



**This electronic thesis or dissertation has been
downloaded from Explore Bristol Research,
<http://research-information.bristol.ac.uk>**

Author:

Kittivorapart, Jane

Title:

**Investigation and Characterisation of Extracellular Vesicles Generated by HbE/
Thalassaemic Patients**

General rights

Access to the thesis is subject to the Creative Commons Attribution - NonCommercial-No Derivatives 4.0 International Public License. A copy of this may be found at <https://creativecommons.org/licenses/by-nc-nd/4.0/legalcode>. This license sets out your rights and the restrictions that apply to your access to the thesis so it is important you read this before proceeding.

Take down policy

Some pages of this thesis may have been removed for copyright restrictions prior to having it been deposited in Explore Bristol Research. However, if you have discovered material within the thesis that you consider to be unlawful e.g. breaches of copyright (either yours or that of a third party) or any other law, including but not limited to those relating to patent, trademark, confidentiality, data protection, obscenity, defamation, libel, then please contact collections-metadata@bristol.ac.uk and include the following information in your message:

- Your contact details
- Bibliographic details for the item, including a URL
- An outline nature of the complaint

Your claim will be investigated and, where appropriate, the item in question will be removed from public view as soon as possible.

Investigation and Characterisation of Extracellular Vesicles Generated by HbE/ β -Thalassaemic Patients

JANEJIRA KITTIVORAPART

School of Biochemistry, Faculty of Life Sciences,

University of Bristol,

University Walk, Bristol, UK

November 2018

A dissertation submitted to the University of Bristol in accordance with the requirements for award of the degree of Philosophy in the School of Biochemistry, Faculty of Life Sciences

Word count: 53,208

ABSTRACT

Thalassaemia is one of the most prevalent inherited haemoglobin disorders with a broad clinical spectrum. The diversity in symptoms cannot be explained purely by patients' genetic background. Several factors have been recognised to contribute to disease severity, and this work has set out to undertake a comprehensive study of some of these contributors in HbE/ β -thalassaemia patients from Thailand.

Extracellular vesicles (EVs) are one factor that may indicate and/or contribute to disease severity. The levels of EVs observed in the plasma of thalassaemic patients are reported to be, on average, four times higher than in healthy controls. Moreover, it is well established that these EVs are associated with an increase in clinically significant procoagulant activity. The work presented in this thesis has investigated the EVs produced from both *in vitro* and *in vivo* origins derived from thalassaemic patients and the quantification and characterisation of their protein constituents.

An erythroid culture system was developed for growing thalassaemic patient progenitor cells into reticulocytes. Using this culture system, thalassaemic and age-matched control reticulocytes were produced, EVs subsequently isolated, and their proteomic profiles assessed using quantitative mass spectrometry. This thesis reports the first *in vitro* reticulocyte EV proteome derived from adults with β -thalassaemia.

Furthermore, *in vivo* EVs isolated from plasma of thalassaemic patients were investigated using quantitative proteomic analysis. Amongst 21 proteins identified with significantly altered abundances in HbE/ β -thalassaemia EVs, haptoglobin, hemopexin, and cathepsin S had the potential to be used as clinical biomarkers. A pilot clinical follow-up trial was designed to examine their application, with promising results. All three protein biomarkers had significantly altered levels in groups of patients with different severity of symptoms, i.e., patients with transfusion-dependent thalassaemia, non-transfusion dependent thalassaemia, thalassaemic carriers, and healthy controls. Additionally, both haptoglobin and hemopexin showed a significant correlation to other haemolytic blood parameters. These findings suggested haptoglobin and hemopexin have utility in thalassaemic patients as a tool for clinical monitoring and as indicators of blood transfusion requirements.

Therefore, in summary, the investigation and characterisation of the extracellular vesicles generated by HbE/ β -thalassaemic patients were successfully completed, protein biomarkers were identified, and their potential clinical application explored.

ACKNOWLEDGEMENTS

I am profoundly grateful to Dr Vanja Karamatic Crew and Dr Ashley Toye for giving me the opportunity of being their PhD student. The patience, motivation, enthusiasm, immense knowledge, and encouragement I have received throughout the journey of my PhD life are much more than one could ask for from a supervisor. I could not have imagined having a better mentor for my study.

I would like to express my gratitude to everyone in the 'F056 lab', Filton for their kind help, supervision, and teaching me most of the techniques I used in this project. My research could not have been completed without their help.

Thanks for all the advice from my progression panel, Dr Mike Jones and Dr Kevin Gaston.

My sincere thanks to Professor David Anstee for giving me the opportunity to be a PhD student in NHSBT, Filton, also I thank his valuable insight guiding my project topic.

A very special thank goes to Tom, a friend and a brother, who always encourage and listen to me. Massive thanks to all his help and, of course, his wonderful cakes!

To all friends in Bristol and throughout the UK, thank you for all the support and understanding. Everything we shared together makes me feel like we are family members than just friends.

Thanks to the Faculty of Medicine, Siriraj Hospital, Mahidol University, for giving me the great opportunity of being in the UK. I would also like to thank everyone, especially Yubolrat, Usanee, Pradermchai and the staff from HLA and QC labs for their help with the samples at Department of Transfusion Medicine, Faculty of Medicine, Siriraj Hospital.

I am grateful for the help of Dr Noppadol Siritanaratkul, the staff, and Dr Bunchoo Suntornopas in the recruitment of patients and controls in the project. Also, Thanks the patients and controls in the project for providing their precious blood samples.

My supporters, Pang, Ku, Nattaya, Pop, thank you for always being there for me.

My heartfelt thanks to my family, my amazing parents who always understand me, continually support, and stand by my side. I extremely appreciate it. To Vee, thanks for always putting a smile on my face every time I frown.

AUTHOR'S DECLARATION

I declare that the work in this dissertation was carried out in accordance with the requirements of the University's *Regulations and Code of Practice for Research Degree Programmes* and that it has not been submitted for any other academic award. Except where indicated by specific reference in the text, the work is the candidate's own work. Work done in collaboration with, or with the assistance of, others, is indicated as such. Any views expressed in the dissertation are those of the author.

SIGNED: DATE:.....

PUBLICATION

Kittivorapart J, Crew VK, Wilson MC, Heesom KJ, Siritanaratkul N, Teye AM. Quantitative proteomics of plasma vesicles identify novel biomarkers for hemoglobin E/ β -thalassemic patients. *Blood Adv* 2018 Jan 23; 2(2): 95-104.

ABSTRACT.....	i
ACKNOWLEDGEMENTS.....	iii
AUTHOR'S DECLARATION	iv
PUBLICATION	v
LIST OF FIGURES.....	xii
LIST OF TABLES.....	xv
LIST OF ABBREVIATIONS	xvii
CHAPTER 1.....	1
1.1 Erythropoiesis	2
1.1.1 Steady-state erythropoiesis	2
1.1.1.1 Key transcription factors of erythropoiesis.....	5
1.1.1.2 Key growth factors that influence erythropoiesis.....	8
1.1.2 Stress erythropoiesis	11
1.1.2.1 Regulators of stress erythropoiesis	13
1.1.3 Animal models of erythropoiesis	15
1.1.4 <i>In vitro</i> erythropoiesis	16
1.1.4.1 Sources of stem cells for <i>in vitro</i> erythropoiesis studies.....	17
1.1.4.2 Culture systems	18
1.1.4.3 <i>In vitro</i> erythropoiesis for the study of thalassaemia	19
1.1.4.4 Other strategies to study <i>in vitro</i> erythropoiesis	20
1.2 Globin genes and their regulators	22
1.2.1 Normal haemoglobin synthesis.....	23
1.2.2 Haemoglobin switching.....	24
1.3 Thalassaemia.....	26
1.3.1 Definition.....	26
1.3.2 Epidemiology.....	26
1.3.3 Pathophysiology.....	27
1.3.4 Classifications of thalassaemia.....	28
1.3.4.1 Beta-thalassaemia	29
1.3.4.2 Haemoglobin E (HbE).....	30
1.3.4.3 Alpha-thalassaemia	32
1.3.5 Clinical manifestations and complications of thalassaemia	33
1.3.5.1 Haemolysis and blood parameters associated with thalassaemia	33

1.3.5.2 Iron overload	35
1.3.5.3 Extramedullary haematopoiesis.....	36
1.3.6 Treatments of thalassaemia.....	36
1.3.6.1 TDT patients.....	37
1.3.6.2 NTDT patients	37
1.4. Genetic factors determining the severity of β -thalassaemia	38
1.4.1. Mutations of the <i>HBB</i> gene.....	38
1.4.2 Co-inheritance of β -thalassaemia	41
1.4.2.1 Clinical features of HbE/ β -thalassaemia	41
1.4.2.2 Co-inheritance of α - and β -thalassaemia	41
1.4.2.3 <i>Cis</i> -regulatory sequences of the β -globin locus	42
1.4.2.4 <i>Trans</i> -acting factors of fetal Hb	43
1.5 Extracellular vesicles	47
1.5.1 Extracellular vesicle definition	48
1.5.2 Mechanisms of EV formation	48
1.5.2.1 Physiological EV release	48
1.5.2.2 EVs formation and release in haemoglobinopathy diseases	51
1.5.3 Methods for EV characterisation	54
1.5.3.1 Electron microscopy	56
1.5.3.2 Flow cytometry.....	56
1.5.3.3 Nanoparticle tracking analysis.....	57
1.5.3.4 Tunable Resistive Pulse Sensing.....	57
1.5.4 Proteomics studies	58
1.5.4.1 Proteomics studies of thalassaemia erythrocytes and plasma	59
1.5.4.2 Proteomics studies of thalassaemic EVs	59
1.6 Project aims.....	62
CHAPTER 2.....	63
2.1 Materials	64
2.1.1 Ethics and consent for patient and control samples	64
2.1.1.1 Blood samples for EV characterisation.....	64
2.1.1.3 Clinical trial recruitment.....	65
2.1.1.3 Fresh CD34 ⁺ cells as control samples	66
2.1.1.4 Genomic DNA of thalassaemic patients and healthy controls.....	67

2.1.2 Commercial chemicals and suppliers	67
2.1.3 In-house buffers and chemicals	69
2.1.4 Antibodies	70
2.1.4.1 Antibodies for Western blot analysis	70
2.1.4.2 Antibodies for flow cytometry	70
2.1.5 Analysis Software	70
2.2 Methods.....	71
2.2.1 CD34 ⁺ isolation from adult peripheral blood	71
2.2.2 Three-stage erythroid culture based on Griffiths <i>et al.</i> (2012).....	71
2.2.3 Three-stage erythroid cultures with corticosteroids.....	72
2.2.4 Cell morphology monitoring	72
2.2.5 Cytospin slide staining.....	73
2.2.5.1 May-Grünwald Giemsa stain	73
2.2.5.2 Leishman's stain	73
2.2.6 Reticulocyte filtration.....	73
2.2.7 EVs isolation	73
2.2.7.1 EVs isolation from <i>in vivo</i> sources (ultracentrifugation)	74
2.2.7.2 EVs isolation from <i>in vitro</i> sources (cultured reticulocytes)	75
2.2.8 Flow cytometry.....	76
2.2.8.1 Flow cytometry for <i>in vivo</i> EVs (plasma-derived samples).....	76
2.2.8.2 Flow cytometry for <i>in vitro</i> EVs (from cultured reticulocytes).....	77
2.2.9 Nanoparticle tracking analysis (NTA)	77
2.2.10 Protein quantitation using Bradford's assay.....	78
2.2.11 Ghost membrane preparation	79
2.2.12 Western blotting	79
2.2.13 Proteomic analysis: TMT labelling and high pH reversed-phase chromatography ..	79
2.2.14 Nano-LC mass spectrometry	80
2.2.15 Proteomics data analysis.....	81
2.2.16 Enzyme-linked immunosorbent assay (ELISA)	81
2.2.17 Statistical analyses	82
CHAPTER 3.....	83
3.1 Introduction	84
3.2 Results.....	85

3.2.1 Cold storage of whole blood has minimal effect on CD34+ isolation.....	85
3.2.2 CD34+ cell yield from 24 ml of peripheral blood.....	87
3.2.3 Glucocorticoids increase erythroid culture yields	88
3.2.4 Effects of corticosteroids on extracellular vesicles isolated from the cultured reticulocytes.....	92
3.2.5 <i>Ex vivo</i> erythropoiesis of thalassaemic cells compared to the matched controls.....	94
3.2.6 Comparative analysis of proteome between red blood cell membranes of thalassaemic samples and the matched controls.....	103
3.2.7 Quantification of <i>in vitro</i> EVs released from cultured reticulocytes.....	106
3.2.8 Quantitative analysis of the proteome of EVs released from cultured thalassaemic reticulocytes and the matched controls	107
3.2.9 Comparison of the proteomic profiles between the <i>in vitro</i> generated EVs and reticulocyte membrane.....	112
3.3 Discussion.....	115
3.3.1 Effects of delaying CD34+ cells isolation on <i>in vitro</i> erythroid culture.....	115
3.3.2 Glucocorticoids increase the yield of erythroid cells and have minimal effects on reticulocyte derived extracellular vesicles composition.....	116
3.3.3 <i>Ex vivo</i> erythropoiesis of thalassaemic erythroid cells compared to the matched controls.....	117
3.3.4 Proteomic comparison of <i>in vitro</i> reticulocyte membranes between patient and control	120
3.3.5 Proteomic comparison of <i>in vitro</i> EVs derived from cultured reticulocytes of HbE/ β -thalassaemia patients.	121
3.3.6 Proteomic profiles of reticulocytes membrane and their derived EVs.....	122
3.4 Chapter summary	123
CHAPTER 4.....	124
4.1 Introduction	125
4.2 Results.....	126
4.2.1 Isolation of extracellular vesicles	126
4.2.2 Quantitative measurements of EVs derived from plasma of HbE/ β -thalassaemia patients.....	128
4.2.3 Exploring the relationship between <i>in vivo</i> EV generation and clinical manifestations of HbE/ β -thalassaemia patients using NTA	129
4.2.4 Proteomic profiles of <i>in vivo</i> circulating EVs.....	131
4.2.4.1 Comparison of proteome profiles of the <i>in vivo</i> circulating EVs derived from plasma of HbE/ β -thalassaemia patients and normal healthy individuals.....	131

4.2.4.2 Immunoblotting to validate the proteomic study.....	138
4.2.4.3 Thalassaemic EV plasma adsorption test	139
4.2.4.4 Comparative analysis of the proteomic profiles of <i>in vivo</i> and <i>in vitro</i> sourced EVs	140
4.3 Discussion.....	141
4.3.1 Determination of the optimised method for EV isolation and quantification	141
4.3.2 The relationship of <i>in vivo</i> EV generation and clinical parameters of HbE/ β -thalassaemia patients	142
4.3.3 Proteomic analysis of the <i>in vivo</i> EV produced from HbE/ β -thalassaemia patients	143
4.4 Chapter summary	146
CHAPTER 5.....	147
5.1 Introduction	148
5.1.1 Overview of haemolysis and biomarkers in thalassaemic patients.....	148
5.1.2 Haemolytic markers and their clinical applications	149
5.1.2.1 Haptoglobin testing	150
5.1.2.2 Hemopexin testing	151
5.1.2.3 Cathepsin S testing	152
5.1.3 Evaluation of haptoglobin, hemopexin and CTSS as predictive parameters of disease severity.....	153
5.1.4 Optimisation of the ELISA assays to detect the very low levels of proteins.....	154
5.2 Results.....	155
5.2.1 Molecular diagnosis, demographic data and laboratory parameters in TDT, NTDT, thalassaemic traits, and control individuals.....	155
5.2.2 Plasma haptoglobin.....	157
5.2.3 Plasma hemopexin	159
5.2.4 Plasma cathepsin S.....	160
5.2.5 The applications of haptoglobin, hemopexin and CTSS in the various clinical classification of thalassaemic patients.....	161
5.2.5.1 NTDT patients	161
5.2.5.2 TDT patients.....	163
5.2.6 The effect of transfusion on haemolytic markers in TDT patients	165
5.3 Discussion.....	169
5.3.1 Clinical severity of thalassaemia	169
5.3.2 NTDT patients.....	170
5.3.3 TDT patients	171

5.4 Chapter summary	173
CHAPTER 6.....	174
6.1 <i>In vitro</i> erythropoiesis of HbE/ β -thalassaemic patients	175
6.1.1 Proteomic study of <i>in vitro</i> -derived thalassaemic EVs.....	176
6.1.2 Future work around <i>in vitro</i> culture of thalassaemia	177
6.1.2.1 Development of synthetic cellular model of human β -thalassaemia	177
6.1.2.2 Monitoring decreased differentiation of erythroid precursor cells.....	178
6.2 Identification and clinical applications of haptoglobin, hemopexin, and cathepsin S as biomarkers	178
6.3 Genetic studies of the thalassaemic patients.....	179
6.4 Final summary.....	180
REFERENCES	181
APPENDIX	218
Appendix I	218
Demographic data, initial diagnoses, laboratory parameters, medications, and ELISA results of all the patients recruited in the clinical follow-up trial	218
Appendix II	223
Primers used for PCR amplifications and Sanger sequencing.....	223
Appendix III	224
Table summarised genetic backgrounds of all the thalassaemia patients recruited in the project.....	224

LIST OF FIGURES

Figure 1.1. Schematic of early and late erythropoiesis with associated cell-specific surface markers (KIT, GPA, CD71).	3
Figure 1.2. An overview of different stages of erythropoiesis from HSCs to reticulocytes and their regulators.	5
Figure 1.3. Model of stress erythropoiesis and its regulators.	13
Figure 1.4. β -globin gene cluster and the sequence of globin synthesis during human development.	24
Figure 1.5. KLF1 regulates globin switching through <i>BCL11A</i> and <i>HBB</i> genes.	45
Figure 1.6. Biogenesis of exosome and microparticle from a mother cell.	50
Figure 1.7. Effects of oxidative stress on β -thalassaemic red cells and EVs generation.	53
Figure 2.1. Workflow diagram of EVs characterisation.	65
Figure 2.2. Scheme of blood collections of the clinical follow-up study.	66
Figure 2.3. Schematic showing the ultracentrifugation technique used to isolate extracellular vesicles from cell plasma or liquid media culture.	74
Figure 2.4. Example of flow cytometry analysis of the EVs derived from the thalassaemic plasma-derived sample.	76
Figure 2.5. An example of nanoparticle tracking analysis.	78
Figure 3.1. Storage effect on CD34 ⁺ cell isolation from buffy coats and erythroid cell proliferation in three-stage culture.	86
Figure 3.2. The average percentages (n=2) of cells at the stated morphological stage of the control sample (D0), 3-day stored sample (D3), and 5-day stored sample (D5).	87
Figure 3.3. The effects of corticosteroid treatment on <i>in vitro</i> erythroid culture.	89
Figure 3.4. Representatives Leishman's stain cytopspins illustrating morphology on day 8 of culture.	90
Figure 3.5. Cell maturation of dexamethasone (DXM) (10^{-6} M), hydrocortisone (HC) (10^{-6} M) and untreated controls, analysed on the days indicated using cytospin images.	91
Figure 3.6. Cell expansion of CD34 ⁺ derived control and HbE/ β -thalassaemia patient erythroblasts shown as cumulative fold increase.	97

Figure 3.7. Cell death as a measure of cell viability of HbE/ β -thalassaemia patients (n=3) and controls (n=3) erythroblasts during culture.....	98
Figure 3.8. Erythroid differentiation of CD34 ⁺ -derived erythroblasts from three thalassaemia patients compared to their matched controls.	101
Figure 3.9. Cell morphologies of <i>in vitro</i> cultured thalassaemic and control erythroid cells.	102
Figure 3.10. Cumulative fold change of two erythroid cultures of thalassaemic samples (PT4 and PT5) and their matched controls (CT4 and CT5).....	103
Figure 3.11. Proteins with altered abundance in thalassaemia patients' <i>ex vivo</i> reticulocyte membranes compared to control reticulocyte membranes.	105
Figure 3.12. Cytospin images of pre-and post-filtered cultured reticulocytes from HbE/ β -thalassaemia patients.	106
Figure 3.13. Functional classification (Gene Ontology; GO) of 286 proteins/genes mutually found in the EV constituents derived from three <i>ex vivo</i> cultured three pairs of thalassaemic and control reticulocyte samples.	108
Figure 3.14. Proteins with altered abundance in HbE/ β -thalassaemia patients' EVs derived from <i>in vitro</i> reticulocytes compared to the matched-control EVs.....	111
Figure 3.15. Proteins shared between the erythroid membrane and EV preparations from <i>in vitro</i> thalassaemic patient (n=3) and matched controls (n=3).	114
Figure 4.1. Comparison of different EV enrichment methods from plasma.	127
Figure 4.2. Schematic of HbE/ β -thalassaemia patients and control samples used for the proteomic analysis of the <i>in vivo</i> generated EVs.....	131
Figure 4.3. Gene Ontology analysis of cellular components on three sets of pooled thalassaemic plasma EV samples.....	133
Figure 4.4. Functional classification of 21 proteins exhibiting an altered abundance according to their functions using STRING:.....	135
Figure 4.5. Western blot analysis of EV samples of two patients.	139
Figure 4.6. Western blot of EVs from patient and control immunostained with anti-hemopexin, demonstrating the expression of hemopexin.	140

Figure 5.1. Boxplot showing variation in haptoglobin level (mgdl^{-1}) between groups of patients and controls as measured by ELISA.158

Figure 5.2. Boxplot showing the variation in hemopexin level (mgml^{-1}) between groups of patients and controls.159

Figure 5.3. Boxplot showing the variation in cathepsin S level (pgml^{-1}) between groups of patients and controls.160

Figure 5.4. Box plots showing different levels of plasma haptoglobin (mgml^{-1}), hemopexin (mgml^{-1}), and CTSS (ugml^{-1}) pre- and post-transfusion.167

Figure 5.5. Haptoglobin pre- and one-hour post-transfusion and concentration (mgdl^{-1}) shown for five visits for each individual patient.168

LIST OF TABLES

Table 1.1. A summary of genetic classification and the phenotype diversities of thalassaemia.	29
Table 1.2. Frequencies of causative <i>HBB</i> mutations reported in Thailand.	39
Table 1.3. Categories of proteins and their expected abundance levels in EVs.....	55
Table 1.4. Proteins identified in EVs isolated from thalassaemia-intermedia (TI) RBCs analysed by MALDI-TOF reported by Ferru and colleagues (2014).	60
Table 1.5. Proteins from platelet-free plasma-derived microparticles of HbE/ β -thalassaemia patients compared to the normal controls analysed by Q-TOF MS and MS/MS analyses reported by Chaichompoo and colleagues (2012).	61
Table 2.1. Primary antibodies used for Western blotting of selected proteins.	70
Table 3.1. Nine up-regulated proteins in the EVs derived from DXM-treated samples when compared to the control samples.....	93
Table 3.2. Characteristics and clinical parameters of five non-transfusion dependent HbE/ β - thalassaemia patients enrolled in the <i>ex vivo</i> erythropoiesis experiment.....	95
Table 3.3. Numbers of CD34 ⁺ cells extracted from 24 ml of peripheral blood in thalassaemic patient (PT) and control (CT) samples.	96
Table 3.4. Numbers of <i>in vitro</i> derived reticulocyte EVs from thalassaemic patients (PT sample) and matched controls (CT sample), determined by flow cytometry and NTA analyses.	107
Table 3.5. Eight proteins observed to be up-regulated in the two EV samples derived from <i>in vitro</i> reticulocytes of HbE/ β -thalassaemia patient (n=3), compared to the matched controls (n=3).	109
Table 3.6. The total number of proteins (>2 unique peptides) identified from the three samples (PT1, PT2, and PT3) from the <i>in vitro</i> erythrocyte membrane preparation and from the <i>in vitro</i> reticulocyte EVs.	113
Table 4.1. Clinical information of the HbE/ β -thalassaemia patients enrolled in this experiment.	128

Table 4.2. Quantification of <i>in vivo</i> sourced EVs from the plasma of HbE/ β -thalassaemia patients. Comparison of NTA and flow cytometry techniques.	128
Table 4.3. The concentration of EVs from circulating plasma vesicles derived from HbE/ β -thalassaemia patients (n=16) with recorded splenic status and controls (n=13).	130
Table 4.4. Clinical parameters of 15 patients enrolled for the EV proteomics.	132
Table 4.5. Proteins with increased abundance in EVs of HbE/ β -thalassaemia patients compared to controls across three separate experiments.	134
Table 4.6. Proteins identified using TMT mass spectrometry as consistently reduced in abundance across three separate experiments in extracellular vesicles of HbE/ β -thalassaemia patients compared to controls.	135
Table 4.7. Haemoglobin levels and the ratio of alteration of the proteins of interest in EVs from six individual HbE/ β -thalassaemia patients measured by TMT.	137
Table 4.8. Statistical correlations between altered ratios of proteins of interest and haemoglobin levels of six individual HbE/ β -thalassaemia patients.	138
Table 5.1. Blood parameters observed in this study, including indications and associated site of haemolysis.	150
Table 5.2. Demographic data and laboratory parameters in different groups of patients, traits, and controls.	156
Table 5.3. Examples of haptoglobin levels (mgml ⁻¹) of two TDT (A01&A03) and NTDT (B07&B08) patients measured by nephelometry and ELISA methods.	157
Table 5.4. A summary of the correlation studies of the NTDT group, using Spearman's rank correlation, except for the marked parameters (✕).	162
Table 5.5. The correlations of tested parameters in the NTDT group.	163
Table 5.6. Summary of the correlation studies of the TDT group using Spearman's rank correlation, except for the marked parameters (✕).	164
Table 5.7. The correlations of tested parameters in the TDT group. All used Spearman's rank correlation. P <0.05 denotes statistical significance.	165
Table 5.8. Statistical analysis of all parameters between pre-and post-transfusion plasma of the TDT group.	166

LIST OF ABBREVIATIONS

AHSP – Alpha haemoglobin stabilising protein
AIHA – Autoimmune haemolytic anaemia
BC – Buffy coat
BCL11A - B-cell lymphoma/leukaemia 11A
BFU-E – Burst forming unit-erythroid
BMP4 – Bone morphogenetic protein 4
CBP – CREB-binding protein
CDA – Congenital dyserythropoietic anaemia
CFU-E – Colony forming unit-erythroid
CI – Confidence interval
CREB – cAMP response element-binding protein
CTSS – Cathepsin S
DNA – Deoxyribonucleic acid
DXM – Dexamethasone
EKLF – Erythroid Krüppel-Like Factor
EM – Electron microscope
EPO – Erythropoietin
EPOR – Erythropoietin receptor
EV – Extracellular vesicle
EVH – Extravascular haemolysis
FOG-1 – Friend of GATA-1
FUBP1 - Fuse binding protein 1
GATA1 - GATA binding protein 1
GDF15 – Growth differentiation factor 15
gDNA – Genomic deoxyribonucleic acid
GPA – Glycophorin A
GR – Glucocorticoid receptor
GWAS – Genome-wide association studies

Hb – Haemoglobin
HbA – Adult haemoglobin
HBA – Alpha globin gene
HBB – Beta globin gene
HbCS – Haemoglobin Constant Spring
HbF – Haemoglobin F
HC – Hydrocortisone
HEMA – Human erythroid massive amplification
HH – Hereditary haemochromatosis
hHPFH – Heterocellular hereditary persistence of fetal haemoglobin
HIF – Hypoxia-inducible factor
HPFH – Hereditary persistence of fetal haemoglobin
HPLC – High performance liquid chromatography
HSCs – Haematopoietic stem cells
Hsp – Heat shock protein
IE – Ineffective erythropoiesis
IGF-1 – Insulin-like growth factor -1
IL – Interleukin
iPSCs – Induced pluripotent stem cells
ISEV – International Society for Extracellular Vesicles
iTRAQ – Isobaric tags for relative and absolute quantification
IVH – Intravascular haemolysis
IVS – Intervening sequence
JAK2 – Janus Kinase 2
KLF1 – Krüppel-like transcription factor 1 gene
LCR – Locus control region
LDH – Lactate dehydrogenase
M/Z – Mass-to-charge ratio
MALDI-TOF – Matrix-assisted laser desorption/ionisation

MAPK – Mitogen-activated protein kinase

MEP – Megakaryocyte-erythroid progenitor cells

MetHb – Methaemoglobin

MNCs – Mononuclear cells

mRNA – Messenger ribonucleic acid

MP – Microparticle

MS/MS – Tandem mass spectrometry

nano-LC-MSMS – Nanoscale liquid chromatography coupled to tandem mass spectrometry

NO – Nitric oxide

NTA – Nanoparticle tracking analysis

NTDT – Non-transfusion dependent thalassaemia

NuRD – Nucleosome remodelling deacetylase

PI3K – Phosphoinositide 3-kinase

PRDX2 – Peroxiredoxin 2

PS – Phosphatidylserine

PSMs – Peptide to spectrum match

PTC – Premature termination codon

QTLs – Quantitative trait loci

RBCs – Red blood cells

RE – Reticuloendothelial system

ROS – Reactive oxygen species

RR – Relative risk

SCD – Sickle cell disease

SCF – Stem cell factor

SILAC – Stable isotope labelling with amino acids in cell culture

SNV – Single nucleotide variant

SOD – Superoxide dismutase enzyme

STAT5 – Signal transducer and activator of transcription 5

TAL-1/SCL – T-cell acute lymphocytic leukaemia protein 1/ stem cell leukaemia

TDT – Transfusion dependent thalassaemia

TEM – Transmission electron microscope

TGF- β – Transforming growth factor- β

TMT – Tandem Mass Tag

TRPS - Tunable resistive pulse sensing

UC – Ultracentrifugation

UTR – Untranslated region

VCAM – Vascular adhesion molecule

ZF – Zinc finger

CHAPTER 1

INTRODUCTION

1.1 Erythropoiesis

Erythropoiesis is a dynamic process whereby stem cells differentiate into fully mature red blood cells (RBCs), also known as erythrocytes. The average RBC lives for 120 days (1), so the body must maintain erythropoiesis continually to replenish the RBC supply for an entire individual lifetime, producing approximately 2 million RBCs per second (2). Insufficient RBC production causes anaemia (3). There are two types of erythropoiesis: steady-state erythropoiesis and stress erythropoiesis, which only occurs during anaemia.

1.1.1 Steady-state erythropoiesis

Human RBCs comprise, on average, 84% of all the cells in the body, totalling approximately 25 trillion cells in circulation (4). Daily, approximately 2×10^{11} new erythrocytes are generated in order to replace the senescent cells lost to clearance (5). This process of RBC production occurs in bone marrow in a stem cell niche. Starting from pluripotent haematopoietic stem cells (HSCs), with $CD34^+$ and $CD90^+$ specific cell surface markers, these cells differentiate into multipotent progenitor cells ($CD34^+CD90^-$). The stem cells possess self-renewal properties and multi-potency to develop into all lineage precursors, i.e., erythroid, myeloid, and lymphoid progenitors. Depending on many factors, for example, the niche or microenvironment of the bone marrow, presence of erythroblastic islands composed of one or more central macrophages and stimulus by cell-cell interactions and growth factors, the stem cells may either self-renew or undergo asymmetric division to generate multipotent progenitors (6, 7). The multipotent progenitors will subsequently differentiate into common myeloid progenitor cells, and megakaryocyte/erythroid progenitor cells ($CD34^+CD38^+CD45RA^-$).

Once they are committed to the erythroid development, the progenitors then undergo the process of erythropoiesis. Erythropoiesis can be divided into two phases: early-stage erythropoiesis and terminal erythroid differentiation. Early erythropoiesis is defined as the process by which the multipotential progenitor cells proliferate and mature into the committed erythroid lineage, as seen in Figure 1.1.

The first committed erythroid progenitor is a burst-forming unit-erythroid (BFU-E), which subsequently divides and differentiates into a colony-forming unit-erythroid (CFU-E). In the bone marrow, BFU-Es are less abundant than CFU-Es, with approximately 0.03% and 0.3%

cells, respectively (8, 9). Less mature BFU-Es differentiate into more mature, rapidly dividing CFU-Es, which can give rise to 8-49 erythroblast colonies in seven days, within three to five cell divisions (10, 11) (Figure 1.1). Further expansion and cell division occur, so that the progenitor cells subsequently develop into the proerythroblasts, the first stage of the terminal erythroid differentiation and the first erythroid cells recognizable by the light microscopy. In normal erythroid cells, haemoglobin (Hb) starts to accumulate and increase in concentration during the terminal differentiation stage, with the highest expression at the reticulocyte/erythrocyte stage (3). The cells also begin to express erythroid-specific membrane proteins, such as glycophorin A (3).

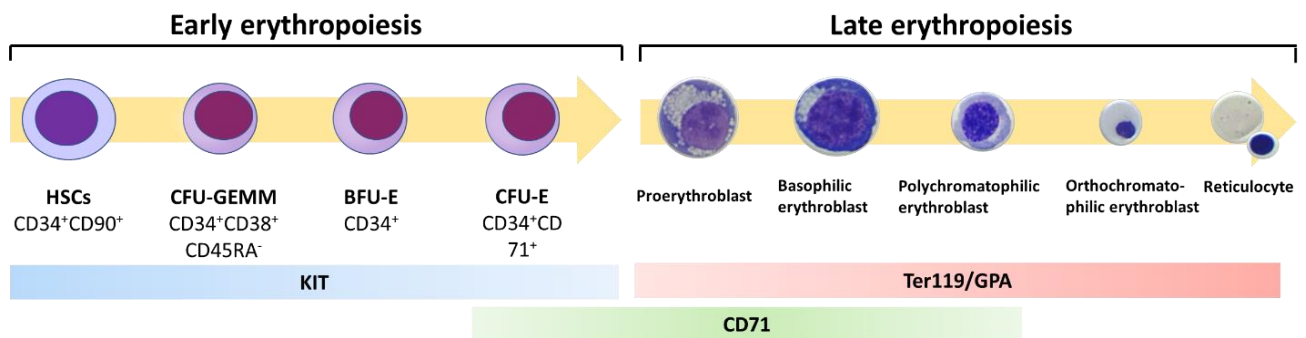


Figure 1.1. Schematic of early and late erythropoiesis with associated cell-specific surface markers (KIT, GPA, CD71).

During early erythropoiesis, the first identifiable committed erythroid cell is BFU-E, which can undergo cell division into large colonies of >500 erythroblasts; while each CFU-E can then give rise up to 8-49 erythroid cells in seven days. The late erythropoiesis or terminal differentiation begins at proerythroblast phase evolving to basophilic, polychromatophilic and orthochromatophilic erythroblast. Morphologic changes are characterised by a decrease in cell size and progressive nuclear condensation, accumulation of haemoglobin in the cytoplasm and erythroid-specific protein expression. Ultimately, the nucleated red cell undergoes enucleation, becoming a reticulocyte. Representative cells were stained with Leishman's stain. (Modified from Dzierzak & Philipsen 2013 *Erythropoiesis: Development and differentiation Cold Spring Harb Perspect Med* 3(4); a011601)(5)

When the progenitor cells progress into the terminal differentiation, their proliferative potential decreases. The cell division occurs approximately four to five times during the cell development from the proerythroblast to the reticulocyte (5). The whole of the terminal differentiation occurs in the bone marrow on the erythroblastic islands, where a central

macrophage can be surrounded by a between five and over 30 differentiating erythroblasts (see reference (12) for a review). The morphology of the cells undergoing terminal differentiation has been studied extensively (5, 13). In brief, the proerythroblasts are large cells with a high nuclear/cytoplasmic (N:C) ratio, prominent nucleoli, and deep blue cytoplasm (Figure 1.1). As the cells differentiate, their morphology gradually changes; they become smaller in size, the nucleoli disappear, and chromatin becomes more dense and clumped. The cytoplasm also changes from blue to greyish pink colour due to the abundance of Hb, visible when using cell stains such as Leishman's or May-Grünwald Giemsa. The next three consecutive erythroblast stages are basophilic erythroblasts, polychromatophilic erythroblasts, and orthochromatic erythroblasts. During the last phase, the cells go through an extensive synthesis of erythroid specific proteins, such as band 3, and form recognisable membrane complexes (14, 15). Ultimately, the nuclei become localised to one side of the cell, and then enucleation occurs, forming the anucleate reticulocytes.

The nascent reticulocytes can be categorised into R1 and R2. R1 reticulocytes are multilobular and confined to the bone marrow, whilst R2 reticulocytes are released into the blood circulation (16). The final maturation stage of erythropoiesis takes place in peripheral circulation when the reticulocytes lose 20% of their plasma membrane surface area and any remaining organelles. Their cytoskeletons, as well as transmembrane proteins, are remodelled, and the cells become mature erythrocytes (9, 17, 18). Recent evidence has suggested that a part of the reticulocyte maturation process requires autophagosomal vesicle release (16, 19) and this is driven by the mechanical shear experienced in the circulation in a process dependent on non-muscle myosin IIA activity (19).

Regulation mechanisms of erythropoiesis are intricate and involve the combined effects of specific cytokines, growth factors and microenvironmental stimuli, as well as the genetic influence of erythroid-specific transcription factors and related genes. Some of the most important regulators of steady-state erythropoiesis will be discussed here. Figure 1.2 summarises the various stages of erythropoiesis and their key regulators.

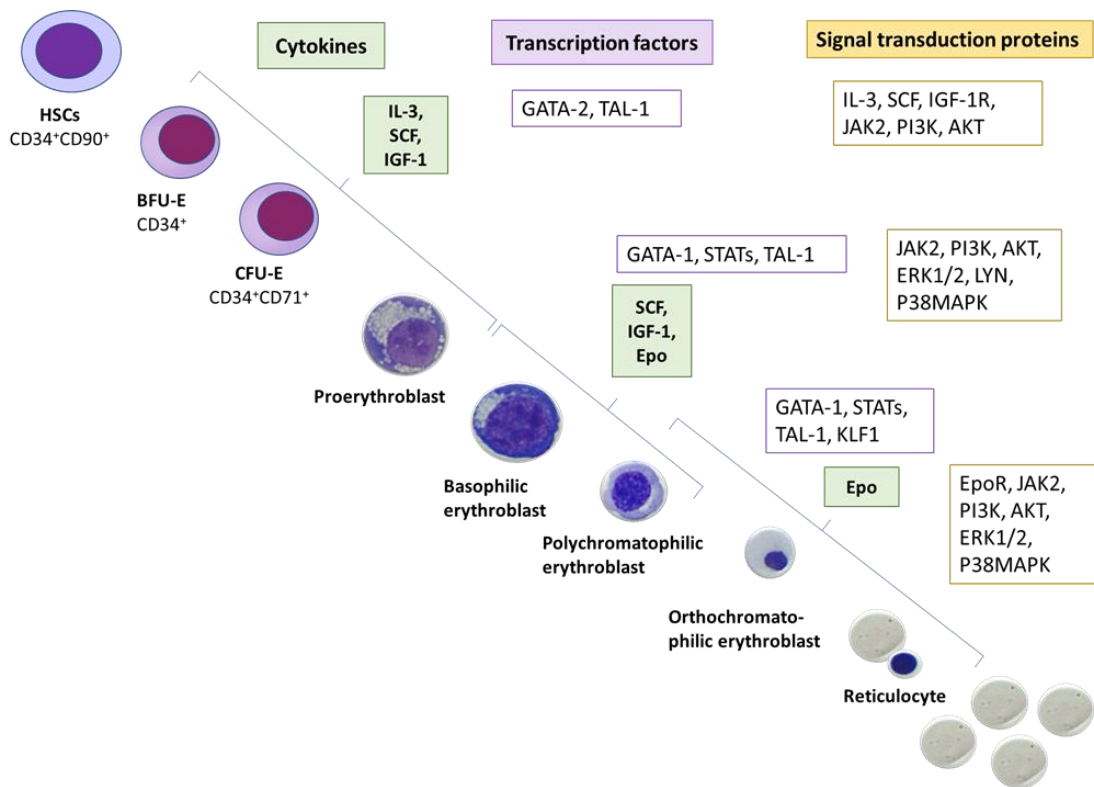


Figure 1.2. An overview of different stages of erythropoiesis from HSCs to reticulocytes and their regulators.

The illustration summarises the regulatory factors at each stage of erythropoiesis, which include transcription factors, cytokines and their signal transduction pathways (Diagram adapted from Xie et al. *Mol Med Rep.* 2019 Feb;19(2):783-791)(20)

1.1.1.1 Key transcription factors of erythropoiesis

1.1.1.1.1 GATA Binding Proteins

This family comprises of six members, GATA 1-6, but only GATA-1/2/3 are essential to the haematopoiesis (21). GATA-1 is a crucial transcription factor in erythropoiesis and a member of GATA transcription factor family of zinc finger (ZF) DNA binding proteins that bind to the (A/T)GATA(A/G) DNA sequences which are recognised as the regulatory sequences of erythroid-specific genes in erythroid and other haematopoietic lineages (22, 23). In HSCs, the GATA-1 expression is suppressed, possibly by the process of DNA methylation of *GATA1* locus, and this mechanism allows the binding of GATA-2 and its expression at the HSCs stage (24). Conversely, following the committed progenitor stage, GATA-1 expression increases over GATA-2 and this highlights the different roles of GATA-1 and GATA-2 in haematopoiesis. The primary function of GATA-2 is regulation of progenitor cell proliferation and maintenance of

these haematopoietic progenitors. GATA-1 is necessary for survival and terminal differentiation of erythroid lineage, with its peak expression level at the proerythroblast stage (25) and declining reciprocally to the maturation of erythroblasts. Thus, the proportion of GATA-1 and GATA-2 expression levels at different time points, or so-called GATA factor switching, orchestrates and drives the physiology of erythropoiesis (26). GATA-1 acts as a transcription activator or repressor towards multiple target genes. For example, GATA-1 activates *EPOR* (27) and *HBB* (28), while suppressing *GATA2* and *KIT* (29). Several transcription factors, e.g., FOG-1, KLF1, TAL1/SCL, interact with GATA-1 to regulate erythropoiesis (29, 30).

1.1.1.1.2 Zinc Finger Protein, FOG Family Member 1

Friend of GATA-1 (FOG-1) is a GATA specific cofactor that facilitates erythroid and megakaryocyte maturation (31), specifically GATA switching during erythropoiesis (32). FOG-1 comprises nine ZF domains and interacts directly with GATA-1 for either activation or repression of GATA-1-dependent genes. The interaction site between GATA-1 and FOG-1 was identified through a study of patients with X-linked thrombocytopenia with dyserythropoietic anaemia who had a missense mutation in *GATA1* encoding V205M amino acid change, which disrupted the interaction between GATA-1 and FOG-1. This location was confirmed by using selectively mutated *GATA1* N-finger constructs in the N-terminal ZF of GATA-1 and shown to primarily occur through amino acids E203, V205 and H222 (33, 34). The erythroid cells affected by mutations failed to differentiate down the erythroid lineage (34). In terms of the globin switching, studies in animal models of FOG-1 with disrupted interaction with Nucleosome Remodelling Deacetylase (NuRD) complex indicated that GATA-1 and FOG-1 in conjunction with NuRD, are important for activation of adult type globin expression, but dispensable for silencing of the human γ -globin *in vivo* (35).

1.1.1.1.3 Krüppel-like factor 1 (KLF1) transcription factor

KLF1 is an erythroid-specific essential transcription factor responsible for the regulation of erythropoiesis and the adult β -like globin gene transcription. KLF1 contains three C2H2-type ZF domains on the C-terminus that binds to a CACCC (NCNCNCCCN) DNA consensus element located in the promoter area of many erythroid genes, including the *HBB* globin genes (36). The essential roles of KLF1 in erythropoiesis were demonstrated in KLF1 null mice that presented with failure of adult β -globin expression and died *in utero* (37, 38). The multifunctional roles of KLF1 are extensively reviewed by Siatecka and Bieker (2011) (39).

KLF1 is critical for β -globin expression, definitive erythropoiesis, and the globin switching from fetal haemoglobin (HbF) to adult haemoglobin (HbA) (40, 41). More than one mechanism of KLF1 regulation of gene expression through erythropoiesis has been identified; i.e., regulation via 3D chromatin architecture, chromatin modification and remodelling, and directly via interaction with transcription activators (42-45). KLF1 plays an important role in sequential globin expression by facilitating the interaction between *cis*-regulatory elements or the locus control region (LCR) and the particular globin gene, so only one gene is activated at any one time by the mechanism of 3D chromatin looping (46-48) (see 1.2.2 for Hb switching). KLF1 is also a key transcription factor responsible for Hb switching from γ - to β -globin by direct binding to *BCL11A* (see section 1.1.1.4) to suppress γ -globin and increase β -globin expression (49, 50). Several transcription co-activators also interact with KLF1 and are differentially expressed throughout erythropoiesis, e.g., GATA-1 (51), TAF9 (52), and TFIID (53), which leads to the differential gene transcription activation. Additionally, KLF1 is capable of regulating gene transcription epigenetically by interaction with chromatin modifying and remodelling complexes (44, 54). For example, the interaction of KLF1 and histone H3 results in the acetylation of cAMP response element-binding protein (CREB) – binding protein (CBP), and this occurs without KLF1 binding to the DNA cognate (44).

1.1.1.1.4 B-cell lymphoma/leukaemia 11A (BCL11A) transcription factor

B-cell lymphoma/leukaemia 11A (BCL11A) is a ZF transcription factor that was first identified as one of the quantitative trait loci (QTLs) defining HbF levels (55-57). Three main isoforms of BCL11A are known: BCL11A-XL, BCL11A-L, and BCL-11A-S (57). The expression of BCL11A depends on the developmental stage of human erythroblasts through a reverse relationship with the HbF expression, i.e., from HbF being absent in the primitive erythroblasts to being robustly expressed in adult cells (57). This interaction was reported in the knockdown of *BCL11A* in human erythroblasts resulting in the increase of HbF expression. Sankaran and colleagues (2008) reported the interaction of *cis*-regulatory elements of BCL11A with β -globin gene cluster by demonstrating that the full-length form of BCL11A was occupying several discrete sites in the β -globin cluster, including the areas necessary for γ -globin silencing (57, 58). The BCL11A binding to a γ -globin gene promoter and its repression serve as an underlying mechanism of the Hb switching (59).

1.1.1.1.5 T-Cell Acute Lymphocytic Leukaemia Protein 1 erythroid differentiation factor or stem cell leukaemia (TAL-1/SCL)

T-Cell Acute Lymphocytic Leukaemia Protein 1 (also known as stem cell leukaemia; TAL-1/SCL) is one of the basic helix-loop-helix transcription factors which dimerise with other members of a class of ubiquitous associates, the E-proteins, and E-box consensus element CANNTG (60). TAL-1/SCL is essential for HSCs development, as was shown through SCL^{-/-} embryonic stem cells that were unable to generate haematopoietic and endothelial cells (61). The expression of TAL-1/SCL is similar to GATA-1, being highly expressed in erythroid cells, megakaryocytes and mast cells. At different stages of erythropoiesis, TAL-1/SCL forms a complex with multiple proteins, e.g., LMO2, Ldb1, E2A, and GATA-1, called the pentameric complex (62). The pentameric complex binds to a DNA motif containing an E-box, CAGGTG and a GATA binding sites, and they collectively promote erythroid differentiation (63). Recently, TAL-1/SCL was identified as a regulator of Fuse binding protein 1 (FUBP1), a transcriptional regulator for HSCs self-renewal and survival. Both the pentameric TAL-1 complex and the activation of FUBP1 by TAL-1 are important in switching from progenitor to erythroid-specific gene expression (64).

1.1.1.2 Key growth factors that influence erythropoiesis

To maintain the constant production of erythrocytes, various growth factors and cytokines play a pivotal role in erythropoiesis by acting on erythroid precursors during differentiation. They promote lineage specification, cell proliferation, prevent apoptosis and control maturation.

1.1.1.2.1 Erythropoietin (EPO)

Erythropoietin (EPO) is a cytokine, a glycoprotein with a molecular weight of 34 kDa, which is synthesised by the proximal tubular region of the kidney during adulthood, and by the liver during embryonic and fetal development. EPO regulates the haematopoiesis via a negative feedback control through downstream signal transduction pathways. EPO has an indispensable role as the lineage regulator throughout the erythropoiesis; from the late BFU-E stage all the way to the erythrocyte stage, with the highest concentrations found in the CFU-E stage (65). However, EPO is not a lineage commitment cytokine, since the EPO specific receptor (EPOR) is not detected in any stage earlier than the late BFU-E (10, 65). The EPO regulation of erythropoiesis is initiated from the association of EPO with EPOR, followed by their further association with Janus kinase 2 (JAK2) tyrosine kinase. JAK2s are then

phosphorylated and become activated. The activated JAK2s induce phosphorylation of EPOR tyrosine sites, which in turn act as docking sites of multiple signalling proteins, e.g., Signal transducer and activator of transcript 5 (STAT5), Phosphoinositide-3 kinase (PI3K)/AKT, and Sch/Ras/Mitogen-activated kinase (MAPK) (66). For example, after being phosphorylated and dissociated from EPOR, STAT5s then dimerise and translocate to the nucleus in order to activate gene transcription. The target genes of STATs include *Bcl-xL*, encoding an anti-apoptotic protein which is essential for normal erythropoiesis (67), or genes encoding negative regulators of JAK/STAT pathway: Protein tyrosine phosphatases, suppressors of cytokine signalling proteins and Protein inhibitor of activated STAT (66) .

The production of EPO is regulated by sensing oxygen in the kidney, which activates *EPO* transcription through hypoxia-inducible factors (HIFs) (68). As the name implies, hypoxia is the crucial regulator of the activity of HIFs through its oxygen-sensitive site, i.e., α -subunit (with two main homologs HIF-1 α and -2 α). HIF-2 α transcription factor was identified as the primary regulator of EPO production *in vivo*. In the hypoxic condition, HIF-2 α acts at kidney interstitial cells, increasing EPO mRNA transcription and stimulating EPO synthesis. Recently, another role of HIF-2 α was discovered via the HIF-2 α knock-down mice model. HIF-2 α was shown to mediate the interaction between erythroblasts and intramedullary endothelial cells via Vascular adhesion molecule-1 (VCAM-1) and its ligand, VLA-4, located on the erythroid lineage (68, 69). HIF-2 also governs iron metabolism by regulating serum iron in the hypoxic conditions through a rise in iron absorption, enhanced serum iron-binding capacity, and iron mobilisation from storage (70).

1.1.1.2.2 Stem cell factor and c-Kit

C-Kit or CD117 is a member of the type III receptor tyrosine kinase family. Binding between the c-Kit receptor and its ligand (Stem cell factor; SCF) results in homodimerization and tyrosine autophosphorylation, creating docking sites for Src homology 2 domain-containing signal transduction molecules (71). SCF is one of the indispensable cytokines regulating haematopoiesis of multiple lineages. Indeed, mice with mutations that inactivate the c-Kit receptor or its ligand, SCF, die during the first trimester of gestation, showing a reduced number of erythroid progenitors in their fetal livers (72). The important erythropoietic signalling pathway activated by c-Kit/SCF is PI-3 Kinase/AKT and RAS/MAPK, facilitating the red cell survival and proliferation, respectively. Another significant role of c-Kit is the

cooperation with EPOR to provide a synergistic effect for BFU-E and CFU-E formation (73). Ratajczak and colleagues (1998) demonstrated that SCF co-stimulated the growth of BFU-E with EPO in a much greater degree when compared to IL-3, IL-9, and Granulocyte colony-stimulating factor (GM-CSF) (74). This synergistic mechanism is potentially explained by c-Kit stimulation by SCF phosphorylated tyrosine residue in the cytoplasmic domain of EPOR, resulting in the activation of EPOR (72).

1.1.1.2.3 Interleukin-3 (IL-3)

Human IL-3 is a 15.2 kDa glycoprotein with a single polypeptide chain. In normal physiology, IL-3 is a multilineage potent growth factor generated by monocytes, CD4⁺ T cells, and stromal cells. *In vitro* studies have shown that IL-3 facilitates the expansion of early multilineage stages, CD34⁺ cells, resulting in an increase in expansion of the more mature progenitor cells in all haematopoietic lineages (75-77). Evidence in animal models has shown that IL-3 combined with EPO were important for BFU-E and CFU-E formation through the JAK/STAT pathway (78, 79). The receptor of IL-3 (IL-3R) has specific binding subunits: α -subunit and β -subunit. The signal transduction of the JAK/STAT pathway is induced by this later subunit; whereas the α -chain of IL-3R involves the activation of STAT-5 (80). Moreover, IL-3 is also related to the other signal transduction pathways, e.g. the Ras and PI3 kinase pathways (80). In the *in vivo* erythropoiesis setting, IL-3 appears to act as a primer to other cytokines, including EPO, to increase erythroid expansion (81).

1.1.1.2.4 Insulin and insulin-like growth factor-1 (IGF-1)

The IGFs family consists of insulin, IGF-1 and IGF-2. The receptors of insulin and IGF-1 are homologous in their structures, and all have downstream effects after being activated on multilineage haematopoiesis (82, 83). However, subsequent research found that only insulin receptor, not IGF-1 receptor, is detected amongst the mRNA and the expressed proteins of CD34⁺SCF⁺ progenitor cells (74). IGF-1 may act through the insulin receptor to enhance *in vitro* erythropoiesis. Both IGF-1 and/or insulin in the presence of EPO are required for the *in vitro* haematopoiesis to support the proliferation of early erythroid progenitors (84, 85). A study focusing on BFU-E colony formation from CD34⁺ cells, stimulated with EPO and IL-3, showed the highest number of colonies when insulin (10 μgml^{-1}) was added early. However, BFU-E colonies stimulated with EPO and SCF still developed normally, even in the absence of insulin or IGF-1 (74).

1.1.2 Stress erythropoiesis

As aforementioned, the steady-state erythropoiesis maintains the homeostasis of erythroid lineage by generating new erythrocytes in order to replace the senescent erythrocytes at a constant rate. Unlike the steady-state erythropoiesis, anaemic or hypoxic stress induces physiological responses needed to increase oxygen delivery to the peripheral tissues. The key component behind this adaptive response is stress erythropoiesis (86). Stress erythropoiesis has been studied and is best understood in the fetal liver in mice models and in the spleen and liver in humans (87).

EPO has been shown to be the primary regulator of steady-state erythropoiesis. As physiological levels of EPO are naturally low, erythroid production depends directly on EPO levels. An exogenous source of EPO can moderately increase erythroid production; however, the main limitation of the pathway is the restriction of CFU-Es (BFU-Es are insensitive to EPO) to undergo only 3-5 cell divisions in their terminal state. Therefore, with such low turnover, the steady-state erythropoiesis is not capable of correcting anaemia in extreme conditions (11) and stress erythropoiesis serves as the rescue mechanism in this circumstance. As explained earlier, hypoxia is the crucial regulator of EPO in erythropoiesis and hypoxia leads to activation of physiological responses required for increased oxygen delivery to the hypoxic tissues. The mechanism is based on increased erythropoiesis via significantly up-regulated EPO production, which in turn amplifies the JAK2/STAT5 pathway (88, 89).

Both the signals and the progenitor cells involved in stress erythropoiesis are distinct from the steady-state erythropoiesis (Figure 1.3). There are a number of auxiliary signalling proteins that are uniquely involved with the stress erythropoiesis, i.e., Bone morphogenetic protein (BMP4)/SMAD5 signalling, Hedgehog, SCF/c-Kit, and Glucocorticoid receptor (GR) (86, 90, 91). Furthermore, the progenitor cells involved in stress and steady-state erythropoiesis are different. While the steady-state HSCs develop from the erythroid committed progenitors, i.e., from the megakaryocyte/erythroid progenitors (MEP), short-term reconstituting HSCs (CD34⁺Kit⁺Sca1⁺Lin⁻) are the progenitor cells characteristic of stress erythropoiesis (92). These stress progenitor cells migrate to the spleen and once located there; they undergo an expansion step whilst still retaining their stem cell characteristics (see Figure 1.3). The transition of these cells into the committed erythroid progenitors requires only the high concentration of EPO, unlike the bone marrow BFU-Es that require the burst-promoting

activity signals (86, 93). Subsequently, the committed cells mature into the stress BFU-Es (CD34⁻Kit⁺Sca1⁺CD71⁺Ter119^{L0}) and eventually undergo terminal erythroid maturation (93, 94). Furthermore, the stress BFU-Es are different from the steady-state bone marrow BFU-Es, when examined by a colony assay, as they form larger colonies at a faster rate (5 vs. 7 days) (86). Microenvironment plays a vital role in the progenitor cells of stress erythropoiesis. Growth differentiation factor 15 (GDF15), a member of the transforming growth factor- β (TGF- β) superfamily, is reported to be required for the *in vitro* model of stress erythropoiesis (93). GDF15 was also recently observed to act *in vivo* on the splenic niche of the stress BFU-Es involved with the maintenance of the hypoxia-dependent transcription of BMP4 (see section 1.1.2.1.1). The knockdown Gdf15^{-/-} mice also failed to respond to anaemic stress due to the defect of their splenic niche (95). Additionally, GDF15 was elevated in several conditions of ineffective erythropoiesis (IE) such as thalassaemia and congenital dyserythropoietic anaemia type I (CDAI) (96). The suppressive role of GDF15 on hepcidin, a key regulator of iron metabolism, is resulted in increased iron level and haemochromatosis in these clinical conditions (97).

Since stress erythropoiesis has entirely distinct components to the steady-state erythropoiesis, including unique erythroid progenitors and their regulators, the following sections will introduce the essential growth factors required for the process.

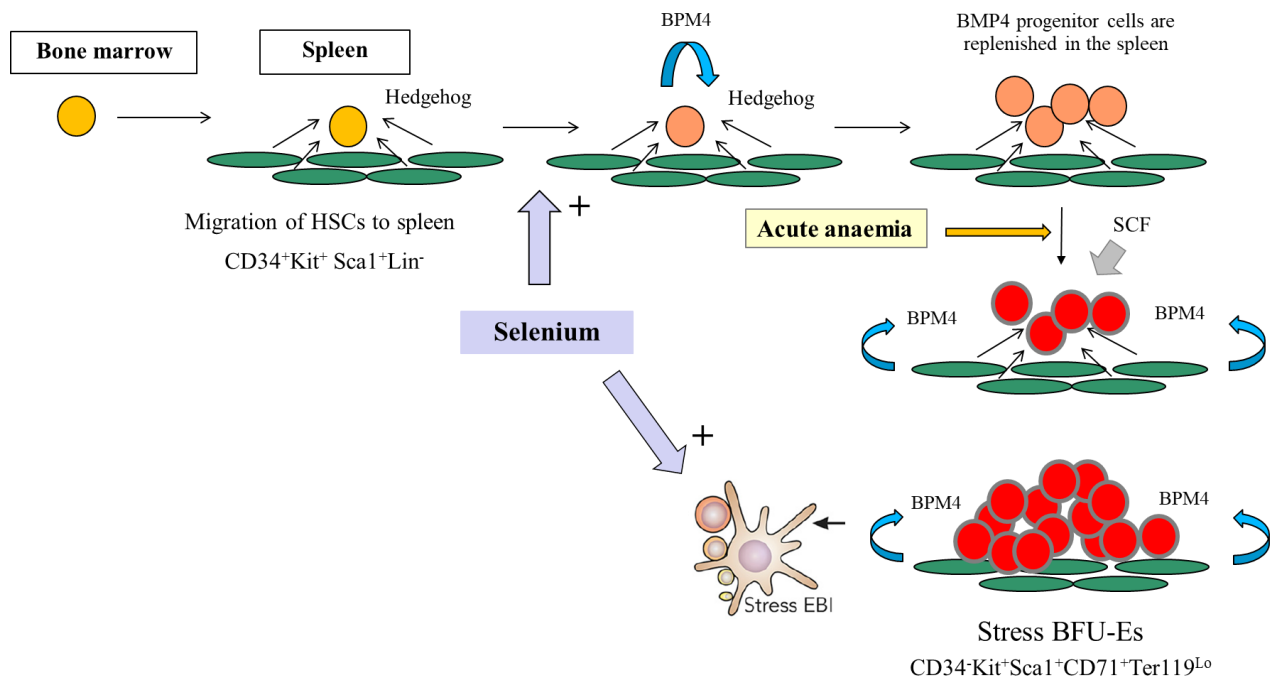


Figure 1.3. Model of stress erythropoiesis and its regulators.

Short-term reconstituting HSCs ($CD34^+Kit^+Sca1^+Lin^-$) migrate from the bone marrow to spleen. The stress progenitor cells are replenished in the spleen promoted by Hedgehog signalling pathway, BMP4, and selenium. Once encountered acute anaemia/hypoxia, the stress progenitor cells develop into stress burst-forming unit - erythroid (BFU-Es) and rapidly undergo terminal erythropoiesis via stress erythroblastic island. EBI-erythroblastic islands (Modified from John M. Perry et al. *Blood* 2009;113:911-918 and Dulmovits and Blanc. *Blood* 2018;131(23):2512-3. (98, 99))

1.1.2.1 Regulators of stress erythropoiesis

1.1.2.1.1 Bone morphogenetic protein 4 (BMP4), SMAD5 and Hedgehog signalling

Once acute anaemia occurs, the spleen progenitor cells will respond to hypoxia through EPO, SCF, and BMP4 pathways. Subsequently, they will expand, differentiate rapidly and mobilise to compensate anaemia. BMP4 and the functional downstream signals carried through the intracellular mediators known as SMAD5 are the key regulators specific to the stress erythropoiesis, as demonstrated by means of *in vitro* experiments (93, 94). BMP4 has multiple roles during stress erythropoiesis, e.g., the expansion of the splenic progenitor cells, the proliferation of the stress BFU-Es, and together with the Hedgehog pathway, the replacement of the short-term reconstituting HSCs which migrate into the spleen (86, 91, 92, 98).

Hedgehog signalling facilitates the recovery and restoration of the splenic progenitor cell population by altering normal marrow progenitor cells to the short-term reconstituting HSCs (CD34⁺Kit⁺Sca1⁺Lin⁻), which then migrate to the spleen (86). However, more recent evidence has suggested that stress erythropoiesis is primarily localised in the bone marrow and is only observed in the spleen when associated with splenomegaly when the process is both prominent and chronic (100).

1.1.2.1.2 Glucocorticoid receptor (GR)

Corticosteroids are synthetic drugs that closely resemble a naturally secreted steroid hormone. Glucocorticoid, for example, dexamethasone (DXM), is one of a class of corticosteroids that signal through the glucocorticoid receptor (GR). GR acts by inducing self-renewal and blocking maturation of erythroid precursors. The unbound receptor is located in the cell cytosol, but once activated by binding of a glucocorticoid, it will translocate to the cell nucleus where it can influence transcription. *In vivo* study of GR defective (*GR^{dim/dim}*) mice model showed the absence of stress erythropoiesis and rapid cell maturation when compared to the wild-type (101, 102). In the *in vitro* erythropoiesis, activated GR directly promotes and maintains proliferation of erythroid progenitors by blocking terminal maturation (101, 103, 104). The underlying mechanisms involve GR inhibiting activities of GATA-1, a crucial transcription factor for erythroid differentiation (see above), and increasing levels of other transcription factors, including c-Myb, c-Kit and RBTN2 (105). These generate positive transcriptional transactivator effects on BFU-E cells by preventing them from exhaustion and, therefore, resulting in increased cell division and cell numbers. DXM entirely inhibited cells differentiation and induced progenitor cells to undergo 15-20 cell divisions in the presence of SCF, EPO, and insulin (104, 106). The self-renewal of BFU-Es takes place, at least in part, through a downstream RNA binding protein ZFP36L2, a transcriptional target of the GR (107). Activated ZFP36L2 in turn binds and down-regulates highly expressed mRNAs during erythroid differentiation. Additionally, it has been observed that DXM added to *in vitro* CD34⁺ cultures together with the erythroid growth factors induced the maturation of stress-specific macrophages, as well as the generation of erythroblastic island-like structures to support erythropoiesis (108, 109). A recent study explored this finding further and identified DXM as a primary regulator driving differentiation of cultured monocytes into the macrophages, which both phenotypic (CD16⁺CXCR4⁺) and functional characteristics resembling the *in vivo* bone marrow resident macrophages (110).

1.1.2.1.3 Selenoproteins

Micronutrients, especially selenium, have recently been highlighted as one of the critical regulators of stress erythropoiesis. Selenoproteins or selenium-containing proteins are essential antioxidant proteins in humans. Thioredoxin reductases and glutathione peroxidases are examples of the functioning forms of selenoprotein family (111). The lack of selenoproteins, particularly selenoprotein W, compromises stress erythropoiesis on multiple levels. Knock-out of selenoprotein W blocked the proliferation of stress erythroid progenitors both *in vivo* in the mice model and *in vitro* in the human stress erythropoiesis cell cultures (112). Selenium-deficient mice manifested anaemia, despite an increase of BFU-Es (113). When oxidative stress was introduced, these mice failed to generate new erythrocytes and died from severe haemolysis. Liao *et al.* (2018) demonstrated the impairment of the expansion and differentiation of the stress erythroid progenitors in the early stage of stress erythropoiesis. The delayed terminal maturation was also observed in selenium-deficient mice during the transition from proerythroblasts to basophilic erythroblasts (99, 114, 115). Moreover, mice with a selenium deficit had fewer red pulp macrophages (CD11b^{lo}/Vcam-1⁺F4/80⁺), as well as a reduced number of splenic erythroblastic islands. (114, 116). These findings highlighted the importance of selenium in the microenvironment for stress erythropoiesis.

Taken together, erythropoiesis is an intricate process of erythrocyte generation, either physiologically in steady-state, or pathologically in stress erythropoiesis. Considerable studies of both *in vitro* and *in vivo* systems have been developed to shed light on this extremely complicated process. The major advantage of the *in vivo* systems over the *in vitro* ones is that they allow the researchers to study the effects of the environmental cues on the erythropoiesis from both bone marrow and splenic niches.

1.1.3 Animal models of erythropoiesis

For the better understanding of *in vivo* erythropoiesis and pathology of related diseases, for example, thalassaemia, rodent models have been developed. Transgenic mouse models have helped elucidate the mechanisms behind the human globin switching, signified the importance of the LCR region (117) and identified the CACCC DNA sequence motif as the binding sites for KLF1 (118). The humanised mouse model, where large segments of the

mouse genome were removed and replaced with equivalent human syntenic regions, was also developed (119). This strategy was later used to identify the upstream regulatory element influencing the α -globin gene expression (120). Furthermore, deletional mouse models of β -thalassaemia were created with the prototype of heterozygous Hbb^{th-3} representing the phenotypes of severe β -thalassaemic patients (121), with reduced expression of hepcidin, and the rescue of Hbb^{th-3} mouse with the high levels of human HbA (122). This evidence suggested functional conservation of the β -globins between the two species, and with this knowledge, new technologies such as gene therapy vectors could be tested in mice models (123). The lentiviral vector with a functional β -globin gene that was successfully delivered to $Hbb^{th-3/+}$ mice provided an improvement of thalassaemic symptoms (124, 125). However, although murine models provided important insight into the *in vivo* pathophysiology of erythropoiesis, there are several species-based differences between human and murine erythropoiesis. These include one-time and two-time globin switching in mouse and human, respectively. The expression of human γ -globin in transgenic mice occurs during the embryonic stage, whilst in humans, the expression commences in the fetal stage (123). Also, a study by An *et al.* (2014) focusing on terminal erythroid differentiation, explored transcriptomic profiles between the two species. The differences were reported in glucose and vitamin C metabolisms, cell membrane composition and mechanisms of stress erythropoiesis. The most prominent difference was a global decrease in gene expression in murine terminal erythropoiesis, not observed in its human counterpart. Hence, care needs to be taken when extrapolating erythropoiesis findings from mice to humans, due to significant species differences (126).

1.1.4 *In vitro* erythropoiesis

In recent decades, there has been a drive to generate efficient *in vitro* cell culture systems that mimic essential features of the *in vivo* erythroid cell proliferation and maturation for purposes of red cell production for disease studies, diagnostic and therapeutic use. Several research groups have successfully produced erythroid cells in small quantities (on a laboratory scale) using a variety of progenitor cell sources, different cell culture conditions and media components. These developments were reviewed herein (127-134).

1.1.4.1 Sources of stem cells for *in vitro* erythropoiesis studies

HSCs can be obtained and successfully cultured from a variety of cellular sources, bone marrow, cord blood, adult peripheral blood, embryonic pluripotent stem cells and induced pluripotent stem cells (iPSCs) (13, 128, 135-138). Although bone marrow sources provide the preferred type of precursor cells due to their high proliferation capacity, their harvesting is more disruptive to patients and can be clinically challenging to justify. Of the different cell sources that can be used for *in vitro* culture, adult peripheral blood and cord blood present the most convenient starting materials, resulting in erythroid cells with the highest enucleation efficiency (139). In particular, adult peripheral blood is one of the most reliable and accessible sources of stem cells, with a special advantage that they can be easily obtained from by-products of blood donations or directly from patients. One of the main drawbacks of this source of progenitor cells is their limited expansion capacity, unlike the immortalised cellular sources such as iPSCs (139). One consideration when using peripheral blood of the patients as a source of progenitor cells is the severity of anaemia in these patients that has to be taken into consideration when requesting blood samples. Several studies of haemoglobinopathy diseases have shown that 20 ml to 30 ml of peripheral blood is an adequate volume for initiating the erythroid cultures (140-143). Alternatively, cord blood progenitor cells are reported to have higher expansion capacity compared to the peripheral blood progenitors (144); however, the cells generated from cord blood predominantly express embryonic and fetal globins, rather than an adult, phenotype (19). Furthermore, small number of Bcam, semaphorin-7A, and some gaseous exchange proteins that include carbonic anhydrase 1 and 2 and aquaporin-1 were reported at a higher level in the adult cells than a cord (145).

Although iPSC and embryonic cell lines have great potential for providing a theoretically inexhaustible source of progenitors, there are ethical issues associated with using embryonic sources (146), the cells have a fetal or embryonic phenotype, and currently these sources have dramatically impaired enucleation when compared to the progenitor cells derived from adult peripheral blood (137).

1.1.4.2 Culture systems

A variety of *in vitro* systems for erythroid cell production has been developed over the last two decades. The success of the 2D liquid culture systems at efficiently producing reticulocytes greatly improved upon the development of recombinant essential growth factors, e.g., EPO (147), SCF (148), and IL-3 (149). The published *in vitro* erythroid culture systems all generally utilise the same combinations of growth factors and media, but with subtle differences in their use of cellular starting material, the number of culture media stages, growth factor concentrations, and inclusion of glucocorticoids (hydrocortisone or dexamethasone).

Two-step liquid culture (with EPO-free media followed by EPO-supplemented media) was first used for peripheral blood mononuclear cells of β -thalassaemia patients; it resulted in the yield of large erythroid colonies and haemoglobinisation by day 14 (150). A different study used a single-step liquid culture with 10^{-6} M hydrocortisone in the presence of EPO, GM-CSF, and IL-3 to grow CD34⁺ cells obtained from various sources: bone marrow, umbilical cord blood, and peripheral blood of healthy controls, sickle cell disease and thalassaemia patients. After a 21-day culture period, enucleation efficiency was reported to be 10% to 40% (151). In 1999, a liquid culture with added dexamethasone was described by von Lindern and colleagues to increase proliferation of erythroblasts (104). Following this, Migliaccio *et al.* (2002) developed Human Massive Erythroid Amplification (HEMA) media and reported to achieve 800-fold erythroid expansion. HEMA culture is a two-stage liquid culture system where mononuclear cells were cultured with cytokines (SCF, IL-3, EPO) and addition of DXM (10^{-6} M) and estradiol (10^{-6} M) for the first 13 days, followed by secondary medium containing only EPO and insulin to promote the cell maturation (131). In 2002, Neildez-Nguyen *et al.* reported a successful *ex vivo* culture of erythroid cells from human cord blood used for an injection of the human CFU-Es (from day 10 of the culture) into a NOD/SCID murine model, which resulted in good survival, proliferation and maturation of human erythroid cells. This provides proof of principle that *ex vivo* erythropoiesis may be a possible source of erythroid cells for clinical transfusion (152). After this, multiple laboratories reported the successful generation of large numbers of reticulocytes (128, 131, 153) – including Dr. Toyne laboratory (University of Bristol, UK). Reticulocytes obtained from a culture of peripheral blood mononuclear cells with the addition of DXM were used to study erythroid membrane multiprotein complex assembly (14)

and the hallmark changes that occur in patients with hereditary spherocytosis and congenital dyserythropoietic anaemia II (154-156).

Most recently, Giarratana *et al.* (2011) described a culture method that used a total of 10^6 CD34⁺ cells as a stem cell source for an erythroid culture maintained in static flasks, producing 3.7×10^{10} of packed reticulocytes, a mini dose sufficient for the first successful autologous transfusion of *ex vivo* generated reticulocytes into a human (132). The authors used an updated three-stage protocol using IMDM medium with transferrin, insulin, heparin, and plasma throughout their culture and included hydrocortisone. In the primary media (day0 – day7), 10^{-6} M hydrocortisone, SCF, IL-3 and EPO was used to culture CD34⁺ cells isolated from peripheral blood, followed by the secondary medium supplemented with SCF and EPO (day7 – day11) and the tertiary medium (day11 – day18) containing only EPO. The erythroid cells achieved 62,000-fold expansion rate with >80% of enucleation (132).

In 2012, Griffiths *et al.* reported a modified three-stage culture media following the same principles of changing the supplemental cytokines in each stage to mimic erythropoiesis and allow cells to proliferate and mature. Note that, hydrocortisone was not used in this culture protocol. The cell expansion achieved was $\geq 10,000$ -fold with enucleation rates of 55% to 95% (128), resulting in approximately 5 ml of packed reticulocytes. Griffiths *et al.* culture method has since been perfected further, producing approximately 10 ml of packed reticulocytes (139). This culture system is being used in the Blood and Transplant Research Unit based in Bristol, UK, to conduct a clinical trial in volunteers (<http://www.bristol.ac.uk/btru/>) and will be the basis of the erythroid culture methodology used in this thesis.

1.1.4.3 *In vitro* erythropoiesis for the study of thalassaemia

In vitro erythroid culture has been widely adopted in thalassaemia disease research to serve two notable purposes – to better understand the pathology of the disease and to explore therapeutic-related aims. There are two major sources of CD34⁺ progenitor cells that have been successfully used for thalassaemic cultures; bone marrow or peripheral blood. Circulating peripheral CD34⁺ cells can be obtained directly from the buffy coat. GM-CSF-mobilised CD34⁺ cells originating from the bone marrow of thalassaemia patients have

typically given better yields than those obtained by the conventional collection from peripheral blood (157, 158).

Since IE is one of the hallmark features of thalassaemia pathology, a study of erythropoiesis of thalassaemic progenitor cells can bestow a better understanding of what occurs *in vivo* in the bone marrow of the patients. Eighteen years ago, Mathias and colleagues reported the application of *in vitro* erythropoiesis to define the process of IE by culturing CD34⁺ cells obtained directly from bone marrow (158). Through their single-step liquid culture protocol (151), they observed the decline of polychromatophilic normoblasts in β -thalassaemia bone marrow cultures, thus concluding that the IE characteristic of thalassaemia can be simulated *in vitro* and that it occurs at the polychromatophilic normoblast stage (159). Lithanatudom *et al.* (2011) used 20 ml of peripheral blood as a source of thalassaemic progenitor cells and demonstrated increased autophagy in HbE/ β -thalassaemia erythroblasts compared to normal erythroblasts (143). Arlet and colleagues (2014) cultured CD34⁺ cells of the β -thalassaemia major patients by using two-phase liquid culture in parallel with healthy donor samples. By confocal microscopy, a chaperone protein heat shock protein 70 kDa (Hsp70) was localised to the cytoplasm, and the low expression of GATA-1 was observed in the nucleus of the thalassaemic erythroid precursors (160). In normal erythropoiesis, Hsp70 protects GATA-1 from destruction by caspase-3 cleavage in the nucleus of erythroblasts (161). In the β -thalassaemia-derived erythroblasts, Hsp70 was sequestered to the cytoplasm due to its binding to the free α -globin chains, which resulted in the cell maturation arrest and apoptosis. In addition to these studies, *in vitro* erythropoiesis of thalassaemic material for therapeutic applications have mainly concentrated on exploring responses of fetal Hb induction manoeuvres, both by hydroxyurea (140-142) and gene therapy (162-164).

1.1.4.4 Other strategies to study *in vitro* erythropoiesis

1.1.4.4.1 Human iPSCs and their benefits for therapeutic research in thalassaemia

Human iPSCs were successfully generated by reprogramming of the somatic cells, human dermal fibroblasts, into the pluripotent cells by transduction of four transcription factors: Oct3/4, Sox2, Klf4, and c-Myc (165). The iPSCs share their phenotypic and pluripotent characteristics with human embryonic stem cells which are able to differentiate into cell types of the three germ layers (165). Therefore, the iPSCs retain the characteristics of embryonic

and fetal erythroid differentiation (138, 166). Initially, several studies explored the potential therapeutic benefits of this cell type for haemoglobinopathy patients. Despite iPSCs' high expression level of the γ -globin chain, it was observed that the globin switching had partially occurred after their transplantation into mice. Moreover, the rate of enucleation was unsatisfactory (167, 168). Thus, it is unlikely that this source of stem cell will replace the conventional sources like bone marrow or cord transplants at present. More research is needed to reduce the risk of tumorigenesis, especially the potential insertional mutagenesis from the use of viral vectors (169). However, these cutting-edge experiments contributed to the robust advancements in medicine. Patient-specific iPSCs in culture have allowed the evaluation of the responses of a particular patient *in vitro* before the actual therapeutic intervention (164, 170). Furthermore, a number of studies have successfully applied gene-editing technology on the iPSCs. Ma *et al.* (2013) generated patient-specific iPSCs and corrected the thalassaemic mutation using TALEN gene editing. These gene-corrected iPSCs showed normal maturation and expressed normal β -globin (171). Recently, Ou *et al.* (2016) generated patient-specific iPSCs from β -thalassaemia patients, cultured them by *in vitro* co-culture with stromal cell lines and used homologous recombination-based CRISPR/Cas9 gene editing before introducing the modified iPSCs to mice models. These genetically edited cells were capable of performing normal HSC function *in vivo* (172). Wattanapanitch and colleagues (2018) had also successfully applied CRISPR/Cas9 gene-editing system to correct HbE mutation by homology-directed repair of HbE/ β -thalassaemia iPSCs (173).

Another application of iPSCs is the creation of immortalised iPSCs lines. The establishment of these cell lines had contributed to a better understanding of the biology of various diseases and facilitated innovative therapeutic strategies. Numerous cell lines have been generated from somatic and peripheral blood haematopoietic cells of patients presenting with various diseases, e.g., neurological diseases, schizophrenia, hypertrophic cardiomyopathy (174-178) and thalassaemia (179-182). A study by Phanthong *et al.* (2017) created the iPSCs line from mesenchymal stromal cells of HbE/ β -thalassaemia patient, then transduced the cells with a lentivirus carrying a modified U7 small nuclear RNA to correct a DNA splicing defect of β -thalassaemia in order to restore the correct splicing of β -globin mRNA. Transplantation of the genetically corrected HSCs into the patient would potentially inhibit disease symptoms (182).

In addition, the iPSCs line carrying the heterozygous form of this splicing defect may also be employed as a model for the disease and for drug screening purposes.

It is worth noting that during the time of this project, immortalised human erythroid progenitor cell lines derived from human iPSC line (HiDEP) generated from amniotic fibroblast-like cells and immortalised using viral transduction of TAL-1 gene at the pro-erythroblast stage have been developed (183). Most recently, the first immortalised adult erythroid cell line Bristol Erythroid Line Adult (BEL-A) derived from human bone marrow was shown to have a higher rate of enucleation than iPSCs (184) and has been successfully gene-edited by CRISPR/Cas9 (185).

1.1.4.4.2 An *in vitro* model of β -thalassaemia major

An artificial model of β -thalassaemia major was created by knocking-down *HBB* gene (*HBB-KD*) in normal CD34⁺ cells obtained from adult peripheral blood. The cryopreserved CD34⁺ cells were cultured in a two-phase, serum-free system and were knocked down using lentiviral vector delivery of short hairpin RNAs. With this method, more than 90% of the β -globin mRNA was silenced when compared to the control. Subsequently, the thalassaemic phenotype of the cells and their Hb profile was assessed. Lee *et al.* (2013) reported the increase of apoptosis of the *HBB-KD* cells at the polychromatophilic normoblast stage, as evaluated by flow cytometry measuring the caspase-3 and annexin V expression. This finding was consistent with their previous assessment of the *in vitro* erythroid culture of CD34⁺ samples obtained from β -thalassaemia major patients (159). In addition, they observed a significantly increased marker of IE, GDF15, in the culture supernatants (see section 1.1.2 for stress erythropoiesis) (186). Thus, this synthetic model was a good representation of human β -thalassaemia and would reduce the confounding factors between erythropoiesis in murine models and humans in future research.

1.2 Globin genes and their regulators

Haemoglobin is the major protein present in mature erythrocytes at approximately 270 million molecules per individual erythrocyte (187). The expression of Hb is varied and chronologically dependent on the human developmental stages (Figure 1.4).

1.2.1 Normal haemoglobin synthesis

The majority (>95%) of adult haemoglobin is HbA, comprised of two globin subunits with two α -globin and two β -globin chains ($\alpha_2\beta_2$). The α -globin gene (*HBA*), encoding the α -globin chain, is located in a gene cluster on chromosome 16. This gene cluster contains, from the 5' end, ζ gene and the pair of *HBA* genes (*HBA1* and *HBA2*). The β -globin gene (*HBB*) is located on the short arm of chromosome 11 among five functional globin genes – ϵ - γ^A - γ^G - δ - β from the 5' to the 3' end (Figure 1.4). These two gene clusters are activated sequentially during development (188, 189).

In humans, during the early embryonic stage when the primary site of erythropoiesis is the yolk sac, Hb Gower 1 ($\zeta_2\epsilon_2$) is the most abundant Hb. After approximately 4 weeks of gestation, Hb Gower 2 ($\alpha_2\epsilon_2$), and Hb Portland ($\zeta_2\gamma_2$) are identified (188). Fetal Hb, HbF ($\alpha_2\gamma_2$), becomes the major Hb in fetal life when the primary site of erythropoiesis transfers to the liver. HbF persists throughout the gestational period, then starts to decline after birth. If the level of HbF is still high in adulthood, this may indicate the hereditary persistence of fetal haemoglobin (HPFH). Besides HbA, HbA2 ($\alpha_2\delta_2$) is also detected in <3.5% of all the haemoglobins in an adult. The higher level of HbA2 denotes deprivation of HbA synthesis, for example, in β -thalassaemia disease (190).

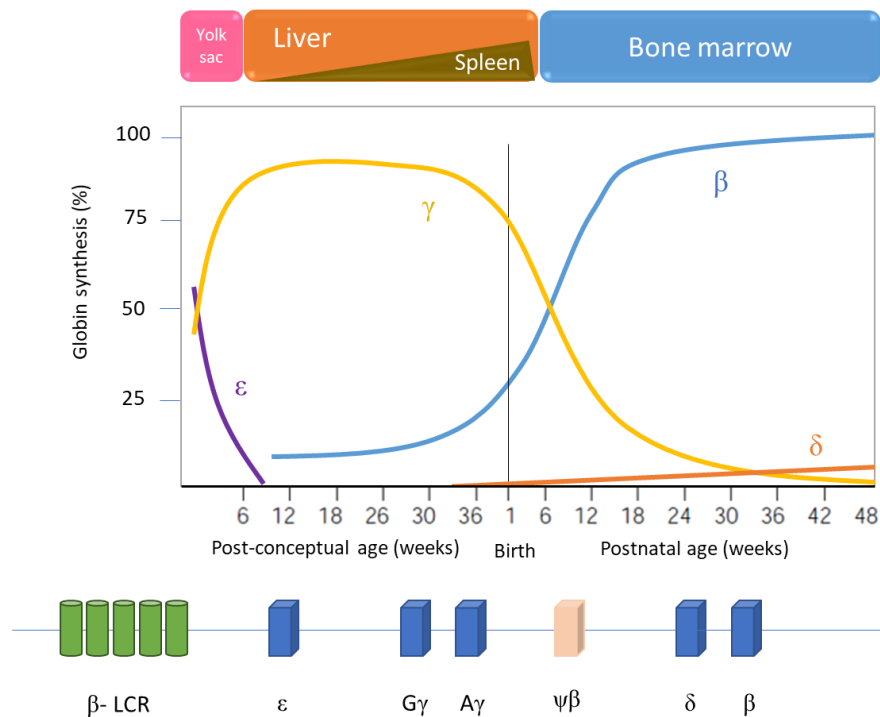


Figure 1.4. β -globin gene cluster and the sequence of globin synthesis during human development.

During the gestational period, embryonic globins ($\zeta\epsilon\epsilon_2$, $\alpha_2\epsilon_2$) are first synthesised in the blood islands of the yolk sac, then the first globin switching occurs. During fetal development, the majority of Hb production is fetal Hb ($\alpha_2\gamma_2$) from the liver and the spleen. Around the time of birth, the second switching from fetal Hb to adult Hb ($\alpha_2\beta_2$) takes place at the β -globin gene locus, and bone marrow becomes the primary site of erythropoiesis. LCR – locus control region. Line colour code: violet – ϵ , yellow – γ , blue – β , and orange – δ globin. (Modified from Weatherall DJ. *Phenotype-genotype relationships in monogenic disease: Lessons from the thalassaemias. Nat Rev Genet. 2001 Apr;2(4):245-55. (191)*)

1.2.2 Haemoglobin switching

Humans possess two distinct erythroid cell lineages – the primitive and the definitive lineage. The primitive lineage originates at the embryonic stage in blood islands of the yolk sac and is later replaced by the definitive erythroid lineage, generated in the fetal liver during the fetal stage and in the bone marrow of the adult. The globin switching occurs within the clonal population of HSCs, rather than through the direct globin replacement at the cell level (192). This project will be focused only on HbF switching, from γ -globin to β -globin chain activation, because of its impact on the severity of β -thalassaemia.

As stated earlier (see section 1.1.1.1, KLF1), KLF1 plays a crucial role in β -globin switching (39). The mechanism involves the configuration of the 3D chromatin structure. In more detail, KLF1 facilitates the long-range DNA interactions, as well as the 3D chromatin looping, which brings the proximal promoter of the β -globin gene to the LCR (47, 48). The KLF1 binding regions are the upstream DNaseI hypersensitivity sites (HS): HS2 and HS3 within the LCR, as well as the adult β -globin proximal promoter. KLF1 binding to the adult β -globin proximal promoter leads to β -globin expression in adult erythroid cells (46). The LCR upregulates one globin gene at a time; therefore, the globin genes require competition for activation by the LCR. This mechanism explains how are the globin genes sequentially expressed in embryonic, fetal, and adult stages of development (193, 194). Since disruption of KLF1 binding would potentially result in an increase of HbF (36), this may be clinically beneficial to β -thalassaemia (195). A knockdown of KLF1 was once considered as a potential therapeutic target. However, the narrow therapeutic window (196) made it very difficult to target KLF1 with small molecule inhibitors (197).

The molecular background of the HbF switching at the β -globin locus requires BCL11A working in synchronisation with GATA-1, FOG-1, and the NuRD complex (see section 1.1.1.1). These transcription regulators bind to the globin gene loci, contributing to the activation of β -globin production and repression of γ -globin gene expression (192, 198). Furthermore, the process of globin switching can also be demonstrated in the *ex vivo* erythroid maturation by modifying the levels of expression of transcription factors KLF1 and BCL11A. Trakarnsanga and colleagues (2014) reported that the transduction of *KLF1* and *BCL11A-XL* successfully drove the globin switching from embryonic (ϵ) to adult β -globin chain in HiDEP-1 cells, a human iPSC line derived from amniotic fibroblast-like cells and immortalised at the pro-erythroblast stage. They also demonstrated that transfection of erythroid cells derived from cord blood with both *KLF1* and *BCL11A-XL* resulted in the increased adult β -globin expression (137). Whereas, the knock-down study of *BCL11A* observed no globin switching and an increase of γ -globin expression in adult erythroblasts (145, 199). All this evidence has highlighted the critical regulatory roles of the two transcription factors, KLF1 and BCL11A, in the process of globin switching.

1.3 Thalassaemia

1.3.1 Definition

The term “thalassaemia” is stemmed from two words, “thalassa” or sea and “haema” or blood, in the Greek language. It refers to inherited human conditions where globin synthesis is partially or entirely suppressed, resulting in imbalanced globin production (200).

Two major types of thalassaemia are α - and β -thalassaemia, depending on which globin is suppressed. For example, β -thalassaemia is characterised by a quantitative reduction of β -globin chain production without any structural changes (201) caused by genetic alterations of the β -globin gene (*HBB*). The mutations of *HBB* in β -thalassaemia show a whole spectrum from ‘mild’ missense mutations (β^+ -thalassaemia) to completely absent alleles (β^0 -thalassaemia) (202). Similarly, mutations occurring in the α -globin gene cluster result in α -thalassaemia.

1.3.2 Epidemiology

Haemoglobinopathies affect around 7% of the world’s population, with an estimated >50,000 births annually being affected by the major forms of thalassaemia (203, 204). Approximately 80 million people are carriers of β -thalassaemia globally. In high incidence regions of Sub-Saharan Africa, Mediterranean basin, the Middle East, Indian subcontinent, Southeast Asia and the Pacific Islands, the frequencies of the carrier state can range from 1% to 20% (203). In 1949, Haldane first proposed the potential advantages presented by heterozygotes β -thalassaemia in malaria resistance (205). Several lines of evidence support the association between the distribution of mutations causing thalassaemia disease and malaria protection, which is endemic in South East Asia region (206, 207). Other reasons explaining the high frequencies of Hb inherited disorders were summarised by Williams and Weatherall (2012); these include the high rate of consanguineous marriages and the longer life expectancy of the affected babies (204).

1.3.3 Pathophysiology

During normal erythropoiesis, two α -globin chains bind to two β -globin chains forming the adult Hb (HbA), whilst in β -thalassaemia, the reduced level of β -globin chain results in a relative excess of α -globin chains. These unmatched α -globin chains accumulate and precipitate in the erythroid membrane as the α -globin inclusion bodies (α_4). The inclusion bodies in turn associate with haemichromes, inducing oxidative species, clustering of band 3 and subsequently generating neoantigen sites for IgG and complement binding (208). IgG and complement bound neoantigens to serve as a senescent signal for the reticuloendothelial (RE) system, i.e. macrophages, to eliminate such affected red blood cells (209). The premature destruction of erythrocytes in the bone marrow occurs as a part of IE.

IE was first described in thalassaemia in 1950 in a study examining ferrokinetic parameters (210). Since then, this pathophysiology has been extensively studied and elaborated on. The process is characterised by apoptosis of the erythroid precursors due to the imbalance of globin chains, leading to intramedullary erythroid destruction, as well as abnormal differentiation and maturation of erythroid progenitors (209, 211, 212). IE is a hallmark of thalassaemia, and it leads to a number of sequelae, including haemolysis, progressive marrow expansion and extramedullary erythropoiesis correlated with the degree of anaemia (213). Nowadays, the understanding of IE in thalassaemia has been dramatically improved, and the pathophysiology of IE was recently extensively reviewed by Oikonomidou and Rivella (2018) (213). A number of different mechanisms contribute to the pathology of IE, e.g., increased apoptosis of the erythroid precursors during the maturation process (159, 211, 214), decreased differentiation of erythroid progenitors (215, 216), oxidative stress in erythropoiesis (217-219), and iron metabolism (220, 221).

Furthermore, another significant pathomechanism of thalassaemia is the reduction of nitric oxide (NO) that leads to the thrombotic events in thalassaemia. In physiological conditions, circulating NO diffuses in and out of erythrocytes; however, in thalassaemic RBCs, NO is not being released from the cells because of the oxidative injury to the binding sites of the intracellular NO and the clustering of band 3. When NO is reduced in circulation, the vasodilator activity is also reduced and eventually will lead to a hypercoagulable state in thalassaemia (222).

1.3.4 Classifications of thalassaemia

Thalassaemia can be classified in two ways – depending on either its genetic or clinical outlook. Genetic classification simply depends on which globin gene is affected. This category can be expanded further, taking into account the impact of the mutations on the globin products: the first group reflects an absent or suppressed globin synthesis, i.e., β -thalassaemia or α -thalassaemia for *HBB* and *HBA* mutations, respectively. The second group includes the alterations of structural Hb, i.e. Hb variants such as HbE, HbC (see Table 1.1) (223).

Conversely, classification into the clinically-associated categories of transfusion dependent thalassaemia (TDT) and non-transfusion dependent thalassaemia (NTDT) focuses on the clinical management of the disease, rather than the actual genotype. The key factor that differentiates patients between TDT and NTDT groups is the necessity of blood transfusion for survival. NTDT patients do not require lifelong regular transfusions for survival, whilst TDT patients do. Note that, NTDT comprises three clinically distinct diagnoses: β -thalassaemia intermedia, HbE/ β -thalassaemia disease, and HbH disease (224).

Table 1.1. A summary of genetic classification and the phenotype diversities of thalassaemia.

Type	Affected gene(s)	Genotype	Phenotype	Transfusion requirement	Reference
β-thalassaemia trait	One allele	<i>HBB</i> β^+/β β^0/β	Asymptomatic	Do not require transfusion	(Chonat and Quinn, 2017)
β-thalassaemia intermedia	Two alleles	<i>HBB</i> β^+/β^+ β^+/β^0	Mild to moderate	None to intermittent transfusion	(Chonat and Quinn, 2017)
β-thalassaemia major	Two alleles (complete absence of β -chain production)	<i>HBB</i> β^0/β^0	Severe anaemia	Transfusion dependence	(Chonat and Quinn, 2017)
α silent carrier	One allele	<i>HBA</i> $-\alpha/\alpha\alpha$	Asymptomatic	Do not require transfusion	(Marengo-Rowe, 2007)
α-thalassaemia trait	Two alleles	<i>HBA</i> $\alpha\alpha/--$ $-\alpha/-\alpha$	Asymptomatic	Do not require transfusion	(Marengo-Rowe, 2007)
HbH disease	Three alleles	<i>HBA</i> $-\alpha/--$	Mild to severe	None to intermittent transfusion	(Marengo-Rowe, 2007)
Hydrops fetalis	Four alleles	<i>HBA</i> $--/--$	Fatal	Incompatible with life	(Marengo-Rowe, 2007)

1.3.4.1 Beta-thalassaemia

The term β -thalassaemia refers to a quantitative reduction of structurally normal β -globin chains usually caused by mutations affecting the *HBB* gene (201). These mutations are heterogeneous (see Table 1.2), leading to variable clinical disease severity from mild to severe, depending either on the degree of the β -globin chain reduction (β^+) or on its complete absence (β^0). Moreover, the co-inheritance between β -thalassaemia and other genetic alterations that involve globin expression could make the disease even more divergent (see section 1.4). However, the severity of β -thalassaemia symptoms correlates well with the quantity of the free α -globin chains (202). The patients with homozygous form of β -thalassaemia (β^0/β^0) usually present to the medical attention in the early years of life and require regular transfusion due to the severe clinical features, e.g. severe microcytic anaemia,

hepatosplenomegaly and failure to thrive. Haematological parameters in the patients are typically characterised by Hb levels $<7 \text{ gdl}^{-1}$, MCV 50-70 fl and MCH 12-20 pg (225). Untreated patients could develop skeleton changes such as deformities of long bones and expansion of flat bones (thalassaemic facies), extramedullary haematopoiesis, and ultimately may not survive the first few years of life (225, 226). However, adequate blood transfusion in conjunction with appropriate iron chelation, has proved to suppress erythropoiesis and ameliorate these symptoms (227).

Patients with β -thalassaemia intermedia usually present at a later age with milder clinical manifestations, and do not require a regular blood transfusion to survive. Their Hb levels range from 7 to 9 gdl^{-1} with a broad clinical spectrum. Patients with severe manifestations could present with delayed growth and development in later life when compared to the β -thalassaemia major. On the other end of the spectrum, patients with mild manifestations can be asymptomatic. Although most β -thalassaemia intermedia patients have mutations that affected both β -globin loci, the result of such genetic alteration is only a partial suppression. Their genetic background can be either homozygosity (β^+/β^+ or β^+/β^0) or compound heterozygosity (HbE/ β -thalassaemia) (228).

1.3.4.2 Haemoglobin E (HbE)

1.3.4.2.1 Pathophysiology of HbE

HbE is one of the abnormal β -globin variants, caused by a single base-pair substitution at *HBB*:c.79G>A (p.Glu26Lys) (229). The underlying altered RNA processing mechanism occurs due to the activation of a new cryptic splice site, which competes with the regular site and results in a reduction of normally spliced mRNA (230). The c.79G>A mutation caused abnormalities in RNA processing, as was demonstrated in expression studies. The alternative splicing of exon 1 at the codon 26 caused the insertion of intron 1 into the transcript and creation of a new stop codon (230). The abnormally spliced mRNA *in vitro* was shown to be unstable and non-functional. Thus, the overall quantity of functional β -globin was reduced, which manifested as a mild β -thalassaemia phenotype (231). The proportion of the aberrantly spliced mRNA from the patients was in line with the severity of the disease. Patients with more severe symptoms had more of the abnormally spliced mRNA (2.9% to 6.1%); whereas patients with higher Hb levels had lower amounts (1.6% to 2.6%) (232). The crystallography

study demonstrated the aetiology of HbE instability through two proposed mechanisms: 1) the change of p.Glu26 to p.Lys26 leading to the loss of stability of H-bonds with p.Arg30 and the modification of $\alpha 1\beta 1/\alpha 2\beta 2$ interfaces and 2) the conformation change of p.His116 and p.His117 from HbE and HbA, respectively, affecting Hb assembly and stability (233). A study of interactions between variants of Hb in a model RBC membrane system showed that HbE induced different redox properties when compared to HbA (234). However, it was unclear how HbE exacerbated the increase of oxidative stress *in vivo*.

There are many factors that contribute to the pathophysiology of HbE/ β -thalassaemia. These include a globin chain imbalance caused by reduced β -chain production, IE, apoptosis and oxidative injury (235, 236). In the steady-state, the instability of HbE is not considered to be a significant contributor to the pathophysiology of the disease, except during episodes of fever. The effect of high temperature on the reduction of the Hb synthesis was demonstrated both *in vitro* (237) and *in vivo* in the patients carrying *HbE* allele (238).

1.3.4.2.2 Phenotypic manifestations of HbE

Both heterozygous, *in trans* with a wild-type allele, and homozygous expression of the *HbE* were shown to contribute to a mild hypochromic microcytic RBCs phenotype (239). A *HbE* heterozygote (β^E/β ; HbE 25-30% of total Hb) may not have any blood parameter changes, except for a modest number of target cells in a blood smear. A *HbE* homozygote (β^E/β^E), will have a similar spectrum of phenotypic severity as a heterozygous form of β -thalassaemia, including the presence of hypochromic microcytic red cells (mean corpuscular volume <80 fl) and slight anaemia (229). Such patients' Hb typing would display HbE $\geq 80\%$, and they usually do not require any treatment or transfusion.

However, when *HbE* combines with a β -thalassaemic allele, the clinical manifestations can be broad, ranging from severe anaemia in TDT to thalassaemia intermedia in NTDT (197, 231). These variations in disease severity are a reflection of the expression of globin alleles other than *HbE*, as well as other genetic factors. Some of these factors are α -thalassaemia co-inheritance and *XmnI* polymorphism (*HBB*:c.-158C>T, rs7482144), which is a mutation in *HGB* promoter and a known modifier of HbF level (237, 240-242). The β -thalassaemia allele alone *in trans* to *HbE* might contribute to this heterogeneity of symptoms, but not in a consistent manner (243). Other than genetic factors, environmental cues also play a role in the severity of HbE/ β -thalassaemia. Premawardhena *et al.* (2005) stratified HbE/ β -thalassaemia patients

into different age groups and observed that the alteration of EPO levels due to age-related changes in adaptation to anaemia and malarial infection correlated with the disease severity (241). The interactions between HbE and β -thalassaemia in various population, including proportions of Hb and haematological profiles, were summarised by Gibbons *et al.* (239) and Vichinsky (244).

1.3.4.3 Alpha-thalassaemia

Normal adult Hb comprises four subunits; two β -globin chains, and two α -globin chains. Thus, deficiency of the α -globin chain production leads to a thalassaemic disease known as α -thalassaemia. Alpha globin genes are members of the *HBA* gene cluster. Deletional mutations in this gene cluster are typical of α -thalassaemia: Hb Bart's hydrops fetalis ($--/--$) and HbH disease ($--/\alpha$). Whereas, non-deletional mutations often lead to abnormality of the α -globin chain, e.g., Hb Constant Spring (HbCS) or Hb Paksé (245). The α -globin gene cluster spans approximately 30 Kb on chromosome 16 (16p13.3) and consists of seven loci, ordered from 5' to 3': *HBZ* – *HBZP1* (pseudozeta) – *HBM* – pseudogene – *HBA2* – *HBA1* – *HBQ1*. The *HBA1* and *HBA2* genes are responsible for α -globin chain production in an adult. They share identical coding sequences but have a different level of transcription, where $\alpha 2$ mRNA predominates over $\alpha 1$ in 70:30 ratio (246). At the protein level, *HBA1* and *HBA2* products are more comparable, with the ratio difference of 60:40 for $\alpha 2$: $\alpha 1$ (247, 248). Thus, it is implied that any mutations present in the *HBA2* gene would have a more pronounced effect than mutations present in the *HBA1* gene.

Unlike in the β -globin locus, the Hb switching in the α -globin locus takes place in the prenatal period when the *HBZ* or ζ -globin expression halts and α -globin synthesis begins (249). Therefore, the patients diagnosed with α -thalassaemia always present at a very early stage of life, ranging from Hb Bart's hydrops fetalis, the most severe form of α -thalassaemia, to HbH disease, a mild to severe α -thalassaemic disease. Because α -globin is a composition of all types of Hb present in adulthood (HbA, HbA₂, HbF), it is an indispensable globin chain. A complete deficit of α -globin chains is seen in Bart's hydrops fetalis when a fetus cannot produce any normal fetal or adult Hb. Without treatment, stillbirths and infant deaths shortly after birth are typical for this pathology. The severity of HbH (β_4) disease is more varied than Bart's hydrops, ranging from very mild to severe symptoms. Moreover, it is well established

that the non-deletional form of HbH disease, for instance, HbH and Constant Spring (HbH-CS) disease, is usually more severe than the 'traditional' deletional HbH disease (250, 251). Not only the causative genes are giving rise to thalassaemia, but the α -globin genes also serve as the notable genetic influencers in β -thalassaemia.

1.3.5 Clinical manifestations and complications of thalassaemia

Clinical phenotypes of thalassaemia show extreme variations, from severe manifestations in thalassaemia major, to slightly less severe in intermedia, through to asymptomatic forms that could only be identified by abnormal blood tests (191). Anaemia is the major and the first clinical presentation of thalassaemia that would bring a patient to a clinician. The main cause of anaemia in thalassaemia is premature red cell destruction by the process of IE (see section 1.3.3) and haemolysis.

1.3.5.1 Haemolysis and blood parameters associated with thalassaemia

One of the significant features of thalassaemia that determine the severity of the disease is the rate of haemolysis, which can occur as intravascular (IVH) or extravascular (EVH) haemolysis. IE is associated with the EVH type. Generally, most of the haemolytic conditions have a predominant site of haemolysis, but these are not mutually exclusive. Kormoczi *et al.* (2006) suggested the concomitant IVH component in the predominantly EVH patients, e.g. patients with hereditary spherocytosis, autoimmune haemolytic anaemia, etc. These observations were based on the altered levels of IVH markers, i.e. reduction of haptoglobin and the increase of lactate dehydrogenase (LDH) (252). The detection of the IVH markers in these conditions could be explained by the release of Hb from macrophages following endocytosis of affected RBCs, or by the release of the affected RBCs from the RE system followed by their lyses in the circulation (252). Monitoring of haemolytic markers is an unbiased way to determine severity, response to treatment and concomitant complications of thalassaemia. Currently, there is no 'gold standard' marker of haemolysis. Hb serves as the most important indicator of haemolysis and treatment monitoring. However, in thalassaemia and other chronic haemolytic conditions where the patients' disease is well tolerated, with some degrees of anaemia, Hb alone would not be a good marker to reflect patients' well-

being and transfusion requirements. Listed below are blood parameters which are used as indicators of the haemolytic status of both EVH and IVH in thalassaemic patients.

1.3.5.1.1 Haemoglobin and haematocrit

World Health Organization designates normal Hb levels for non-pregnant women at $\geq 12 \text{ gdl}^{-1}$ and for men at $\geq 13 \text{ gdl}^{-1}$ (253). The Hb values below these cut-off points would be categorised as anaemia. Although Hb is the most significant predictive marker for acute haemolytic conditions such as the autoimmune haemolytic anaemia (254) or even the haemolytic crisis in thalassaemia, it might not represent the *bona fide* severity in chronic haemolytic diseases, for instance, in a non-haemolytic crisis of thalassaemia intermedia. In the latter cases, it is necessary to compare the current Hb results with the historic Hb values in order to interpret the clinical severity. Thus, in patients with thalassaemia intermedia, their baseline Hb can be decreased to $6\text{-}7 \text{ gdl}^{-1}$ (or Hct of $\sim 20\%$) without the need for transfusion or treatment (255). Hb and Hct are also the most common markers used to monitor the improvement of the patients, especially after a transfusion.

1.3.5.1.2 Plasma haemoglobin and percentage of haemolysis

Plasma haemoglobin concentration that represents 'free Hb' diffused in the plasma is usually tested to determine the presence of IVH. In the normal state, the reference ranges of total free Hb in plasma are $0.0\text{-}15.2 \text{ mgdl}^{-1}$ (256). The level of plasma Hb is measured by spectrophotometry at different wavelengths and calculated based on the Harboe method (257). Percentage of haemolysis can also be calculated from the plasma Hb value.

1.3.5.1.3 Reticulocytes

One of the parameters associated with thalassaemia is reticulocytosis due to increased release of reticulocytes from the bone marrow into the peripheral blood. The normal physiological reticulocyte count is approximately 0.5% - 1.5% of RBCs. A higher number of reticulocytes indicates the enhanced response of the marrow to anaemia. Reticulocytes are also good indicators of the causes of anaemia, as their low number denotes a problem with erythrocyte production or bone marrow diseases.

1.3.5.1.4 Indirect bilirubin (unconjugated bilirubin)

When RBCs break down, the globin chains are recycled, and the iron is reused. The haem is degraded into bilirubin. Hb degradation contributes to 70% to 90% of the total bilirubin. The initial form of bilirubin is the free unconjugated bilirubin, which is bound by albumin and

transferred to the liver. This complex is then dissociated, and hepatocytes conjugate bilirubin into water-soluble form (conjugated bilirubin) which is subsequently excreted into the gastrointestinal tract. In EVH, the level of the unconjugated form of bilirubin is elevated because of the saturation of hepatocyte functional capacity to process the excess bilirubin (258). In haemolysis, the conjugated bilirubin level is usually normal. Other conditions that might have unconjugated hyperbilirubinemia are cirrhosis/liver diseases, Gilbert's syndrome, etc. This syndrome is a prevalent benign condition with a high bilirubin baseline due to the decrease of the conjugating enzyme (259).

1.3.5.1.5 Lactate dehydrogenase

Lactate dehydrogenase is an enzyme associated with the glycolysis pathway with a function of converting pyruvic acid to lactate. Thus, LDH is found ubiquitously in all cell types, with a high concentration in cardiac muscles, liver, muscles, kidneys, lungs and erythrocytes. Because LDH is pervasive, there are many conditions with elevated LDH (normal ranges are 122 – 222 U⁻¹ in an adult), notably where the turn-over rate of cells is increased, e.g. in lymphoma, several types of solid cancer, myocardial infarction, megaloblastic anaemia and haemolysis. LDH is known to be a good clinical parameter of IVH, but the levels of LDH can also be slightly elevated in EVH (260). Therefore, LDH is useful to distinguish between these two types of haemolysis. Additionally, LDH is also useful in treatment monitoring because its levels being in concordance with a degree of haemolysis (259).

To summarise, there is no specific marker of haemolysis. In clinical practice, usually, more than one haemolytic parameter is monitored and taken into consideration together with the signs and symptoms to make an accurate diagnosis and predict the severity of the disease.

1.3.5.2 Iron overload

Transfusion iron overload is the inevitable complication of TDT patients (see section 1.3.6). Iron in the form of either labile cellular or non-transferrin bound iron can lead to increased storage in organs and tissues susceptible to iron accumulation (261). These tissues include vital organs, e.g., myocardium, hepatocytes and pancreatic tissue. In addition, an excess of labile cellular iron can mediate the formation of reactive oxygen species (ROS), particularly hydroxyl radicals, according to Fenton reaction (209). ROS generation worsens the organelle damage and can subsequently result in cell death and fibrogenesis (262). Overall, unchelated

transfusion iron overload is one of the leading causes of death in thalassaemic patients. However, NTDT patients, even those who never receive a transfusion, can develop iron overload as well, albeit with much slower kinetics (263). Such iron overload is related to IE, anaemia, and increased EPO production, which altogether suppresses hepcidin, a key enzyme that regulates ferroportin in intestinal cells and hepatocytes; causing a subsequent increase in iron absorption and release of stored iron, respectively (264). The adequacy of transfusion therapy can prevent and correct anaemia and inhibit this pathogenic mechanism in TDT patients; therefore, this type of iron overload from hepcidin suppression is more commonly found in NTDT patients.

1.3.5.3 Extramedullary haematopoiesis

Due to the limited areas of erythroid production in thalassaemia, thalassaemia major patients would develop extramedullary haematopoiesis (EH), or haematopoiesis that occurs in organs other than bone marrow (265). EH can cause localised symptoms if compressing on nerve plexus or spinal cord, leading to a disability in the patients. Adequate blood transfusion is reported to suppress the occurrence of this complication (225).

1.3.6 Treatments of thalassaemia

Treatments and management of thalassaemic patients are chosen according to the severity of the disease, and the guidelines for both TDT and NTDT patients are issued by the Thalassaemia International Federation (224, 225). The conventional therapies for thalassaemia comprise red blood cell transfusion, iron chelation, splenectomy, hydroxyurea, and haematopoietic stem cell transplantation, while several novel and specific treatments are also proposed, e.g. gene therapy, gene editing, novel medications including JAK2 inhibitor, activin receptor-II ligand traps, etc. Note that, a recently published report has comprehensively reviewed this topic (266) and in this manuscript, only the principal treatment, red blood cell transfusion, will be discussed together with some unsolved problems and non-standardised practices regarding blood transfusion therapy.

1.3.6.1 TDT patients

Transfusion therapy is the mainstay of treatment of thalassaemic patients. Transfusion to this group of patients helps to correct anaemia, promote normal growth, and permit daily activity level (267). Transfusion also suppresses IE, which in turn prevents downstream complications, including extramedullary haematopoiesis and skeletal changes from marrow hyperplasia (228). A recent survey of 717 thalassaemic patients from 11 medical institutions in the US revealed current clinical practices compared to recommended guidelines. The threshold to initiate transfusion in the TDT group was Hb $<7 \text{ gdl}^{-1}$ on two separate occasions, or Hb $>7 \text{ gdl}^{-1}$ with the presence of complications (268). All centres used pretransfusion Hb level to guide transfusion therapy. Target Hb varied from >8 to $>10 \text{ gdl}^{-1}$ (268) when the guidelines of management of TDT patients recommended maintaining pre-transfusion Hb at 9 to 10.5 gdl^{-1} , or higher in patients with a history of cardiovascular diseases (225). This survey indicated the gap in management between clinical practice and the ideal therapy in the TDT group and implied that there might be other factors to be considered in order to reach the transfusion decision, rather than only the pre-transfusion Hb level. These factors, for example, could be the quality of life or laboratory parameters that may correlate better with the disease pathology, rather than solely the drop of Hb. The other inconsistent practice identified in the survey was how much blood was required per transfusion treatment, especially in adult patients. The current practices in the review were varying from fixed-dose (2-3 units) to calculated dose based on the pre-transfusion Hb (268). While under-dosed transfusion would not reach the clinical goal, the over-dosed transfusion could result in unnecessary exposure to alloantigens and an additional risk of transfusion complications, both infection- and non-infection related.

1.3.6.2 NTD patients

Regarding the NTD group, the indications of blood transfusion are less well established (255) when intermittent transfusion would benefit patients with known acute stress or episodes of anaemia (pregnancy, surgery, infections). Currently, there is no minimum threshold for this group of patients; therefore, the real practices can be very diverse from centre to centre. According to the recent survey of 11 institutes, the decision to administer transfusion to the patients was based on symptoms, regardless of Hb level (7 from 11 institutes). Patients were transfused with a minimum Hb of $<6 \text{ gdl}^{-1}$ (two from 11 centres), $<7 \text{ gdl}^{-1}$ (one centre), and <9

gdl⁻¹ (one centre) (268). The research outlined in this thesis could potentially ameliorate the use of Hb pre-transfusion level as the only indicator of transfusion, as potential biomarkers in this patient group will be assessed.

1.4. Genetic factors determining the severity of β -thalassaemia

The focus of this project is β -thalassaemia; therefore, this section will introduce the known genetic factors that alter the clinical severity of β -thalassaemia. The known genetic modifiers of β -thalassaemia can be categorized based on their origins into two groups: the *HBB* gene, and the other genes that influence phenotypic diversity among the same β -thalassaemia *HBB* genotypes. Two of these other loci are related to the co-inheritance of α -thalassaemia and the QTL that affect the level of the γ -globin chain expression, leading to an increase of HbF levels (197). These two modifiers have a direct effect on the degree of globin chain imbalance, the key pathophysiology of β -thalassaemia. The co-inheritance of mutations in *HBA1* and *HBA2* genes encoding α -globin chains will result in a deficit of α -globin synthesis, which would alleviate the clinical severity of β -thalassaemia. The QTL associated with HbF also alleviates the disease severity in a similar manner. While HbF levels increase, the γ -globin will bind to the α -globin chain, and subsequently reduce the excess unbound α -globin pool (202, 269).

1.4.1. Mutations of the *HBB* gene

More than 350 β -thalassaemic alleles have been reported to date (data from <http://www.ithanet.eu/db/ithagenes>). The frequencies of β -thalassaemic alleles vary in different geographical areas. The four most common mutations identified in Thailand are listed in Table 1.2.

Table 1.2. Frequencies of causative *HBB* mutations reported in Thailand.

Mutations	Average frequencies (%)
<i>HBB</i> :c.79G>A (HbE)	44.50
<i>HBB</i> :c.124_127delTTCT or <i>HBB</i> :c.126_129delCTTT	37.26
<i>HBB</i> :c.52A>T	21.99
<i>HBB</i> :c.19G>A (HbC)	8.58

Data from <http://www.ithanet.eu/db/ithamaps?country=TH>

The mutations and mechanisms altering the expression of the β -globin gene can affect any stage of gene processing, from transcription, RNA processing, to translation.

1) Transcriptional mutations

This type of mutation can be found in the 5' UTR promoter region of the *HBB* gene, including the critical CACCC, CCAAT, and ATAA box DNA sequences which are located approximately 100 bp upstream of the starting point of the transcription. Frequently, the transcriptional mutations cause only a mild reduction of β -globin synthesis, resulting in β^+ or β^{++} thalassaemic phenotype (197). However, people with different chromosomal backgrounds, carrying the same transcriptional mutation, can manifest in extremely different forms of thalassaemia, from a very mild to transfusion-dependent disease (270). For example, individuals from Black ethnic group homozygous for -29A>G have only a mild severity; whilst, the same mutation in Chinese people causes severe anaemia that requires a regular transfusion (270).

2) RNA processing mutations

In *HBB*, the mutations that affect mRNA processing change either RNA polyadenylation or RNA splicing. They usually result in various degrees of disease severity, except for the mutations of the GT or AG sequences in the exon-intron splice sites that result in β^0 -thalassaemia. HbE variant is one of such splice site mutations, affecting the RNA processing by creating a cryptic splice site at codon 26 of exon 1 of the *HBB* gene (see section 1.3.4.2.2 for HbE thalassaemia). A cryptic splice site can be used preferentially to the regular splice site, generating abnormal and non-functional mRNA (271).

3) Translational mutations

Both nonsynonymous and nonsense mutations that introduce premature stop codons are common amongst *HBB* mutations (197). Most of these nonsense mutations are offset by the nonsense-mediated mRNA decay, and only a few nonsense mutations are known to escape this surveillance mechanism, leading to a dominantly inherited β -thalassaemia (272).

4) Other mutations

Large deletions are rarely found as causes of β -thalassaemia; either deletion restricted to the *HBB* gene or extensive deletion involving the upstream β -LCR. Interestingly, HbF and HbA2 levels can be elevated because of certain types of deletions. The proposed mechanisms postulate that these deletions include the β -globin promotor (i.e., CACCC, CCAAT, and TATA sequences), the target of transcriptional regulation, resulting in *cis* enhancement of β -LCR with γ and δ genes (273). Moreover, *trans*-acting mutations have been reported; one such mutation that affects transcription factor is in *GATA1* sequence encoding N-finger region, which affects the DNA binding. The affected family presented with X-linked thrombocytopenia and mild β -thalassaemia features (274).

5) The dominant form of β -thalassaemia

Generally, β -thalassaemia is known as an autosomal recessive inherited disorder. However, a dominant inherited form can occur, where only one allele can cause clinical disease (275, 276). Patients heterozygous for causative mutations presented with moderate to severe β -thalassaemic symptoms and the abnormal haematology parameters (277). Hb analysis showed an increased level of HbA2, as seen in usual cases of β -thalassaemia major (277). Various types of mutations were reported to be causative mutations of this dominant type (278, 279), such as single nucleotide variations and small insertions/deletions. These mutations lead to malfunction and unstable β -globin chain products that are not able to form normal adult Hb with α -globin chains. Consequently, the pathophysiology of the dominant disease mimics the β -thalassaemia disease with recessive inheritance. One striking difference between the two modes of inheritance of β -thalassaemia is that the prevalence of the dominant form is not aligned with the malarial pandemic areas (197).

1.4.2 Co-inheritance of β -thalassaemia

1.4.2.1 Clinical features of HbE/ β -thalassaemia

The remarkable heterogeneity of clinical presentations of HbE/ β -thalassaemia patients would require a strategy of categorising these patients based on several parameters, along with the long observation period, to determine the most appropriate clinical courses. The Sri Lankan patients in the longitudinal study by Premawardhena and colleagues (2005) were monitored for their clinical and laboratory parameters over the course of eight years (241, 280, 281). The severity of the disease was graded from 1-5, as described in the literature (241). The attempts to shift the management of patients from TDT into NTDT categories were reported to be successful in a number of cases. The phenotypic instability of HbE thalassaemia seemed to be improved with older age, and in those cases, less transfusion was needed (281, 282). This phenomenon is likely reflecting a decrease of EPO production in response to the similar level of Hb with ageing. Furthermore, HbF levels played a significant role in altering oxygen affinity in RBCs and EPO level was not correlated with the Hb oxygen saturation (283). The overall oxygen saturation levels of the HbE thalassaemic patients were significantly higher than of those suffering from other β -thalassaemia. Thus, such patients were able to adapt better to severe anaemia (283). Nonetheless, when focusing on HbE/ β -thalassaemia patients, only minimal differences in Hb values (Hb 5.6 gdl⁻¹ vs. 4.9 gdl⁻¹) and HbF levels (1.61 gdl⁻¹ vs. 1.31 gdl⁻¹) were observed in the mild and severe forms, respectively. Thus, other factors could be involved in the clinical presentation of these patients.

1.4.2.2 Co-inheritance of α - and β -thalassaemia

Alpha thalassaemia is one of the primary genetic modifiers of β -thalassaemia, since a loss of α -globin synthesis, would tilt the imbalance between α -non- α globin. The compound heterozygotes will have less of the redundant α -globin and thus present with less severe symptoms. The extent of α -gene deletion and the type of β -thalassaemia allele will determine the clinical manifestations (202). For example, co-inheritance of single α -globin gene deletion ($-\alpha/\alpha\alpha$) with β^0 -thalassaemia would only slightly change the clinical severity. Individuals who carried only one allele of functioning α -globin gene (HbH disease) with the homozygous β -thalassaemia could present with NTDT spectrum (197).

1.4.2.3 *Cis*-regulatory sequences of the β -globin locus

After the β -globin switching, HbF levels are normally reduced to approximately 1% of total Hb in adulthood. In a condition where the fetal Hb silencing is incomplete, fetal HbF will be expressed at a high level; this condition is referred to as HPFH (284). Two forms of HPFH are identified: the pancellular and the heterocellular, depending on the presence of HbF in all or some RBCs, respectively. HPFH is caused either by large deletions of the β -globin gene cluster involving δ - and β -globin genes or by point mutations affecting the upstream promoter region of the *HBG* (285).

1.4.2.3.1 *Deletional type of HPFH*

Individuals with large deletions encompassing the γ - and β -globin genes express only HbF and are healthy (286). The deletions usually involve a loss of δ - and β -globin genes and result in $(\delta\beta)^0$ -thalassaemia, together with HPFH. The diversity of these deletions was described by Wienert *et al.* (2018) (287). Interestingly, the area around the β -pseudogene is important to the binding of BCL11A (59, 288). The deletion of this region would disrupt the interaction between BCL11A, one of the critical fetal globin repressors, and the LCR of the β -globin gene cluster, as shown by the 3D chromosome architecture mapping (289). This observation was confirmed with CRISPR/Cas9 gene-editing to excise this particular region of DNA. The CRISPR/Cas9 edited cells expressed higher levels of HbF (286).

1.4.2.3.2 *Non-deletional type of HPFH*

Point mutations in the promoter region of the γ -globin gene, approximately c.1-115 and c.1-200 upstream of the start of the coding region, can cause the non-deletional form of HPFH (288). These two DNA positions were confirmed as the binding sites of BCL11A and ZBTB7A, two important fetal globin gene repressors (50, 59, 290). The other regulatory single point mutation was revealed at c.1-175T>C upstream of the γ -globin gene. This mutation creates a *de novo* binding site of the T-cell acute leukaemia lymphocytic leukaemia protein 1 (TAL1) (291). Recently, Wienert and colleagues (2018) published a list of these regulatory mutations and the corresponding HbF levels (287). All the regulatory mutations interfere with the fetal globin gene repressors and γ -globin gene interactions, subsequently triggering the persistence of fetal Hb in affected individuals. Ultimately, enhance levels of HbF has beneficial effects on patients with co-inherited β -haemoglobinopathies, both in SCD and β -thalassaemia (269, 292, 293).

1.4.2.3.3 Co-inheritance of HPFH and β -thalassaemia

As discussed above, HbF is a major type of circulating Hb in fetus and newborn. In an adult, HbF is restricted to only a small amount of total Hb (<1%) and confined to the F cells. However, various acquired and genetic disorders can cause the persistence of high HbF levels, varying from mild to almost 100% increased (294). These conditions include $\delta\beta$ -thalassaemia, β -thalassaemia, and HPFH. Additionally, the combination of these conditions can alter disease severity (294). For example, Thein and Weatherall (1989) reported one Indian family with β -thalassaemia major (β^0/β^0) with the unusually mild clinical manifestations. The cause of the mild manifestation was identified as the co-inherited non-deletional HPFH. The linkage analysis study of five generations of this family has shown that the genetic determinant for the HPFH was independent of the β -globin gene cluster (292). Regarding HbE/ β -thalassaemia, the HbF levels can be varied, ranging from 8.9% to 66% and the increase of HbF levels is correlated with the increase of total Hb (242). The higher levels of HbF were also reciprocally correlated with the α/γ -synthesis ratio, and this could explain the greater capacity for γ -globin chain synthesis (242). Rees *et al.* (1999) described two mechanisms contributing to the elevated HbF levels in this group of patients: erythroid mass expansion resulting from increased EPO, as well as the selection of cells with more γ -globin chain production (295).

1.4.2.4 Trans-acting factors of fetal Hb

HbF was shown to be inherited as a quantitative genetic trait, in a study of a pair of twins. This study identified that the variance observed in HbF quantity in the individuals was inherited and that *Xmnl-HBG2* polymorphism was responsible for this variation (296). Genetic linkage and genetic association studies in one family identified the intergenic region *HBS1L-MYB* on chromosome 6q as the second QTL (297). Subsequently, due to the advancement of genome-wide association studies (GWAS), the *BCL11A* gene was identified as responsible for regulating HbF levels (55), enabling a better understanding of globin switching process (57, 298, 299). Clinical studies of co-inheritance of these three QTLs and β -thalassaemia alleles showed a milder disease severity (197).

1.4.2.4.1 KLF1 and globin chains expression

KLF1 is one of the crucial transcription factors during the erythropoiesis, first described by Miller and Bieker in 1993 (41) (see section 1.1.1.1, KLF1). Its mechanism of action is based on

three conserved KLF1 Krüppel-like zinc fingers interacting with the *HBB* gene promoter region, the CACC box (300). Studies of induced homozygous deletion of *KLF1* gene in mice models showed fatal anaemia, which was more severe than a pure loss of *HBB* expression (37, 38). With its various erythroid gene targets, this transcription factor plays different roles at each stage of the erythropoiesis, from erythroid lineage determination at an early stage to globin switching, and finally, facilitating cell differentiation and enucleation (39, 301). Recently, Gnanapragasam *et al.* (2016) reported that *KLF1*-null erythroid cells (*klf1*^{-/-}) were unable to enucleate, and the rescue procedure successfully restored the enucleation (302). The *klf1*^{-/-} mouse models manifested clinical symptoms similar to the β -thalassaemia major disease (37, 38). In one of its most critical roles, KLF1 is responsible for the transition from fetal Hb to adult Hb (HbA, $\alpha_2\beta_2$) through two mechanisms. Firstly, KLF1 has a direct effect on β -globin gene expression by interacting with DNase 1 hypersensitive sites HS2 and HS3 of the LCR, and the CACCC-box consensus sequences at the proximal promoter of β -globin (48, 303). Secondly, the indirect suppression of γ -globin is regulated by BCL11A, a repressor of γ -globin gene expression (304, 305). A direct link between KLF1 and BCL11A was demonstrated when a knockdown of *KLF1* resulted in a decrease of BCL11A levels and in an increase of γ -globin to the β -globin ratio in both human and mice models (49) (see Figure 1.5). *KLF1* was reported as one of the γ -globin gene modifiers in a Maltese family with HPFH studied by genome-wide linkage analysis. The test identified a candidate mutation on chromosome 19p13.12-13. Subsequently, Sanger sequencing analysis identified the causative nonsense mutation encoding Lys288Ter in the *KLF1* (50). A number of *KLF1* mutations that alter the levels of HbF have been reported (36, 306). A role of KLF1 in ameliorating the severity of thalassaemia was also observed. In one study of targeted Sanger sequencing of *KLF1* in the Chinese population (n=922), the frequency of the *KLF1* mutations was observed to be more prevalent in Southern region of China where thalassaemia is known to be endemic. Moreover, all of the *KLF1* variants were observed in β -thalassaemia intermedia, but not in thalassaemia major patients (195). However, conversely, a recent study of *KLF1* variants among HbE/ β^0 -thalassaemia patients in the Thai population reported the increase of HbF levels (up to $52.3 \pm 2.4\%$) in the HbE/ β^0 -thalassaemia patients carrying the *KLF1* mutations, which did not significantly alleviate the clinical severity (307).

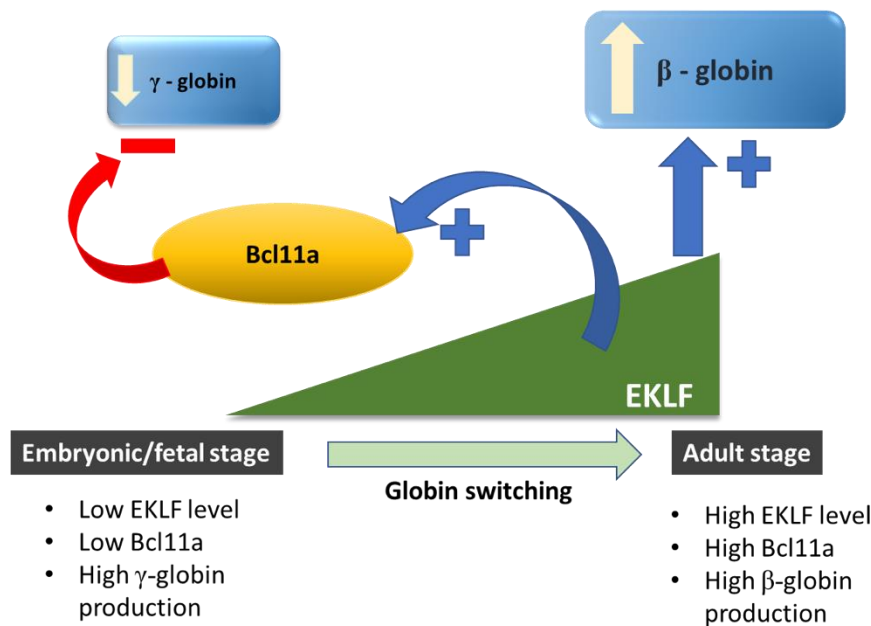


Figure 1.5. KLF1 regulates globin switching through *BCL11A* and *HBB* genes.

Reduced expression of KLF1 (EKLf) during the embryonic/fetal stage leads to a decrease of BCL11A levels and in an increase of γ -globin to β -globin ratio. Whereas, the high KLF1 expression in the adult stage results in increase of BCL11A and the β -globin level (*Modified from Bieker J. Nat Genet 2010; 42(9):733-4)(305).*

1.4.2.4.2 *BCL11A* as a HbF quantitative trait loci

Since the high HbF level is a significant genetic modifier of β -thalassaemia and sickle cell disease, transcription factors that increase this level will also have an ameliorating effect on the haemoglobinopathies. The advent of GWAS disclosed the role of this gene in erythropoiesis as a γ -globin gene repressor implicated in HbF regulation, as described in section 1.1.1.1.4 (Figure 1.5) (55, 56). Full-length BCL11A will bind to many discrete regulatory regions of the β -globin gene cluster of the human adult erythroblasts. This interaction results in another role of BCL11A as an activator of the β -globin gene expression. Several studies tried to identify the specific binding regions of this γ -globin repressor. Primarily, the *cis*-acting elements of the BCL11A on the β -globin cluster include the HS3 of the LCR, the area upstream of the δ -globin gene and the intergenic area downstream of the γ -globin gene (57, 308). By using array comparative hybridization, a small 3.5 Kb intergenic region near the 5' end of the δ -globin gene was identified as one of the binding sites of the BCL11A. Chromatin immunoprecipitation studies revealed the other trans-acting factors binding to this site, including GATA-1, HDAC-1, and H3K27me3 (308). Functional studies illustrated that the

binding of BCL11A and its interaction with GATA-1 and SOX6 mediates re-configuration of the *HBB* locus and represses γ -globin expression (58, 309).

The mechanisms of the γ -globin gene repression were demonstrated by a fine-mapping study of the variant rs1427404 in the intron 2 of *BCL11A* that was located in the erythroid-specific enhancers (57, 310). This SNV was subsequently validated by using a gene-editing CRISPR/cas9 method (311). Recently, the exact binding nucleotides for the ZF domain of BCL11A have been revealed as the distal TGACCA consensus binding motif in the promoter of the γ -globin gene. The overall evidence confirmed that BCL11A represses γ -globin expression (59, 291).

To date, BCL11A is one of the three major HbF QTLs associated with heterocellular HPFH (hHPFH) (197). The hHPFH has been reported to affect the phenotypic disease severity of haemoglobinopathies in conjunction with both homozygous and heterozygous β -thalassaemia (201, 269). Generally, these two forms of β -thalassaemia and SCD homozygotes could have high HbF level not caused directly by genetic disorders. They are more likely to be the result of increased erythropoiesis due to the IE, and preferential survival of the erythroid population that carries HbF (298).

1.4.2.4.3 *Xmnl*-*HBG2*

The single nucleotide variation c.1-158C>T in the *HBG2* promoter (*HBG2*:g.-158C>T) that is digested by the *Xmnl* restriction enzyme (*Xmnl*-*HBG2*, rs782144 SNP) was identified as one of the occurring mutations in HbS. Carriers of this type of mutation have a higher HbF level, and subsequently, milder clinical manifestation when compared to individuals who do not have this mutation (312). In addition, this SNV was reported to associate with hHPFH (313). *Xmnl*-*HBG2* is one of the most commonly identified QTLs underlying quantitative trait of HbF, at a frequency of 0.32 - 0.35 (298). Garner and colleagues (2000) confirmed the influence of this SNV on adult RBS with elevated HbF levels (F cells) through a study of healthy adult twins (296). However, this *cis*-acting *Xmnl*-*HBG2* module does not explain the entire variance of HbF in both the healthy population and in the haemoglobinopathy patients.

1.4.2.4.4 *HMIP-2* (rs9399137)

Linkage analysis of one large family with β -thalassaemia and HPFH (272) and an association study between chromosome 6q segment and the level of F cells (314) revealed an association between *HBS1L*-*MYB* intergenic polymorphism (*HMIP*) 2 on chromosome 6q as one of the

QTLs for HbF levels. The SNV rs9399137 was demonstrated to affect the regulatory regions that interact with critical erythroid transcription factors and the MYB expression levels (315).

1.4.2.4.5 TFIIH (*SSL1* transcription factor and nucleotide excision repair)

The important transcription factor TFIIH performs two significant roles in eukaryotes; firstly, in nucleotide excision repair of DNA damage, and secondly, as a basic transcription factor component of the RNA polymerase II (316). TFIIH consists of nine subunits, and the XPD helicase is one of these subunits. This subunit is encoded by the gene *ERCC2/XPD*. Mutations in this gene can result in two clinical features – xeroderma pigmentosum (XP) and trichothiodystrophy (TTD) (317). In 2001, Viprakasit and colleagues reported an association between TTD patients and mild β -thalassaemic phenotypes. The clinical findings included hypochromic microcytic red blood cells, mildly decreased Hb levels and increased HbA₂ levels, the hallmark of β -thalassaemia. Moreover, the globin study identified the down-regulated levels of β -globin and reduced β -globin mRNA when compared to α -globin, but without any mutations detected in the *HBB* gene (317). Therefore, the general transcription factor TFIIH has a ‘trans’-acting effect on *HBB*, but not on the α -Hb genes (*HBA1* and *HBA2*), illustrating different mechanisms between α and β genes initiation of transcription.

1.5 Extracellular vesicles

Cells release membrane-enclosed sacs or extracellular vesicles (EVs), both in pathological conditions and as a part of physiological processes. EVs can be found in circulation and have been an attractive target for a wide range of research, due to their unique characteristics of an enclosed membrane filled with biomolecules such as RNA and proteins derived from the cells of origin. EVs play a role in cell-to-cell communication (318) and trafficking of biological molecules between cells, including their immunological roles as a host defensive mechanism and immunogenic trigger mediator (319). Not only the constituents of EVs are important, the negative charge on EV surface created by the uneven distribution of lipid bilayer and the exposure of phosphatidylserine (PS) is also crucial to coagulation cascade and homeostasis (320). With all these qualities, numerous studies of EVs had been published, exploring their roles as diagnostic aids, prognosis predictors and therapeutic targets.

1.5.1 Extracellular vesicle definition

In 2018, International Society of Extracellular Vesicles (ISEV) has declared the use of the term “extracellular vesicle” for a particle with enclosed lipid bilayer that does not contain a functional nucleus (321). EV is a generic term for a wide variety of vesicles released from the cell, including apoptotic bodies, microparticles or microvesicles and exosomes (322). The classification relies on EV size and biogenesis. An exosome is the smallest particle with a diameter <150 nm, arising from multivesicular bodies in cells and fusing its membrane with the cell plasma membrane before releasing its content into the extracellular space. An apoptotic body is the largest particle (1-5 µm in size), and as its name implies, it is generated by shedding out of the cells when they undergo apoptosis. Microparticles or ectosomes have a diameter between these two extremes, i.e. ~100 to 1000 nm, and are released from the cells by direct blebbing from their plasma membranes, but are not uniquely linked with the process of apoptosis (323, 324). Due to the difference in biogenesis, the protein markers contained in each class of EVs are also different. Therefore, to define precisely any particular EV type would require the specific markers, as reviewed recently by Shah *et al.* (325). Note that, in this thesis, the term EVs will be used to refer to either exosomes or microparticles.

Because of the wide diversity in terminology, the ISEV has established the standard guideline for the definition of EVs and set the criteria for the minimal requirements that would discriminate EVs from non-EV components (321, 322).

1.5.2 Mechanisms of EV formation

1.5.2.1 Physiological EV release

In the normal physiological process, EVs are shed from activated or senescent cells. Figure 1.6 displays the mechanism of biogenesis of EVs. Although this process can occur in any cell, this review will focus mainly on erythrocytes.

1.5.2.1.1 Biogenesis of microparticles

Microparticle (MPs) formation is distinct from the exosome biogenesis. MPs form via direct membrane blebbing and shedding of plasma membrane. This involves two main steps: 1) a cytoskeletal reorganisation such as actin filament rearrangement and 2) cell membrane phospholipid rearrangement with the PS exposure (326, 327). In a resting stage, PS is located

on the intracellular side of the RBCs phospholipid bilayer. This arrangement is maintained by flippase, a transmembrane lipid transporter (Figure 1.6). When cells are activated, intracellular Ca^{2+} is increased. The increased Ca^{2+} triggers floppase and scramblase, which in turn induce loss of asymmetry of the membrane and externalise PS (327, 328). Additionally, when erythrocytes become aged and are fated to undergo apoptosis, band 3 molecules are clustered together forming neoantigens on the cell surface that are recognised by the immune system (329). PS exposure plays an essential role in initiating RE-mediated phagocytosis and clearance of apoptotic and senescent cells (330).

1.5.2.1.2 Biogenesis of exosomes

As previously mentioned, exosomes originate from multivesicular bodies as internal vesicles, inwardly budding from the endosomal membrane. The vesicles are released into extracellular space by fusion with the plasma membrane (331). Mankelov and colleagues (2015) observed the mechanisms of removal of cellular organelles via autophagy through the inside-out reticulocyte vesiculation, i.e., via PS-exposed autophagic vesicles (16). Their observations have confirmed that EVs are released from reticulocytes as a part of the physiologic red cell maturation process.

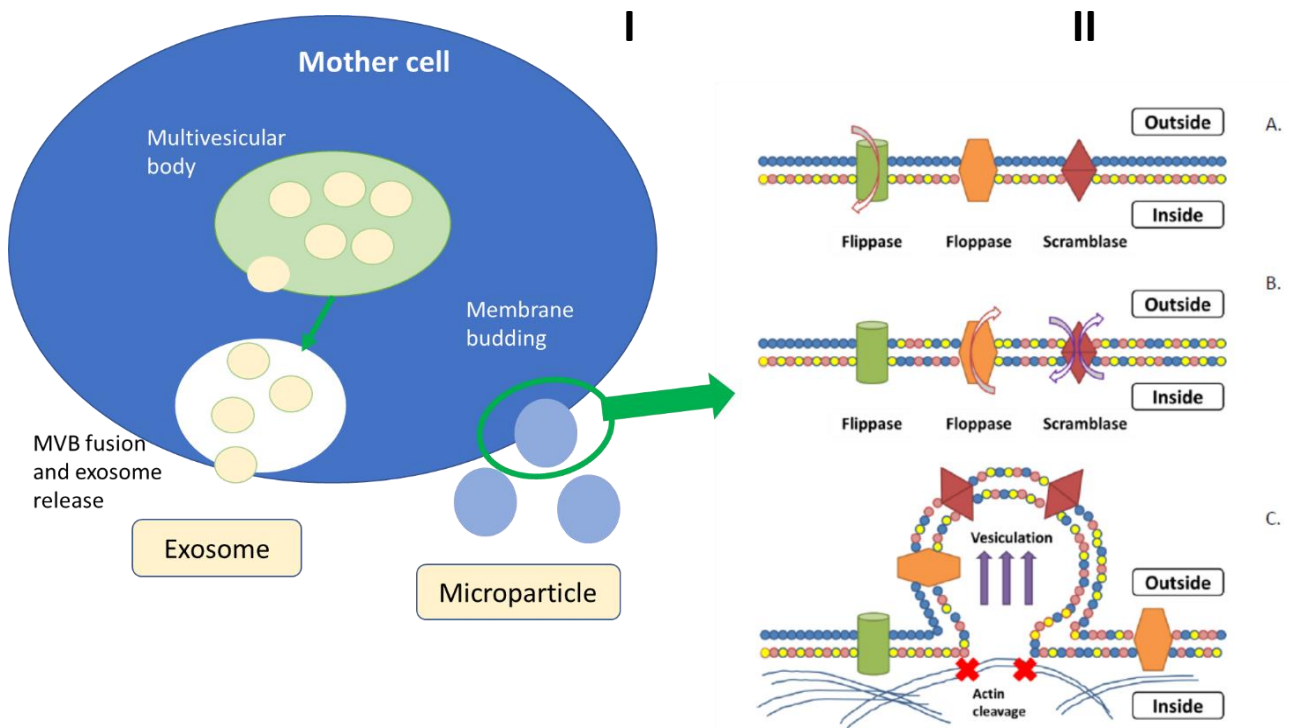


Figure 1.6. Biogenesis of exosome and microparticle from a mother cell.

(I) Exosome originates from the multivesicular body inwardly budding from the endosomal membrane before fusing with the plasma membrane and releasing exosomes into the extracellular space. The mechanism of microparticles formation is depicted in (II). In the resting stage, (IIA) Flippase maintains the arrangement of phospholipid bilayer of erythrocytes. Once the cell is activated, (IIB) Floppase and Scramblase are triggered and inhibit Flippase; consequently, loss of asymmetry of the membrane and externalisation of phosphatidylserine lead to microparticle formation (IIC) by cleavage of cytoskeleton and vesiculation of the imbalanced membrane structure.

Hence, in normal physiological conditions, RBC EVs are generated in two phases: during the maturation of reticulocytes and at the senescent state of aged erythrocytes. In summary, exosomes are formed from multivesicular bodies and released only during the development of RBCs in the bone marrow. RBC MPs are formed during the normal cell ageing process in circulation by budding off directly from the plasma membrane caused by the rearrangement of the phospholipid bilayer and fragmentation of RBC cytoskeleton due to the complement-mediated calcium influx (332).

1.5.2.2 EVs formation and release in haemoglobinopathy diseases

Sickle cell disease and β -thalassaemia are the two most common haemoglobinopathy disorders worldwide. Both conditions share the abnormalities of a β -globin chain, either in structure or deficient production. This aberrant globin synthesis leads to pathological erythrocytes and is associated with EVs formation since the affected cells are fragile and have increased susceptibility to oxidative injury and shear stress (333). This thesis will focus mainly on EVs in thalassaemia disease.

1.5.2.2.1 EVs formation and release in sickle cell disease

EVs in SCD are mainly generated from erythrocytes, platelets, and endothelial cells, and have been recognised as a participant in chronic inflammation and renal vaso-occlusions in both a murine model (334) and in human (335). EVs contribute to the pathophysiology of SCD by transferring free haem to the endothelial cells; subsequently, free haem mediates oxidative stress, vascular dysfunction, and may ultimately trigger vaso-occlusion (336). Moreover, EVs can behave as a nitric oxide scavenger that reduces NO bioavailability and therefore aggravates the vaso-occlusion observed in SCD (337). The quantity of EVs present in the plasma of SCD patients is reported to be significantly increased during both a steady-state and also in a painful crisis of SCD patients (338, 339).

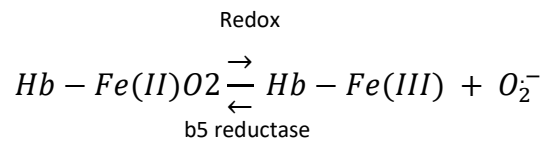
1.5.2.2.2 EVs formation and release in thalassaemia

Oxidative stress plays a significant role in initiating and mediating the pathophysiology of β -thalassaemia (217). The mechanism of increased oxidative stress in β -thalassaemic RBCs is well-established. It is initiated from the free α -globin chains, with their aggregation and precipitation occurring on the erythroid membranes. Such precipitated globin chains are highly unstable, and when bound to free iron, they lead to the generation of reactive oxygen species (ROS), as described by the Fenton reaction (see equations 1-4 below) (209). The resulting oxidative damage affects cells on multiple levels, causing following cellular injury events: PS exposure, membrane lipid peroxidation, cross-linking and clustering of band 3, promoted band 3 tyrosine phosphorylation, activating of the K-Cl co-transport. Subsequently, all these events lead to RBC membrane destabilisation and, eventually, EV release (340-343) (see Figure 1.7).

For an individual with a *HbE* allele (see section 1.4.2.1), the instability of HbE due to the shift of the redox system is further aggravated by the increase of haemin, haemichromes, and

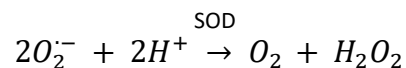
labile iron (234, 344). This process results in pathologic changes in erythrocytes and EV formation (see Figure 1.7) (343). The labile iron interacts with the membrane lipid peroxidation as described in equations below: in normal erythrocyte physiology, oxygenated Hb autoxidizes to methaemoglobin [metHb, Hb Fe(III)] at an insufficient rate, which in turn produces superoxide ions ($O_2^{\cdot-}$) (345), as depicted in equation 1.

Equation 1

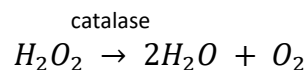


This type of ROS is unstable and rapidly converts to hydrogen peroxide (H_2O_2) by superoxide dismutase (SOD) enzyme (equation 2). Subsequently, an H_2O_2 molecule is neutralized into oxygen and water by the catalase enzyme (equation 3). Another enzyme that plays a vital role in neutralizing peroxide is PRDX2, especially during RBCs exposure to oxidative stress conditions (346). If the hydrogen peroxide is not neutralized, the Fenton reaction will occur (equation 4). The conversion of Fe^{2+} in Hb into Fe^{3+} in metHb is another primary source of ROS production, where reactive hydroxyl radicals ($\cdot OH$) are highly toxic to cells and cannot be neutralized by antioxidative enzymes. Other products of Fenton reaction are free iron and haem degradation products such as biliverdin.

Equation 2

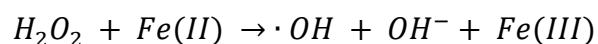


Equation 3



Equation 4

(Fenton reaction)



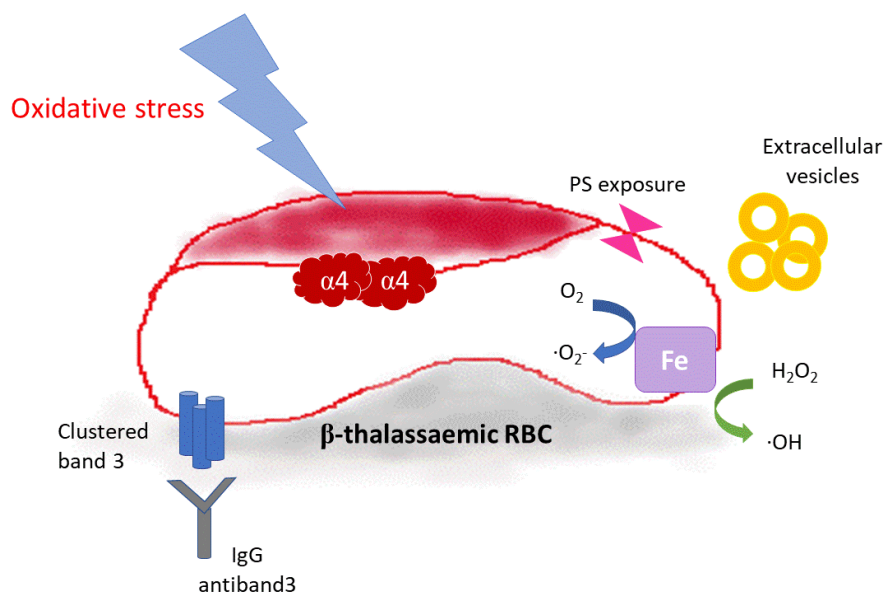


Figure 1.7. Effects of oxidative stress on β -thalassaemic red cells and EVs generation.

Oxidative stress is increased in β -thalassaemic red cells both via the Fenton reaction from haemichrome and from the aggregation of excess Hb in the form of Heinz bodies (α_4). It contributes to multiple abnormalities in erythrocyte membrane perturbation. Firstly, it causes a loss of membrane phospholipid asymmetry and phosphatidylserine (PS) exposure and/or EVs production. Secondly, it enhances band 3 clustering and disturbs the band 3-ankyrin-complex, resulting in the formation of aberrant neoantigens recognised by IgG anti-band 3 antibody. These two mechanisms precipitate red cell clearance by macrophages. (modified from De Franceschi L *et al. Oxidative stress and beta-thalassaemic erythroid cells behind the molecular defect. Oxidative medicine and cellular longevity*.2013;2013; 985210)(340))

Thalassaemic EVs have been described as different from EVs released by normal individuals in both quantitative and qualitative terms. Westerman *et al.* (2008) quantified the thalassaemic EVs from thalassaemia intermedia patients and noted that their numbers were four times greater than in normal controls (347). Haemichromes were identified as the main content of EVs through a proteomics study of the thalassaemic EVs (348). The haemichrome binding sites were also reported, which were identified as the cytoplasmic domains of less glycosylated band 3 molecules. These band 3 molecules are more susceptible to oxidation and phosphorylation by Syk kinase (p72sSyk kinase). The elevation of band 3 tyrosine phosphorylation reduces the connection between red cells membrane and cytoskeleton proteins, for instance, spectrin, ankyrin, etc. (340, 349). Therefore, they can become uncoupled from RBCs cytoskeleton and released in EVs (348). The thalassaemic EVs are

related to coagulation because of the externalisation of PS and the presence of the markers of thrombin generation. All these changes potentiate the thrombotic risks in thalassaemic patients, especially splenectomised patients (333).

1.5.3 Methods for EV characterisation

Several methods have been developed to explore EV characteristics, including their size distribution, concentration, and comparison of constituents. The ISEV has provided the framework for the identification of EVs and defined the minimal requirements for their characterisation. Two conditions must be satisfied in order to claim the presence of EVs in an isolate:

- Isolation must be from the extracellular fluid, e.g. cell culture medium, plasma, or body fluids.
- The method employed to isolate EVs has to restrict the mechanical disruption of cells; otherwise, this could result in co-isolation of contaminant intracellular compartments which would interfere with the purity of EVs (322).

Regarding the EV characterisation, the recognised EV-enriched proteins should be reported along with the proteins not expected to be enriched in EVs. Classification of the categories of proteins expected to be present in EVs and their examples are described in Table 1.3.

Table 1.3. Categories of proteins and their expected abundance levels in EVs.

Protein categories †		Examples	Expected abundance
I	Transmembrane or lipid-bound proteins	Tetraspanins (<i>CD9, CD63, CD81</i>), integrins (<i>ITG*</i>), cell adhesion molecules (<i>CAM*</i>), heterotrimeric G proteins (<i>GNA*</i>)	Enriched or present
II	Cytosolic proteins	Membrane binding proteins: <i>TSG101, RAB</i> , signal transduction proteins	Enriched or present
III	Intracellular proteins	Proteins derived from other cell compartments – endoplasmic reticulum (<i>calnexin</i>), Golgi (<i>GM130</i>), nucleus (histones family)	Absent or under-represented
IV	Extracellular/secreted proteins	Acetylcholinesterase, serum albumin, extracellular matrix – fibronectin, collagen, cytokines, growth factors matrix	Variable association with EVs

† The quantities of one or more protein of category I, II, and III should be reported.

* Denotes other possible genes in the same family. Modified from *J Extracell Vesicles*. 2014 Dec 22; 3: 26913

Characterisation of the vesicles should include their physical characteristics and constituents. The physical characteristics comprise morphology, concentration, and size distribution, all of which can be measured using various methods, for example, electron microscopy, atomic force microscopy, flow cytometry, imaging flow cytometry, tunable resistive pulse sensing (TRPS), dynamic light scattering and nanoparticle tracking analysis (NTA). The EV composition can be studied by mRNA transcriptomics, protein studies, e.g., Western blot analysis, mass spectrometry.

1.5.3.1 Electron microscopy

Electron microscopy (EM) techniques are one of the long-established methods for EV morphology and size assessments (350, 351). With choices of various types of EM, they provide different levels of information. For scanning EM, EVs are fixed and dehydrated on a glass substrate before sputter coating with a metal such as gold, gold-palladium or platinum to prevent charging of the specimen and to increase signal conduction (352). This technique has revealed topographic data of the 3D surface of the particles. Transmission EM (TEM) allows detailed imaging of membrane-intact vesicles by embedding concentrated EV suspensions in a mixture of methylcellulose and uranyl acetate, which are then applied to the grid and fixed (353). Subsequently, EV pellets can be fixed and analysed as cross-sections (353). Moreover, TEM can also be used as immune-EM when incorporating immunoglobulins coupled with nanogold particles to detect specific epitopes on EVs (351). Further modification of the method is a cryo-EM, which analyses samples at a temperature of -100°C and enables the assessment of EVs in the frozen state. This avoids the impact of dehydration and/or distortion of samples by fixation (354). The major limitation of all types of EM is that the concentration of particles cannot be evaluated.

1.5.3.2 Flow cytometry

Flow cytometry is a key method used for characterising EVs by investigating their cellular origin and estimating the concentration of EVs suspended in fluids. However, an important drawback of flow cytometry is the limited sensitivity of the instruments, as conventional flow cytometers have a low detection threshold limit of particle size of approximately 300–400 nm (355). Moreover, flow cytometry analysis is subjective, relying on the operator setting the optimum gating strategy and interpreting the results. The technique involves a specific wavelength laser beam directed at the suspended particles that are arranged in a line by a sheath fluid. A light scattering of particles is detected and analysed to collect information about their size and granulation (356). This method has been used in a number of studies, where known quantities of the commercially available counting beads were added to each sample and flow cytometry was used for measuring and calculating the numbers of EVs (357, 358). Such an EV quantifying method is accurate and reproducible (357).

1.5.3.3 Nanoparticle tracking analysis

Nanoparticle tracking analysis (NTA) is one of the most accurate techniques for measuring the size and concentration of EVs in a liquid suspension (359, 360). NTA works on the principle that particles which undergo Brownian motion will scatter light emerging from a light source, including any intensity fluctuations. A camera records these movements for an individual particle, and the NTA software determines the particle sizes at a specific temperature, their velocity and diffusivity using the Stokes-Einstein equation. After repetitive tracking (at least five records), all the information is integrated and calculated to create graphs of size distribution and concentration of EVs (see 2.2.9, Chapter 2 for methods of operation). This technique requires an accurate optimization of sample dilution and standardisation of the camera and analysis settings (360). Whilst flow cytometry has a drawback of limited sensitivity, NTA is not capable of distinguishing between a mixture of EV and non-vesicular structures of the same size, such as protein aggregates. Therefore, the numbers of counted particles could potentially be higher than the exact EV numbers (361).

1.5.3.4 Tunable Resistive Pulse Sensing

Similar to NTA, the Tunable Resistive Pulse Sensing (TRPS) technology is able to detect EV concentration and size distribution. The principle of TRPS is the detection of transient changes of the electrical resistance generated when the particles travel through a size-tunable nanopore in a polyurethane membrane. When a particle enters the aperture, an equal volume of electrolyte is displaced, and this generates a voltage pulse proportional to the volume of the particle (362, 363). Unlike NTA, this technique is independent of the refractive index of a particle. The caveat of using this method to measure inhomogeneous solutions is the potential for clogging of the aperture by large size particles or high molecular weight proteins. Additionally, damaged membranes of vesicles can induce conductivity and interfere with the electrical output (364). TRPS was not used in this thesis for EV analysis as it was not available.

1.5.4 Proteomics studies

Proteomics is an approach that provides information on both identification and quantification of protein constituents of interest in EVs. In the past, the techniques used to study protein expression were based on antibody-dependent methods such as Western blot analysis (365, 366) and flow cytometry analysis (367, 368). With the advantages of high specificity and accessibility, these methods have a significant limitation in their inability to identify new and unknown proteins. This limitation can be overcome by using mass spectrometry (MS). This technique measures the mass-to-charge ratio (M/Z) of ions in simple or complex protein mixtures (369). MS-based techniques have enabled the discovery of novel proteins. In addition, with the application of isotope-labelling, the relative quantification is possible. Post-translational modifications can also be monitored by this technique (370).

Quantitative proteomics is based on the isotope-labelling approach achieved by the introduction of the internal standard into amino acids. The labelling techniques are varied, e.g., metabolic-labelling, stable isotope labelling of amino acids in cell cultures (SILAC), chemical-labelling, tandem mass tag (TMT), and isobaric tags for absolute and relative quantification (iTRAQ) (371). SILAC is an approach for *in vivo* incorporation of two isotopic labels – light or heavy form into two cell samples of interest. After an appropriate number of cell differentiation cycles, the isotope label will replace the ‘native’ amino acid in all synthesised proteins (372). However, the drawback of SILAC is that it requires special media to prevent the conversion of intracellular isotope-coded arginine to proline that would interfere with the quantitative proteomics experiments (373). Both TMT and iTRAQ targets are known as isobaric tags that work on the basis that peptides from differently labelled samples have identical mass but can be differentiated from other peptides by the different isotope-encoded reporter ions in the lower mass range region of tandem MS (MS/MS) (371). However, recently, a technique of quantitative proteomics without tagging has become a possibility, known as a label-free method, which is based on data comparison between signal intensities or the number of peptide-to-spectrum matches (PSMs) of an individual protein obtained from more than two independent experiments (371).

1.5.4.1 Proteomics studies of thalassaemia erythrocytes and plasma

Proteomic analysis has been used as an effective tool to investigate the pathophysiology and information of functions and interactions of proteins in multiple diseases, including thalassaemia. Two studies focused on the thalassaemic erythrocytes highlighted the increased oxidative stress and ROS exposure of these cells. Bhattacharya and colleagues (2010) used of 2-DE and matrix-assisted laser desorption/ionisation (MALDI) -MS/MS-based study to identify several redox proteins were up-regulated in HbE/ β -thalassaemia cell lysate, namely, peroxiredoxin-2 (PRDX2), thioredoxin, catalase, Cu-Zn SOD, carbonic anhydrase 1, Hsp70, and alpha haemoglobin stabilising protein (AHSP) (374). The other studied using 2-DE and liquid chromatography (LC)-MS/MS technique in peripheral blood-derived erythroid precursors between HbE/ β -thalassaemia and controls observed the quite resemble set of protein as in Bhattacharya's study along with a few glycolysis proteins and δ - and β -globins (218). Proteomic analysis is also utilised as a follow-up tool for pre-and post-treatment examining plasma samples of HbE/ β -thalassaemic patients (375, 376).

1.5.4.2 Proteomics studies of thalassaemic EVs

The study of protein components of EVs can be conducted using the same methods and approaches as those used on whole cells, e.g., Western blotting, fluorescent activated cell sorting and MS-based technologies (377). The workflow of protein identification (known as bottom-up proteomics) starts from efficiently isolating the EVs, then isolating the proteins by 1D or 2D gel electrophoresis or gel-free liquid chromatography, and then digesting the extracted proteins into peptides and analysing these by MS. A number of studies of EV proteomes have adopted the successful use of gel electrophoresis for analysis of EV protein composition. However, the main limitation of these studies is that only a limited number of proteins can be explored further; for instance, Mears *et al.* (2004) and Xiao *et al.* (2012) examined proteome profiles of EVs in melanoma and identified only 41 and 11 proteins, respectively (378, 379).

In thalassaemia EVs, there have been two reported proteomics studies conducted prior to the research described in this thesis. Ferru *et al.* (2014) performed SDS-PAGE followed by Western blot analysis, then excised the protein bands and analysed them with MALDI – time of flight (MALDI-TOF) to identify the protein constituents of EVs isolated from thalassaemia

intermedia RBCs (348). A study by Chaichompoo and colleagues used 2D-gel electrophoresis followed by hybrid mass spectrometry (Q-TOF) MS and MS/MS analyses to successfully identify 29 proteins from circulating EVs derived from HbE/ β -thalassaemia patients. (380). Both studies detected proteins involved with oxidative stress and chaperone proteins, for example, catalase, PRDX2, and Hsp70, all with increased abundance in the thalassaemic EVs compared to the controls. Table 1.4 and Table 1.5 display full lists of these proteins. (348, 380).

Table 1.4. Proteins identified in EVs isolated from thalassaemia-intermedia (TI) RBCs analysed by MALDI-TOF reported by Ferru and colleagues (2014).

Proteins identified in EVs isolated from TI-RBC	Proteins that were found only in EV from TI-RBC
Band 3	Serotransferrin
Haemoglobin chain α	Ig μ chain C region
Haemoglobin	Alpha enolase
HSP90	
HSP71	
HSP70	
Catalase	
Selenium binding protein 1	
GADPH	
Carbonic anhydrase	
Peroxiredoxin-2	

Table 1.5. Proteins from platelet-free plasma-derived microparticles of HbE/ β -thalassaemia patients compared to the normal controls analysed by Q-TOF MS and MS/MS analyses reported by Chaichompoo and colleagues (2012).

Proteins increased in EVs	Proteins decreased in EVs	Proteins detected only in thalassaemic EVs
Apolipoprotein E	Apo-B100 precursor	Biliverdin-IX beta reductase isozyme I
Chain A, cyclophilin A complexed with dipeptide Gly-Pro	ASCC3 protein	hCG205366, isoform CRA α
Chain A, the molecular basis for the recognition of phosphorylated and phosphoacetylated histone H3 by 14-3-3	Chain A, heat shock 70kd protein, 42kd ATPase N-terminal domain	Haemoglobin mu chain
Chain A, X-ray structure of the complex between carbonic anhydrase I and the phosphonate antiviral drug foscarnet	Chain A, a three-dimensional structure of dimeric human recombinant macrophage colony-stimulating factor	Matrilin 1, cartilage matrix protein, isoform CRA_b
Chain B, oxygen affinity modulation by the N-termini of the beta chains in human and bovine haemoglobin	Fibrin beta	Myosin VIIB
Cytochrome P450, family 20, subfamily A, polypeptide 1, isoform CRA_c	Guanine nucleotide-binding protein G(q) subunit alpha	Peroxiredoxin 6
Haemoglobin mu chain	Immunoglobulin heavy chain variable region	Protein Rei, Bence-Jones
Hsp90AA1 protein	Pantothenate kinase 3, isoform CRA_b	Zinc finger protein 233
Immunoglobulin light chain	RNA polymerase II 140kDa subunit	
N-ethylmaleimide-sensitive factor attachment protein, alpha		
Trabeculin-alpha		
WWOX delta5-8		

1.6 Project aims

Thalassaemia is one of the most common monogenic disorders worldwide with the wide ranges of disease manifestations, especially in the case of HbE/ β -thalassaemia patients. It is still unexplained why these two conditions, which individually are relatively benign, can combine into a wide range of disease severities, including a transfusion-dependent thalassaemia. This work will set out to utilise recent developments in *ex vivo* erythroid cell culture and proteomics techniques to explore the differences between HbE/ β -thalassaemic patients and healthy controls, with the aim of identification of potential biomarkers for predicting clinical severity and transfusion requirements.

More specifically, this work aims will:

- Compare and monitor the *ex vivo* expansion and differentiation in HbE/ β -thalassaemic cells compared to healthy controls.
- Quantitate EVs produced by HbE/ β -thalassaemic patients, both from *in vitro* (reticulocyte derived) and *in vivo* (plasma) origins.
- Examine and compare the proteome of EVs derived from HbE/ β -thalassaemic patients and healthy controls, from both *in vivo* and *in vitro* origins.
- Evaluate the potential diagnostic applications in thalassaemia of any of the proteins identified using comparative proteomics. The identified proteins will be compared between groups of subjects with a spectrum of disease severity: transfusion-dependent thalassaemia, non-transfusion transfusion dependent thalassaemia, carriers of thalassaemia, and healthy controls.

CHAPTER 2

MATERIALS AND METHODS

2.1 Materials

2.1.1 Ethics and consent for patient and control samples

To initiate the patient recruitment, ethical approval was requested and granted from the Institutional Review Board (IRB) Committee, Siriraj Hospital, Bangkok, Thailand. Alongside this, a Material Transfer Agreement (MTA) regarding patient samples was authorised between NHS Blood and Transplant (NHSBT, Filton, Bristol, UK) and Faculty of Medicine, Siriraj Hospital. For the clinical follow-up trial (Chapter 5), additional ethical approval was obtained from the IRB Committee, Medical Service Department, Bangkok. Following the approvals, all sample collections proceeded according to the Declaration of Helsinki and with the informed consent of all the patients and controls. To protect anonymity, all controls and patient samples were given individual codes, and only the Chief Investigator was able to access patient identities and records.

2.1.1.1 Blood samples for EV characterisation

All patient samples used in this study were collected at the Division of Haematology, Department of Medicine, Faculty of Medicine Siriraj Hospital, Bangkok, Thailand, between October 2015 and April 2016. The control samples were selected to be age and sex-matched to the patient samples, n=22. For patients, a total of 27 mononuclear cell (MNCs) samples were prepared from 24 ml EDTA blood. From the same cohort of patients, EVs were derived from 21 samples of EVs were derived from 3.2% sodium citrate blood, and 20 HbE/ β -thalassaemia plasma samples were collected and processed. The control samples were selected to be age and sex-matched to the patient samples; n=22 (five patient samples did not have matched controls). The patient recruitment, the type of samples taken, and their processing are summarised in Figure 2.1. For half of the EDTA blood samples, the MNCs separation was performed immediately on the day of collection in Thailand. All the MNCs from this cohort were frozen using 10% DMSO with 90% fetal calf serum. All cellular and plasma samples were frozen at -20°C and shipped frozen on dry-ice; whereas, fresh EDTA tubes were shipped in ambient temperature to NHSBT Filton, UK.

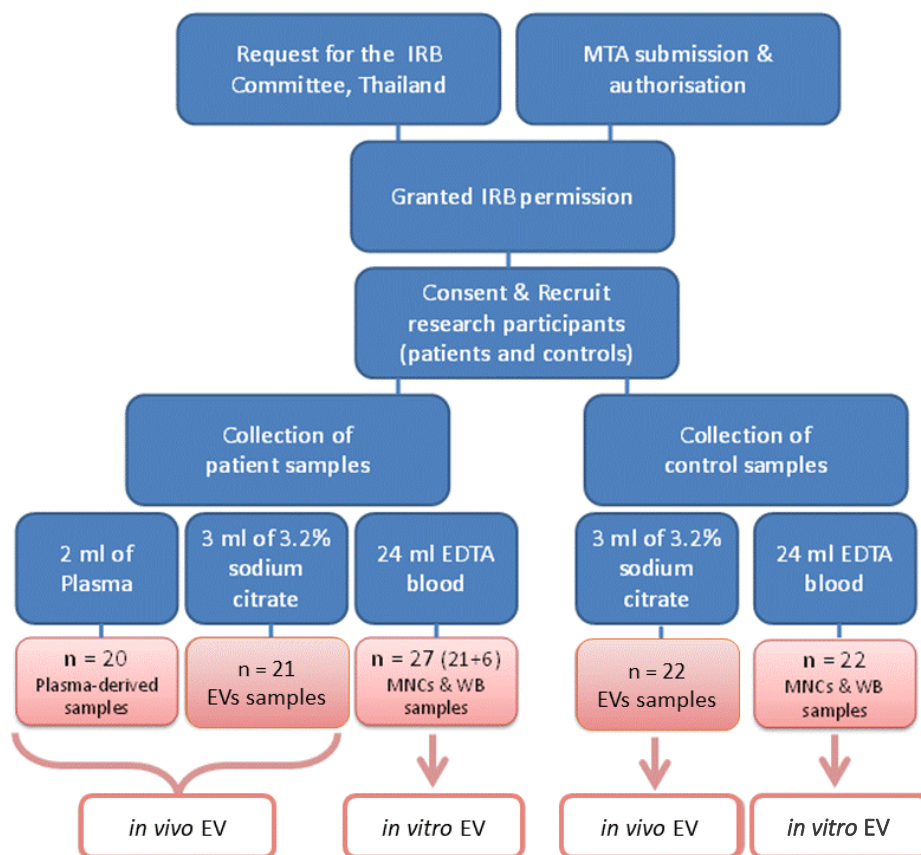


Figure 2.1. Workflow diagram of EVs characterisation.

The chart summarises permissions requested, sample collection, types and numbers of samples, and the analysis conducted. IRB = International Review Board, MTA = Material Transfer Agreement, EVs = extracellular vesicles.

2.1.1.3 Clinical trial recruitment

All the patients and controls for the clinical follow-up trial (discussed in Chapter 5) were recruited between October 2017 to June 2018. The samples included 12 transfusion-dependent thalassaemic (TDT) patients, 18 non-transfusion-dependent thalassaemic (NTDT) patients, eight thalassaemic carriers, and seven healthy controls. Blood samples from the TDT patients were collected during their regular hospital visits for transfusion. EDTA blood samples were taken at pre-transfusion and one-hour post-transfusion sampling points for five visits; therefore, ten samples were collected from an individual patient. The NTDT patients were invited to have their blood collected every three months for a total of three visits. The thalassaemic carriers and the controls had their blood collection on the day of recruitment. For the trial organisation and type of samples see Figure 2.2. Over the period of recruitment, all blood samples were successfully collected from the TDT group. However, 16 visits of

patients in the NTDT group were lost to follow-up. One patient was excluded from the study due to tuberculosis infection; others were non-compliant to follow-up.

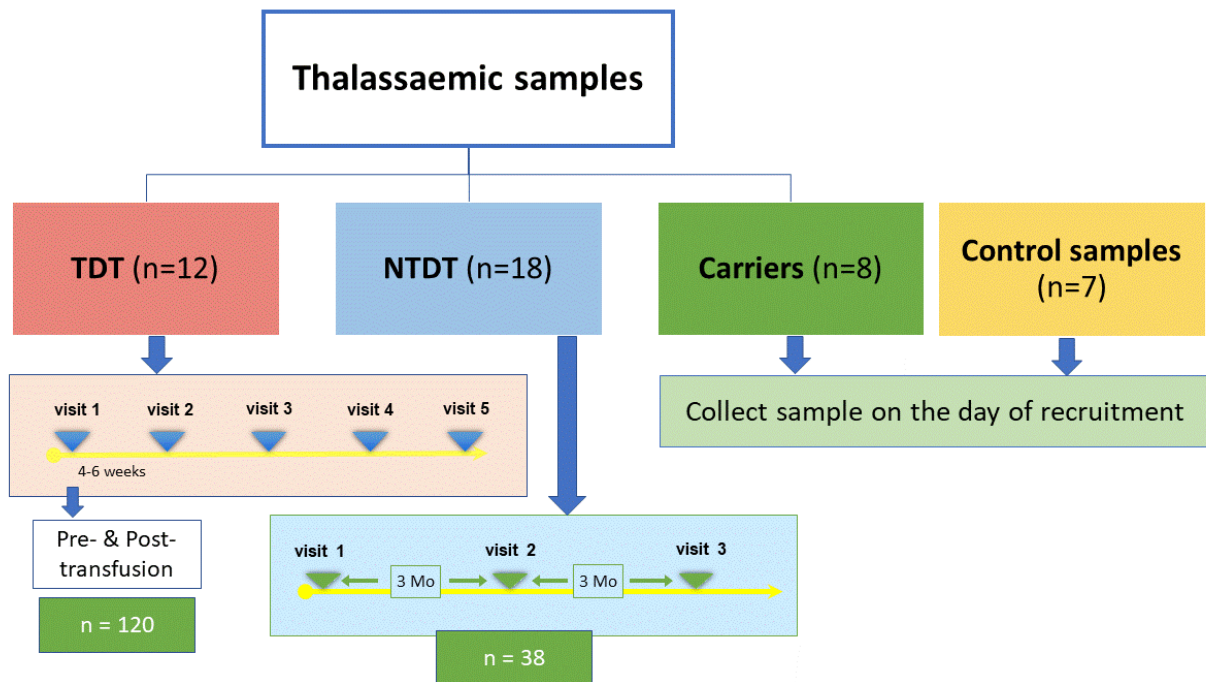


Figure 2.2. Scheme of blood collections of the clinical follow-up study.

In a total of five visits every four to six weeks per patient, pre- and post-transfusion samples were collected from 12 TDT patients (n=120). NTDT patients (n=18) had their blood sample collected at three visits, but due to non-compliances, a total number of NTDT samples was 38. Carrier and control samples were collected at the day of recruitment.

2.1.1.3 Fresh CD34⁺ cells as control samples

The fresh CD34⁺ samples used as controls in the optimisation of *ex vivo* cell cultures were derived from two sources; by-products of blood donations, and three healthy volunteers. Volunteers' blood was obtained to determine the minimum volume of blood needed for CD34⁺ cell isolation in section 3.2.2, Chapter 3. EDTA blood (24 ml) from three healthy volunteers was collected after the written permission and consent had been obtained. All other fresh CD34⁺ samples used in this thesis were isolated from by-products of blood donations, either buffy coats or apheresis cones provided by Non-Clinical Issue Department (NCI, NHSBT Filton, Bristol, UK).

2.1.1.4 Genomic DNA of thalassaemic patients and healthy controls

All the patients' genomic DNA (gDNA) was extracted from the recruited patients and seven controls at the Faculty of Medicine, Siriraj Hospital, and shipped for further tests to NHSBT, Filton, UK. All gDNA obtained were quantified by Qubit Fluorometer® (Thermo Fisher Scientific, Loughborough, UK) according to the manufacturer's instructions. All patients and controls provided written consent for genomic DNA work.

2.1.2 Commercial chemicals and suppliers

Chemicals

1,2-Bis(dimethylamino)ethane (TEMED)
2-Mercaptoethanol
30% Acrylamide solution
Albumin for bovine serum (BSA, Fraction V)
Bradford Reagent
Bromophenol blue
Citrate-dextrose solution (ACD)
Citrate-phosphate dextrose (CPD)
Complete protease inhibitor cocktail tablet
Coomassie brilliant blue G
Dexamethasone
Dimethyl sulfoxide (DMSO)
Disodium phosphate (Na₂HPO₄)
Dried skimmed milk
Dulbecco's phosphate buffered saline
Ethanol absolute (EtOH)
Ethidium bromide (EtBr)
Fetal calf serum
Giemsa's stain solution
Gel loading buffer
Glycerol
Glycine

Suppliers

Sigma-Aldrich, Poole, UK
Sigma-Aldrich
Severn Biotech Ltd, Kidderminster, UK
Sigma-Aldrich
Sigma-Aldrich
VWR International Ltd, Lutterworth, UK
Sigma-Aldrich
Sigma-Aldrich
Roach Diagnostics Ltd, Burgess Hill, UK
Sigma-Aldrich
Sigma-Aldrich
VWR International Ltd
Premier Foods, Stafford, UK
Sigma-Aldrich
Fisher Scientific, Loughborough, UK
Sigma-Aldrich
Fisher Scientific
VWR International Ltd
Sigma-Aldrich
Fisher Scientific
Severn Biotech Ltd

Hank's balanced salt solution (HBSS)	Sigma-Aldrich
Histopaque®-1077 Hybri-Max™	Sigma-Aldrich
Human holotransferrin	R&D systems, Abingdon, UK
Human serum group AB	Sigma-Aldrich
Human serum albumin (HSA)	Irvine Scientific, Wicklow, Ireland
Hydrocortisone	Sigma-Aldrich
Interleukin-3	R&D systems
Iscove's modified Dulbecco's medium (IMDM)	BD BioScience, Wokingham, UK
Leishman's eosin-methylene blue stain (Gurr®)	VWR International Ltd
May-Grunwald's stain solution	Sigma-Aldrich
Methanol (MeOH)	Fisher Scientific
Penicillin/Streptomycin	Sigma-Aldrich
Phenylmethanesulfonyl fluoride (PMSF)	Sigma-Aldrich
Phosphate buffered saline (PBS)	Sigma-Aldrich
Potassium bicarbonate (KHCO ₃)	Sigma-Aldrich
Potassium chloride (KCl)	VWR International Ltd
Potassium dihydrogen phosphate (KH ₂ PO ₄)	VWR International Ltd
Recombinant human insulin	Sigma-Aldrich
Sodium chloride (NaCl)	Sigma-Aldrich
Sodium dihydrogen phosphate (NaHPO ₄ .7H ₂ O)	VWR International Ltd
Sodium dodecyl sulphate (SDS)	Sigma-Aldrich
Sodium hydrogen carbonate (NaCO ₃)	Fisher Scientific
Sodium hydroxide (NaOH)	Fisher Scientific
Stem cell factor	R&D systems
Tris base/boric acid/EDTA (TBE) buffer	Sigma-Aldrich
Triton-100	Sigma-Aldrich
Trypan blue solution	Sigma-Aldrich
Trypsin	Sigma-Aldrich
Tween-20	Sigma-Aldrich
<u>Protein markers</u>	
Magic Mark XP	Life Technologies, Warrington, UK
Novex Sharp	Sigma-Aldrich

Reagent kits

Human Cathepsin S ELISA kit (ab155427)	Abcam, Cambridge, UK
Human Haptoglobin ELISA kit (ab108856)	Abcam
Human Hemopexin ELISA kit (ab108859)	Abcam
MiniMACS® Direct CD34 progenitor cell isolation Kit	Miltenyi Biotech Ltd, Woking, UK
MiniMACS® magnetic Multi-stand	Miltenyi Biotech Ltd
MiniMACS® MS column	Miltenyi Biotech Ltd
MiniMACS® LS column	Miltenyi Biotech Ltd
Western Lightning Plus-ECL	PerkinElmer, Seer Green, UK

2.1.3 In-house buffers and chemicals

'310' buffer (iso-osmotic, phosphate buffer): Na_2HPO_4 103 mM, NaH_2PO_4 155 mM, pH 7.4.

Buffered water: diluted Sorenson buffer, 1:20 dilution in distilled water

Lysis buffer: 1 in 20.5 dilutions of 310 buffer with water containing 1x complete protease inhibitor and 0.5 mM PMSF.

MACS buffer: 5 tablets of PBS (1 tablet/100 ml H_2O) dissolved in 500 ml distilled H_2O + 0.6% citrate phosphate dextrose, pH 7.2 + 0.5% BSA (Fraction V), stored at 4°C.

Red cell lysis buffer: 150 mM NaCl, 1 mM EDTA.2 H_2O and 10 mM KHCO_3 , pH 7.5 with NaOH, filtered through a polyethersulfone vacuum filtration unit (Nalgene® Labware, Thermo Fisher Scientific), stored at -20°C. Aliquoted buffer was thawed at 37°C in a water bath before use.

Sorenson buffer: KH_2PO_4 33 mM, Na_2HPO_4 33 mM, pH 6.8.

Tris-buffered saline (TBS) Tween: 25mM Tris, 0.15M NaCl, 0.02% Tween-20 (Sigma-Aldrich), pH 7.7.

Trypan blue solution: 0.4% solution diluted 1:10 with 1xPBS.

2.1.4 Antibodies

2.1.4.1 Antibodies for Western blot analysis

Primary antibodies used in Western blotting analyses of proteins of interest are listed in Table 2.1.

Table 2.1. Primary antibodies used for Western blotting of selected proteins.

Protein	Clone	Animal	Source	Dilution	2 nd Ab	Expected bands	Pos CT	Gel	Reduced
GPA	CVDP RIFP	Rabbit	In-house	1 in 2000	DaR 1:2500	Monomer 43 kDa Heterodimer 68 kDa Dimer 86 kDa	RBC mb	10%	yes
AHSP		Rabbit monoclonal	A kind gift from Dr.Rebecca Griffith	1 in 500	DaR 1:2500	12 kDa	RBC lysate	15%	yes
Catalase	polyclonal	Rabbit	Abcam	1 in 2000	DaR 1:2500	60 kDa	RBC lysate	10%	yes
Haptoglobin	EPSISR7	Rabbit monoclonal	Abcam	1 in 10000	DaR 1:2500	45 kDa	RBC lysate	10%	yes
Hemopexin	polyclonal	Rabbit	Abcam	1 in 50-100	DaR 1:2500	52 kDa	RBC lysate	10%	yes
Cathepsin S	polyclonal	Rabbit	Abcam	1 in 1000	DaR 1:2500	25 kDa (predicted 37 kDa)	Spleen lysate	12.50%	yes

2nd Ab – secondary antibody, Pos CT – positive control

Secondary antibody for Western blot analysis: donkey anti-rabbit IgG (Jackson Immuno Research Laboratories INC., Ely, UK).

2.1.4.2 Antibodies for flow cytometry

FITC conjugated BRIC256 (Glycophorin A, extracellular domain/ CD235a) mouse IgG1 (IBGRL Research Products, NHSBT Filton, UK).

2.1.5 Analysis Software

Software

Kaluz software

SPSS v.18

Developer

Beckman Coulter Inc, High Wycombe, UK

IBM Analytics, New York, USA

2.2 Methods

2.2.1 CD34⁺ isolation from adult peripheral blood

Buffy coats provided starting material for isolation of CD34⁺ progenitor cells, which were to be used in cell culture experiments. Buffy coats (approximately 50 ml) were diluted (1:1 v/v) with Hank's buffer salt solution (HBSS) with 1% citrate-dextrose solution (HBSS-C), then mononuclear cells (MNCs) were separated using gradient separation with Histopaque-1077. Mononuclear cells were then purified by washing out contaminating platelets with HBSS-C, as well as lysing remaining red blood cells with in-house ammonium chloride-based lysis buffer solution. After a 10-minute incubation, lysed red cells were removed by washing with HBSS-C. Subsequently, cells were washed with cold MACS buffer by centrifugation at 400g for 5 minutes at 20°C. Cells were then resuspended with 300 µl MACS buffer, 100 µl MACS CD34⁺ magnetic beads and 100 µl MACS blocking antibody per 10⁸ MNC cells and incubated at 4°C in MACS continuous spinning device for 30 minutes. Cells were washed and resuspended in 5 ml of chilled MACS solution. Next, CD34⁺ cells were purified with MACS LS column with a sieve, attached to MiniMACS[®] magnetic multi-stand, by letting the unlabelled cells pass through the column, then washing the column with 1 ml of MACS buffer three times. The LS column was removed from the magnet, and the CD34⁺ cells were eluted with 5 ml of MACS buffer into a 15 ml Falcon tube (Thermo Fisher Scientific). For better purity, the separating steps on a magnet were repeated with MACS MS column and following three washes with 500 µl MACS buffer, CD34⁺ cells were eluted into a Falcon tube with 1 ml of MACS buffer. After centrifugation, the pellet containing the cells was resuspended in IMDM medium. Cells were stained with trypan blue at the concentration of 1:1 (v/v) to check viability and number of CD34⁺ cells. The Neubauer chamber (NanoEnTek Inc) was used for manual cell counting.

2.2.2 Three-stage erythroid culture based on Griffiths *et al.* (2012)

The three-stage culture system was based on changing the supplemented medium according to the growth stage of erythroid cells. Principle ingredients for all stages of the cell culture were IMDM base medium, 30 µlml⁻¹ 3% (v/v) human, male, group AB serum, 2 mgml⁻¹ human serum albumin, 10 µgml⁻¹ recombinant human insulin, 3 Uml⁻¹ erythropoietin and 1 Uml⁻¹ unfractionated heparin. In the first stage of culture, days 0 to 7, the primary medium

contained 1 ngml⁻¹ IL-3, 10 ngml⁻¹ stem cell factor, and 200 µgml⁻¹ hHolotransferrin. The secondary stage medium was applied from day 8 to day 10 of erythroid expansion; from this stage onwards, IL-3 was omitted, and transferrin concentration was increased to 500 µgml⁻¹. The tertiary stage of the culture (day 11 onwards) involved omitting SCF from the medium and retaining the other components until the end of the culture. Cells were seeded into stationary plastic tissue culture flasks at a density of 1 x 10⁵ cellsm⁻¹. The culture cells were all kept at 37°C in a humid atmosphere of 5% CO₂ in the air. Cells were counted every day and maintained by the addition of fresh medium in the range of 1 x 10⁵ and 2 x 10⁵ cellsm⁻¹ during the first phase, then between 3 x 10⁵ and 5 x 10⁵ cellsm⁻¹ during the remaining culture period. Morphology of cells was monitored by cytopsin slide preparations.

2.2.3 Three-stage erythroid cultures with corticosteroids

Cells were grown following Griffiths *et al.* (128) culture protocol, as described in section 2.2.2, in an incubator with 5% CO₂ and humidified air. The dosages of dexamethasone (DXM) and hydrocortisone (HC) used in this study were 10⁻⁶ M. Steroids were added at the start of the cultures and were removed from the culture medium on day 11 by washing the cells with HBSS and placing them into the steroid-free tertiary medium (cells were treated with steroids during days 0 to 11 of culture). Numbers of cells were regularly monitored on alternate days throughout the experiment and maintained between 1 x 10⁵ and 2 x 10⁵ cellsm⁻¹ during the first phase, then between 3 x 10⁵ and 5 x 10⁵ cellsm⁻¹ until the end of culture. Morphology of cells was monitored by cytopsin slide preparations.

2.2.4 Cell morphology monitoring

Cell morphology and maturation were assessed by visual analysis of cytopsin slides on alternate days of the culture. After labelling cytopsin slides, the cell preparations were resuspended in 10% HSA at a concentration of approximately 4 x 10⁵ cellsm⁻¹ in a total volume of 300 µl and added to the cytopsin slides. The slides were placed in the cytopsin cassettes and centrifuged at 1365rpm for 5 minutes. Cells were visualised by staining, described in section 2.2.5, and analysed under a light microscope.

2.2.5 Cytospin slide staining

Cytospin slides were air dried and dyed using either May-Grünwald Giemsa stain or Leishman's stain.

2.2.5.1 May-Grünwald Giemsa stain

Slides were fixed with absolute methanol for 10 – 20 minutes and stained with May-Grünwald's stain for five minutes, followed by Giemsa's stain for 10 – 15 minutes. Lastly, slides were rinsed in buffered water (pH 6.8) for one to two minutes and air-dried.

2.2.5.2 Leishman's stain

Leishman's Eosin-Methylene blue stain was used to fully cover slides for 1 minute. Buffered water was applied for 5 minutes. Lastly, slides were rinsed with buffered water (pH 6.8) for 1 – 2 minutes and air-dried.

2.2.6 Reticulocyte filtration

On day 21 of the cultures, cultured cells were harvested via centrifugation at 400g for 5 minutes. They were washed once with HBSS; then the cell suspension was loaded into a leukocyte reduction filter (Pall Corporation, Portsmouth, UK). HBSS was used to pre-wet the filter and was passed through the filter after finishing cells filtration.

2.2.7 EVs isolation

Ultracentrifugation (UC) method was used for isolation of EVs from all the *in vivo* sources. When EVs were generated *in vitro*, the filtration method was used for non-proteomics study and UC was used for EV preparation for proteomic analysis. The diagram illustrating the steps of EVs isolation using UC methods is depicted in Figure 2.3 (347).

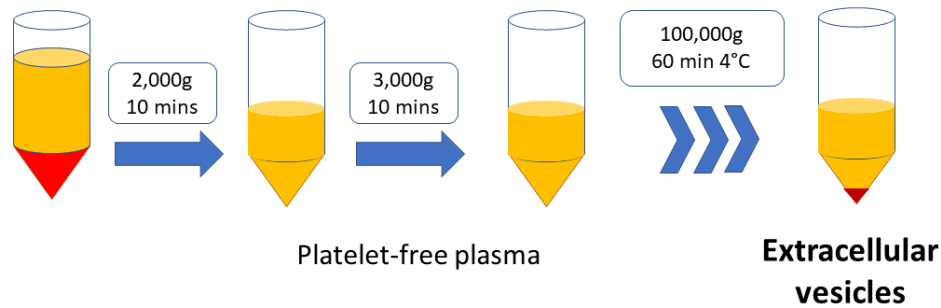


Figure 2.3. Schematic showing the ultracentrifugation technique used to isolate extracellular vesicles from cell plasma or liquid media culture.

Plasma/culture media was centrifuged to remove cellular components and debris by lighter spins at 2000g for 10 minutes and 3000g for 10 minutes; then the EV pellet was obtained by the ultracentrifugation process by Optima L-100XP centrifuge (Beckman Coulter) using fixed-angle rotors set at 100000g at 4°C for 60 minutes.

2.2.7.1 EVs isolation from *in vivo* sources (ultracentrifugation)

2.2.7.1.1 EVs isolation from plasma-derived samples

Twenty cases of HbE/ β -thalassaemia patients were used in the study as plasma only samples. Approximately 2 ml of plasma that remained from the blood samples taken for routine complete blood count was collected in each case. The cell separation was undertaken as soon as possible to minimise *ex vivo* EV generation. Plasma samples were, therefore, processed at the Siriraj Hospital (Bangkok) for EV extraction on the day of collection. They were centrifuged using a series of centrifugation speeds: 500g for 5 minutes to remove cellular debris, followed by 2000g for 10 minutes at 4°C to get the platelet-free plasma, and then 3000g for 10 min at 4°C. All the centrifuged plasma-derived samples were frozen at -20°C and shipped on dry ice to NHSBT Filton (Bristol) for further investigations.

2.2.7.1.2 EVs isolation from 3.2% sodium citrate blood samples

A total volume of 3 ml of 3.2% sodium citrate blood was collected at the same sampling time for the same study participants as the EDTA blood collection, because calcium ions are chelated by citrate, and this is claimed to prevent the vesiculation process, or *in vitro* EV generation related to blood sample handling and storage. Moreover, it has been shown that EV levels elevated *in vivo* remained detectable (381, 382). The 3.2% sodium citrate samples were intended to represent the *in vivo* EV generation in thalassaemic patients and controls. They underwent centrifugation as described above for the plasma samples, but with an additional, final step where the samples underwent UC for 100000g for 60 minutes at 4°C. All

samples were processed within 12 hours of their collection in order to minimize iatrogenic EV production. The EV pellets were diluted with 100 µl PBS and frozen at -20°C before transporting to NHSBT, Filton.

2.2.7.2 EVs isolation from *in vitro* sources (cultured reticulocytes)

In vitro EV production was assessed from cultured filtered reticulocytes. At day 21 of erythrocyte culture, cells were filtered with a leukocyte filter, LeuKoGuard™ (Pall Corporation), to purify reticulocytes. After filtering, reticulocytes were washed with a fresh particle-free tertiary medium which had been pre-centrifuged by UC at 100000g for 1 hour to remove any remaining EVs from the AB serum and resuspended with this new medium at a concentration of 1×10^7 cellsml⁻¹. Reticulocytes were stored at 37°C and 5% CO₂ and humidified air for 72 to 96 hours prior to vesicle isolation. This process was designed to augment particles released from the reticulocytes for further experiments.

2.2.7.2.1 Ultracentrifugation method for *in vitro* generated EVs

The isolation procedure was completed, as shown in detail in Figure 2.3; samples were centrifuged at 2000g 10 min at 4°C, then the supernatant was removed and centrifuged again at 3000g. These two centrifugation steps served to remove any intact cells from the sample. Supernatants were decanted and used for the last UC (Optima L100 XP, Beckman Coulter) at 100000g at 4°C for 1 hour. Supernatants were discarded, and the EV pellets were collected and diluted with filtered PBS in the volume appropriate for the downstream application.

For proteomic analysis, 30 µl of PBS was added to dissolve the pellet, as well as 1 mM of PMSF and cOmplete™ protease inhibitor (PI) to stop the proteolytic process in the sample; then it was stored at -20°C, ready to quantify and analyse.

2.2.7.2.2 Ultrafiltration method for *in vitro* generated EVs

The Filtration technique by using an MF-Millipore®, 0.22 µm pore size (Merck KGaA, Darmstadt, Germany) was employed to enrich EVs for the non-proteomic study samples. The filter device was equilibrated with PBS once, and the sample was added and centrifuged at 4000g for 30 minutes. The sample was collected, and the filter membrane was washed multiple times to ensure complete EV recovery.

2.2.8 Flow cytometry

Flow cytometry was used to quantify EVs in samples of both *in vivo* and *in vitro* origins.

2.2.8.1 Flow cytometry for *in vivo* EVs (plasma-derived samples)

Plasma samples were thawed. A total of 4 µl of each sample was added to 40 µl of commercially available counting beads (Flow-Count™ Fluorospheres; Beckman Coulter Inc.) and then diluted with 436 µl phosphate buffer solution (PBS) in order to obtain an optimal dilution of 1:100. The optimal concentration of EVs was previously determined in preliminary experiments (data not shown). As illustrated in Figure 2.4, from the side scatter (SS) and forward scatter (FS) logarithmic graph, EVs were localised in “A” region. The Flow-Count beads were identified in the “C” area of the logarithmic graph (SS against FS) by their distinct size when compared to EVs. The numbers of erythrocyte vesicles were calculated from the formula used in a previous study (358) as follows:

$$RBC\ vesicles/\mu l = \left(\frac{\text{no. of antibodies positive events (A)}}{\text{no. of beads in C region}} \right) \times \frac{\text{Bead count per test}}{\text{Sample volume } (\mu l)} \times DF$$

All the tests were performed with Navios™ Flow Cytometer (Beckman Coulter Inc.). The flow cytometry results were analysed with the help of Kaluza® software (Beckman Coulter Inc).

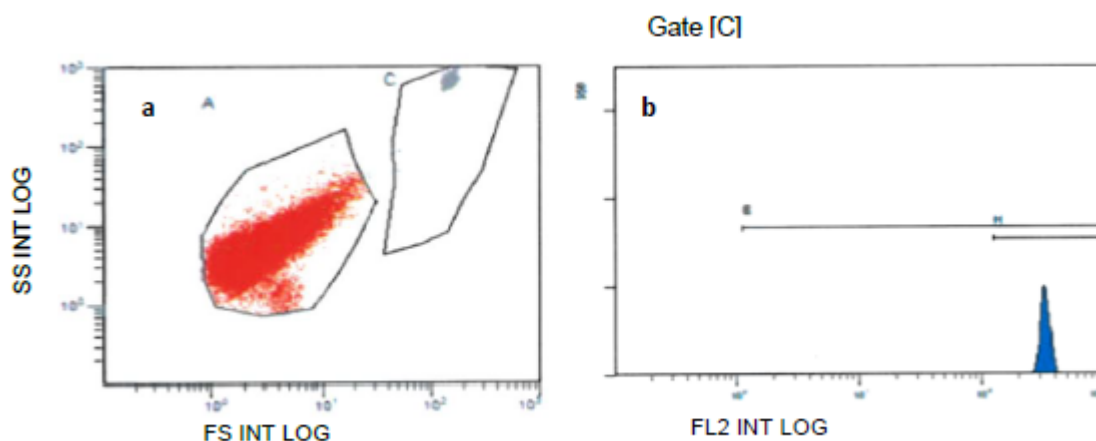


Figure 2.4. Example of flow cytometry analysis of the EVs derived from the thalassaemic plasma-derived sample.

(a) Dot plot of forward scatter (FS) and side scatter (SS) of EVs at A region with Flow-Count beads represented in C region. (b) Histogram of Flow-Count beads in C region.

2.2.8.2 Flow cytometry for *in vitro* EVs (from cultured reticulocytes)

Following UC spin, the *in vitro* EVs obtained from cultured reticulocytes were diluted with 200 μl of PBS and stored at -20°C . At the time of use, these EV samples were to be thawed and labelled with antibodies, as well as counting beads, in the same manner as the EVs derived from plasma samples. For *in vitro* EV samples, all the tests were performed with NaviosTM Flow Cytometer (Beckman Coulter Inc.), and the flow cytometry results were analysed with the help of Kaluza[®] software (Beckman Coulter Inc).

2.2.9 Nanoparticle tracking analysis (NTA)

Plasma samples, the same samples used for flow cytometry testing, were prepared by thawing the frozen plasma and diluting it with PBS at ratio 1:1000 (v/v). An optimal concentration for each sample was determined by titration in a preliminary experiment (data not shown) for $2-10 \times 10^8$ of particles ml^{-1} , which contained approximately 20-60 microspheres/microscope field. The NTA instrument used for characterising EV was a NanoSight LM10 (Malvern Panalytical Ltd, Malvern, UK), software version 2.3. The instrument was standardised prior to measuring the samples with polystyrene latex microspheres, 100 nm and 200 nm in size. The sample chamber was rinsed with PBS to remove all the remaining particles. The sample was infused into 1 ml syringe and then connected to the chamber. The content was slowly introduced to avoid creating air bubbles. After loading of the sample, the temperature probe was connected to the analytical box to monitor temperature during the analytic process. The laser beam as the source of light was switched on, and the optimal analysing area was identified. The best zone for analysis was the space next to the reference spot, the 'thumbprint-like shape', as illustrated in Figure 2.5. The camera level was adjusted to identify the proper saturation of EVs spot, and a video was captured, where the length of video recording was related to the concentration of particles and polydispersity of samples. A low concentration and low polydispersity of vesicles required shorter recording times. Five movies were recorded for each sample and were allocated to a single quantifying method. In terms of video analysis, the detection threshold was adjusted according to the concentration of EVs in one microscopic view. The positions of EVs in the field were identified by the presence of red crosses, whereas the blue crosses represented noise or too low threshold.

Fluid viscosity was set at 1.0, according to PBS viscosity. A total of five movies were recorded per sample, and these were analysed altogether to increase the level of accuracy (360).

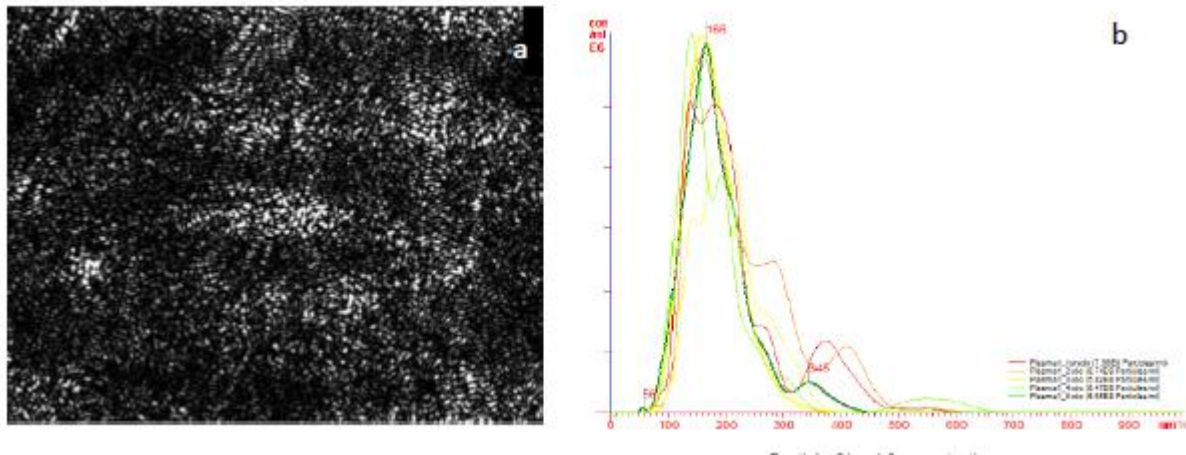


Figure 2.5. An example of nanoparticle tracking analysis.

(a) The reference point, the “thumbprint” area. Modified from Gardiner C *et al.* Extracellular vesicle sizing and enumeration by nanoparticle tracking analysis. *J Extracell Vesicles* . 2013; 15,2. (b) Graph of NTA analysis of plasma sample 1. It demonstrates a median particle size of 166 nm, where each line represents one video movie with a total of 5 videos analysed for each sample. Details at the right lower quadrant state concentrations of particles for each video analysis.

Size distribution of EV was measured by D-value. D-value is one of the most frequently used parameters describing particle size distribution in fluid suspension. The current NTA technique was modified from the grain size distribution (GRADISTAT) described by Blott and Pye in 2001 by producing an S-curve of cumulative mass (see (383) for more information). D-values at D10, D50, and D90 are the diameter which, when particles are arranged in order of ascending mass (mass is equivalent to volume in spherical shape particles), divides the sample’s mass into 10%, 50%, and 90%. Thus, D50 represents mid-point value where 50% of particles have a particular size. The approximate ranges of size can be obtained from D10 and D90 (384).

2.2.10 Protein quantitation using Bradford’s assay

Bradford protein dye reagent was used for measuring protein concentration in the EV samples intended for proteomic analysis. Duplicate sample aliquots of 10 μ l were added into the Bradford reagent (Sigma-Aldrich) at 1:10 concentrations and then incubated at room

temperature for 2 minutes. The Camspec M550 Double Beam SPF Scanning UV/Vis spectrophotometer (Spectronic Camspec Ltd, Leeds, UK) was used for light absorbance measurements at a wavelength of 595 nm. Subsequently, the average values for each sample were plotted against the standard curve created using standard bovine serum albumin at different concentrations of 0, 5, 10, 20, 30 and 40 $\mu\text{g}\mu\text{l}^{-1}$.

2.2.11 Ghost membrane preparation

All of the buffers, centrifuge tubes and rotor (Beckman centrifuge) were chilled at 0°C to avoid re-sealing of membranes and Hb contamination. Cells were washed twice in cold PBS, followed by two washes in 310 buffer. Subsequently, cells were lysed in a large volume of the lysis buffer (>30 times cell volume), followed by centrifugation at 15000rpm for 10 minutes at 4°C. The first supernatant was collected and kept as a cytoplasmic fraction. The lysis step was repeated until the membrane pellet became white. The samples were stored at -20°C.

2.2.12 Western blotting

EV proteins were diluted at 1:1 (v/v) with SDS sample buffer. The samples were incubated at 95°C for 3 minutes before being solubilized with 5% (w/v) 2-mercaptoethanol. The samples were separated on 10% to 12.5% polyacrylamide gels and transferred to polyvinylidene difluoride membranes in a semi-dry transfer system using the blotting apparatus. The membranes were blocked for 1 hour with 5% milk supplemented with 0.05% Tween 20 in PBS [PBS-T], then the primary antibodies were added and incubated at 4°C overnight. After sequential PBS-T washing was performed three times, the secondary antibody was added to each membrane and incubated for 1 hour. Chemiluminescent detection was carried out using ECL Plus reagent (Western Lightning; PerkinElmer) and visualised in Kodak Image Station 4000R (Carestream Health, Inc., Rochester, NY, USA).

2.2.13 Proteomic analysis: TMT labelling and high pH reversed-phase chromatography

Proteomic samples were processed by the University of Bristol Proteomics Facility (Bristol, UK). Aliquots of 100 μg of samples per experiment were digested with trypsin (2.5 mg trypsin

per 100 mg of protein; 37°C, overnight), labelled with TMT reagents according to the manufacturer's protocol (Thermo Fisher Scientific) and the labelled samples were pooled in equal ratios. An aliquot of the pooled sample was evaporated to dryness and resuspended in buffer A (20 mM ammonium hydroxide, pH 10) prior to fractionation by high pH reversed-phase chromatography using an Ultimate 3000 LC system (Thermo Fisher Scientific). In brief, the sample was loaded onto an Xbridge BEH C18 column (130Å, 3.5 mm, 2.1 mm x 150 mm; Waters) in buffer A, and peptides were eluted with an increasing gradient of buffer B (20 mM ammonium hydroxide in acetonitrile, pH 10) from 0% to 95% over 60 minutes. The resulting fractions were evaporated to dryness and resuspended in 1% formic acid prior to analysis by nano-LC-MS/MS using an Orbitrap Fusion Tribrid mass spectrometer (Thermo Fisher Scientific).

2.2.14 Nano-LC mass spectrometry

High pH reversed-phase fractions were further fractionated using an Ultimate 3000 nano high-performance LC system in line with an Orbitrap Fusion Tribrid mass spectrometer (Thermo Fisher Scientific). Peptides in 1% (v/v) formic acid were injected onto an Acclaim PepMap C18 nano-trap column (Thermo Fisher Scientific). After washing with 0.5% (v/v) acetonitrile, 0.1% (v/v) formic acid, peptides were resolved on a 250-mm x 375-mm Acclaim PepMap C18 reversed-phase analytical column (Thermo Fisher Scientific) over a 150-minute organic gradient, using 7 gradient segments (1%-6% solvent B over 1 minute, 6%-15% B over 58 minutes, 15%-32% B over 58 minutes, 32%-40%B over 5 minutes, 40%-90% B for 1 minute, held at 90%B for 6 minutes, and then reduced to 1% B for 1 minute) with a flow rate of 300 nLmin⁻¹. Solvent A was 0.1% formic acid, and solvent B was aqueous 80% acetonitrile in 0.1% formic acid. Peptides were ionized by nanoelectrospray ionization at 2.0 kV using a stainless-steel emitter with an internal diameter of 30 μm (Thermo Fisher Scientific) and a capillary temperature of 275°C. All spectra were acquired using an Orbitrap Fusion Tribrid mass spectrometer controlled by Xcalibur 2.0 software (Thermo Fisher Scientific) and operated in data-dependent acquisition mode using a synchronous precursor selection – MS3 workflow. Fourier transform mass analysers (FTMS)1 spectrum was collected at a resolution of 120000, with automatic gain control (AGC) target of 200000 and maximum injection time of 50 milliseconds. Precursors were filtered with an intensity threshold of 5000, according to

charge state (to include charge states 2-7) and with monoisotopic precursor selection. Previously interrogated precursors were excluded using a dynamic window (60 seconds 6 10 ppm). The MS2 precursors were isolated with a quadrupole mass filter set to a width of 1.2 m/z. Ion-trap tandem mass spectrometry (ITMS2) spectra were collected with an AGC target of 10000, the maximum injection time of 70 milliseconds, and collision-induced dissociation collision energy of 35%. For FTMS3 analysis, the Orbitrap was operated at 50000 resolution with an AGC target of 50000 and a maximum injection time of 105 milliseconds. Precursors were fragmented by high-energy collision dissociation at a normalized collision energy of 60% to ensure maximal TMT reporter ion yield. Synchronous precursor selection was enabled to include up to 5 MS2 fragment ions in the FTMS3 scan.

2.2.15 Proteomics data analysis

The raw data files were processed and quantified using Proteome Discoverer software v1.4 (Thermo Fisher Scientific) and searched against the UniProt human database (385) (134,169 sequences) using the SEQUEST algorithm. Peptide precursor mass tolerance was set at 10 ppm, and MS/MS tolerance was set at 0.6 Da. Search criteria included oxidation of methionine (115.9949) as a variable modification and carbamidomethylation of cysteine (157.0214) and the addition of the TMT mass tag (1229.163) to peptide N termini and lysine as fixed modifications. Searches were performed with full tryptic digestion, and a maximum of 1 missed cleavage was allowed. The reverse database search option was enabled, and all peptide data were filtered to satisfy a false discovery rate of 5%.

2.2.16 Enzyme-linked immunosorbent assay (ELISA)

All ELISA tests in the project were carried out according to the manufacturer instructions (all Abcam): Haptoglobin (ab108856), Hemopexin (ab108859), and Cathepsin S (ab155427). The ELISA plates were read with 450 nm filter using Tecan Microplate Reader (Reading, UK). Note that, due to the limited sensitivity of the kits, the dilutional tests were carried out to obtain the optimal dilution for haptoglobin and hemopexin in the TDT and NTDT groups. The optimal dilutions used in the project were 1:50 and 1:4 for the haptoglobin and hemopexin tests, respectively.

2.2.17 Statistical analyses

All statistical analyses in this project were carried out using SPSS software v.18 (IBM Corporation). Test for normality was performed by Kolmogorov-Smirnov test for normality, to test whether the hypothesis of skewed samples can be rejected. 95% confidence interval (CI) means the probability of 0.95 to contain the true mean of the population. Statistical significance determines with P-value <0.05 , when P-value <0.0001 designates highly statistical significance.

Associations between two continuous variables were analysed by either Pearson correlation or Spearman's rho correlation test for parametric or non-parametric relationships, respectively. The one-sided hypothesis was performed only when the correlations between two parameters can be predicted either increased or decreased. The bootstrapping statistic, i.e., resampling from the sample to estimate the sampling distribution in the real population, was applied to increase the confidence to represent the population. Comparisons of means were calculated using unpaired *t*-test to analyse the differences of means between the two independent groups and paired *t*-test where repeat samples from the same patients are analysed. If more than two samples were compared, one-way analysis of variance (ANOVA) was performed. For non-Gaussian distributed samples, Mann-Whitney-*U* and Kruskal-Wallis tests were applied for two independent groups and more than two groups, respectively.

CHAPTER 3

***IN VITRO* ERYTHROPOIESIS STUDIES OF HBE/ β -THALASSAEMIC PATIENTS**

3.1 Introduction

There are now numerous *in vitro* erythroid culture systems that are reported to successfully produce reticulocytes originating from human CD34⁺ progenitor cells or peripheral blood mononuclear cells, as discussed in Chapter 1 section 1.1.4 (105, 127, 128, 151, 386). Several studies have successfully used *in vitro* culture methods to study patient samples, for example, hereditary spherocytosis (14, 387, 388) and also the ineffective erythropoiesis observed in the haemoglobinopathy patients (143, 159, 389). Also, *in vitro* erythropoiesis has been used in clinical trials of medications for haemoglobinopathy patients (140-142). More recently, erythroid culture systems have been developed and optimised to generate large numbers of reticulocytes, enough for a mini dose to take forward for a clinical trial (128, 139, 390). These new bulk culture systems have yet to be utilised for the study of haemoglobinopathy patients.

In Thailand, thalassaemic disease is one of the major national health problems due to its high prevalence (<http://www.ithanet.eu/db/ithamaps>). The molecular background of thalassaemia is a loss of a globin gene(s) or the presence of an abnormal globin gene(s), therefore causing a decrease or absence of globin chain synthesis. In β -thalassaemia, the excess α -globin polypeptide forms a haemichrome, which results in increased reactive oxygen species (ROS) and also extracellular vesicle (EV) production (340, 358). The oxidative stress generates EVs directly by causing a loss of membrane phospholipid asymmetry and exposure of phosphatidyl serine which also acts as a senescent signal attracting the reticuloendothelial clearance of RBCs (340). Another mechanism proposed to cause EV generation in thalassaemia is due to an elevation of band 3 tyrosine phosphorylation which reduces the connection between red cells membrane and cytoskeleton proteins, for instance, spectrin, ankyrin, etc. (340, 349). While substantial evidence has focused on the proteomes of haemoglobinopathic erythrocytes (374, 391, 392), only two studies have examined EVs shed from thalassaemic red cells (348, 380) (see 1.5.4.2, Chapter 1). Both studies observed that proteins with altered abundance in thalassaemia intermedia samples were antioxidant proteins, e.g., heat shock proteins and peroxiredoxin, and α -haemoglobin (Hb) (348, 380). The experiments described in this chapter will set out to culture CD34⁺ progenitors isolated from peripheral blood of HbE/ β -thalassaemic patients and controls, using an adapted three

stage *in vitro* erythroid culture process which is optimised to produce large numbers of reticulocytes (128). These cultures will be used to explore whether any alterations specific to HbE/ β -thalassaemia can be detected in the erythroid cells during the erythroid-specific development and maturation, or in EV release from reticulocytes.

3.2 Results

3.2.1 Cold storage of whole blood has minimal effect on CD34⁺ isolation

The control and HbE/ β -thalassaemia patient blood samples used in this study were to be shipped from Thailand, with an anticipated transit time ranging from two to five days. To determine the effects of shipping of blood samples, randomly selected buffy coat (BC) samples (n=3) were split into EDTA tubes and either used for CD34⁺ isolation on the first day as a control (D0 sample), or stored at 4°C for three days (D3 sample) and five days (D5 sample) before isolation of CD34⁺ cells (Figure 3.1A). The isolated CD34⁺ cells were then cultured, as described in section 2.2.2 in Chapter 2. Cell expansion rates and morphology were monitored using cell counts and cytospin preparations on alternative days throughout the 21-day culture period.

CD34⁺ cells were successfully isolated from all stored EDTA samples. The fresh samples isolated on D0 yielded the highest numbers of CD34⁺ cells in all buffy coat samples (n=3; mean \pm SD; $9.97 \times 10^5 \pm 6.24 \times 10^5$ cells). The average number of CD34⁺ cells isolated from D3 and D5 samples were $3.86 \times 10^5 \pm 1.17 \times 10^5$ cells and $5.37 \times 10^5 \pm 2.23 \times 10^5$ cells, respectively. Once cultured, the average cumulative fold increase of D3 CD34⁺ isolated samples gave the steepest proliferative growth curve with up to 91-fold increase. D5 samples had 47-fold, and the control D0 samples 29-fold cumulative fold increase. Figure 3.1B illustrates the cumulative fold increase of the D0, D3, and D5 samples in different stages of the 21-culture period of the Griffiths *et al.* based three-stage cell culture media protocol (128). Stage I designated the primary stage (day 0 to 7), stage II the secondary stage (day 8 to 11), and stage III the tertiary stage of the culture (day 12 onwards). Figure 3.1C shows the average fold increase of the three samples in the three-stages.

Note that, two of the three samples in the D5 groups had to be terminated at day 15 of culture due to bacterial infection. Therefore, surprisingly, although the two controls (D0) had the highest initial CD34⁺ cell count, the expansion rates of these samples were not superior to the samples that had been stored cold for longer. The D3 samples tended to have the greatest fold increase overall. However, more repeat experiments are needed to confirm this finding.

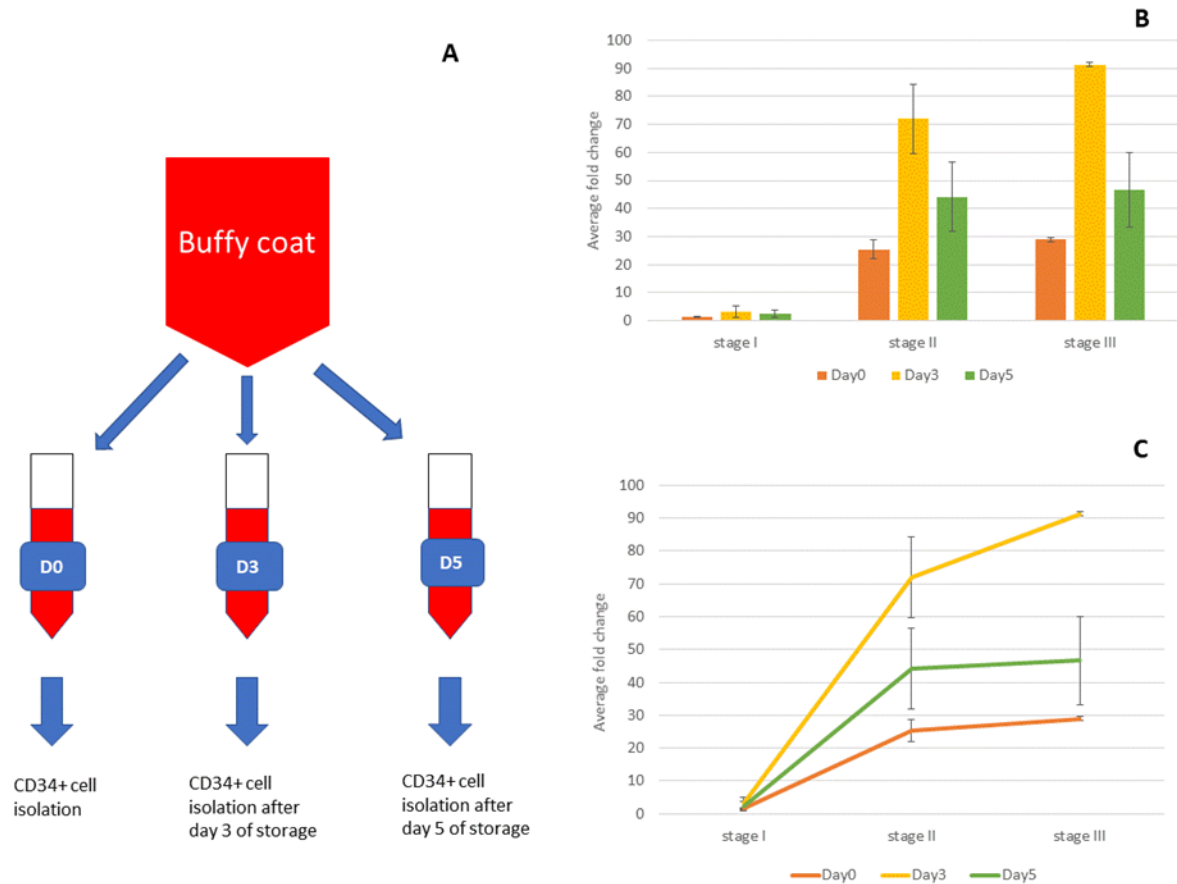


Figure 3.1. Storage effect on CD34⁺ cell isolation from buffy coats and erythroid cell proliferation in three-stage culture.

(A) Three EDTA tubes were generated from three separate buffy coat samples (n=3). CD34⁺ cell isolation was then performed on day 0 (D0), day 3 (D3), and day 5 (D5) following storage at 4°C. **(B)** and **(C)** Cumulative fold change of three samples at different stages of culture and the average fold changes of each stage, respectively. Stage I, II, and III represent day 0 to 7, day 8 to 11, and day 12 to 21 of the 21-day culture period, respectively. The cultures were performed using Griffiths *et al.* (128) three-stage process as described in Chapter 2, and all cultures were maintained until day 21, except for two cultures of D5 that were terminated on day 15 due to bacterial infection.

Throughout the experiment, erythroid differentiation of all of the samples was monitored by morphological analysis of cytopsin preparations on alternate days (from day 5 of culture

onwards). The maturation of cells appeared normal, and reticulocytes were observed from day 13 of D0 sample, and day 14 of both D3 and D5 samples. Comparatively, the stored samples matured faster than the control (D0) in concordance with their storage time, i.e., the D5 sample matured faster than D3 sample (Figure 3.2). However, further repeat experiments are needed to confirm this observation. It could have been concluded though, from these experiments, that a three-day delay of fresh blood stored on ice during shipping from Thailand to Bristol would not be detrimental to the CD34⁺ isolation and planned culture experiments.

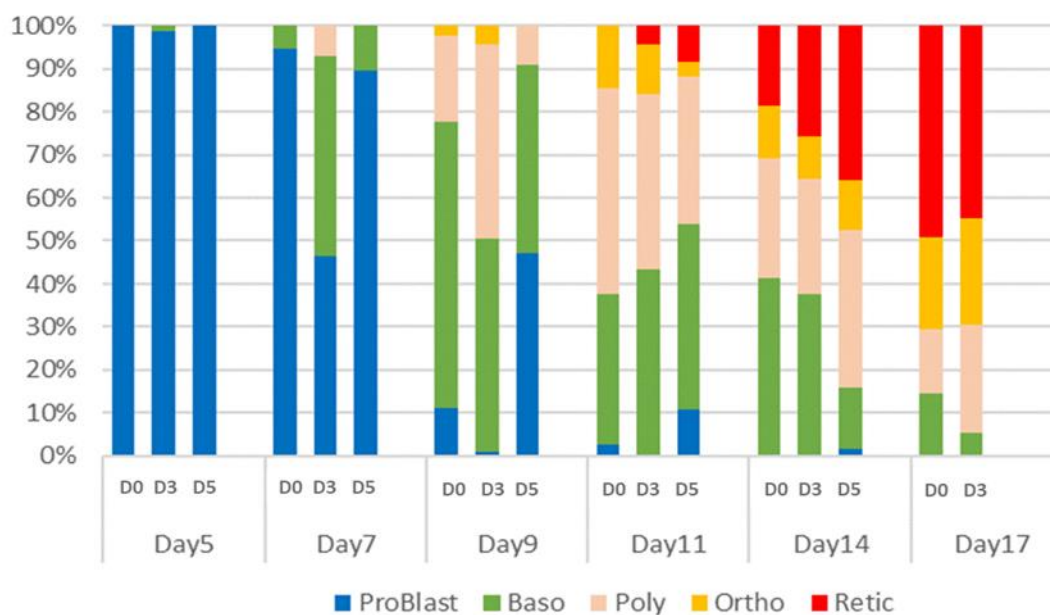


Figure 3.2. The average percentages (n=2) of cells at the stated morphological stage of the control sample (D0), 3-day stored sample (D3), and 5-day stored sample (D5).

The samples stored at 4°C were observed to mature faster than the controls, in concordance with their storage time. Note that at day 17 of the culture sample D5 was terminated early due to bacterial infection. Problast: proerythroblast, Baso: basophilic erythroblast, Poly: polychromatophilic erythroblast, Ortho: orthochromatophilic erythroblast, Retic: reticulocyte

3.2.2 CD34⁺ cell yield from 24 ml of peripheral blood

Since one of the significant features of thalassaemic patients is anaemia, the volumes of blood samples available from the patients were restricted to the lowest minimum threshold. According to previous studies in such patients, the lowest amount of whole blood used for *in vitro* erythroid culture was 20 ml; however, the numbers of progenitor cells isolated from this volume of blood were not reported (141). In the current project, the volume of blood

collected from each patient and control individual obtained from Thailand was agreed with the patients' clinicians to be 24 ml. To determine whether this amount of blood is sufficient for the CD34⁺ cell isolation, three UK-based volunteers were enrolled to provide 24 ml of fresh whole blood each. CD34⁺ isolation was performed (see section 2.2.1, Chapter 2), except for the omission of the MACS LS column (Milteny BioTec) step due to the small numbers of cells. The CD34⁺ cell numbers isolated were 4×10^4 cells, 1.56×10^4 cells, and 1.25×10^5 cells from volunteer 1, 2, and 3, respectively. This work provided confirmation that 24 ml blood volume would provide enough CD34⁺ for erythroid culture experiments.

3.2.3 Glucocorticoids increase erythroid culture yields

There is substantial evidence in the literature that suggests the effectiveness of glucocorticoids at promoting proliferation in the early stages of erythroid cell development (104, 390). Dexamethasone (DXM) has been used successfully in the erythroid cultures carried out previously at the University of Bristol (133, 184). An alternative steroid hydrocortisone (HC) has also been used previously in erythroid culture to produce reticulocytes (132).

Isolated peripheral blood CD34⁺ cells from three donors were cultured using Griffiths *et al.* (2012) three-stage culture system as normal or with the addition of either DXM and HC as described in the materials and methods (section 2.2.2, Chapter 2). Thus, the initial number of cells from a donor available for each arm of the experiment was 2.6×10^5 , 5.6×10^5 , and 6.1×10^5 cells. The observed proliferation rates are depicted in Figure 3.3. During the primary stage of culture (day 0 to day 8), there was no detectable difference between the three experimental culture conditions. DXM and HC were removed from the cultures, and the cells washed on day 11 of culture. During the late stage of cultures (day 13 onwards), the cumulative fold increase of all of the cells cultured with steroids was dramatically higher than the controls, with the highest points of 3.82- and 3.35-fold greater expansion than the control group for HC and DXM, respectively (Figure 3.3). Both groups with corticosteroid additives were observed to have the highest fold expansion on day 16; whilst, the control group reached its proliferative peak on day 14.

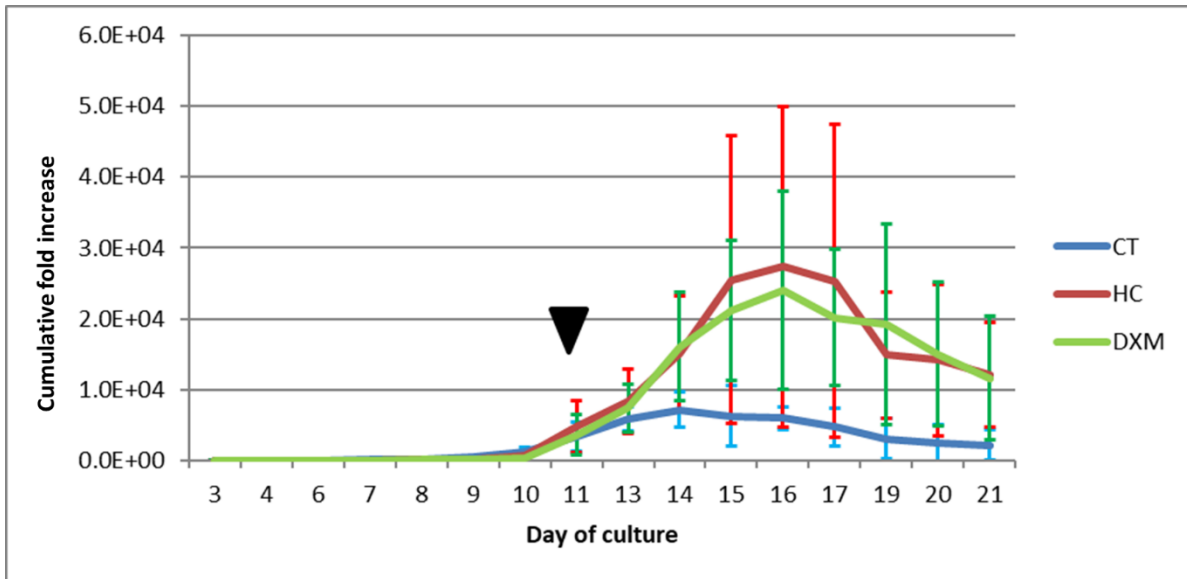


Figure 3.3. The effects of corticosteroid treatment on *in vitro* erythroid culture.

CD34⁺ cells were isolated from three buffy coat units; each unit was split into three experimental arms: control CT, HC additive (10⁻⁶ M), and DXM additive (10⁻⁶ M). Cells were cultured under identical conditions except for where a glucocorticoid addition is indicated. Steroids were removed from all the cultures on day 11 post-isolation (black arrow on the graph). The proliferation rates were monitored and compared across the three treatment arms. Standard errors are shown as error bars (CT in blue, HC in red, and DXM in green colour).

Additionally, the morphology of cells in erythroid cultures was examined periodically by cytospin method. At the same time points on day 8, 12, and 20, in the majority of the glucocorticoid-treated erythroid cell populations, cell morphology was more immature compared to the controls in all experiments (Figure 3.4 and Figure 3.5).

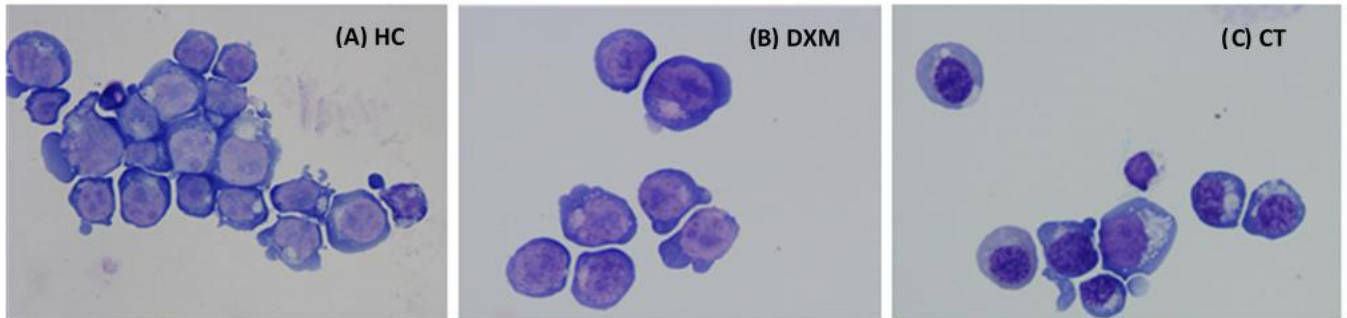


Figure 3.4. Representatives Leishman's stain cytopspins illustrating morphology on day 8 of culture.

(A) = hydrocortisone-treated (10^{-6} M), **(B)** = dexamethasone-treated (10^{-6} M), and **(C)** = control. At day 8, the majority of cell populations from (A) and (B) were proerythroblasts characterised by their large size, fine nuclear chromatin, and presence of nucleolus, whilst cells in (C) were more mature with the appearance of basophilic erythroblasts (smaller in size, with deep blue cytoplasm with perinuclear halo and coarse nuclear chromatin) and polychromatophilic erythroblasts (homogeneous reddish cytoplasm with coarse clumping nuclear chromatin).

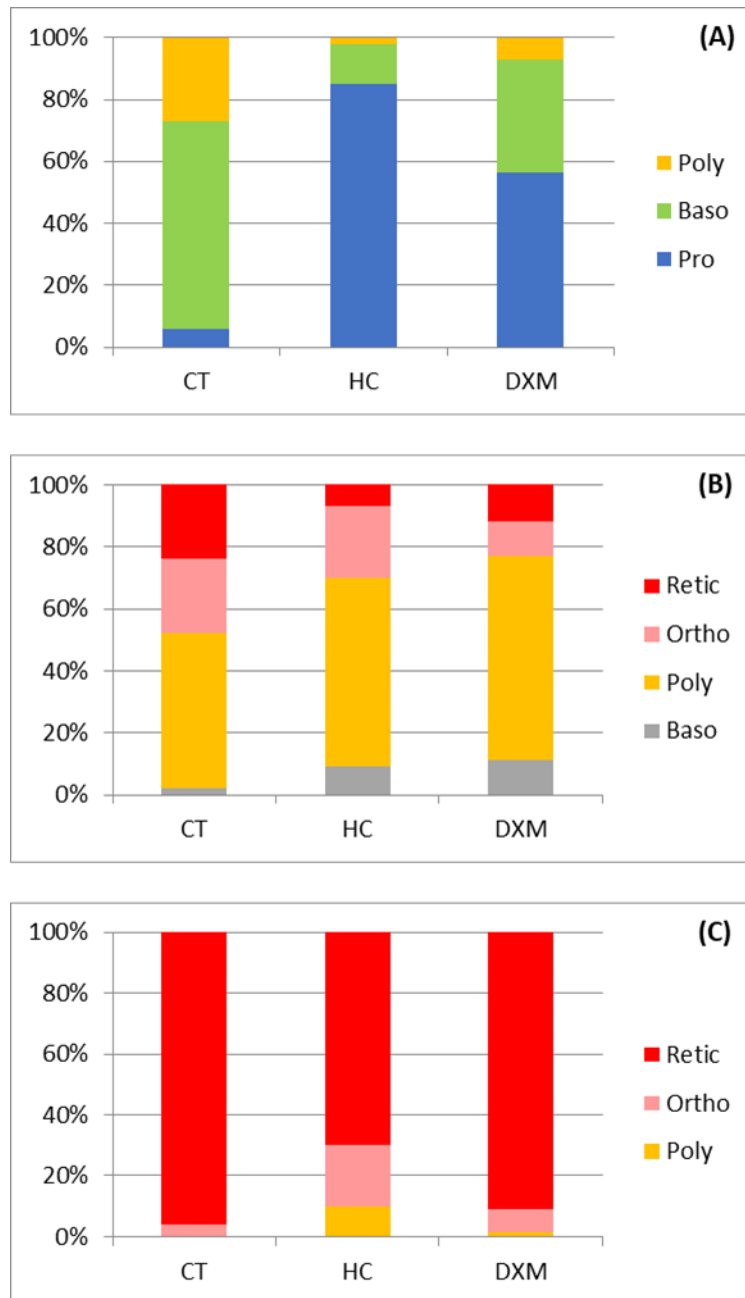


Figure 3.5. Cell maturation of dexamethasone (DXM) (10^{-6} M), hydrocortisone (HC) (10^{-6} M) and untreated controls, analysed on the days indicated using cytopspin images.

A minimum of 200 cells was counted per sample to represent the whole population at a one-time point, then the average numbers from the three samples were calculated. **(A)** day 8 of culture - the majority of cells in control were basophilic erythroblasts; while proerythroblasts were the main population for both steroid-treated samples, **(B)** day 13 of culture and **(C)** day 20 of culture. At day 20, DXM-treatment gave a similar number of enucleated cells (91%) as the control sample (96%); whereas, HC was observed to be lower (70%).

The data from this experiment confirmed the effectiveness of the inclusion of corticosteroids as erythroid lineage proliferation enhancers by delaying cell maturation. In all culture conditions reticulocytes were isolated using leukofilters and the total number reticulocytes obtained at the end of the cultures for the three groups were $8 \times 10^6 \pm 1.5 \times 10^5$ cells for the control, $3.28 \times 10^7 \pm 3.9 \times 10^6$ for HC treated cells and $4.74 \times 10^7 \pm 2.1 \times 10^7$ for DXM treated. The number of reticulocytes generated using corticosteroid was sufficient for use in EV isolation as approximately 1×10^7 reticulocytes are needed to form a visible EV pellet after centrifugation procedure (personal communication; Dr.Tosti Mankelow, NHSBT Filton, 2015). DXM was selected for use in all future experiments as this produced a higher number of reticulocytes.

3.2.4 Effects of corticosteroids on extracellular vesicles isolated from the cultured reticulocytes

To determine whether the inclusion of corticosteroids in the culture system affects the composition of *in vitro* EVs released from day 21 cultured reticulocytes, the DXM and control reticulocyte samples were washed as described (see section 2.2.7, Chapter 2) and then incubated in EV-free tertiary stage media (see section 2.2.7.2, Chapter 2) for 72-96 hours at 37°C. The samples were then processed for isolation of EVs by ultracentrifugation technique as described in Figure 2.3, Chapter 2. Pellets of EVs were harvested and prepared for proteomics study (see 2.2.13, Chapter 2). The protein content of the EVs was measured using Bradford assay (see 2.2.10, Chapter 2) and then normalised to 100 µg per sample.

Subsequently, the control and DXM treated reticulocyte derived EV samples were processed for TMT labelling at the University of Bristol Proteomics Facility (as described Chapter 2, 2.2.13 section) and samples were run on an Orbitrap Fusion Tribid machine (Thermo Fisher Scientific). A total of 2,956 proteins was detected from EV samples derived from standard cultured reticulocytes and reticulocytes cultured with DXM for the first 11 days of culture. The results were filtered at high stringency for proteins that contained two or more unique peptides, and as a result, 1,406 proteins with altered expression were detected in EVs from the two samples. Analysis using the String Database (<http://string-db.org/>; v10.5; 14 May 2017) identified 523 proteins, of these 310 proteins (59.27%) were classified as extracellular vesicle proteins (GO:1903561). According to cellular component ontology (GO) by the String

Database, the majority of the identified proteins were membrane-bound organelle (GO:0043227; 390, 74.57%) and organelle (GO:0043226; 383, 73.23%).

To assess the differences between control and DXM exposed cultures, a cut-off ratio difference was set as ≤ 0.5 and ≥ 2 , where a protein difference was judged to be significantly changed between the samples. The bioinformatics data was analysed with PANTHER software (<http://www.pantherdb.org/>; v13.1; Feb 2018) and WebGestalt software (<http://www.webgestalt.org/option.php>; Jan 2013). Only nine proteins were identified when the cut-point ratio differences were applied. These are listed in Table 3.1 and include; c-Kit (accession P10721), alpha-2 antiplasmin (P08697), myosin, and zinc finger protein 512 (B4DES6). These results suggest that the addition of DXM into the *in vitro* erythroid culture process had a minimal effect on the EV protein content, and therefore does not preclude its use. This experiment has also demonstrated the feasibility of isolating EVs from *in vitro* cultured reticulocytes.

Table 3.1. Nine up-regulated proteins in the EVs derived from DXM-treated samples when compared to the control samples.

Accession	Protein name	Unique Peptide	Ratio HC/CT	Ratio DXM/CT
F5H810	Noelin (Fragment)	2	3.188	2.397
J3KT17	Galectin	2	3.116	3.805
A2NYU8	Heavy chain Fab (Fragment)	2	2.976	2.454
P10721	Mast/stem cell growth factor receptor Kit	11	2.682	2.033
B4DES6	cDNA FLJ52441, highly similar to Zinc finger protein 512	3	2.578	2.442
Q9UL88	Myosin-reactive immunoglobulin heavy chain variable region (Fragment)	2	2.533	2.518
B4DUJ8	cDNA FLJ54160, highly similar to Carbonic anhydrase 3 (EC 4.2.1.1)	2	2.361	2.295
P08697	Alpha-2-antiplasmin	17	2.113	2.115
B1N7B6	Cryocryoglobulin CC1 heavy chain variable region (Fragment)	2	2.059	2.514

3.2.5 *Ex vivo* erythropoiesis of thalassaemic cells compared to the matched controls

Ineffective erythropoiesis is one of the most important pathophysiologies in thalassaemic patients. This process occurs mainly in the bone marrow resulting in the destruction of the erythroid lineage (See Chapter 1, section 1.3.3). To monitor the process *in vitro*, three samples (n=3) of CD34⁺ cells from HbE/ β -thalassaemia patients were cultured alongside CD34⁺ cells from normal healthy age- and gender-matched individuals. This part of the study focused on comparing features of the *in vitro* erythropoiesis of HbE/ β -thalassaemia patient erythroblasts (proliferation, maturation, and viability of cells) to the age- and gender-matched control cells.

The three pairs of HbE/ β -thalassaemia patient (PT1, PT2, PT3; see Table 3.2 for patients' demographic and laboratory data) and the age- and gender-matched control samples (CT1, CT2, CT3) were cultured in parallel from isolated CD34⁺ cells.

Table 3.2. Characteristics and clinical parameters of five non-transfusion dependent HbE/ β -thalassaemia patients enrolled in the *ex vivo* erythropoiesis experiment.

No.	Sex	Age	Diagnosis	Splenic Status	Transfusion History	Hb Analysis	Hb (g ^l ⁻¹)	Hct (%)	MCV (fl) (82-97)	Platelet Count (x10 ³ μ l ⁻¹) (157-420)	WBC (x10 ³ μ l ⁻¹) (5.3-10)	N (%) (59-69)	Ferritin (ngml ⁻¹)
1	M	24	β^0/β^E	Intact	Intermittently	6.3%A2 54.8%E 38.9%F	80	26	53	123	7.4	64.4	595.5
2	M	52	β^0/β^E	Intact	Never	12.5%A2 55.6%E 31.9%F	86	25.5	68	325	5.6	57.5	N/A
3	F	33	β/β^E	Intact	Intermittently	N/A	66	19.9	60	204	6.05	47.6	392
4	F	21	β^0/β^E	Intact	2 years ago (Pregnancy)	10.2%A2 35.5%E 54.3%F	89	26.9	58	227	8.8	59.7	310
5	M	19	β^0/β^{E*}	Intact	1 year ago	60.9%E, 28%F	4.9	18.5	57	49	7.16	40.2	335

*Patient 5 had complications of hypersplenism & haemochromatosis: primary hypothyroidism, secondary hypogonadism. N – neutrophils, N/A – not available

Each progenitor cell sample, in both patients and controls, was derived from ~24 ml of peripheral blood. The starting numbers of CD34⁺ cells are summarised in Table 3.3.

Table 3.3. Numbers of CD34⁺ cells extracted from 24 ml of peripheral blood in thalassaemic patient (PT) and control (CT) samples.

Sample pair	Patient (cells)	Control (cells)
PT1/CT1	2.0 x 10 ⁵	1.5 x 10 ⁵
PT2/CT2	1.2 x 10 ⁵	1.1 x 10 ⁵
PT3/CT3	9.0 x 10 ⁴	1.8 x 10 ⁵

During erythroid cell culture (see section 2.2.3, Chapter 2) two of the three patient samples exhibited higher proliferation rates when compared to their age and sex-matched controls; 11500- (PT1) vs. 488-fold increase (CT1) and 3122- (PT3) vs. 63-fold increase (CT3). However, this pattern was not observed in the third pair of patient and control samples, with 618- and 731-fold increases for PT2 and CT2 samples, respectively (Figure 3.6). Cell viability was measured daily by trypan blue staining and manual cell counting. The cell death (average values and standard errors, n=3) in both groups was calculated. Due to the limited number of cells in the samples, only one method of cell viability measurement was performed throughout. There was no significant difference in cell viability observed between these two groups (Figure 3.7).

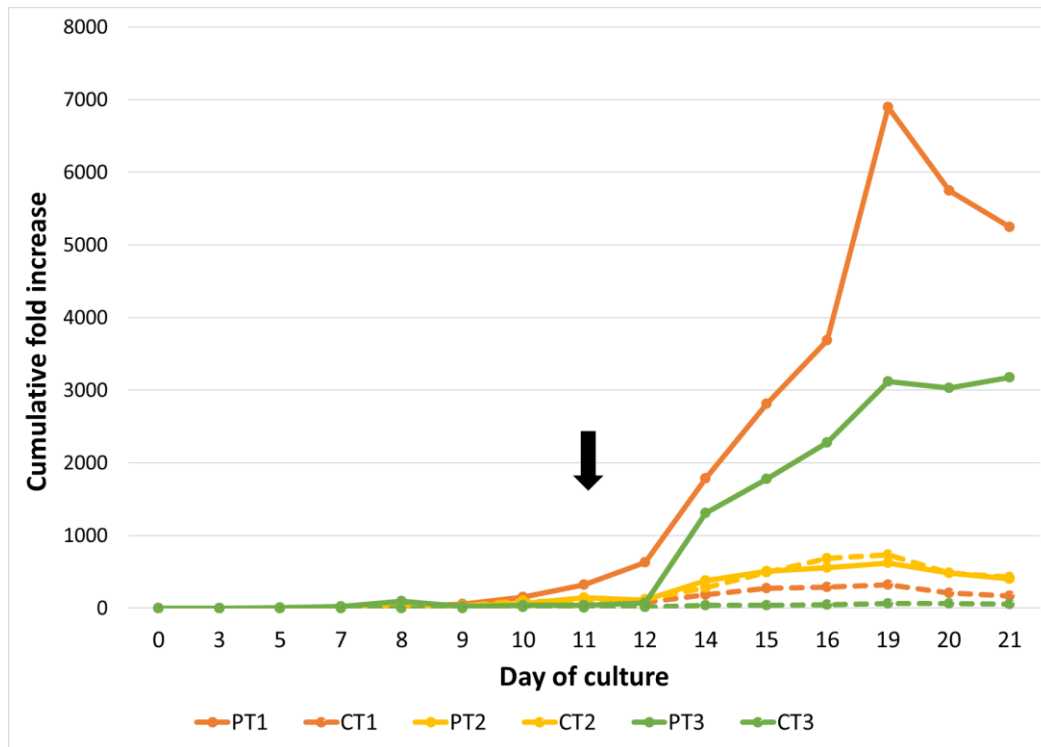


Figure 3.6. Cell expansion of CD34⁺ derived control and HbE/β-thalassaemia patient erythroblasts shown as cumulative fold increase.

CD34⁺ cells were isolated from 24 ml of peripheral blood of three thalassaemic patients (PT1, PT2, PT3; solid colour lines) and their matched controls (CT1, CT2, CT3; dash lines). All cells were cultured using the Griffiths *et al.* (128) three-stage media with DXM added on D0 to D11 (10⁻⁶ M). DXM was removed from the culture system on D11 (black arrow); the cells were washed and moved to the fresh tertiary media. PT1 and PT3 showed better proliferation compared to their matched controls CT1 and CT3; however, the same trend was not observed in the PT2 and CT2 samples, which exhibited similar proliferation rates.

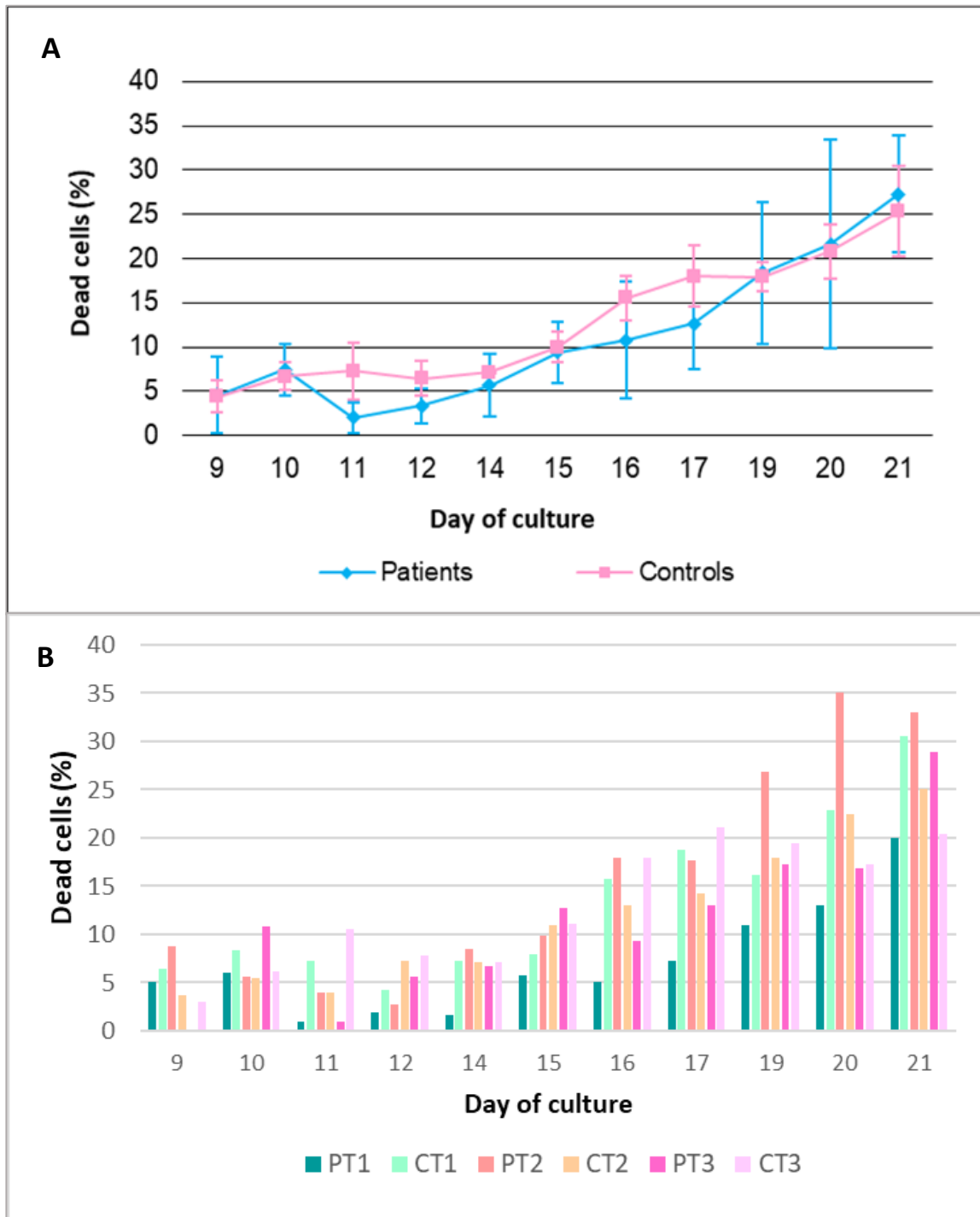


Figure 3.7. Cell death as a measure of cell viability of HbE/ β -thalassaemia patients (n=3) and controls (n=3) erythroblasts during culture.

Dead cells were manually counted daily using trypan blue and displayed as a percentage of the total counted cells as **(A)** average value with SD and **(B)** an individual sample. There was no distinct difference in cell viability between patients and controls. In particular, no increase of the cell mortality rate was observed during the polychromatophilic stage (day12 to day17).

Regarding maturation, the thalassaemic cells were found to have a faster rate of differentiation, particularly in the early stage of the culture between day 7 and day 9 (Figure 3.8). This trend was observed to alter in the later stages, where between day 12 and day 17 the majority of thalassaemic cells were at the polychromatophilic stage (Figure 3.9), whilst more of the control cells had matured to reticulocytes (23% vs. 42% of reticulocytes on day 17). At the end of the culture, on day 21, enucleation rates were lower in thalassaemic samples when compared to the matched controls in all three samples – 34% vs. 75% (PT1 vs. CT1), 75.5% vs. 81% (PT2 vs. CT2), and 46% vs. 82% (PT3 vs. CT3).

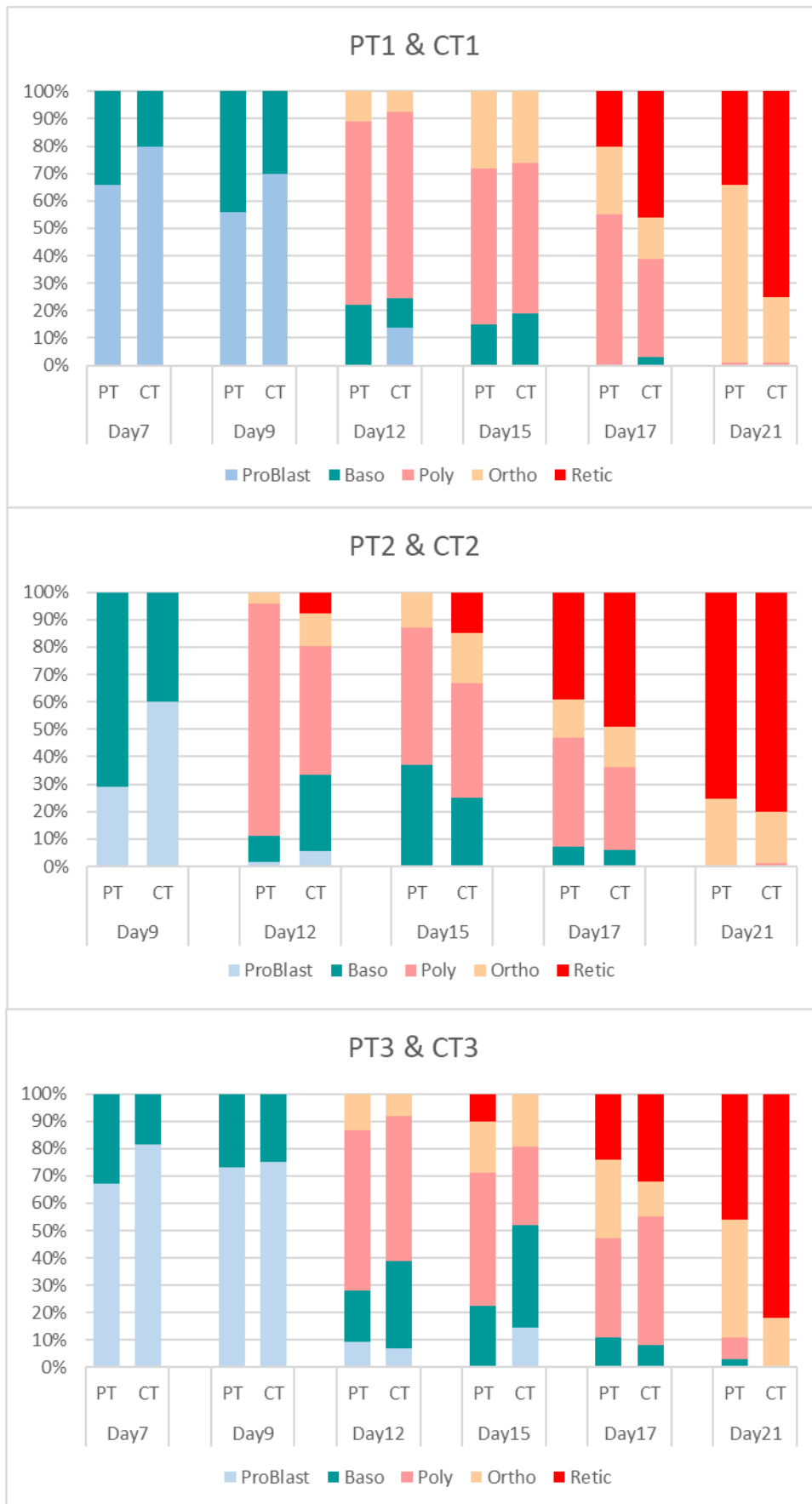


Figure 3.8. Erythroid differentiation of CD34⁺-derived erythroblasts from three thalassaemia patients compared to their matched controls.

The cultured cells were derived from three HbE/ β -thalassaemia patients, and three matched control samples. Cell morphology was assessed using cytopsin technique stained with Leishman's stain at different time points of the culture (day 7, 9, 12, 15, 17, 21), except for sample PT2 where the cell count at day 7 was too low to perform the analysis. In a differential count, 200 to 500 cells were counted per sample to represent the total cell population. The thalassaemic cells, when compared to the controls, were observed to have a faster rate of differentiation in the early stages of the culture (day 7 to day 9), but then remained longer at the polychromatophilic stage (during day 12 to day 17) when the control cells were regularly matured to reticulocytes. In the tertiary stage (day 12 to day 21), cell maturation of two thalassaemic samples was slower than the controls (PT1 and PT3). Enucleation rates were also lower in these thalassaemic samples (PT1 and PT3) when compared to their matched controls. The PT2 sample did not show a different rate of maturation and had equivalent enucleation rate to the control (CT2) at day 21.

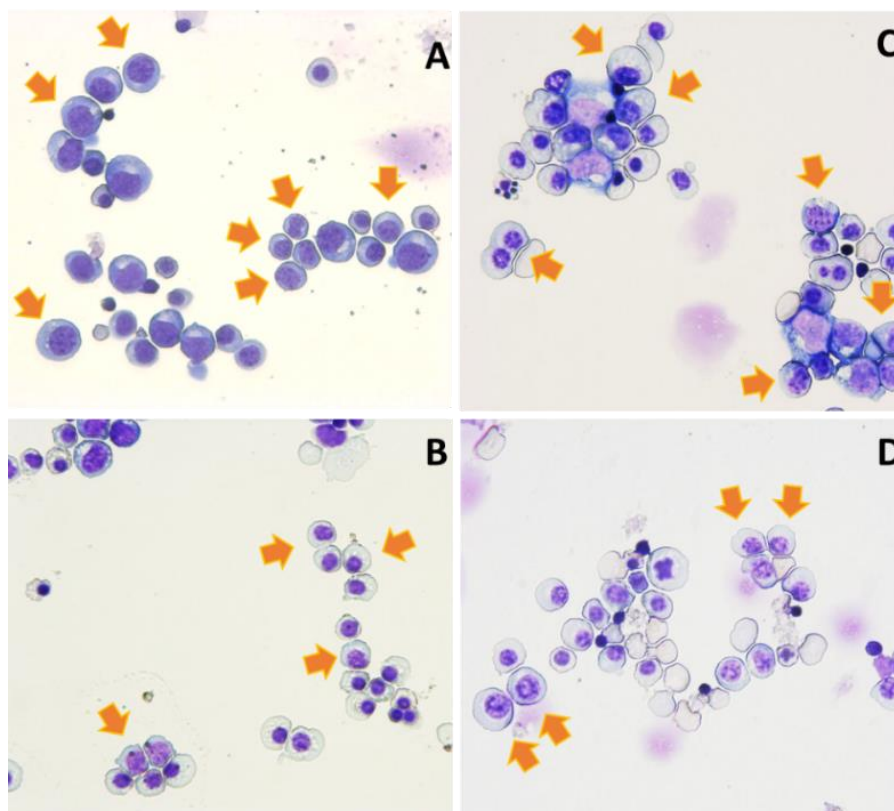


Figure 3.9. Cell morphologies of *in vitro* cultured thalassaemic and control erythroid cells. (A and B) and their matched controls (C and D) observed at different time points during *ex vivo* erythropoiesis – day 12 (A and C), and day 15 (B and D). The thalassaemic patient cells appear to be delayed at the polychromatophilic stage, suggesting the maturation is hindered or disturbed. Slides were prepared by cytopspin technique and stained with Leishman’s stain. Arrows indicate cells in their polychromatophilic stage.

Two additional pairs of HbE/ β -thalassaemia patients (PT4, PT5) (see Table 3.2 for clinical details) and matched controls (CT4, CT5) were also cultured. The cell proliferation, viability rates, and maturation rates for PT4/CT4 and PT5/CT5 were comparable to the initial three sample pairs. The PT4 sample proliferated particularly well, exceeding the age-matched control (514 vs. 23; 22.3-fold difference) and the PT5 sample and control (583 vs. 12.8; 45.5-fold difference), as shown in Figure 3.10. Eucleation rates on day 21 of the culture of these samples were 53.5% (PT4), 70% (CT4), 55% (PT5), and 79% (CT5).

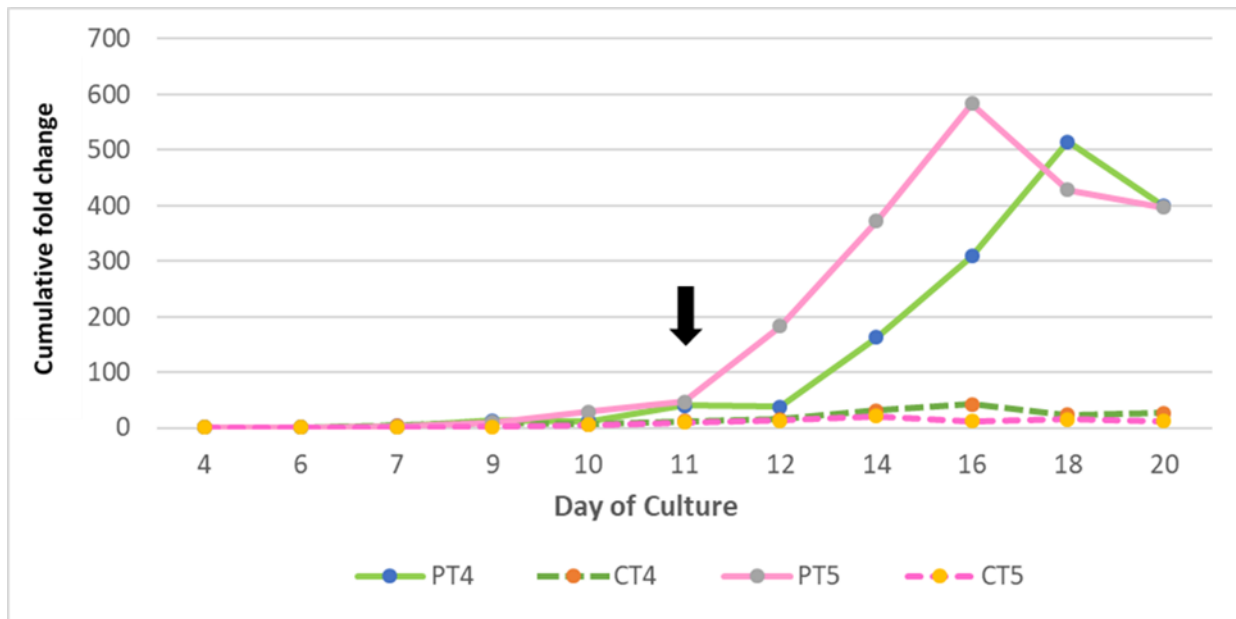


Figure 3.10. Cumulative fold change of two erythroid cultures of thalassaemic samples (PT4 and PT5) and their matched controls (CT4 and CT5).

MNCs were isolated in Thailand from 24 ml of peripheral blood, frozen at -20°C and transferred to Bristol, UK. CD34^{+} cells were isolated from the thawed cells and grown in Griffiths *et al.* (128) three-stage liquid media with DXM additive (10^{-6} M) during the primary and secondary stages of the culture; a black arrow indicates the day of steroid removal (day 11). Both PT4 and PT5 cells (solid lines) proliferated better than their matched controls CT4 and CT5 (dash lines).

3.2.6 Comparative analysis of proteome between red blood cell membranes of thalassaemic samples and the matched controls

To explore the effects of thalassaemic pathology on *in vitro* thalassaemic reticulocytes, *in vitro* generated membrane preparations of three sets of patient reticulocytes (from PT1, PT2, PT3) and their matched controls (CT1, CT2, CT3) on day 21 were prepared as outlined in Chapter 2 (section 2.2.11). The white membranes obtained were collected and measured for protein concentration using Bradford's assay (see section 2.2.10, Chapter 2). Membrane samples were normalised to 100 μg of the total protein before quantitative proteomics analysis was performed. The proteomic analysis using TMT nano-LC-MS/MS analysis initially identified 4,620 proteins, with 2,539 proteins identified when filtered for two or more unique peptides. When using a cut-off ratio of ≥ 2 or ≤ 0.5 to determine a significant change between patient and control samples, a total of 2,510 proteins were shared across all three samples. There were no proteins detected that were observed to be unique to thalassaemic samples. When

these observed proteins were categorized with regard to cellular component origins using WebGestalt (<http://www.webgestalt.org/>; Mar 2013), approximately two-thirds (69%) of proteins were membrane-bounded organelle (GO:0043227), 40% were extracellular vesicle (GO:1903561), and 34.5% were macromolecular complex (GO:0032991) proteins. There were 70 up-regulated proteins found across all patient samples when compared to controls (Figure 3.11A). These could be categorised, based on a biological process and protein class, into proteins involved in the binding, catalytic proteins, signal transducers, structural molecular, and translation regulator activities. The biological processes associated with these identified proteins were classified as follows: chaperone binding proteins such as AHSP, prefoldins, Von Hippel-Lindau binding protein 1; microtubule motor function proteins which facilitate dynein, tubulin, and myosin activities; RNA binding proteins or spliceosome proteins; and inhibitor factors of protein synthesis, e.g., eukaryotic translation inhibitor factor 3. In addition, proteins involved with iron metabolism were also increased in their abundance in patients' red cell membrane samples, e.g., ferritin light chain, ferritin heavy chain, and transferrin receptor. Interestingly, nucleolar proteins, i.e., proteins found in the nucleus that binds to nucleic acids, for example, nucleophosmin 1, nucleolin and nucleoporin, were detected. This suggests that the red cell membranes could have been contaminated with nucleated erythroblasts, therefore reflecting the limitations of the filtering process or these were residual proteins leftover after enucleation. Examination of the post-filter cytopspins confirmed the presence of a small number of contaminating nucleated cells (Figure 3.12). There were 51 proteins that exhibited reduced abundance in the patient samples relative to the controls. The majority of these were annotated as protein binding (35 proteins), transporter (12 proteins), and nucleotide-binding categories (11 proteins) (Figure 3.11B). Also found in this group were proteins with molecular function involved in ion channel and ATPase activity, e.g., ABCB6, ATPase family and stomatin. Additionally, various β -globin fragments were less abundant in the three patients' samples, potentially because the control erythroid cells contained more normal β -globin chains than the patients. Haptoglobin and hemopexin, the critical free Hb and haem scavengers, were found to be less abundant in the patients. Haptoglobin was decreased in two out of three samples (ratio 0.056, 0.652, and 0.306 for PT1/CT1, PT2/CT2, and PT3/CT3, respectively); while, hemopexin was reduced in only one sample below the 0.5 cut-off level (ratio 0.38, 0.79, and 0.82 for PT1/CT1, PT2/CT2, and PT3/CT3, respectively).

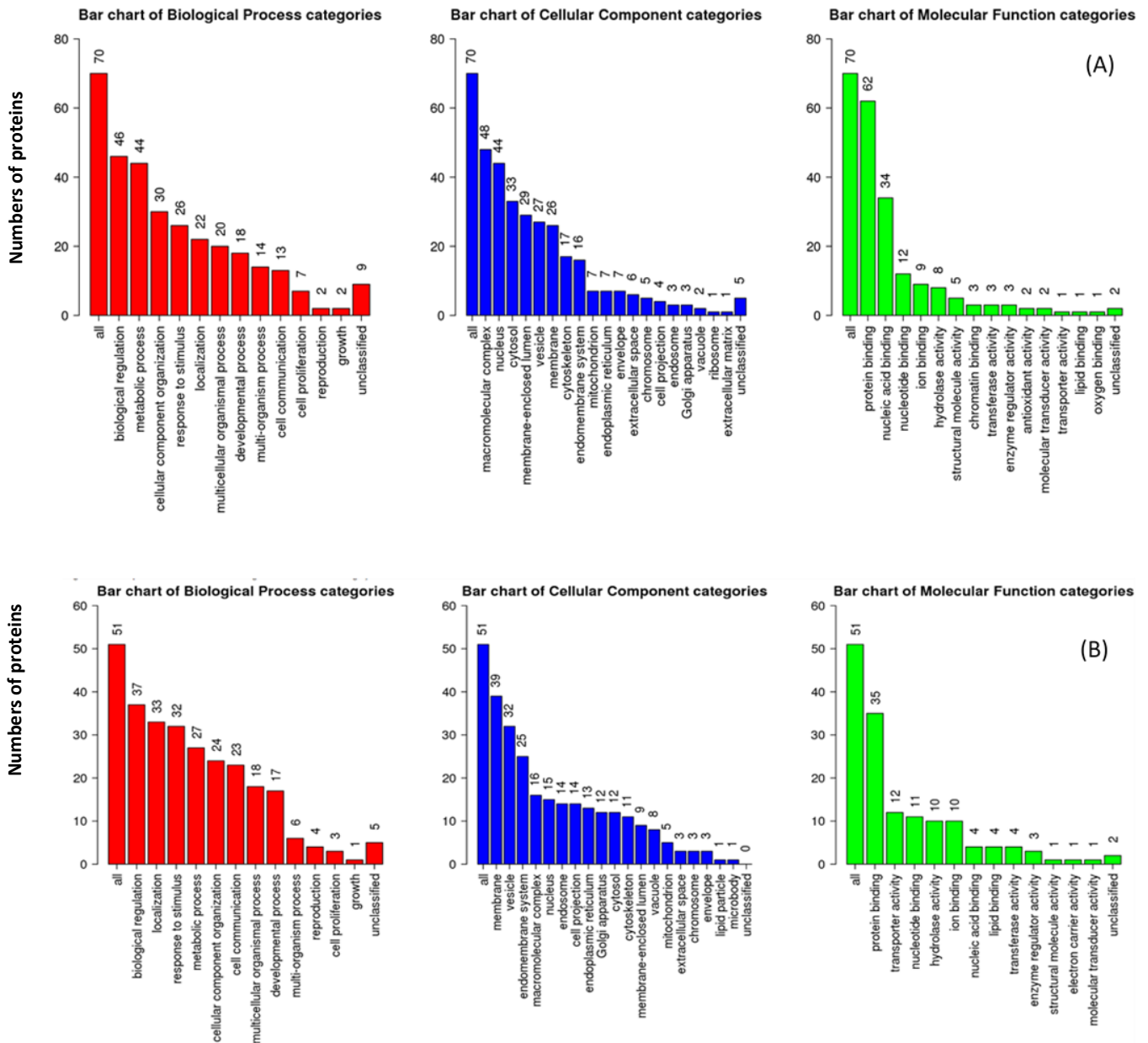


Figure 3.11. Proteins with altered abundance in thalassaemia patients' *ex vivo* reticulocyte membranes compared to control reticulocyte membranes.

The proteomic data using Webgestalt software analysis, **(A)** 70 functional classes of proteins with increased abundance in the patient reticulocyte membrane samples were observed when compared to matched controls. The proteins were categorised according to their biological process, cellular component, and molecular function. **(B)** 51 functional classes of proteins with reduced abundance in thalassaemic reticulocyte membranes relative to matched controls.

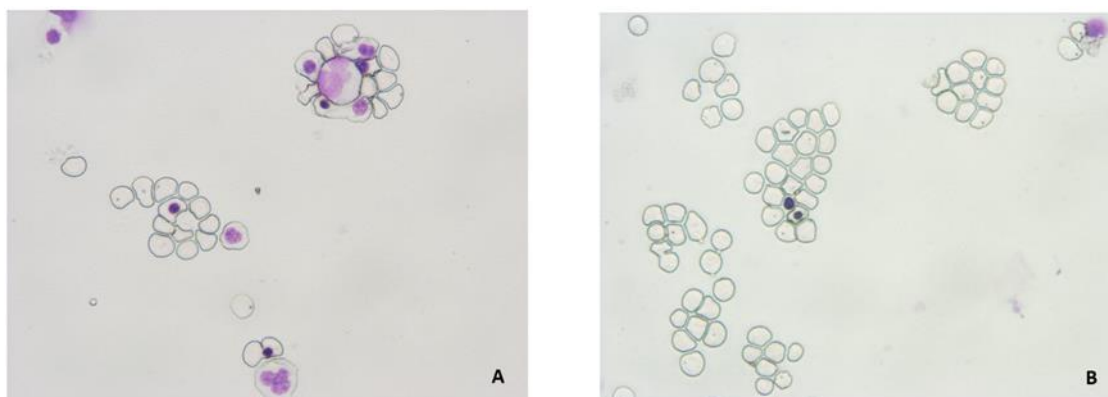


Figure 3.12. Cytospin images of pre-and post-filtered cultured reticulocytes from HbE/ β -thalassaemia patients.

Cytospins were made on day 21 of cultures from **(A)** pre-filtered reticulocytes and **(B)** post-filtered reticulocytes, with contaminating nucleated red blood cells visible in image B.

3.2.7 Quantification of *in vitro* EVs released from cultured reticulocytes

In the previous report, the number of plasma-derived EVs of β -thalassaemic patients was four times higher than controls (347). One potential source of this increased EVs is from the patient's reticulocytes. Therefore, the quantitative difference between the EVs isolated from the *in vitro* reticulocytes of thalassaemic patients and controls was examined next. EVs were isolated as described in section 2.2.7.2 in Chapter 2 and prepared by ultrafiltration (MF-Millipore[®], 0.22 μm pore size) using the process described in section 2.2.7.2.2, Chapter 2. The EVs obtained from cultured reticulocytes were quantified using flow cytometry and nanoparticle tracking analysis (NTA) (see methods described in section 2.2.8 and 2.2.9 of Chapter 2 for flow cytometry and NTA, respectively).

EV concentrations of four thalassaemic samples and their matched controls are presented in Table 3.4. The average numbers of EVs detected by both flow cytometry and NTA were comparable between the patient (1.06×10^8 particles μl^{-1}) and control samples (1.03×10^8 particles μl^{-1}). The NTA method was more sensitive than flow cytometry for detection of EVs in both thalassaemia and the control samples (Table 3.4), in keeping with the method's superior ability to detect small-sized particles. In summary, there was no quantitative

difference of EVs derived from cultured reticulocytes of HbE/ β -thalassaemic patients and the healthy controls.

Table 3.4. Numbers of *in vitro* derived reticulocyte EVs from thalassaemic patients (PT sample) and matched controls (CT sample), determined by flow cytometry and NTA analyses.

PT sample	FC (particles μl^{-1})	NTA (particles μl^{-1})	CT sample	FC (particles μl^{-1})	NTA (particles μl^{-1})
PT1	1.40×10^5	8.24×10^7	CT1	3.06×10^4	6.18×10^7
PT2	5.30×10^4	6.66×10^7	CT2	7.26×10^4	5.16×10^7
PT3	8.64×10^5	6.70×10^7	CT3	2.00×10^5	N/A
PT4	3.15×10^5	2.10×10^8	CT4	2.20×10^5	1.95×10^8
Mean (\bar{x})	3.43×10^5	1.06×10^8	Mean (\bar{x})	1.31×10^5	$1.03 \times 10^{8*}$

FC – flow cytometry, NTA – nanoparticle tracking analysis; N/A – no available result;

* average was calculated from three samples

3.2.8 Quantitative analysis of the proteome of EVs released from cultured thalassaemic reticulocytes and the matched controls

The proteomic composition was assessed of *in vitro* generated EVs from leuko-filtered cultured reticulocytes of the PT1, PT2, PT3 and their matched controls CT1, CT2, and CT3 obtained as described in section 3.2.5 above using methods described in Chapter 2, section 2.2.7. Each sample was normalised to 100 μg of total protein before being subjected to quantitative proteomics analysis at Proteomics Facility Unit, University of Bristol. The TMT and MS/MS analysis was performed by Orbitarp nano-LC-MS/MS (Thermo Fisher Scientific).

A total of 1707 proteins were identified in this quantitative proteomics experiment. There were no proteins identified that were unique to thalassaemic samples. When filtered for proteins containing ≥ 2 unique peptides, the number of detected proteins was reduced to 655. Of these, 286 proteins were common to both thalassaemic and control samples, and when subjected to Webgestalt (<http://www.webgestalt.org/option.php>; Mar 2013), 193 (72%) of these were identified as known constituents of extracellular vesicles (Gene Ontology (GO):1903561). Based on the GO molecular function, the majority of the identified proteins

were involved in the catalytic (42%) and the binding (32.7%) activity (see Figure 3.13). Relative quantifications of proteins in the patients were compared to control samples with a cut-off values of ≥ 2 or ≤ 0.5 -fold difference.

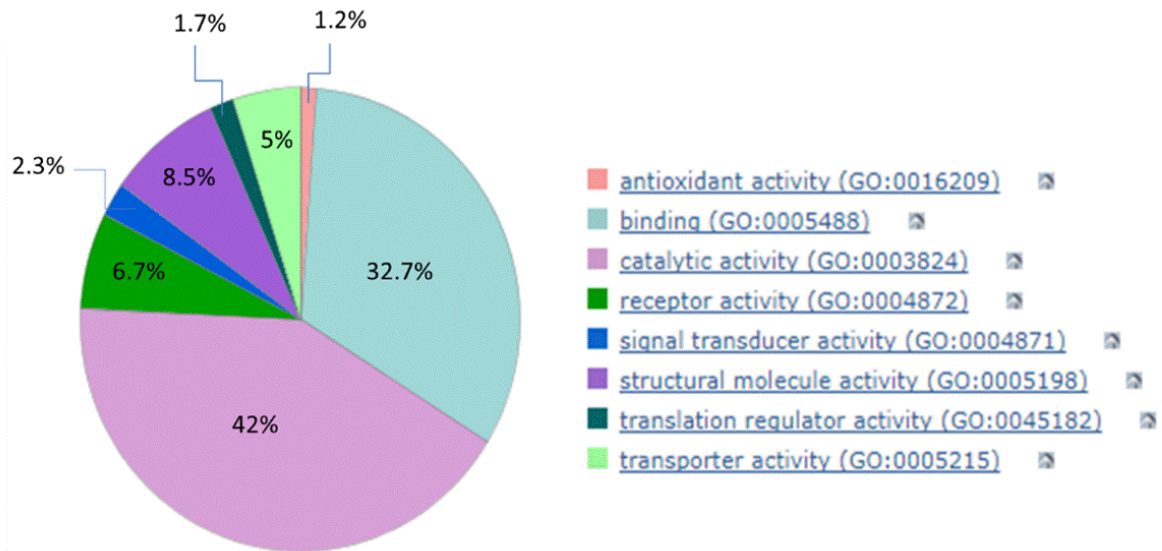


Figure 3.13. Functional classification (Gene Ontology; GO) of 286 proteins/genes mutually found in the EV constituents derived from three *ex vivo* cultured three pairs of thalassaemic and control reticulocyte samples.

Cultured reticulocytes were filtered, washed, and then incubated for 72-96 hours before the EV isolation. EV proteins were normalised to 100 μg protein concentrations using Bradford's assay, and then EV proteome was investigated by TMT and MS/MS analysis. The analysis by Webgestalt and Panther-db software was performed to identify and compare the proteome of the EVs derived from reticulocytes of thalassaemic patients and healthy controls. The pie chart shows similarity analysis of observed proteins to GO function classes using Panther-db software.

Two out of three patient EV samples (PT1 and PT3) had eight commonly shared proteins with greater abundance than the control samples (Table 3.5). The categorization of these proteins in terms of the cellular component, molecular function, and biological process is depicted in Figure 3.14.

Table 3.5. Eight proteins observed to be up-regulated in the two EV samples derived from *in vitro* reticulocytes of HbE/ β -thalassaemia patient (n=3), compared to the matched controls (n=3).

Protein	Accession	Unique peptide	PT1/CT1	PT2/CT2	PT3/CT3	Function/ Contribution	Reference
Lamin B2	Q03252	2	8.423	0.056	17.024	Dynein binding Maturation & enucleation	JW Shin <i>et al.</i> , 2013 (393)
T-complex protein 1-α	P17987	5	2.302	0.869	2.401	Chaperone Maturation & enucleation	Ozdemir <i>et al.</i> , 2016 (394)
TRIM58	Q8NG06	3	2.001	0.252	3.823	Dynein binding Maturation & enucleation	Thom <i>et al.</i> , 2014 (395)
Rac GTPase activating protein 1	B2RE34	6	2.490	0.611	10.035	Tubulin binding Maturation & enucleation	Kalfa and Zheng, 2014 (396)
LIS1 (PAFHA1B1)	P43034	2	2.139	0.566	4.922	Tubulin binding Maturation & enucleation	Zimdahl <i>et al.</i> , 2014 (397)
Catalase	P04040	22	2.047	0.278	4.764	Antioxidant enzyme	Ghaffari S, 2008 (398)
SBP1 (HSP56)	Q13228	7	2.278	0.670	3.161	Antioxidant enzyme	Leecharoenkiat <i>et al.</i> , 2011 (218)
ALAD	B7Z3I9	4	2.286	0.255	3.534	Haem synthesis	Ponka and Schulman, 1993 (399)

Five out of the eight proteins identified were known to be involved in the process of erythroid maturation and enucleation, namely lamin B2, t-complex protein 1, tripartite motif containing 58 (TRIM58), Rac GTPase activating protein 1 and platelet-activating factor acetylhydrolase 1b, regulatory subunit 1 (Lis1). Another two proteins found to be increased in the patients were catalase and selenium binding protein 1 (SBP1), which were categorised as antioxidant proteins. A protein involved in haem synthesis, namely delta-aminolevulinic acid dehydratase (ALAD), was also more abundant in the patient compared to the control reticulocytes derived EV samples.

There were also 90 proteins observed with reduced abundance in the patients' EVs when compared to EVs from the control group. These proteins were involved in DNA replication, ribosomal proteins, complement activation proteins, i.e., C4a, C4b, C5, and coagulation pathways such as alpha-2 antiplasmin, protein S, apolipoprotein, etc. (Figure 3.14B)

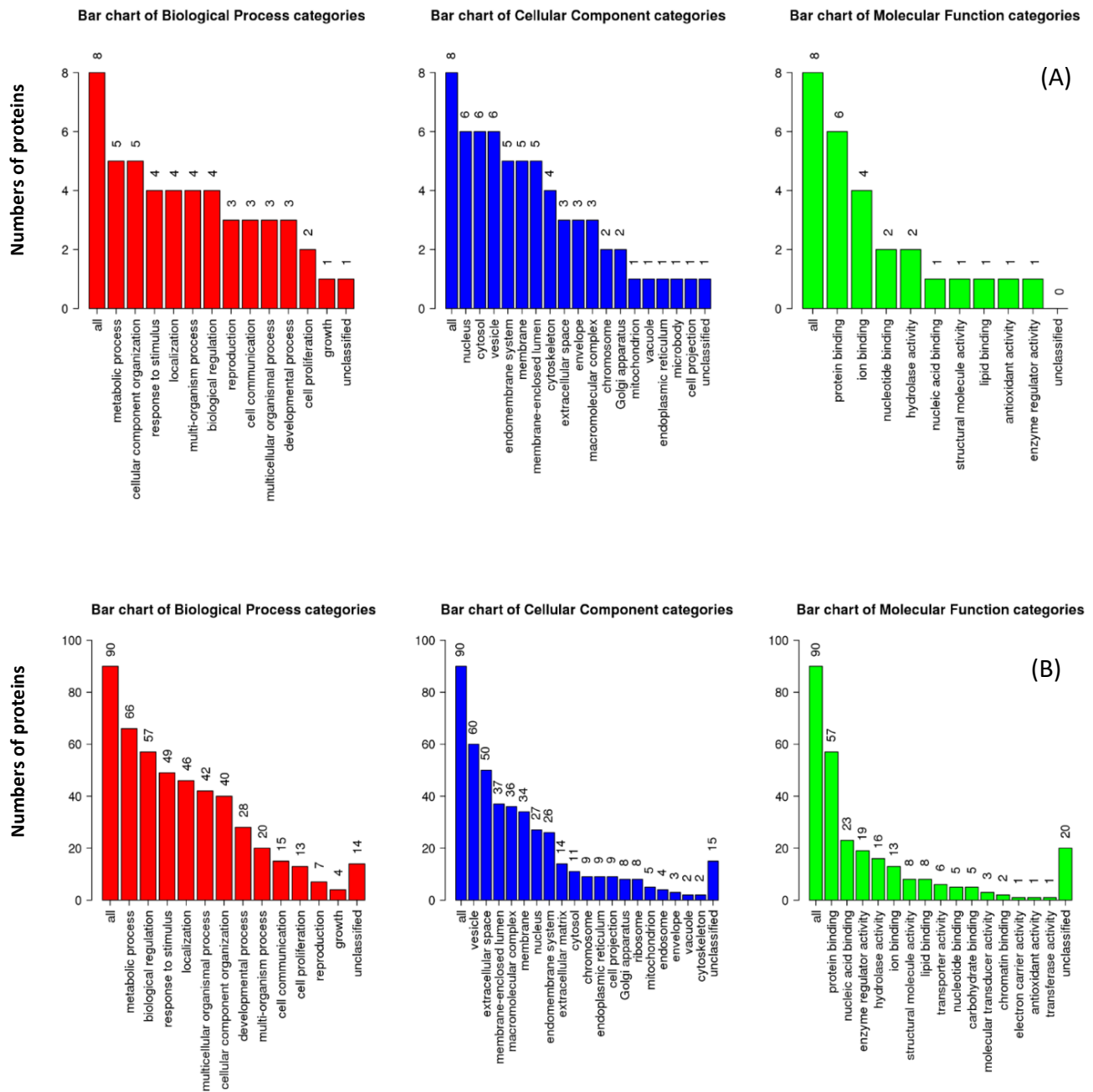


Figure 3.14. Proteins with altered abundance in HbE/ β -thalassaemia patients' EVs derived from *in vitro* reticulocytes compared to the matched-control EVs.

(A) Eight proteins had increased abundance in patient samples when compared to matched controls. Here the eight proteins are categorised according to their biological process, cellular component, and molecular function. **(B)** 90 proteins were detected with reduced abundance in thalassaemic EVs relative to healthy controls, categorised according to their biological process, cellular component, and molecular function. Charts were prepared from functional enrichment analysis using Webgestalt 2013 web tool.

In an additional experiment, two further pairs of thalassaemic and control samples (PT4 vs. CT4 and PT5 vs. CT5) isolated from reticulocytes produced in the previous *in vitro* erythropoiesis experiment (section 3.2.5) were compared by their proteome profiles using the tandem mass tag (TMT) and mass spectrometry (MS/MS).

A total of 3094 proteins were initially identified in EVs released from the *in vitro* reticulocytes, cultured over 21 days of erythroid culture course. When data were filtered for proteins that contained two or more unique peptides, the number was reduced to 1,490 proteins. Sample PT4 had 970 proteins of higher abundance than the matched control, with 21 proteins that were found only in PT4 sample. These included seven of the eight previously identified proteins of interest that were observed in the previous patients EV comparison (only lamin B2 was absent in PT4). However, for PT5 sample, there were no proteins observed in higher quantity than in control, in fact, there were 1148 proteins present in lower levels than its control, suggesting a possible problem with this sample or the control used.

Other significant proteins that were found with an increased level in patients were Hb delta chain, mutant β -globin (fragment), and peroxiredoxin-2 (PRDX2). Hb delta chain, which binds to α -globin chain to form HbA₂, was observed to be increased in two patient samples (PT3 and PT4); while, the mutant β -globin, representing an aberrant HbE was more abundant in the three patient samples (PT1, PT3, and PT4) than in their matched controls. PRDX2, one of the critical redox proteins, was found to be significantly increased in two of five patient samples (PT3 and PT4).

3.2.9 Comparison of the proteomic profiles between the *in vitro* generated EVs and reticulocyte membrane

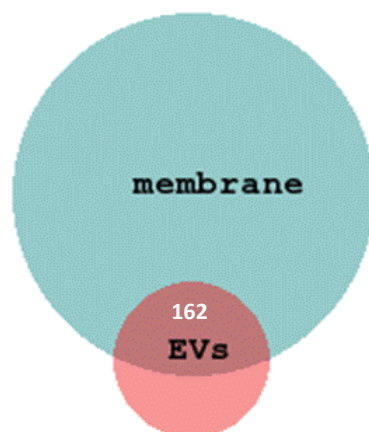
The degree of similarity between proteomes of EVs released from the *in vitro* reticulocytes of samples PT1, PT2, and PT3 (section 3.2.8), and the proteomes of their reticulocyte membranes (section 3.2.6) were explored. The number of proteins mutually shared between the membrane and EV proteomes is shown in Table 3.6. A total of 162 common proteins were found across all three samples in both their *in vitro* erythroid membrane and EV preparations from the same patients (n=3) (Figure 3.15A).

Table 3.6. The total number of proteins (≥ 2 unique peptides) identified from the three samples (PT1, PT2, and PT3) from the *in vitro* erythrocyte membrane preparation and from the *in vitro* reticulocyte EVs.

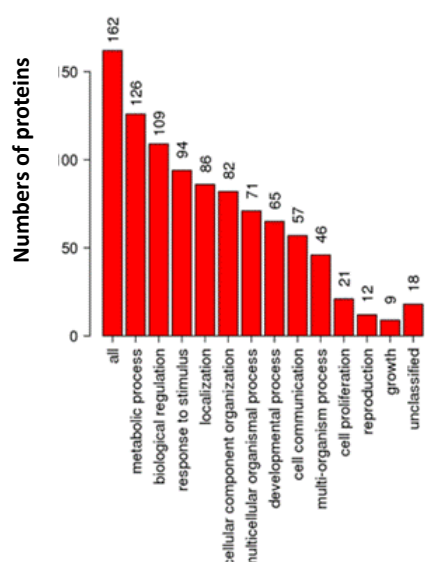
Sample	Membrane proteins	EV proteins	Mutual proteins
PT1	2522	632	173
PT2	2531	651	178
PT3	2518	616	166

A number of the commonly shared proteins between the red cell membrane and EVs in PT1, PT2 and PT3 was 173, 178, and 166 proteins, respectively, of which 162 proteins were shared between all three samples (Figure 3.15A).

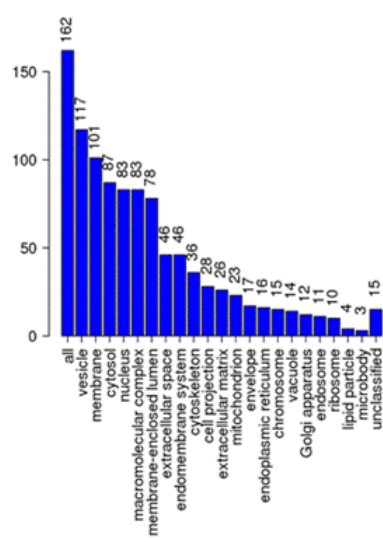
(A)



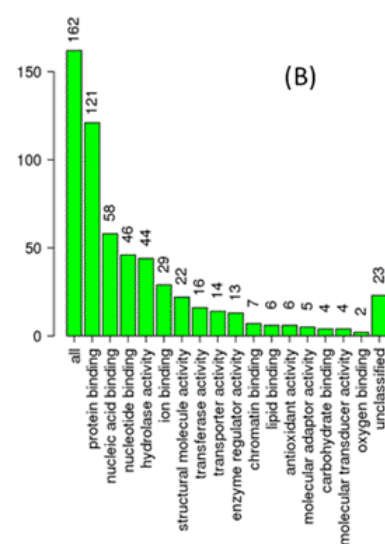
Bar chart of Biological Process categories



Bar chart of Cellular Component categories



Bar chart of Molecular Function categories



(B)

Figure 3.15. Proteins shared between the erythroid membrane and EV preparations from *in vitro* thalassaemic patient (n=3) and matched controls (n=3).

(A) Venn diagram of 162 common proteins found across both erythroid membrane and EV groups from the same *in vitro* patients (n=3) and matched control samples (n=3); **(B)** Three categories of GO (biological process, cellular component, and molecular function) depicting the 162 shared proteins.

The 162 common proteins shared between reticulocyte membranes and EVs were analysed using Webgestalt software (<http://www.webgestalt.org/>) (see Figure 3.15B). Based on their cellular component, the samples contained 117 out of 162 (72%) of known EV constituents, whilst 101 (62%) of the total 162 proteins were of vesicular origin. The majority of these were protein binding (GO:0005488, 75%), whilst 126 proteins (GO:0044237, 77%) were found to be

involved with the metabolic process. Also detected were proteins that can be annotated as ribosomal proteins, proteins with antioxidant activity, for example, catalase, SBP1, PRDX2, PRDX6, and Hb subunit mu, Hb subunit delta, proteins in the coagulation cascade and platelet activation, e.g., serpin, fibronectin, coagulation factor V, plasminogen, etc. Moreover, haptoglobin and hemopexin were also present, including other high prevalence erythroid proteins as defined by Bryk *et al.* (2017), such as AHSP, PRDX2, biliverdin reductase B, transferrin receptor, TRIM58, and lamin B2 (400).

3.3 Discussion

This chapter describes the successful *in vitro* culture and investigation of the proteomic profiles of *in vitro* generated HbE/ β -thalassaemia erythroid membranes and extracellular vesicles. A collaboration was initiated between the Siriraj Medical Research Center, Bangkok, Thailand, and NHSBT, Bristol, UK, whereby patient and control blood samples were shipped from Bangkok to Bristol for the purposes of this project. Sample handling and the transport process were evaluated, and experiments were designed to optimise erythroid cell culture conditions for low sample volumes. Since the goal of the experiments was to generate as many reticulocytes from anaemic patients as possible, the erythroid culture method described by Griffiths *et al.* (128) was successfully optimised further by the inclusion of DXM to generate the maximum number of reticulocytes from as minimal patient sample possible. Using this method, a peripheral blood sample of 24 ml was shown to be sufficient to provide CD34⁺ HSCs for *in vitro* erythroid culture.

3.3.1 Effects of delaying CD34⁺ cells isolation on *in vitro* erythroid culture

Due to the potential delay in CD34⁺ isolation because of the need to ship fresh blood samples from Thailand to Bristol, the work described in this chapter explored the effects of storage time on CD34⁺ cell yield and viability. It was observed that the numbers of isolated HSCs were not significantly different when blood samples were stored before CD34⁺ isolation. This was in agreement with the observations of Moroff *et al.* (2004), in which CD34⁺ blood progenitor

cells were successfully harvested after up to 72 hours of storage at 1-6°C (401). These findings were also consistent with other reports, where the storage time of blood (up to 5 days) did not have a significant effect on the numbers of CD34⁺ cells obtained (401, 402). The only difference observed between the CD34⁺ isolation from fresh and stored blood was a potential impact on cell maturation. The D5 and D3 samples maturation rates were slightly higher than D0 samples, as observed in Figure 3.2, but more samples should be tested to confirm this finding. In this project, the overall time delay experienced for delivery of fresh blood samples from Thailand to Bristol was three days. Therefore, the transportation process was within the acceptable range and was not anticipated to have a detrimental impact on the erythroid cultures.

In addition, to further mitigate the possibility that storage could affect the cells, peripheral blood mononuclear cells were also shipped frozen and similar results were observed using these cells. There are multiple reports in the literature that have studied the freeze-thaw process of cord blood as a source of progenitor cells (403-405). In the study most relevant to this work, Martinson *et al.* (1997) compared fresh apheresis samples with samples stored in liquid nitrogen (n=7) and found no difference between CD34⁺ cell numbers isolated and more importantly, no significant difference between fresh and frozen/thawed samples regarding the progenitor cells obtained, including their ability to proliferate and mature during erythroid culture (402).

3.3.2 Glucocorticoids increase the yield of erythroid cells and have minimal effects on reticulocyte derived extracellular vesicles composition.

As discussed in Chapter 1, section 1.1.2, there is considerable evidence in the literature suggesting the effectiveness of glucocorticoids in promoting proliferation in the early stages of erythroid cell development (101, 103, 104). The glucocorticoids DXM or HC were added to the Griffiths *et al.* (128) three-stage culture system (see the protocol in section 2.2.3, Chapter 2) between day 0 and day 11 and this was shown to improve erythroid progenitor proliferation (2.81 ± 0.78 fold for HC and 2.49 ± 1.24 for DXM compared to the controls), with total reticulocytes obtained at the end of the cultures for three groups being $8 \times 10^6 \pm 1.5 \times 10^5$ cells, $3.28 \times 10^7 \pm 3.9 \times 10^6$ cells, and $4.74 \times 10^7 \pm 2.1 \times 10^7$ cells for CT, HC, and DXM,

respectively. A delay in terminal differentiation in the culture incorporating DXM or HC was also evident, as previously reported (104, 406).

Proteomics studies were carried out on the EV samples isolated from *in vitro* cultured reticulocytes filtered at the end of culture period of control and the DXM stimulated cultures. This experiment confirmed that the steroid addition did not significantly alter the EV proteome profiles and could, therefore, be applied to the cultures without significantly affecting the interpretation of the proteomics data. Nine proteins with increased expression were observed to be released in EVs isolated from *in vitro* cultured reticulocytes in both steroid treatment arms (DXM and HC). Of these nine identified proteins, c-Kit has been reported to have its role in haematopoiesis, not only promoting proliferation but also delaying differentiation (72, 104). This protein acts as a cell-surface receptor to the cytokine Kit ligand (KITL)/stem cell factor (SCF) and its downstream effect results in cell proliferation and cell survival regulation (73, 407). The results of our study were in agreement with a published study of DXM treatment resulting in the maintained expression of c-Kit (104). Varricchio *et al.* (2012) demonstrated the synergistic effects of KITL/SCF increasing the proliferation of erythroblasts in the presence of DXM which was postulated that KITL/SCF triggers glucocorticoid receptor expression via ERK pathway (90).

Among the nine identified proteins (as listed in Table 3.1) was ZNF512, which carries four putative zinc finger motifs necessary to transcription regulation and alpha-2-antiplasmin protein which inactivates plasmin in the process of fibrinolysis (408), a known EV constituent protein (GO:0072562). Overall, other than the alteration in the proteins highlighted above, there was a minimal qualitative difference in EV proteomes between control and steroid-treated cultured cells, suggesting that DXM treatment does not influence the composition of the EVs, although it does increase the cell proliferation, justifying its use in our experiments.

3.3.3 *Ex vivo* erythropoiesis of thalassaemic erythroid cells compared to the matched controls

The erythroid cell proliferation and differentiation were monitored in *ex vivo* erythroid cultures of HbE/ β -thalassaemia patients and healthy matched controls sourced from Thailand. Previously, reports have observed that cultured erythroid cells of HbE/ β -

thalassaemia patients showed a 2.5-fold greater expansion rate than normal controls on day 7 of culture (409). In our study, the proliferation of HbE/ β -thalassaemia patients illustrated greater fold increase of cell proliferation in four of the five separate cultures, relative to the matched controls (Figure 3.6 and Figure 3.10).

This finding was also consistent with a study by Leecharoenkiat *et al.* (2011) where *in vitro* erythroid culture of HbE/ β^0 -thalassaemia erythroblasts (n=3) was shown to have a greater expansion rate than the normal control erythroblasts (218). However, our results were in contrast with Mathias *et al.* (2000), who reported cell proliferation from thalassaemia major (β^0/β^0) patients being significantly lower than the control (159). The key explanation of the discrepancy between the studies could be the presence of SCF in our culture system (410).

Regarding cell maturation, thalassaemic erythroblasts differentiated faster than their matched controls in the early stage of erythropoiesis (day 7 to day 9); whilst, the cells remained at the polychromatophilic stage from day 12 to day 17 (Figure 3.8 and Figure 3.9). This finding was in agreement with other studies of β -thalassaemic erythroblast cultures (159, 218). However, it was difficult to fully compare these data to other studies, due to their use of different culture systems and different types of β -thalassaemia.

Among the tested thalassaemic samples of this study, PT2 matured faster than the other samples and had the lowest pronormoblast population on day 9 of the culture (29%). The short period of the early phase of erythropoiesis of this sample probably explained why PT2 had the lowest proliferative fold change, given that no increased number of dead cells was observed. Our work showed similarities with Mathias *et al.* who observed a slightly faster maturation of β^0/β^0 thalassaemic cells during the early stage of erythropoiesis up to day 7, i.e., an increase in the proportion of basophilic normoblasts over pronormoblasts between day 4 and day 7 of the culture (159). In later stages, the delay of erythroid maturation was observed in both this study (Figure 3.8) and the study by Mathias *et al.* When considering the patient's clinical parameters, PT2 had the highest Hb (Hb 8.6 gdl⁻¹; Table 3.2) than the other two (PT1 & PT3) samples. However, neither the greatest proliferation rate (Figure 3.6) nor the slowest differentiation rate (Figure 3.8) was observed in PT3 sample who had the lowest Hb level (Hb 6.6 gdl⁻¹) in this study. Altogether, there was no apparent relationship between *in vitro* erythroid proliferation rates and severity of anaemia in the HbE/ β -thalassaemia patients

identified in this study. Note that, statistical analysis was not performed due to the small sample size.

When focusing on the cell death rates, in our project, they were comparable between patients and controls at the polychromatophilic cell stage, which would otherwise have indicated IE (159, 236). At the stage of the culture when polychromatophilic normoblasts were prominent in patients' cells (day 12, Figure 3.9), the death rate did not increase (Figure 3.7). We hypothesise that the three-stage culture system used here and/or the addition of corticosteroids to the culture ameliorate the effect of ROS towards HbE/ β -thalassaemic erythroid cells in a yet undetermined way. One possible explanation is that the inclusion of SCF in the growth medium could be one of the factors reducing apoptotic rates in thalassaemic cells in our culture system. In support of this supposition, a published study of culture system with SCF additive with or without DXM showed that SCF could reduce the apoptotic rates of β -thalassaemia erythroblasts to the level comparable to the control cells (410). According to this study by Gabbianelli *et al.* (2008), cultured thalassaemic erythroid cells were able to successfully differentiate and complete the terminal maturation. Other studies of the *in vitro* erythropoiesis of β -thalassaemia, such as a study by Leechooenkiat and colleagues (2011) which used the culture protocol containing SCF, reported that there was no increase in apoptotic cells during and after the polychromatophilic normoblast stage of the cultured HbE/ β -thalassaemia erythroblast compared to the normal controls (218). Mathias *et al.* (2000) did observe a higher death rate at the same stage of maturation, indicating the occurrence of ineffective erythropoiesis in their study of β -thalassaemia major erythroblasts (159) but the culture protocol of the latter work was a one-stage culture system previously described by Malik *et al.* (1998) that used hydrocortisone but did not contain SCF (151).

To date, there was no available data comparing the proliferation rate between β -thalassaemia patients with their clinical data. In the current study, when considering the patients' clinical parameters (Table 3.2), neither the Hb nor the HbF levels were consistent with the proliferative fold change. However, the decreased of apoptotic rates of β -thalassaemia major and β -thalassaemia intermedia observed in the work of Gabbianelli *et al.* (2008) was in concordance with the higher levels of HbF directly measured in the *in vitro* erythropoiesis system (410). This suggests that there may be other factors that influence the *in vitro*

synthesis of HbF, and the *in vivo* HbF levels or the severity of the patients do not associate with the proliferation rate or survival of *in vitro* erythroblasts.

In conclusion, our experiments have demonstrated an increased proliferative fold change of *ex vivo* erythropoiesis of HbE/ β -thalassaemic erythroblasts using this specific culture system with a slightly faster maturation rate in the early stage of erythropoiesis when compared to the matched controls. However, the extent of cell proliferation did not relate to the clinical parameters of the patients. There was no observed increase in a dead cell proportion in thalassaemic samples but at delayed differentiation from the polychromatic stage was observed. This may be explained by the optimal three-staged culture system that we used for the patient culture and potentially by the presence of SCF, which has been suggested to reduce apoptosis in thalassaemia samples (410).

3.3.4 Proteomic comparison of *in vitro* reticulocyte membranes between patient and control

Numerous proteomic studies of reticulocytes and erythrocytes have been published, endeavouring to determine the underlying mechanisms of erythroid maturation process (19, 145, 400, 411, 412). This body of work revealed the composition of the reticulocyte membrane (prepared from reticulocytes at day 21 of the *in vitro* erythropoiesis, section 2.2.11, Chapter 2), comprising over 2,000 proteins, through top-down proteomics analysis (145, 400). The proteins identified in our project within reticulocyte membranes were in agreement with those reported in the previous studies. Of these proteins, the thalassaemic membranes, when compared to control reticulocyte membranes, had increased amounts of protein markers known to be lost during reticulocyte maturation. The reported proteins included the transferrin receptor (CD71), β -tubulin, myosin-9, and myosin-10 (19, 411). The composition of proteins we have observed provided further evidence that the cultured thalassaemic reticulocytes may be more immature than the normal control reticulocytes, which also agreed with the delay in maturation observed in the patient cultures compared to controls (as in section 3.2.5; Figure 3.8).

Most previous proteomics studies conducted on β -thalassaemic erythroid cells used *in vivo* source of erythrocytes (348, 374). Only one published report has studied proteome of *in vitro*

cultured erythroid cells of HbE/ β^0 -thalassaemia disease, and this study identified 18 proteins with altered abundance between thalassaemic erythroblasts and controls on day 7 and day 10 of the culture (218). Leecharoenkiat *et al.* (2011) carried out 2-DE gel electrophoresis, followed by quantitative proteomics analysis with MS/MS. This report observed that proteins involved with the metabolic state (11 out of 18) were up-regulated in HbE/ β^0 -thalassaemia when compared to normal erythroblasts. The up-regulated proteins were, for example, flavin reductase, enolase 1 alpha, aldolase, glucosidase, carbonic anhydrase 1, triosephosphate isomerase, GAPDH, and PRDX2 (218). Our study was in accordance with this finding, where the majority of proteins with increased expression in thalassaemic reticulocytes were proteins involved with the biological and metabolic process, unlike proteins identified from *in vivo* produced erythrocyte membranes where most of the proteins are involved in oxidative injury (374). The authors postulated that thalassaemic erythroblasts had higher active metabolic state than controls and measured the changing ratio of NADH/NAD⁺ to confirm this hypothesis (218). There are several important differences between the study by Leecharoenkiat *et al.* and our project. Firstly, our study used TMT nano-LC-MS/MS, a highly sensitive technology for proteomics analysis, which had the power to identify more than 2,000 proteins. Secondly, Leecharoenkiat *et al.* focused on erythroblasts on day 7, 10, and 14 of erythroid culture, whilst our source of erythroid membranes was filtered reticulocytes on day 21 of the culture. This is one of the most important differences between the two studies, as a comparison at different stages of cell maturation would naturally result in diverse types of proteins detected (19, 411). Lastly, culture protocols used were different; no steroid was added to the Leecharoenkiat's culture system.

3.3.5 Proteomic comparison of *in vitro* EVs derived from cultured reticulocytes of HbE/ β -thalassaemia patients.

While substantial evidence has focused on the proteomes of haemoglobinopathic erythrocytes (374, 391, 392), only two studies have examined EVs shed from *in vivo* thalassaemic red cells (348, 380). Both studies observed that proteins with altered abundance in thalassaemia intermedia samples were antioxidant proteins, e.g., heat shock proteins and peroxiredoxin, and α -globin (348, 380). To our knowledge, this work is the first to explore proteomic profiles focusing on EVs derived from *in vitro* pathological adult reticulocytes.

When compared between *in vitro* EVs of thalassaemic and control reticulocytes, the proteomic results did not identify proteins associated with increased oxidative stress. Most of the proteins were known constituents of EVs that are involved in the maturation of reticulocytes and the enucleation process (see Table 3.5). Only two antioxidant proteins were more abundant in the patient over control EVs – namely, catalase and selenium binding protein 1. In addition, the PT2 sample did not show the increased abundance of these eight proteins (as listed in Table 3.5) over the matched control. This finding is in agreement with the proliferative growth of this sample, which was not greater than its matched control (see Figure 3.3). Therefore, we could potentially conclude that the proteomics of *in vitro* thalassaemic EVs derived from cultured reticulocytes did not provide substantial evidence of increased oxidative injury or increased apoptosis, but only illustrated the slower maturation of thalassaemic cells when compared to the normal controls. Importantly, this result agreed with the previous culture data (presented in section 3.2.5), where maturation was delayed, and IE was not detected in the *in vitro* erythropoiesis of the patients' thalassaemic cells.

One recent study reported 367 unique proteins identified from exosomes derived from *in vitro* cultured cord blood reticulocytes (413). This number of proteins was comparable to the 286 proteins identified in EV samples in our study. A comparison of the composition of the EVs from cord blood reticulocytes identified a similar number of the membrane and cytosolic proteins. Membrane proteins identified by Diaz-Varela *et al.* (2018) include transferrin receptor, transporter proteins (Na⁺/K⁺ transporting ATPase, glucose transporters, neutral amino acid transporters), integrin alpha and beta, CD44, CD59 glycoproteins, etc., while common exosome proteins were not observed in either study – i.e. flotillin, stomatin, CD55, and acetylcholinesterase. Several histone proteins, LDH, GADPH, 6-phosphogluconate dehydrogenase, S100, Rab GTPase, and galectin were key cytosolic proteins identified; our finding was in agreement with these observations (413).

3.3.6 Proteomic profiles of reticulocytes membrane and their derived EVs

Regarding our proteomic findings, the proteins with altered levels, observed either in *in vitro* cell membranes or in reticulocyte EVs, were proteins contributing to the physiological mechanisms such as binding activity, metabolic activity, or even enucleation process, and not

the proteins known to respond to stress or stimuli (See Figure 3.11B and Figure 3.14B). The anticipated alterations in antioxidant proteins and ROS pathways reported previously was not observed. This may mean that the cells experience less ROS stress in our culture system or that the cells are losing these proteins when the membranes were prepared. The follow-up study with the whole cell lysate would elucidate this finding. Therefore, the proteome profiles of *in vitro* reticulocyte membranes and EVs obtained here were similar in the patient and the control samples. However, the proteome of whole-cell lysates of patients and matched controls would be needed to fully validate that such cultured reticulocytes are genuinely similar to each other. Notably, the subtle differences detectable among the proteomes could be explained by the differences in the maturation stage between individual samples.

3.4 Chapter summary

In summary, the addition of DXM to the Griffiths *et al.* (2012) three-stage culture media was shown to be an effective way to enhance the proliferation of *in vitro* thalassaemic erythroid cells, even when using a low starting number of CD34⁺ progenitor cells isolated from small blood. The numbers of filtered reticulocytes obtained by this cell culturing methodology were sufficient for pelleting and enrichment of EVs used in experiments further described in this chapter. In addition, the *ex vivo* erythropoiesis of thalassaemic cells did not exhibit the ineffective erythropoiesis observed by Mathias *et al.* (159), but this more consistent with other reports (216, 218, 409, 410).

The experiments described in this chapter have generated the *in vitro* reticulocyte membrane and EV proteome from thalassaemic patients and matched controls for the first time. Surprisingly, the proteomics of both EVs and *in vitro* reticulocyte membranes from patients and controls were very similar, and we did not observe any prominent increased in antioxidant proteins expression in the patient samples, as we had originally anticipated. The proteomics findings corroborated the *in vitro* erythropoiesis experiment of culturing thalassaemic cells, where IE was not observed in the patients' samples or was masked due to the culture methodology used. These results led us next to explore the proteomic profiles of *in vivo* sources of extracellular vesicles in thalassaemic patients, discussed in the next chapter.

CHAPTER 4

CHARACTERISATION AND PROTEOMICS ANALYSIS OF THE *IN VIVO* GENERATED EXTRACELLULAR VESICLES

4.1 Introduction

The observed heterogeneity of clinical presentation of Haemoglobin E (HbE)/ β -thalassaemia patients cannot be explained entirely by the patients' genetic background. Several factors play a role in this heterogeneity, such as incomplete (β^+) or complete (β^0) loss of the β -globin chain, association with hereditary persistence of fetal haemoglobin, the degree of disparity between α - and non- α -globin chains, the starting onset and requirement for blood transfusion therapy (as reviewed in Chapter 1) (189). There is emerging evidence suggesting that extracellular vesicle (EV) generation may contribute to the variation of clinical manifestations of thalassaemic patients (340, 414). As discussed in Chapter 1 section 1.5, the protein composition of EVs can mirror the ongoing pathology of the cells of origin, and even indicate the severity and prognosis of the disease (323), as *in vivo* generated EVs originate from various cell sources, e.g., erythrocytes, endothelial cells, and platelets. EVs can also contribute to disease pathology or complications and are widely observed in many RBC diseases, e.g., red cell membrane disorders (415), sickle cell anaemia (16, 416), and thalassaemia (348, 358, 380). For example, EVs of platelet origin were observed to associate with the hypercoagulable state in transfusion-dependent β -thalassaemia major patients (417), whilst the red blood cells-derived EVs from thalassaemia intermedia patients contain an enzyme that involved in redox maintenance (348). This accumulating evidence suggests that the further study of *in vivo* generated EVs may inform our understanding of the pathophysiology of thalassaemia. Therefore, the work described in this chapter will set out to investigate the *in vivo* EVs derived from plasma of HbE/ β -thalassaemic patients with the aim of determining whether there are any detectable EV properties that may be useful in the clinical management of thalassaemic patients.

To be able to undertake this study successfully, firstly the best method for EVs isolation and quantification from plasma needed to be determined prior to the qualitative study of the EVs present in thalassaemic patients.

4.2 Results

4.2.1 Isolation of extracellular vesicles

In order to assess the best methodology for EV isolation from plasma, both UC and filtration methods were explored (see Chapter 2 section 2.2.7.1 for methods used). The NTA technique (see Chapter 1 section 1.5) was used to assess the effectiveness and recovery yield of EVs obtained by these two different isolation methods.

Two thalassaemic plasma samples, collected in 3 ml citrate tubes, were centrifuged at 2000g for 10 minutes in order to separate and discard all the cellular components. They were then frozen at -20°C and transported on dry ice from Thailand to NHSBT Filton, UK. The samples were divided into two aliquots each and processed for UC or filtration as described. The first aliquot was used for UC isolation method; the pellet was resuspended with PBS and diluted for testing by NTA, according to the sample preparation protocol for NTA described in section 2.2.9 in Chapter 2. The remaining supernatant was centrifuged with UC for the second time using the identical settings; a sample was taken and then repeated UC once more (three times in total). Vesicle size and enrichment were evaluated after each centrifugation step by NTA. The second plasma aliquots were filtered by using a MF-Millipore®, 0.22 µm pore size filter (Merck, Darmstadt, Germany) as described in (section 2.2.7.1 in Chapter 2). Size distribution and concentration of the isolated EVs were measured using NTA, and then a comparison was made between the two isolation methods.

As anticipated, the concentrations of plasma derived EVs were observed to be lower in the original primary plasma samples when compared to concentrated plasma following either sequential centrifugations or filtration, confirming that both methods successfully enriched the original plasma. The concentrations of EVs obtained after three UC (mean ± SE; $8.91 \times 10^8 \pm 3.82 \times 10^6$ particlesml⁻¹) were slightly lower than those obtained after only one ultracentrifugation ($9.88 \times 10^8 \pm 1.68 \times 10^7$ particlesml⁻¹). The overall differences in yield were within 15% between the 1st UC and the 3rd UC (Figure 4.1A); while in both samples, the EV sizes after three UC (161.2 ± 0.74 nm) were lower than after one UC (213.1 ± 3.39 nm) (Figure 4.1B). This suggests that repeated UC can affect the integrity of EVs, and therefore, all the experiments in this project used only a one-time UC protocol for EV isolation by the differential centrifugation technique.

The differences in EV density between the two enrichment methods, one-time UC and filtration were $9.88 \times 10^8 \pm 1.68 \times 10^7$ particlesml⁻¹ and $8.87 \times 10^8 \pm 3.82 \times 10^6$ particlesml⁻¹, respectively; as shown in Figure 4.1C. The concentration of EVs after three-time UC ($8.91 \times 10^8 \pm 3.82 \times 10^6$ particlesml⁻¹) and the post-filtration were comparable (Figure 4.1C). Regarding the distribution of particle size, the filtration technique provided a more homogeneous particle population, and particle enrichment (Table 4.2, Figure 4.1B and D) attained a satisfactory range (i.e. <220 nm, which correlated to the filter pore size).

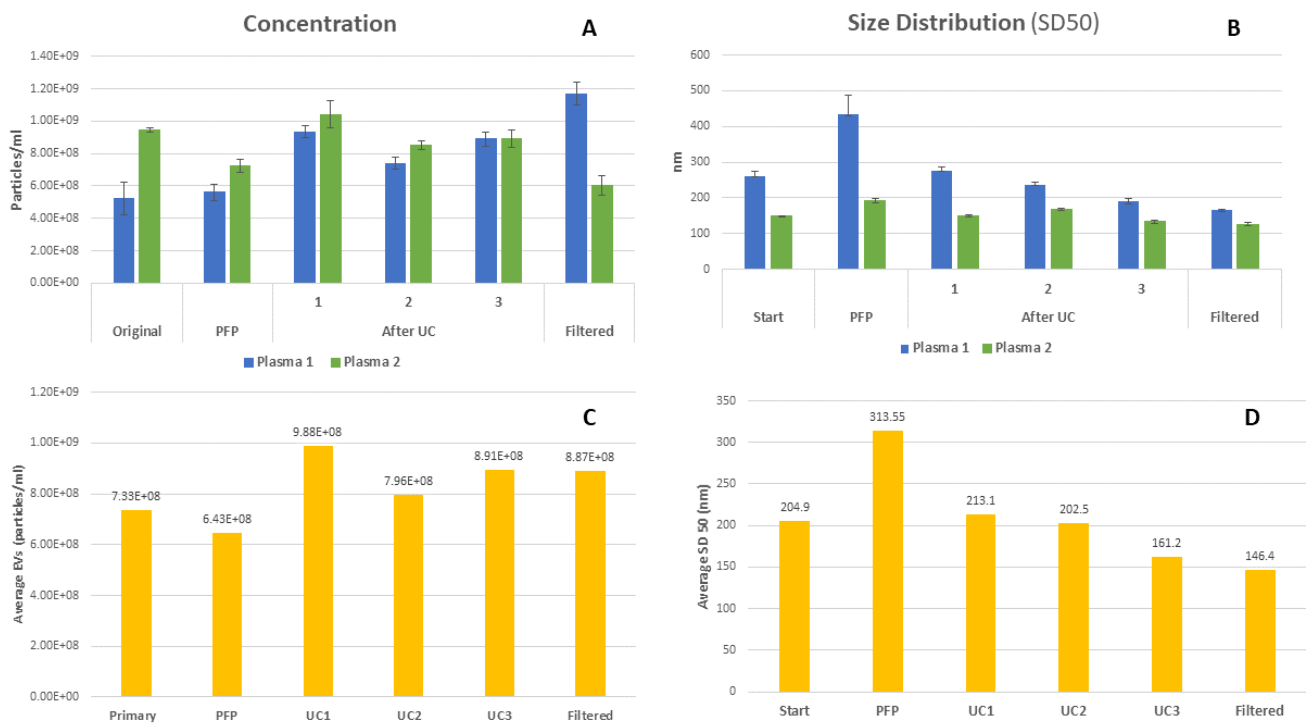


Figure 4.1. Comparison of different EV enrichment methods from plasma.

Two thalassaemic plasma samples tested. Bar graphs depict (A) individual and (C) average concentrations of EVs obtained from the primary plasma, platelet-free plasma (PFP), plasma following one (UC1), two (UC2), or three (UC3) time(s) ultracentrifugation, and plasma following filtration. Size distribution (SD50) of EVs is shown in (B) for individual samples and (D) for average values. SD50 in particle size distribution designates distribution value (D-value) which is the intercept for 50% (D50) or midpoint of the cumulative mass of particles in a particular sample, according to an arrangement of particle diameters. Note that, in order to determine size ranges, D10 and D90 are also required (383). All parameters were measured by nanoparticle tracking analysis (NTA; NanoSight Ltd; Malvern Panalytical) following the protocol described in section 2.2.9 in Chapter 2.

4.2.2 Quantitative measurements of EVs derived from plasma of HbE/ β -thalassaemia patients

Plasma samples of four thalassaemic patients (Table 4.1) were centrifuged to separate cellular components and then were frozen for transportation and storage. Although the freezing/thawing process is known not to affect the numbers of vesicles in cell-free plasma (352), this process was kept to a minimum. At the point of testing, the samples were thawed and aliquoted. Average EV concentrations of $1.38 \times 10^7 \pm 4.65 \times 10^6$ particles μl^{-1} for plasma sample 1, 2, 3, and 4 were measured by flow cytometry using commercial counting beads (see section 2.2.8 in Chapter 2); whereas the average concentrations of EVs from the same set of samples identified by NTA (see section 2.2.9, Chapter 2) were $7.65 \times 10^8 \pm 1.13 \times 10^8$ particles μl^{-1} for sample 1 to 4. The individual vesicle numbers obtained using these two methods are summarized in Table 4.2. When considered alongside clinical parameters of these patients (Table 4.1), the splenic status of the patients did not show any statistical association with the numbers of circulating plasma EVs measured by either method (data not shown).

Table 4.1. Clinical information of the HbE/ β -thalassaemia patients enrolled in this experiment.

Patient	Hb (gdl ⁻¹)	Splenic status	Transfusion history
P1	8.9	intact	Last transfusion 2 years ago (during pregnancy)
P2	7.0	intact	Intermittently (last transfusion 4 weeks ago)
P3	7.2	Post-splenectomy	Last transfusion over 5 years ago
P4	5.8	Post-splenectomy	Intermittently

Hb – haemoglobin

Table 4.2. Quantification of *in vivo* sourced EVs from the plasma of HbE/ β -thalassaemia patients. Comparison of NTA and flow cytometry techniques.

Sample	NTA (particles μl^{-1})	FC (particles μl^{-1})	Size distribution (nm)	Splenic status
Plasma 1	$7.07 \times 10^8 \pm 5.12 \times 10^7$	1.20×10^7	178 \pm 20.6	Intact
Plasma 2	$4.77 \times 10^8 \pm 1.33 \times 10^8$	2.13×10^7	175 \pm 29.5	Intact
Plasma 3	$8.77 \times 10^8 \pm 3.48 \times 10^7$	2.05×10^7	181 \pm 30.4	Splenectomy
Plasma 4	$1.00 \times 10^9 \pm 5.0 \times 10^8$	1.36×10^6	189 \pm 37	Splenectomy

NTA was displayed as an average of five video recordings per sample in a format mean \pm SE. NTA – nanoparticle tracking analysis, FC – flow cytometry

The size distribution of the EV samples obtained by NTA as D50 values (see definition of D50 in section 2.2.9, Chapter 2) was 178, 175, 181, and 189 nm for sample 1, 2, 3, and 4, respectively (see Table 4.2). Therefore, the quantities of EVs detected by NTA technology were higher than those obtained by flow cytometry. This result is consistent with the known limitations of flow cytometry, as this methodology cannot detect particles of less than 400 nm.

4.2.3 Exploring the relationship between *in vivo* EV generation and clinical manifestations of HbE/ β -thalassaemia patients using NTA

Plasma samples of the non-transfusion dependent HbE/ β -thalassaemia patients (n=16) and age- and gender-matched controls (n=13) were analysed for their EV concentrations using NTA. Clinical information of the patients was taken into account when exploring the relationship with the numbers of vesicles. Table 4.3 depicts numbers of EVs of the patients and controls, their haemoglobin (Hb) levels, platelet counts, and the splenic status. The statistical significance was defined as P-value <0.05.

In the HbE/ β -thalassaemia patient group, the Hb levels ranged from mild to severe anaemia with a mean Hb of 7.57 ± 1.50 gdl⁻¹ (mean \pm SD) for the whole group. Individually, the levels were 8.48 ± 1.24 gdl⁻¹ for the non-splenectomised (n=8), and 6.66 ± 1.19 gdl⁻¹ for the splenectomised groups (n=8). This difference between the groups was statistically significant (unpaired *t*-test; P-value = 0.0096), indicating that the clinical background of the splenectomised patients was more severe than the non-splenectomised ones. Average EV abundance detected in the patients, measured through NTA, was slightly higher than in the controls, but the difference was not statistically significant ($8.39 \times 10^7 \pm 4.65 \times 10^7$ particles μ l⁻¹ vs $7.87 \times 10^7 \pm 4.02 \times 10^7$ particles μ l⁻¹, respectively; unpaired *t*-test; p-value = 0.753). Also, the numbers of EVs in patient samples did not correlate with a degree of anaemia (Hb level). The EV levels were increased in splenectomised patients when compared to the patients who have the intact spleen; but this result was not statistically significant (Mann-Whitney-*U* test; p-value = 0.059). However, as previously observed (418), there was a significant correlation between platelet counts and the number of EVs in the patient group (Spearman's rho $r = 0.62$; p-value = 0.01, two-tailed).

Table 4.3. The concentration of EVs from circulating plasma vesicles derived from HbE/ β -thalassaemia patients (n=16) with recorded splenic status and controls (n=13).

Patient	Concentration (particlesμl⁻¹)	Hb (gdl⁻¹)	Platelet count (x10³/μl)	Splenic status	Control	Concentration (particlesμl⁻¹)
P1	3.49 x 10⁷	7.3	195	intact	C1	3.28 x 10⁷
P2	6.8 x 10⁷	6.7	717	splenectomised	C2	6.69 x 10⁷
P3	4.49 x 10⁷	8.6	325	intact	C3	7.52 x 10⁷
P4	8.24 x 10⁷	8.9	227	intact	C4	6.18 x 10⁷
P5	6.66 x 10⁷	7.0	134	intact	C5	5.16 x 10⁷
P6	3.41 x 10⁷	8.2	164	intact	C6	3.51 x 10⁷
P7	9.07 x 10⁷	7.5	755	splenectomised	C7	7.02 x 10⁷
P8	9.01 x 10⁷	7.9	858	splenectomised	C8	6.86 x 10⁷
P9	5.36 x 10⁷	7.7	301	intact	C9	8.11 x 10⁷
P10	7.53 x 10⁷	10.9	251	intact	C10	6.5 x 10⁷
P11	2.09 x 10⁸	5.8	733	splenectomised	C11	1.95 x 10⁸
P12	1.11 x 10⁸	9.2	398	intact	C12	1.11 x 10⁸
P13	8.46 x 10⁷	5.7	946	splenectomised	C13	1.09 x 10⁸
P14	1.78 x 10⁸	7.9	795	splenectomised		
P15	6.7 x 10⁷	7.2	765	splenectomised		
P16	5.22 x 10⁷	4.6	698	splenectomised		
Mean (\bar{x})	8.39 x 10⁷				Mean (\bar{x})	7.87 x 10⁷
SD	4.65 x 10⁷				SD	4.02 x 10⁷

4.2.4 Proteomic profiles of *in vivo* circulating EVs

4.2.4.1 Comparison of proteome profiles of the *in vivo* circulating EVs derived from plasma of HbE/ β -thalassaemia patients and normal healthy individuals

Fifteen HbE/ β -thalassaemia patients and 15 healthy controls were recruited in order to explore the proteomics of EVs in this study (see Table 4.4 for their clinical parameters). The circulating EVs were isolated from plasma of HbE/ β -thalassaemia patients and control samples as outlined in Chapter 2, by using UC technique. To reduce biological variation between individuals, quantitative proteomics of the circulating EVs were carried out across three separate sets of pooled-patient (n =5) and pooled matched control samples (n=5), as detailed in Chapter 2, section 2.2.1.4. Schematic representation of the samples used in these experiments is displayed in Figure 4.2.

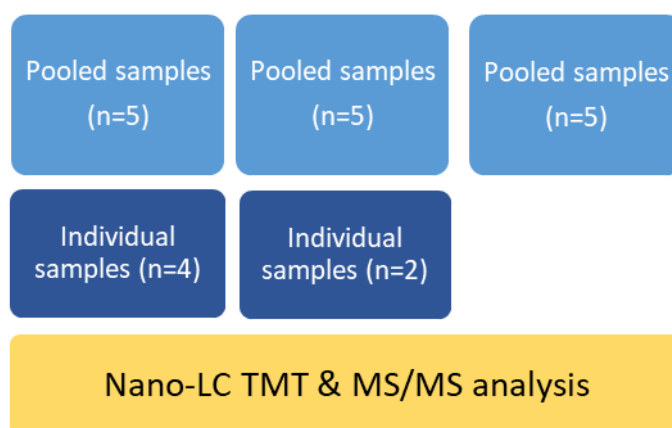


Figure 4.2. Schematic of HbE/ β -thalassaemia patients and control samples used for the proteomic analysis of the *in vivo* generated EVs.

Three sets of pooled HbE/ β -thalassaemia samples comprising a total of 15 individual samples were used for Nano-LC Tandem Mass Tag (TMT) with mass spectrometry analysis (MS/MS). Furthermore, six unrelated individual thalassaemic samples were also used for proteomic comparisons. All thalassaemic samples were compared to their matched controls.

Table 4.4. Clinical parameters of 15 patients enrolled for the EV proteomics.

PT	Sex	Splenectomy status	Hb Analysis	Hb (gdl ¹)	Hct (%)	MCV (fl) (82-97)	Nucleated RBC (/100 WBC)	Platelet Count (x10 ³ /ul) (157-420)	WBC (x10 ³ /ul) (5.3-10)	Neutrophil (%) (59-69)	Lymphocyte (%) (34-42)	Ferritin (ngml ⁻¹)
1	M	Intact	6.3%A2 54.8%E 38.9%F	80	26	53	7	123	7.4	64.4	29.4	595.5
2	M	Intact	55.6%E 31.9%F	86	25.5	68	N/A	325	5.6	57.5	36	N/A
3	F	Intact	N/A	66	19.9	60	N/A	204	6.05	47.6	45.3	392
4	F	Intact	35.5%E 54.3%F	89	26.9	58	N/A	227	8.8	59.7	30.9	310
5	F	Intact	N/A	70	22.2	69	N/A	134	10.5	59.2	35.2	1101
6	M	Intact	60.9%E2 8%F	49	18.5	57	34	49	7.16	36.8	57.4	334.7
7	M	Yes	34.5%E 65.5%F	79	27.4	65	229	858	14.9	34.3	56.3	387
8	M	Yes	N/A	79	26.5	81	274	795	17.51	42.6	40.8	1263
9	F	Yes	41.3%A 5.6%A2 14.4%F 38.7%E	67	21.5	75	151	717	20.7	36.5	48.6	5328
10	F	Yes	0.3%A 3.1%A2 94.9%F	46	16	79	490	698	39.9	62	28	766
11	M	Intact	44.1%E 55%F	68	23.4	58	N/A	221	7.1	64.4	29.5	336.7
12	F	Intact	N/A	77	23.8	56	N/A	301	8.6	54.6	35.1	N/A
13	F	Yes	N/A	72	24.2	71	258.4	765	17.7	41.1	49	N/A
14	F	Yes	N/A	58	20.4	72	534.3	733	8.6	26.1	65.5	N/A
15	F	Intact	N/A	92	28	60	2	398	8.06	67.1	26.8	645

N/A – not available

When filtered for proteins with >2 unique peptides, a total of 685, 1127, and 859 unique proteins were identified in each of the three individual experiments. Approximately 80% of the proteins detected in each experiment were known constituents of EVs, matching the Gene Ontology system (GO:1903561) from the AmiGO v1.8 database (Figure 4.3A). There was a total of 212 proteins detected that were common across all experiments (Figure 4.3B). The isolated EVs contained proteins from a mixture of cellular sources, including platelet proteins. The list of all proteins detected in this experiment is available as the supplemental data of the published article by Kittivorapart et al. (2018) (419). Table 4.5 lists 19 proteins in the EV samples that were identified to be consistently more abundant in the HbE/ β -thalassaemia patient samples than the controls, across all three experiments. There were only two proteins detected with differentially reduced abundance in the patient samples (Table 4.6). The classification of these proteins is shown in Figure 4.4 using STRING: Functional protein association network (www.string-db.org).

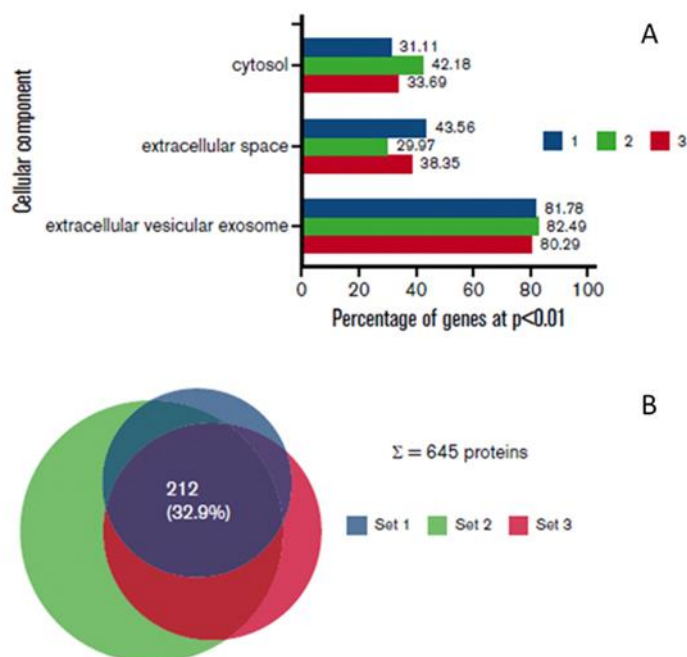


Figure 4.3. Gene Ontology analysis of cellular components on three sets of pooled thalassaemic plasma EV samples.

(A) Bar graphs show the cellular composition of the samples detected, with the majority of the identified proteins being EVs constituents (81.78%, 82.49%, and 80.29% from the sample set 1, 2, and 3, respectively). **(B)** Venn diagram of the total number of EV proteins identified, which was 645 proteins, with 212 proteins shared across all three experiments (419).

Table 4.5. Proteins with increased abundance in EVs of HbE/ β -thalassaemia patients compared to controls across three separate experiments.

Accession	Gene ID	Description	1 st experiment		2 nd experiment		3 rd experiment	
			Unique peptides	Patient/Control ratio	Unique peptides	Patient/Control ratio	Unique peptides	Patient/Control ratio
Chaperone proteins								
Q9NZD4	51327	Alpha hemoglobin stabilizing protein	6	47.40	4	43.46	5	31.70
P11142	3312	Heat shock cognate 71kDa protein	17	2.56	29	7.44	21	4.53
P0DMV9	3303 or 3304	Heat shock 70kDa protein 1A or 1B	17	10.65	27	13.41	24	14.02
P07900	3320	Heat shock 90kDa protein alpha family class A member1	12	4.03	21	13.54	16	4.77
P17987	6950	T-complex protein1 subunit alpha	2	3.78	10	5.79	2	2.49
B3KX11	7203	T-complex protein1 subunit gamma	2	2.47	12	8.70	4	2.37
Iron metabolism								
P02792	2512	Ferritin light chain	3	15.59	5	13.59	3	11.44
P02786	7037	Transferrin receptor protein	3	13.03	2	6.52	41	20.25
Antioxidant								
P04040	847	Catalase	14	2.69	26	6.35	17	3.80
P00441	6647	Superoxide dismutase	6	2.47	9	9.72	6	2.21
P32119	7001	Peroxiredoxin 2	8	2.40	11	8.45	7	6.88
Haemoglobin								
P02042	3045	Hemoglobin subunit delta	6	7.22	6	14.51	6	9.62
RBC cytoskeleton								
P02549	6708	Spectrin alpha chain, erythrocytic 1	16	2.70	98	3.80	61	2.97
P16157	286	Ankyrin-1	25	2.43	53	3.39	28	3.05
Other proteins								
P25774	1520	Cathepsin S	2	3.47	4	3.89	3	3.01
P00915	759	Carbonic anhydrase 1	8	5.66	6	13.76	8	6.37
P30043	645	Flavin reductase (NADPH)	8	4.63	6	9.51	7	5.64
P37837	6888	Transaldolase	6	2.08	11	6.99	6	2.47
P26641	1937	Elongation factor1-gamma	5	2.89	12	6.39	9	4.98

Table 4.6. Proteins identified using TMT mass spectrometry as consistently reduced in abundance across three separate experiments in extracellular vesicles of HbE/ β -thalassaemia patients compared to controls.

Accession	Gene ID	Description	1 st experiment		2 nd experiment		3 rd experiment	
			Unique peptides	Patient/Control ratio	Unique peptides	Patient/Control ratio	Unique peptides	Patient/Control ratio
Haemoglobin and haem scavenger								
P02790	3263	Hemopexin	26	0.04	29	0.08	31	0.05
P00738	3240	Haptoglobin	19	0.05	24	0.09	19	0.14

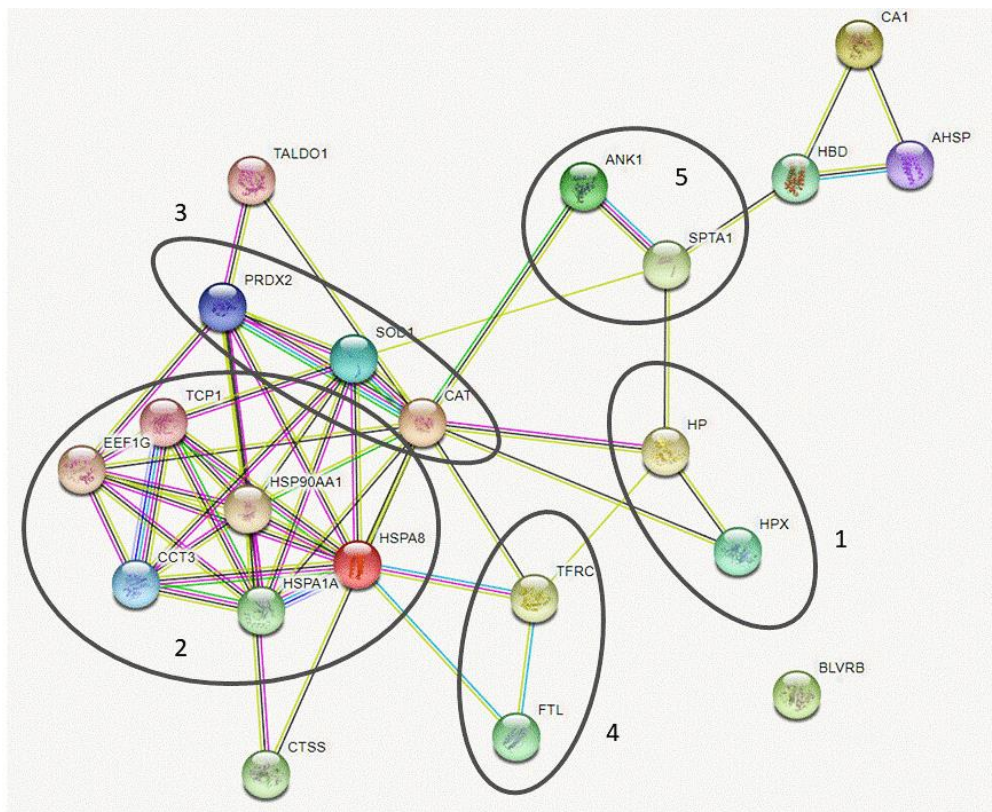


Figure 4.4. Functional classification of 21 proteins exhibiting an altered abundance according to their functions using STRING:

1- haem and haemoglobin scavengers, 2- chaperone proteins, 3- antioxidants, 4- iron metabolism and 5- cytoskeleton proteins. Network image was created from String-db.org. The group 1 haem and haemoglobin scavenger proteins were the only proteins detected as downregulated.

Proteins with increased abundance in the HbE/ β -thalassaemia patient over control samples could be categorised according to their molecular functions as chaperone proteins, proteins involved with iron metabolism, antioxidant proteins, and erythrocyte-specific proteins (Table 4.5). Among these, the protein with the highest ratio difference between patients and

controls was alpha haemoglobin stabilising protein (AHSP), a red blood cell-specific protein that prevents α -globin precipitation (420), which exhibited between 31- and 47-fold increase in thalassaemic EVs. Other chaperone proteins identified were Hsp70, Hsp90, and T-complex protein 1 subunit α and γ . Three antioxidant proteins that were increased in thalassaemic EVs were catalase, superoxide dismutase (SOD1), and peroxiredoxin-2 (PRDX2). Flavin reductase, a broad specificity oxidoreductase that catalyses the nicotinamide adenine dinucleotide phosphate (NADPH) reduction contributing to haem catabolism and provides reducing power for the release of ferritin-bound iron, was increased. Proteins involved in iron metabolism were also increased (ferritin and transferrin), alongside carbonic anhydrase-1, transaldolase (a pentose phosphate pathway enzyme) and the erythrocyte cytoskeleton proteins spectrin and ankyrin. These data strengthened the hypothesis that the circulating plasma EVs are derived in part from erythrocyte lysis (374). Finally, an increase in the quantity of cathepsin S, a potent elastolytic protease, was detected in thalassaemic EVs, which may have, therefore, originated from activated myeloid cells (421).

Only two proteins, hemopexin and haptoglobin, were consistently and significantly reduced (12.5- to 25-fold and 7.1- to 20-fold reduction, respectively) in the HbE/ β -thalassaemia patients compared with control EV samples across the three experiments (see Table 4.6). The data were consistent with the pathophysiology of thalassaemia, with the haemolysis causing a dramatic decrease in these Hb/haem scavengers. In addition to the pooled samples, where a sufficient amount of EV protein sample was isolated, individual patient samples were also included within the same TMT MS experiments.

Proteomics analysis of six HbE/ β -thalassaemia patients' individual samples across two separate experiments corroborated the pooled results. All of the proteins identified as having increased quantity in the pooled patient EVs had increased abundance in each individual sample, namely, AHSP, Hsp70, HspA8, Hsp90, TCP1 subunit α and γ , flavin reductase (NADPH), SOD1, catalase, PRDX2, and ferritin (see details in Table 4.7). Moreover, the fold increase of EV proteins in the individual samples correlated well with the severity of anaemia of the HbE/ β -thalassaemia patients. Levels of Hb were used as an indicator of anaemia in the patients. Ratios of the antioxidant proteins, AHSP, Hsp70, and TCP1- α showed statistically significant reverse correlation with Hb levels, summarised in Table 4.8. The results of these experiments were published in Kittivorapart *et al.* (2018) (419).

Table 4.7. Haemoglobin levels and the ratio of alteration of the proteins of interest in EVs from six individual HbE/ β -thalassaemia patients measured by TMT.

Patient Sample Number	Hb (gdl ⁻¹)	AHSP	Hsp70	Hsp71	Hsp90	TCP1- α	TCP1- γ	Flavin reductase	CTSS	SOD1	Catalase	PRDX2	Ferritin	Haptoglobin	Hemopexin
1	8.0	31.29	9.52	1.89	2.56	1.76	1.82	3.63	3.57	1.48	2.19	1.50	7.14	0.04	0.04
3	6.6	100.00	22.82	5.99	13.14	11.81	3.57	19.43	5.54	8.01	7.63	7.83	76.76	0.14	0.08
4	8.9	19.44	6.93	1.90	2.90	2.19	1.79	3.73	2.44	1.26	1.64	1.16	7.31	0.09	0.04
5	7.0	39.91	8.65	2.13	3.57	4.19	3.39	5.58	2.81	1.59	2.80	1.99	7.90	0.05	0.06
8	7.9	47.54	15.98	11.99	15.42	6.02	6.40	6.53	4.98	7.51	5.56	5.27	14.50	0.11	0.14
9	6.7	91.82	20.73	11.61	25.87	14.27	18.42	23.19	2.96	23.95	15.65	21.87	5.79	0.08	0.15

Hb - haemoglobin, AHSP – alpha haemoglobin stabilising protein, Hsp – heat shock protein, TCP – T-complex protein, CTSS – cathepsin S, SOD1- superoxide dismutase, PRDX2 – peroxiredoxin 2, Ferritin LC- ferritin light chain

Table 4.8. Statistical correlations between altered ratios of proteins of interest and haemoglobin levels of six individual HbE/ β -thalassaemia patients.

	Correlation coefficient	P-value, 2-tailed
Chaperone proteins		
AHSP	-0.943	0.005**
Hsp70	-0.829	0.042*
HspA8	-0.543	0.266
Hsp90	-0.657	0.156
TCP1-alpha	-0.829	0.042*
TCP1-gamma	-0.714	0.111
Antioxidants		
Catalase	-0.886	0.019*
SOD1	-0.886	0.019*
PRDX2	-0.886	0.019*
Flavin reductase	-0.829	0.042*
Haem scavengers		
Haptoglobin	0.371	0.468
Hemopexin	0.714	0.111
Other protein		
Cathepsin S	-0.543	0.266

Negative correlation coefficients denote negative correlations.*P<0.05 represents statistical significance of >95%. **P<0.01 represents statistical significance of >99%.

4.2.4.2 Immunoblotting to validate the proteomic study

The alterations in abundance of catalase, AHSP, hemopexin, and haptoglobin from these plasma-derived EVs were also confirmed in individual samples by Western blot analysis, following a method described in section 2.2.12, Chapter 2. Two pairs of patients and age- and sex-matched controls were tested to represent proteins in the EVs of the patient and control groups (as demonstrated in Figure 4.5). The upregulation of AHSP and catalase was demonstrated in patient samples when compared with their matched controls. Haptoglobin and hemopexin were markedly decreased in both patients (Table 4.6).

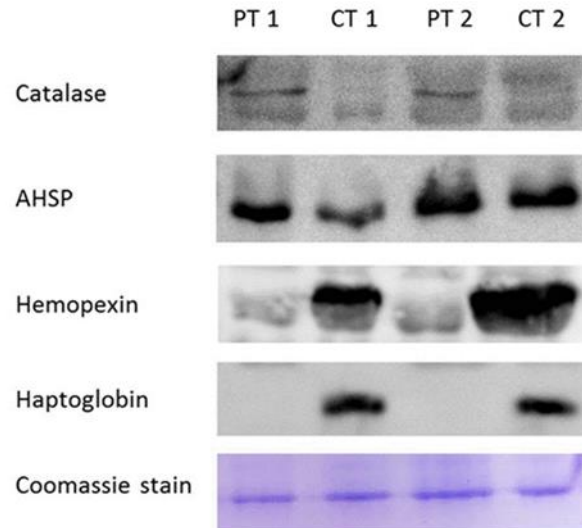


Figure 4.5. Western blot analysis of EV samples of two patients.

EV samples of two patients (PT1 and PT2) and EVs of two age- and sex-matched controls (CT1 and CT2) immunostained with antibodies to the indicated proteins. In concordance with proteomics results, the patients' EVs had an increase in abundance of AHSP and catalase when compared with control samples, and markedly decreased haptoglobin and hemopexin protein levels. An example of Coomassie-stained gel is shown to demonstrate the accuracy of loading.

4.2.4.3 Thalassaemic EV plasma adsorption test

The depletion of both hemopexin and haptoglobin from the EVs observed in this study may be an indicator of their continual clearance from patient's plasma, which was in turn reflected in the low amount of these proteins associated with EVs. To test this hypothesis, thalassaemic patients' EV pellets were washed and then incubated for 72 hours with EV-depleted normal fresh plasma. Using Western blotting, we observed that incubation of normal plasma caused the restoration of haptoglobin and hemopexin levels in patients' EVs (Figure 4.6).

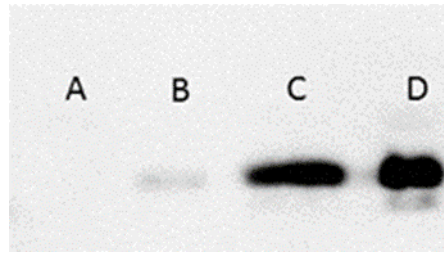


Figure 4.6. Western blot of EVs from patient and control immunostained with anti-hemopexin, demonstrating the expression of hemopexin.

(A) washed patient's EV (B) washed matched control's EV (C) patient's EV after incubated with normal fresh plasma (D) EV of the donor of fresh plasma.

4.2.4.4 Comparative analysis of the proteomic profiles of *in vivo* and *in vitro* sourced EVs

The proteomic results of the constituents of EV samples derived from the *in vitro* reticulocytes (from section 3.2.8, Chapter 3) were then compared to the results of the proteomic studies of the EVs isolated from the plasma of thalassaemic patients and normal matched-controls. The primary objective of the analysis was to determine whether the EVs released by reticulocytes are responsible for some of the EV content detected in the plasma. As aforementioned, approximately 70% (section 3.2.8, Chapter 3) and over 80% (Figure 4.3, this Chapter) of the proteins from *in vitro* and *in vivo* sources, respectively, were known EV protein constituents (GO:1903561) from the AmiGO v1.8 database. The source of both *in vitro* and *in vivo* EV proteins analysed in this project were therefore confirmed to be derived from EVs. Moreover, many proteins are known to be in reticulocytes or erythrocytes, for instance, Hb, AHSP, transferrin receptor, and cytoskeleton proteins (e.g., ankyrin, β -tubulin, spectrin, myosin 9), etc., were shared by both types of EVs.

Regarding EVs from the *in vitro* reticulocyte source, the majority of the more abundant proteins were involved in the enucleation process (Chapter 3, Table 3.5). Whereas, up-regulated proteins from the *in vivo* patients' EVs were associated with the stress-response mechanisms of the thalassaemic erythrocytes, as shown in Table 4.5.

Less abundant proteins in the EVs from *in vitro* reticulocyte origin in the patient samples did not exemplify the pathophysiology of thalassaemia (e.g., metabolic proteins, ribosomal proteins, complement activation proteins, etc.), unlike the less abundant proteins identified in EVs, derived from circulating patient plasma. EVs from the latter group showed evidence

of haemolysis when compared to EVs from healthy controls, indicated by the decreased quantity of haptoglobin and hemopexin. It should be noted that the EVs from circulating plasma of the patients would have originated from multiple cellular sources, i.e., erythrocytes and platelets, whereas the *in vitro* EVs were exclusively derived from the cultured reticulocytes. Overall, these findings indicated that the mechanism of EV generation between the *in vitro* and *in vivo* erythropoiesis was different.

4.3 Discussion

This chapter has focused on the analysis of HbE/ β -thalassaemia EV samples for their characteristics in terms of quantities, sizes distribution, and protein constituents, to determine if EVs are one of the factors that can possibly contribute to the severity of the disease or help disease management.

4.3.1 Determination of the optimised method for EV isolation and quantification

According to the results displayed in Figure 4.1, the overall EV yields by the chosen isolation methods were slightly different. The EV sizes after three UC (161.2 ± 0.74 nm) were lower than after one UC (213.1 ± 3.39 nm); therefore, the one-time UC was deemed better than the three-time UC, for this method does not affect the integrity of EVs. Hence, one-time UC was the method of choice used to isolate EV for the proteomic work in this project. UC method was preferable because the EV obtained from the filtration technique may be contaminated with proteins aggregates (377, 422). When time and labour were compared between one-time UC and filtration techniques, the latter proved to be a good alternative method for EV enrichment, when EVs were not used for the proteomic study.

Regarding the EV quantification technique, there are several methods available for investigation and characterisation of EVs. The benefits and limitations of each technique were briefly reviewed in Chapter 1. In this chapter, two of the most frequently used methods of quantifying EVs – flow cytometry and NTA, were compared. The higher concentrations of EVs were observed with the use of NTA over flow cytometry in both EVs generated *in vivo* (Table

4.2) and *in vitro* (see Table 3.4, Chapter 3). These observed results were consistent with the known sensitivities of the techniques used (423, 424).

Although the NTA has superior sensitivity when compared to conventional flow cytometry, this methodology does have limitations. For NTA that uses the refractive index and tracks individual particle scattering to determine the size and concentration of particles in a solution, which makes it difficult to accurately assess the actual number of particles in non-homogeneous samples. EVs are naturally highly polydisperse in character; thus, large EVs can obscure the smaller size EVs in the samples and lead to inaccurate measurements (360). However, to date, NTA is one of the methods of choice to quantify and assess size distributions of the EV samples (425) due to its superior sensitivity and, therefore, was the main method used in this thesis to quantify EVs in the tested samples.

4.3.2 The relationship of *in vivo* EV generation and clinical parameters of HbE/ β -thalassaemia patients

In this project, the enrolled patients were all thalassaemia intermedia or non-transfusion dependent patients (NTDT) with average Hb baseline of 7.6 gdl⁻¹; ranging from 4.6 to 10.9 gdl⁻¹ (see Table 4.3). The concentrations of the *in vivo* EVs between the patient and control groups did not show a significant difference. This may be explained by the fact that the majority of the previous publications that assessed the numbers of EVs in thalassaemic patients used conventional flow cytometry, which as discussed above has size limitation (347, 358, 380). This observation was in disagreement with the previous studies, which reported a greater number of EVs in splenectomised patients using conventional flow cytometry method (347, 358). However, Levin *et al.* (2018) carried out an analysis of 35 severe β -thalassaemia patients (TDT patients) using NTA, showing a significant increase ($p < 0.05$) in EV concentration in patients over controls (426). Another explanation of the discrepancy is that the specific type of thalassaemia patient explored here (HbE/ β -thalassaemia) is responsible for the observed differences.

Levin *et al.* (2018) reported that the numbers of EVs in subgroups of patients that underwent splenectomy and patients with the intact spleen were not statistically significant, which was in line with observations made in this thesis (426). This evidence indicated that the severity of the disease, but not the splenic status, potentially influences vesicle production. Whereas, platelet counts of the patients had a strong correlation with the number of EVs (Table 4.2);

thus, this relationship confirmed the suggestion that a substantial quantity of circulating plasma EVs of the thalassaemic patients have likely originated from the platelets (418).

Although flow cytometry was examined as a method of choice, utilising this method would have affected the identification of different subgroups of EVs due to the lower sensitivity of the method and its inability to detect particles <300 - 400 nm. From literature, there is evidence of the use of diverse EV enrichment methods in different studies. For example, Pattanapanyasat and colleagues (2004) did not isolate EVs from plasma, but had directly stained the fixed plasma (with 1% paraformaldehyde to limit the number of newly generated *in vitro* EVs) with glycophorin A (GPA) antibody and analysed it by flow cytometry (358). This approach would potentially include other sources of GPA⁺ particles in the analysis, e.g., products of red cell lysis, debris and apoptotic bodies, leading to false-positive results.

Ultimately, there were likely to be other influential factors involved in the formation of thalassaemic EVs, other than their quantity, for example, the EV composition that would reflect anaemic levels in HbE/ β -thalassaemia patients. Thus, the proteome profile of thalassaemic EVs was investigated as a next step.

4.3.3 Proteomic analysis of the *in vivo* EV produced from HbE/ β -thalassaemia patients

We observed that antioxidant proteins, chaperone proteins, proteins involving in iron metabolism, haemoglobin subunit δ , cathepsin S (an inflammatory marker), and erythroid proteins were consistently increased in quantity in HbE/ β -thalassaemic patients across all three pooled samples (Table 4.5), and this was also observed in six individual samples (Table 4.7). Taken together, the observed alterations in protein content in the thalassaemic EVs are consistent with the known increase in oxidative burden due to peripheral haemolysis reported in previous studies (348, 374, 375) and this study has substantially extended the number of known proteins with an altered concentration in HbE/ β -thalassaemic patients' EVs. The increased abundance of antioxidant and chaperone proteins in thalassaemic EVs was also observed by Ferru *et al.* (2014), who detected alterations of Hsp70, PRDX2, and catalase (348). In our study, we detected these proteins with at least two-fold greater abundance in thalassaemic EVs when compared with EVs from control individuals. The presence of these antioxidant proteins likely reflects the stress response mechanism in thalassaemic

erythrocytes, and we propose this could be a result of either EVs shedding from the viable erythrocytes or being generated from red cell lysis. This is also consistent with the detection of red blood cell-specific proteins in EVs here by us and by other studies (427).

Chaperones are another group of proteins that exhibited an increased abundance in the patients' EVs. These proteins facilitate the refolding of damaged proteins resulting from oxidative stress in erythrocytes (428). AHSP, a specific erythroid chaperone significant in erythropoiesis and exclusively binding to the α -Hb chain, has the greatest fold differences in patients' EVs, consistent with the known disturbance in β -globin in thalassaemic erythrocytes. Several genotype-phenotype studies exploring the association between the AHSP gene and severity of thalassaemia could not identify any correlation (429-431). However, Bhattacharya *et al.* (2010) reported an increase of AHSP expression in thalassaemic erythrocytes, which likely reflects the original source of AHSP in EVs (374).

The proteomics also identified a higher quantity of ferritin and transferrin receptor in EVs, two crucial iron-binding molecules. Transferrin receptor is known to be lost during reticulocyte maturation (9), suggesting that these may also be a source of EVs and raised ferritin correlates with the increased iron status of the patients (Table 4.1). Our study focused on NTDT patients who develop iron overload due to increased iron absorption and acceleration of iron released from the reticuloendothelial system (432). The mean serum ferritin in our study is 1035 ngml^{-1} (normal value 300 ngml^{-1} , from 10 of 15 patients) with some patients requiring chelation. The heightened iron level observed in these patients represents an important source of oxidative stress in thalassaemic erythrocytes, which may explain why EVs from thalassaemic patients have more iron-binding substances and antioxidant proteins in the plasma than healthy individuals.

Haptoglobin and hemopexin were decreased in our patient EV samples, and both are free Hb and free-haem scavenging plasma proteins, respectively. Free Hb and haemin, ferric Hb, can unleash an oxidative catastrophe to the vascular endothelium and parenchymal tissue (433). These proteins bind the toxic substances and transport them to the reticuloendothelial tissue to be eliminated (433, 434). Importantly, we demonstrated that circulating plasma EVs flexibly adsorb haptoglobin and hemopexin (Figure 4.6), thus indirectly reflecting the availability and concentration of these proteins in the plasma.

Overall, this report has undertaken the most detailed proteomic study to date, describing the constituents of circulating EVs of HbE/ β -thalassaemic patients, and providing quantitative differences of protein expression in EVs in comparison with age- and sex-matched healthy individuals. When compared with the pathophysiology of the disease, the observed proteomic changes typify the protective mechanisms used by the thalassaemic patients. Antioxidants, iron sequestering proteins, and chaperones were the predominant proteins that exhibited an increased abundance in thalassaemic EVs. We also report for the first time that the quantity of haptoglobin and hemopexin, the free Hb and haem-eliminating proteins, are reduced in thalassaemic patients' EVs. Furthermore, the alterations of an abundance of these proteins correlated with Hb levels of the patients (Table 4.7 and Table 4.8). As far as we are aware, these plasma proteins are not routinely tested for in the plasma of thalassaemic patients. Similar reductions in haptoglobin and hemopexin were reported recently in the plasma of paediatric patients with sickle cell disease (435) and were proposed as potential biomarkers of clinical severity of haemolysis in these patients. Thus, we have shown that these plasma markers are also applicable for HbE/ β -thalassaemic patients, where a deficit in haptoglobin and hemopexin availability reflects the severity of systemic haemolysis. Finally, we have also detected the altered levels of cathepsin S, a potent elastolytic protease that could be useful as an inflammatory plasma marker to monitor the degree of inflammation in thalassaemia (421). Future studies to evaluate the clinical application of these plasma biomarkers for monitoring the severity of thalassaemia and transfusion requirements were carried out and are described in the following chapter.

4.4 Chapter summary

In summary, the work described in Chapter 4 has demonstrated that the circulating plasma derived EVs of HbE/ β -thalassaemia patients can be successfully isolated using the UC technique, and quantified by the NTA method. The association between the concentrations of EVs in non-transfusion dependent β -thalassaemia patients and the severity of their clinical manifestations was investigated, and it was shown that there was no statistical correlation between Hb levels, splenic status and the concentration of EVs. There was a significant correlation between the numbers of detected circulatory EVs and the numbers of platelets in these patients.

Importantly, we have successfully identified the differences in protein constituents between the EVs of HbE/ β -thalassaemia patients and healthy controls. When compared with the pathophysiology of the disease, the observed proteomic changes typified the protective mechanisms used by the thalassaemic patients. Antioxidants, iron sequestering proteins, and chaperones were the predominant proteins that exhibited an increased abundance in thalassaemic EVs. We have also reported for the first time that the quantity of haptoglobin and hemopexin, the free Hb and haem-eliminating proteins, was reduced in thalassaemic patients' EVs. Furthermore, the alteration of levels of these proteins correlated with Hb levels of the patients. Similar reductions in haptoglobin and hemopexin were reported recently in the plasma of pediatric patients with sickle cell disease (435), where these proteins were proposed as potential biomarkers of clinical severity of haemolysis in these patients. Thus, we have shown that these plasma markers could also be applicable to the HbE/ β -thalassaemia patients, where a deficit in haptoglobin and hemopexin availability reflects the severity of systemic haemolysis. Finally, we have detected the altered levels of cathepsin S, a potent elastolytic protease that could be useful as an inflammatory plasma marker to monitor the degree of inflammation in thalassaemia. In the next chapter, we will assess the clinical applications potential of these plasma biomarkers for monitoring the severity of thalassaemia and/or determining the transfusion requirements in the different clinical severity of thalassaemic patients.

CHAPTER 5

CLINICAL STUDY OF HAPTOGLOBIN, HEMOPEXIN, AND CATHEPSIN S IN THALASSAEMIA

5.1 Introduction

5.1.1 Overview of haemolysis and biomarkers in thalassaemic patients

According to the pathophysiology of thalassaemia (see section 1.3.3, Chapter 1), the haemolytic process in this disease is predominantly extravascular haemolysis (EVH), owing to the occurrence of substantial ineffective erythropoiesis (IE) in this disease (209). There is very limited evidence of intravascular haemolysis (IVH) in thalassaemia, unlike that observed in sickle cell disease (SCD), where one-third of the total haemolysis is intravascular due to the irreversibly sickled cells and oxidative damage that occurs within the erythroid membrane (436).

Currently, there is no 'gold standard' or a specific marker of haemolysis. Only Hb serves as the most important indicator of haemolysis and treatment monitoring. However, unlike in the acute anaemia situation, monitoring Hb only has a limitation in chronic haemolytic diseases, such as thalassaemias, where the patients can tolerate a degree of anaemia. Thus, low Hb does not always directly reflect the well-being and the transfusion requirement in such patients. In clinical practice, usually, more than one parameter is monitored and interpreted together with the patient's signs and symptoms to make a precise diagnosis and to predict the severity of the disease. Several markers have been proposed as potential severity predictors in haemoglobinopathy diseases, for instance, soluble CD163 in SCD patients (437, 438), LDH levels associated with complications of SCD (260, 439) and also Hsp70 levels in β -thalassaemic disease (426).

In Chapter 4, haptoglobin, hemopexin and several other proteins were shown to have significantly altered abundance in thalassaemic patient plasma EVs (Chapter 4, Table 4.5). Haptoglobin and hemopexin are known plasma proteins and free Hb and haemin scavengers. They are one of the clinical indicators of IVH (433). These two proteins have been reported as reduced in SCD (433, 435, 440). Although there is general medical knowledge that haptoglobin is decreased in thalassaemia, hitherto, only a few studies have clinically evaluated both markers in thalassaemic patients (441-443). In 1969, researchers observed the absence of haptoglobin from 26 of the 35 thalassaemia major cases and seven of 42 thalassaemic trait cases using starch-gel electrophoresis technique. The absence of the

haptoglobin bands was not associated with the patients' HbF levels (441). A study by Vinchi *et al.* (2016) reported the decreased levels of haptoglobin and hemopexin in β -thalassaemia major and intermedia patients, but no exact levels were stated (443). Furthermore, no studies have assessed the relationship, if any, between the two proteins and the other indicators of haemolysis. There are currently no reports that would have explored the effects of blood transfusion on the levels of these proteins in haemoglobinopathy patients, probably due to the lack of recognition of IVH component in the thalassaemic patients.

In this chapter, the alterations of haptoglobin, hemopexin and cathepsin S (CTSS) blood levels were examined in a cohort of thalassaemic patients of varying clinical severity, with the ultimate aim of assessing the use of these proteins as biomarkers of thalassaemia severity and for potentially tailoring blood transfusion requirements to individual patients.

5.1.2 Haemolytic markers and their clinical applications

The expansion of erythron mass in thalassaemia occurs simultaneously with ineffective erythropoiesis (IE) and haemolysis. Several blood parameters have been used as haemolytic markers in general practice (see section 1.3.5.1, Chapter 1 and Table 5.1), not only facilitating the diagnosis and the severity of a disease prediction but usually also designating the type of haemolysis occurring in the patients, i.e., EVH or IVH. These markers include soluble transferrin receptor (sTfR), haematocrit (Hct) and erythropoietin levels; when used together, they can determine the erythropoietic status of a patient (444, 445). Anaemia, as measured by the decrease of Hb and Hct levels, would stimulate EPO production in kidneys and lead to the elevated serum EPO. STfR is a circulating transferrin receptor, consisting of two transferrin receptor monomers which bind one transferrin molecule. The concentration of sTfR can be measured by an immunoassay (446). Increased sTfR levels are an indicator of haemolysis and IE, as shown in both α - and β -thalassaemia (211, 447).

Table 5.1. Blood parameters observed in this study, including indications and associated site of haemolysis.

Parameters	Site of haemolysis	Indications
Haemoglobin (Hb)	n/a	Severity of anaemia, monitoring response after treatment
Haematocrit (Hct)	n/a	
Plasma haemoglobin	Intravascular	Diagnosis/severity of IVH
Percent of haemolysis	Intravascular	Not routinely tested
Corrected reticulocyte count	n/a	Differentiate causes of anaemia, the response of bone marrow
Indirect bilirubin (IDB)	Extravascular	Severity of EVH
Lactate dehydrogenase (LDH)	Predominantly intravascular	Diagnosis, monitoring response to therapy
Haptoglobin	Predominantly intravascular	Severity of haemolysis
Hemopexin	Intravascular	Not routinely tested
Cathepsin S	n/a	Not routinely tested

n/a – not applicable; data were derived from Kormoczi et al. *Eur J Clin Invest.* 2006; 36(3): 2029.(252)

5.1.2.1 Haptoglobin testing

Haptoglobin is a plasma protein synthesised by hepatocytes and encoded by the *HP* gene. Two allelic variations (*HP1* and *HP2*) lead to three haptoglobin isoforms, namely, Hp1-1, Hp1-2 and Hp2-2 (448). Each protein isoform has unique properties, such as the affinity towards Hb, binding capacity and a difference in molecular weight that can be assessed by gel electrophoresis (448). Haptoglobin binds to free Hb in the circulation after RBCs lysis. Generally, haptoglobin has a half-life of five days when unbound; however, its half-life is shortened to only a few minutes after forming the complex with Hb (449). Macrophages and the cells in the reticuloendothelial system rapidly remove this complex from the circulation (252), and thus, the level of haptoglobin is almost instantly depleted after the occurrence of haemolysis (usually in <1 hour) (450). Once depleted, it takes approximately 14 days for haptoglobin to be restored to the normal physiological level (449).

There are several methods for testing haptoglobin levels, for example, spectrophotometry which measures the changes of light absorption after haptoglobin forms complexes with Hb, immunoreactive methods such as nephelometry, or the enzyme-linked immunosorbent assay (ELISA) (451). The latter method is relatively quick and easy to perform, very sensitive and accurate, but requires specific antibodies (451). Additionally, false positive results indicating reduced haptoglobin level, albeit without haemolysis, could be detected in certain situations, for instance, liver impairment, ahaptoglobinemia, haemodilution and some types of solid cancer (451, 452). Since there is no 'gold standard' test for a definitive diagnosis of haemolysis, it is difficult to validate the accuracy of haptoglobin tests. One study using nephelometry reported 83% sensitivity and 96% specificity of the test when detecting the IVH if the haptoglobin level was less than 25 mgdl⁻¹ (452).

In our study, haptoglobin levels of all the patients were measured by using two separate methods, nephelometry and ELISA. The nephelometry technique was performed in Thailand, while the ELISA test was carried out at NHSBT Filton, Bristol, UK. ELISA was selected for testing due to the high sensitivity and high-throughput qualities of the method. The results of both techniques were compared individually for each patient and each sampling time.

However, it should be noted that there are limitations to using the haptoglobin level alone as a measurement of haemolysis or a diagnostic tool because as the acute phase reactant agent, haptoglobin would be present in a high level in inflammatory and infectious conditions (252). We also have to be mindful of the restrictions of the haptoglobin-Hb complex clearance, which is dependent on the quantity of available unbound specific receptor molecules on macrophages (CD163⁺) that can also be targeted by monoclonal antibodies or drug-conjugates (449).

5.1.2.2 Hemopexin testing

Hemopexin is one of the abundant plasma proteins and the protein with the highest affinity for haem binding. It is encoded by the *HPX* gene located on chromosome 11 and comprised of 10 exons. Hemopexin protein is produced in hepatic parenchymal cells (453). Unlike haptoglobin, hemopexin is not considered to be an acute phase reactant protein, and thus, its physiological levels are more constant than the haptoglobin levels. The half-life of

hemopexin is approximately seven days; whereas, when formed into a complex with free haem, its half-life is reduced to seven hours (453). Hemopexin assay is not routinely used as a test for haemolysis, but it can indicate the degree of IVH. Muller-Eberhard *et al.* (1968) reported the decrease of hemopexin level after haptoglobin was 'used up' in mild to moderate haemolysis associated with haemolytic diseases such as AIHA and paroxysmal nocturnal haemoglobinuria (PNH), i.e., hemopexin levels were moderately reduced when haptoglobin levels were low (440). The plasma of patients with a more severe degree of anaemia associated with thalassaemia major, HbE/ β -thalassaemia disease and sickle cell disease was depleted of both haptoglobin and hemopexin (440). Similar to haptoglobin, hemopexin can be tested with nephelometry and turbidimetry techniques. The specific hemopexin antisera for nephelometry is available commercially (453). However, since nephelometry is not one of the routine assays performed in Thailand, in our project, hemopexin levels were measured using the ELISA technique only. Normal ranges of hemopexin in an adult are 0.2 – 1.5 mgml⁻¹ (449).

Careful interpretation of hemopexin results is required because, besides haemolysis, hypohemopexinemia is observed in certain other conditions, for instance, liver cirrhosis due to impaired production of hemopexin (454), fulminant rhabdomyolysis with high myoglobin concentrations and acute intermittent porphyria, where hemopexin binds to porphyrins (455). Importantly, the level of plasma haptoglobin can help to differentiate the causes of low hemopexin, for example, in porphyria and rhabdomyolysis, only hemopexin is decreased while the haptoglobin level is normal (453). On the other hand, when only haptoglobin is decreased, and hemopexin levels are normal, the cause can be either mild IVH that does not consume hemopexin or congenital ahaptoglobinemia (453).

5.1.2.3 Cathepsin S testing

Whilst the haptoglobin and hemopexin were the only two proteins found to be less abundant in thalassaemic *in vivo* EVs, cathepsin S (CTSS) was one of the more abundant proteins (Chapter 4, Table 4.5) in these patients. It is a member of a family of cysteine peptidases found predominantly in lymph nodes and spleen (456). Macrophages and other antigen-presenting cells hold CTSS activity, where CTSS regulates autophagy (421, 457). This type of cathepsin can typically work in both weak acidic (optimum pH 6.5) and in neutral conditions (pH 7.5),

while other cathepsin members are able to work only in acidic environments (456, 458). The protein is encoded by the *CTSS* gene located on chromosome 1q21.3. The assay normally used to measure the CTSS level is the ELISA method, with the minimum detectable dose of 4 pgml⁻¹. The increased level of CTSS denotes the inflammation reactions and myeloid stimulation such as in rheumatoid arthritis (421, 459). Since CTSS was identified in the proteomics study to be increased in the thalassaemic *in vivo* EVs compared to the controls (see Chapter 4), we proposed to monitor CTSS as a potential marker of inflammation in patients with different severity of thalassaemia compared to the healthy controls.

5.1.3 Evaluation of haptoglobin, hemopexin and CTSS as predictive parameters of disease severity

For this clinical longitudinal study, patients presenting with different severities of thalassaemia were recruited to repeatedly test their levels of haptoglobin, hemopexin and CTSS and alongside haemolysis parameters. The patients recruited were a collection of transfusion dependent thalassaemia (TDT), non-transfusion dependent thalassaemia patients (NTDT), thalassaemia traits (carriers) and healthy controls. The aspects of enrolment and the patient classification are shown in detail in section 2.1.1.3 and Figure 2.2 in Chapter 2. Briefly, the patients were stratified based on clinical severity (section 1.3.5, Chapter 1) after providing full informed consent. The first group was TDT patients (n = 12), whose pre-transfusion and one-hour post-transfusion blood tests were collected over five visits to the haematology clinic, and thus, the number of individual tests conducted in this patient group was 120. The NTDT patient group (n = 18) provided samples over three visits with three-monthly intervals between the visits. However, some of these patients missed the follow-up testing, and the total number of tests conducted for this group was 38. The numbers of individuals in thalassaemic trait and healthy control groups were eight (n = 8) and seven (n = 7), respectively (see Figure 2.2, Chapter 2). Note that, utilising in-house Sanger sequencing methods (PCR and sequencing primers are detailed in Appendix II), we performed genetic testing of all the enrolled patients in the TDT and NTDT groups in order to confirm the diagnosis of these patients. The results are listed in Appendix III.

The blood samples from each research participant were investigated for a complete blood count (CBC), reticulocyte counts, LDH, indirect bilirubin (IDB), haptoglobin level (by

nephelometry technique) and plasma Hb. Subsequently, plasma was separated by centrifugation and frozen before the transfer to NHSBT Filton, UK, for further investigations. Haptoglobin, hemopexin and CTSS ELISA tests were optimised and used to measure the levels of haptoglobin, hemopexin and CTSS according to the manufacturer's protocols (Abcam).

5.1.4 Optimisation of the ELISA assays to detect the very low levels of proteins

Initially, the ELISA methodology had to be optimised to enable the measurements of the low concentrations of haptoglobin and hemopexin proteins encountered in thalassaemic patients. Firstly, samples were diluted with provided diluents according to the manufacturer's protocols, i.e., 1: 1000 for haptoglobin and 1: 400 for hemopexin and were tested according to the original protocols. As anticipated, due to the low levels of haptoglobin and hemopexin, most of the tests resulted in the out of range values as described by the manufacturer. Note that, according to the manufacturer's protocols, the minimum detectable dose (i.e., sensitivity) of haptoglobin and hemopexin levels are 0.07 and 0.03 μgml^{-1} , respectively. Following the optimising of the methods using serial dilutions, the optimal dilution of haptoglobin was determined as 1:100 for all the TDT and NTDT samples; while, the assay for hemopexin on patient plasma performed the best at 1:4 dilution. The samples prepared using these dilutions gave results within the detectable ranges of the ELISA assays. All the trait, as well as the control samples, were diluted and tested according to the manufacturer's protocols (see section 2.2.16, Chapter 2 for more details).

5.2 Results

5.2.1 Molecular diagnosis, demographic data and laboratory parameters in TDT, NTDT, thalassaemic traits, and control individuals

For the patients in TDT group (n=12), the genetic testing revealed that they comprised of HbE/ β^0 -thalassaemia (n=8), HbE/ β^+ -thalassaemia (n=2), one case of HbH-CS, and one compound heterozygote between HbE (β^E/β^E) and HbCS ($\alpha\alpha^{CS}/\alpha\alpha^{CS}$). Whereas patients in NTDT group (n=15) included patients with diagnoses of HbH-CS (n=6), HbH-Pakse (n=1), HbH disease (n=1), AE Bart's disease (n=1), three homozygous HbE (β^E/β^E), two cases of HbE/ β^0 -thalassaemia, and one compound heterozygote of β^E/β^E and ($\alpha\alpha^{CS}/\alpha\alpha$). The patients' genetic backgrounds are summarised in Appendix III. A summary of all laboratory tests, age, and splenic status of the patients recruited to the clinical follow-up trial is provided in Table 5.2.

Table 5.2. Demographic data and laboratory parameters in different groups of patients, traits, and controls.

Parameter	TDT (n =12)			NTDT (n = 18)	Traits (n =8)	Controls (n = 7)
	Total	Pre-Tx	Post-Tx			
Age (years)	30.7±4.0			46.4±3.5	34.4±3.6	36.3±1.9
Intact spleen	6/12 (50%)			17/17 (100%)	8	7
CBC	n = 120	n = 60	n = 60	n = 38	n = 8	n = 7
Hb (gdl ⁻¹)	7.90±0.13	6.88±0.11	8.84±0.17	9.29±0.23	13.06±0.69	13.96±0.52
Hct (%)	25.30±0.38	22.57±0.35	27.98±0.45	31.41±0.68	41.54±2.11	42.93±1.40
WBC (mm ⁻³)	9832.90±484.41	9628±722.76	10145±657.08	6420.83±267.39	7587.5±663.44	7728.57±529.02
Platelet (x10 ³ mm ⁻³)	453.82±28.24	467.27±41.22	433.93±38.43	199.60±8.25	303.25±0.14	282.00±0.26
Reticulocyte count (%)	6.63±0.61	5.96±0.85	7.20±0.89	3.88±0.38	1.53±0.17	1.46±0.09
Harboe assay						
Plasma Hb (mgdl ⁻¹)	0.09±0.01	0.06±0.01	0.12±0.01	0.05±0.01	0.05±0.02	0.04±0.02
Haemolysis (%)	0.87±0.06	0.72±0.07	1.01±0.1	0.36±0.04	0.20±0.06	0.16±0.04
Blood chemistry						
Total bilirubin (mgdl ⁻¹)	3.40±0.20	3.20±0.28	3.55±0.46	1.80±0.18	0.47±0.05	0.40±0.03
Indirect bilirubin (IDB; mgdl ⁻¹)	2.80±0.20	2.63±0.27	2.93±0.28	1.34±0.16	0.29±0.03	0.22±0.02
LDH (U ⁻¹)	582.69±26.92	576.37±45.93	587.50±28.09	529.98±47.30	341.63±20.26	318.14±23.17
Ferritin (ngml ⁻¹)	2733.24±220.60	2732.03±352.70	2715.18±350.53	511.85±62.28	290.51±93.74	171.93±48.64
ELISA						
Haptoglobin (mgdl ⁻¹)	5.44±1.02	7.43±0.96	3.45±0.93	26.18±5.09	275.10±65.60	206.22±51.27
Hemopexin (mgml ⁻¹)	0.015±0.001	0.015±0.001	0.016±0.001	0.021±0.002	1.834±0.325	1.862±0.341
Cathepsin S (pgml ⁻¹)	13472.00±391.92	13333.56±565.92	13537.03±547.13	8042.15±1089.04	3942.28±685.18	4444.88±696.28

Data represented as mean ± SE. CBC – complete blood count; ELISA – enzyme-linked immunosorbent assay.

5.2.2 Plasma haptoglobin

Normal reference ranges of plasma haptoglobin are between 30 – 200 mgdl⁻¹ (460). In this study, haptoglobin was one of the parameters tested in the UK from the plasma shipped from Thailand using ELISA technique (Abcam). Haptoglobin analysis was also simultaneously carried out in Thailand with the nephelometry technique. The results of the two methods were observed to show a similar trend. However, a statistical correlation is not possible to calculate due to the different limits of detection of the two methods (see Table 5.3 for the examples and the full list in Appendix I). The similarity trend between the two methods is also a validation of the dilutional preparation of the samples for the ELISA test in our study.

Table 5.3. Examples of haptoglobin levels (mgml⁻¹) of two TDT (A01&A03) and NTD (B07&B08) patients measured by nephelometry and ELISA methods.

TDT patients	Visit	Transfusion	Haptoglobin levels (mgml ⁻¹)	
			Nephelometry	ELISA
A01	1	Pre	<0.07	0.005381
		Post	<0.07	0.006048
	2	Pre	<0.027	0.006053
		Post	<0.027	0.004298
	3	Pre	<0.027	0.003871
		Post	<0.027	0.004124
	4	Pre	<0.027	0.006262
		Post	<0.027	0.007895
	5	Pre	0.59	0.346042
		Post	0.67	0.318589
A03	1	Pre	0.4	0.416789
		Post	0.4	0.008691
	2	Pre	0.3	0.434014
		Post	0.2	0.010845
	3	Pre	0.31	0.321481
		Post	<0.027	0.006107
	4	Pre	0.04	0.059143
		Post	<0.027	0.013820
	5	Pre	0.13	0.047934
		Post	0.14	0.099071
NTDT patients	Visit			
B07	1		0.7	0.073020
	2		0.58	0.073262
	3		0.34	0.035271
B08	1		<0.07	0.000371
	2		<0.027	0.000158
	3		<0.027	0.000199

Regarding the ELISA test, levels of haptoglobin of the TDT group were measured as $5.44 \pm 1.02 \text{ mgdl}^{-1}$ (mean \pm SE) and $26.18 \pm 5.09 \text{ mgdl}^{-1}$ for the NTD group. Haptoglobin in thalassaemia traits and controls was $275.10 \pm 65.60 \text{ mgdl}^{-1}$ and $206.22 \pm 51.17 \text{ mgdl}^{-1}$, respectively. Due to the non-normally distributed data, the Kruskal-Wallis test was performed, and it showed a statistically significant difference between all groups ($P < 0.0001$). The statistically significant differences between TDT and NTD groups were examined using Mann-Whitney U -test ($P = 0.013$) (Figure 5.1).

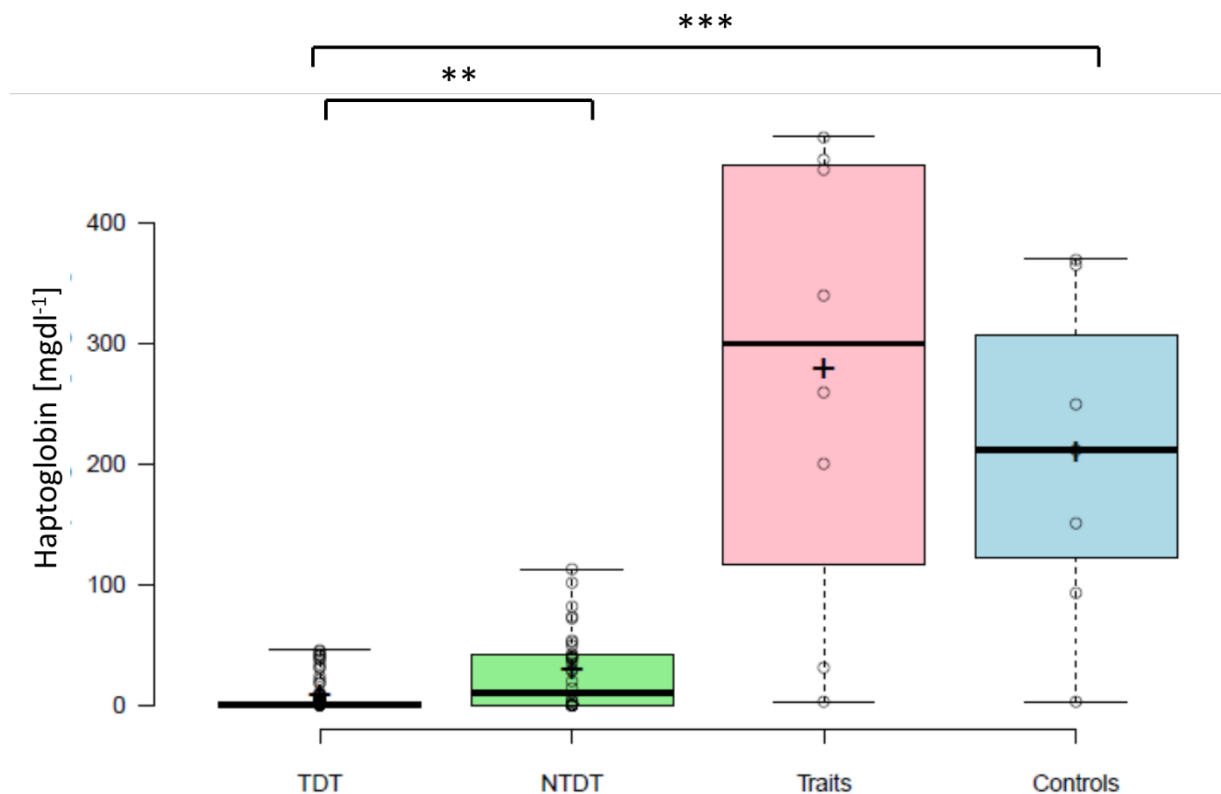


Figure 5.1. Boxplot showing variation in haptoglobin level (mgdl^{-1}) between groups of patients and controls as measured by ELISA.

TDT ($n=120$), NTD ($n=38$), thalassaemia traits ($n=8$), and controls ($n=7$). The box spans the interquartile range. The median and mean observation for a particular group is represented by horizontal lines and plus signs, respectively. Data were analysed by Kruskal-Wallis test and Mann-Whitney U -test. $**P < 0.05$; $***P < 0.0001$.

5.2.3 Plasma hemopexin

Plasma hemopexin is not a routine laboratory test in Thailand. Therefore, all the plasma samples were tested only at NHSBT Filton, Bristol, UK. Normal hemopexin level ranges from 0.5 – 2 mgml⁻¹ (440). In the TDT group, average hemopexin level was 0.015 ± 0.001 mgml⁻¹, and this level was significantly lower than in the NTDT group which had an average measurement of hemopexin 0.021 ± 0.002 mgml⁻¹ at P =0.0011 (unpaired *t*-test; 95%CI - 0.0098 to -0.0025). The significant difference in hemopexin levels was observed across all groups (Kruskal-Wallis test; P <0.0001), whilst the hemopexin levels between traits and controls were not significantly different. Their levels were on average 1.834 ± 0.325 mgml⁻¹ and 1.862 ± 0.341 mgml⁻¹ for traits and controls, respectively.

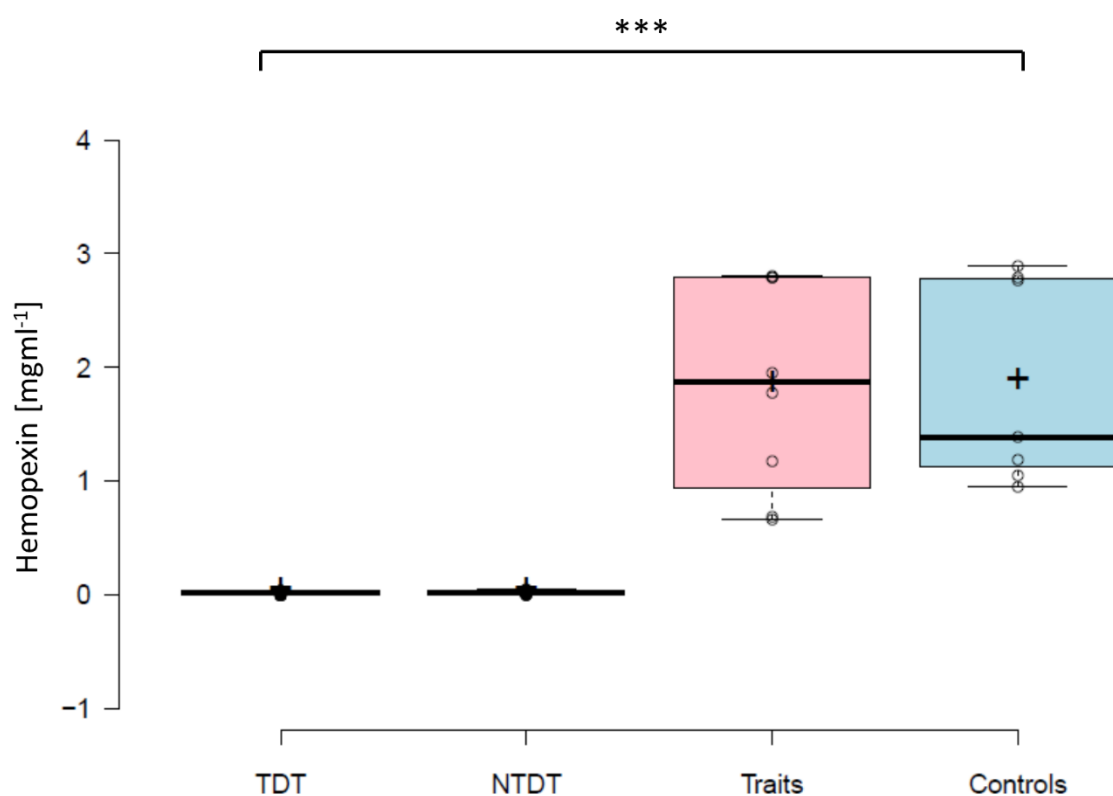


Figure 5.2. Boxplot showing the variation in hemopexin level (mgml⁻¹) between groups of patients and controls.

A markedly reduced level of hemopexin was observed in both the TDT (n = 120) and NTDT groups (n=38). The box spans an interquartile range. The median and mean observation for a particular group is represented by horizontal lines and plus signs, respectively. Data were analysed by Kruskal-Wallis test and unpaired *t*-test. ***P <0.0001.

5.2.4 Plasma cathepsin S

CTSS is a new parameter proposed here to monitor the level of inflammation in haemoglobinopathy diseases. Levels of CTSS are predicted to increase in accordance with the increased activity of the reticuloendothelial system anticipated in thalassaemia. This study used ELISA to measure the level of CTSS from blood plasma in all groups. Across all groups of patients and controls, the CTSS were significantly different (one-way ANOVA; $P < 0.0001$). TDT patients exhibited the highest level of CTSS at an average of $13435.29 \pm 392.03 \text{ pgml}^{-1}$, while CTSS levels in NTDT were lower, measured as an average of $8042.15 \pm 1089.04 \text{ pgml}^{-1}$. The differences between the two groups were statistically significant (t-test; P (two-tailed) < 0.0001 ; 95%CI 3563.65 to 7222.64). CTSS in traits and controls were 3942.28 ± 685.18 and 4444.88 ± 696.28 , respectively.

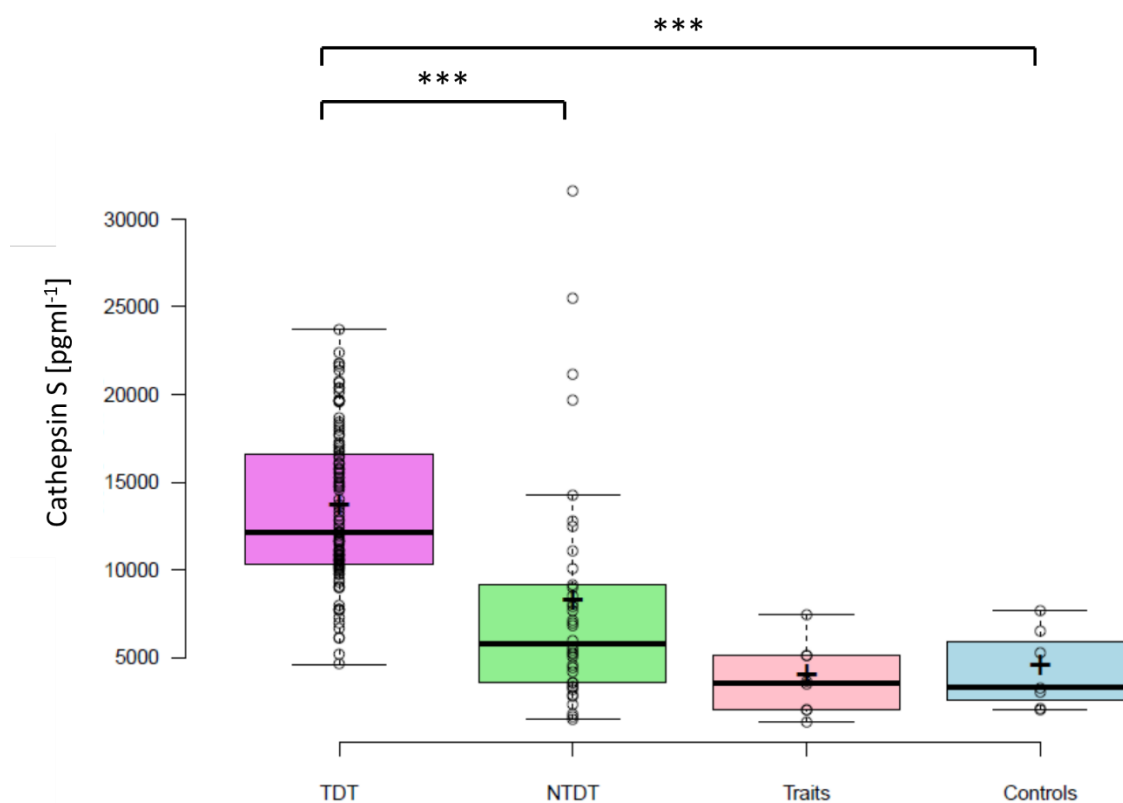


Figure 5.3. Boxplot showing the variation in cathepsin S level (pgml^{-1}) between groups of patients and controls.

These were statistically significant ($P < 0.0001$) across all samples analysed using one-way analysis of variance (ANOVA). The higher CTSS level in the TDT ($n=120$) compared to the NTDT ($n=38$) group was also statistically significant. The box spans an interquartile range. The median and mean observation for a particular group are represented by horizontal lines and plus signs, respectively. *** $P < 0.0001$.

5.2.5 The applications of haptoglobin, hemopexin and CTSS in the various clinical classification of thalassaemic patients.

The analyses performed were based only on clinical classification of thalassaemia, not a genetic diagnosis, for several reasons. Firstly, in each individual clinical group, the majority of patients were homogeneous, i.e., eight HbE/ β^0 -thalassaemic patients out of 12 (67%) in the TDT group, and nine α -thalassaemia from 15 (60%) NTDT patients (see Appendix III). Therefore, statistical analysis made based on clinical or genetic backgrounds would be comparable. Secondly, statistical analysis of small sample size (<30) will be detrimental the validity of the results (461). Thirdly, the primary aim of this study was to utilise the three proteins as clinical biomarkers. Finally, since genetic testing was not available and cost-efficient in the context of developing countries, majority of thalassaemia patients are treated based only on the clinical severity, not their genetic basis, or type of thalassaemia.

5.2.5.1 NTDT patients

The measured plasma haptoglobin, hemopexin and CTSS were analysed by ELISA method as described in previously (Table 5.2). The correlation analysis was performed across 38 tests ($n = 38$), $P < 0.05$ (one-tailed) described the statistical significance for haptoglobin and hemopexin and $P < 0.05$ (two-tailed) for CTSS. $P < 0.0001$ denoted a highly statistical significance between the measured parameters. The results are displayed in Table 5.4. Additionally, the correlations between the three proteins and the haemolysis parameters are presented in Table 5.5.

The correlations of all the haemolytic parameters with Hb were also analysed using Spearman's rank one-tailed hypothesis. Factors that significantly correlated with Hb were Hct ($P < 0.0001$; 95%CI 0.733 to 0.894; $r = 0.841$) and IDB ($P < 0.0001$; 95%CI -0.773 to -0.343; $r = -0.592$). The alteration of Hb levels did not significantly correlate with plasma Hb, percent haemolysis, LDH, or corrected reticulocyte counts. Plasma IDB correlations with LDH and reticulocyte counts were highly significant ($P < 0.0001$); whereas, LDH also showed significant correlations with reticulocyte count, plasma Hb, and haemolysis percentage.

Table 5.4. A summary of the correlation studies of the NTD group, using Spearman's rank correlation, except for the marked parameters (※).

Parameters	Correlation (one-tailed)	95% Confidence interval	Correlation coefficient (r)
Haptoglobin			
Haemoglobin**	P = 0.016	0.011 to 0.636	0.347
Haematocrit	P = 0.283	-0.243 to 0.400	0.096
Plasma Hb**	P = 0.003	-0.717 to -0.111	-0.447
Haemolysis (%)**	P = 0.001	-0.732 to -0.135	-0.484
LDH***	P <0.0001	-0.819 to -0.540	-0.717
Indirect bilirubin***	P <0.0001	-0.799 to -0.439	-0.663
Reticulocyte counts***	P <0.0001	-0.720 to -0.320	-0.555
Hemopexin			
Haemoglobin	P = 0.423	-0.367 to -0.327	-0.032
Haematocrit	P = 0.085	-0.522 to -0.118	-0.227
Plasma Hb**	P = 0.011	-0.643 to -0.057	-0.378
Haemolysis (%)**	P = 0.016	-0.622 to -0.002	-0.352
LDH**※	P = 0.039	-0.522 to 0.030	-0.290
Indirect bilirubin**	P = 0.009	-0.590 to -0.133	-0.384
Reticulocyte counts**	P = 0.006	-0.596 to -0.148	-0.403
Cathepsin S (two-tailed)			
Haemoglobin	P = 0.035	-0.552 to -0.061	-0.343
Haematocrit	P = 0.670	-0.377 to -0.301	-0.071
Plasma Hb***	P <0.0001	0.322 to 0.772	0.587
Haemolysis (%)***	P <0.0001	0.398 to 0.774	0.614
LDH***	P <0.0001	0.476 to 0.843	0.702
Indirect bilirubin***	P <0.0001	0.490 to 0.806	0.683
Reticulocyte counts***	P <0.0001	0.404 to 0.792	0.629
WBC**	P = 0.035	0.011 to 0.629	0.342
Platelet **※	P = 0.001	-0.713 to -0.228	-0.536

Correlation analyses of haptoglobin and hemopexin followed one-tailed, while CTSS followed two-tailed hypothesis. LDH – lactate dehydrogenase, WBC – white blood cell, Hb – Haemoglobin; **P <0.05 statistically significant, ***P <0.0001 statistically highly significant. ※ used Pearson correlation. Minus r (-r) indicates the inverse relationship.

Table 5.5. The correlations of tested parameters in the NTD T group.

Parameters	Correlation	95% Confidence interval	Correlation coefficient (r)
Haptoglobin v Hpx	P(1-tailed) = 0.050	-0.070 to 0.557	0.270
Haptoglobin v CTSS***	P(2-tailed) <0.0001	-0.744 to -0.503	-0.653
Hpx v CTSS	P(2-tailed) = 0.117	-0.564 to -0.077	-0.258

All used Spearman's rank correlation. P <0.05 denotes statistical significance. ***P <0.0001 statistically highly significant. Hpx-hemopexin

5.2.5.2 TDT patients

When applied to TDT patients in our study, the haptoglobin, hemopexin, and CTSS assays and statistic analyses were similar to the NTD T group. The results are displayed in Table 5.6, and the correlations between the three parameters are presented in Table 5.7.

The correlations of all the haemolytic parameters with Hb were also analysed using Pearson or Spearman's rank one tailed hypothesis. Factors that correlated significantly with Hb were Hct (P <0.0001; 95%CI 0.928 to 0.964; r = 0.949), plasma Hb (P <0.0001; 95%CI 0.131 to 0.432; r = 0.282), IDB (P = 0.005; 95%CI -0.376 to -0.086; r = -0.237), reticulocyte counts (P = 0.013; 95%CI -0.328 to -0.078; r = -0.205) and hemopexin (Table 5.6).

Table 5.6. Summary of the correlation studies of the TDT group using Spearman's rank correlation, except for the marked parameters (✖).

Parameters	Correlation (one-tailed)	95% Confidence interval	Correlation coefficient (r)
Haptoglobin			
Haemoglobin	P = 0.350	-0.141 to -0.225	0.035
Haematocrit	P = 0.179	-0.094 to 0.264	0.085
Plasma Hb ✖	P = 0.099	-0.241 to 0.029	-0.119
Haemolysis (%) ✖	P = 0.074	-0.243 to 0.007	-0.133
LDH***	P <0.0001	-0.783 to -0.555	-0.683
Indirect bilirubin**	P =0.008	-0.316 to -0.103	-0.218
Reticulocyte counts***	P <0.0001	0.316 to 0.592	0.467
Hemopexin			
Haemoglobin***	P <0.0001	0.179 to 0.519	0.351
Haematocrit***	P = 0.004	0.059 to 0.407	0.240
Plasma Hb ✖	P = 0.053	-0.001 to -0.272	0.149
Haemolysis (%) ✖	P = 0.224	-0.089 to -0.206	0.070
LDH [‡]	P = 0.045	-0.050 to 0.348	0.155
Indirect bilirubin***	P <0.0001	-0.530 to -0.209	-0.377
Reticulocyte counts***	P <0.0001	-0.471 to -0.085	-0.299
Cathepsin S (two-tailed)			
Haemoglobin	P = 0.459	-0.110 to -0.245	0.068
Haematocrit	P = 0.045	0.014 to 0.351	0.183
Plasma Hb	P = 0.832	-0.196 to -0.161	0.020
Haemolysis (%)	P = 0.263	-0.291 to -0.074	-0.103
LDH ✖***	P <0.0001	-0.474 to -0.217	-0.359
Indirect bilirubin**	P = 0.010	-0.401 to -0.058	-0.235
Reticulocyte counts [‡]	P = 0.046	-0.027 to 0.385	0.182
WBC	P = 0.075	-0.039 to 0.300	0.132
Platelet ✖	P = 0.051	-0.002 to -0.350	0.179

Correlation analyses of haptoglobin and hemopexin followed one-tailed, while CTSS followed two-tailed hypothesis. LDH – lactate dehydrogenase, WBC – white blood cell, Hb – Haemoglobin; **P <0.05 statistically significant, ***P <0.0001 statistically highly significant. ✖ used Pearson correlation. Minus r (-r) indicates the inverse relationship. [‡] Asymptotic P value (P<0.05 but 95%CI crosses zero).

Table 5.7. The correlations of tested parameters in the TDT group. All used Spearman’s rank correlation. P <0.05 denotes statistical significance.

Parameters	Correlation	95% Confidence interval	Correlation coefficient (r)
Haptoglobin v Hpx [‾]	P(1-tailed) = 0.002	-0.004 to 0.503	0.260
Haptoglobin v CTSS**	P(2-tailed) =0.015	0.031 to 0.387	0.221
Hpx v CTSS**	P(2-tailed) = 0.017	-0.377 to -0.038	-0.218

**P <0.05 statistically significant. [‾] Asymptotic P-value. Hpx-hemopexin

5.2.6 The effect of transfusion on haemolytic markers in TDT patients

The majority of TDT patients enrolled in this study (n =12) were β^E/β^0 thalassaemia patients (n = 7; 58%), with 2 cases of β^E/β^+ thalassaemia (n = 2; 16%), one case of β^0/β thalassaemia with unknown cause of anaemia and negative direct antiglobulin test, one case of homozygous HbE with Hb constant spring (HbCS), and one case of HbH-CS disease (see Appendix III for the genetic backgrounds of the patients in this study). The mean pre-transfusion Hb baseline was $6.88 \pm 0.11 \text{ gdl}^{-1}$ (Table 5.2). For each patient, all of the laboratory parameters were measured at the pre-transfusion stage and one-hour post-transfusion for each of the five visits. Blood products used for transfusion were leukocyte-reduced red cell units, with one to two units per dose (one visit). The interval between transfusions ranged between four and six weeks. Statistic methods used to compare the two dependent groups were paired t-test for normally distributed data (only Hct), and Wilcoxon Signed-Rank test for the other parameters with a skewed distribution.

Of all the monitored parameters in this study, only Hb, Hct, plasma Hb, and % haemolysis significantly altered their levels pre- and one-hour post-transfusion (Table 5.8). Figure 5.4 depicts the differences between pre-transfusion and post-transfusion plasma levels of the three markers. There were no statistically significant changes observed between the pre- and post-transfusion blood levels of the three proteins.

Table 5.8. Statistical analysis of all parameters between pre-and post-transfusion plasma of the TDT group.

Parameters	Z-score or 95% CI	P-value (two-tailed)
Haemoglobin***	-6.736	<0.0001
Haematocrit***※	95%CI -6.29 to -4.91	<0.0001
Plasma Hb***	-5.597	<0.0001
Haemolysis (%)**	-3.2871	0.001
LDH**	-3.144	0.002
Indirect bilirubin***	-5.017	<0.0001
Reticulocyte counts	-2.216	0.0264
WBC (mm⁻³)	-0.39	0.6965
Platelet (mm⁻³) ***	-4.518	<0.0001

Wilcoxon Signed-Rank test was carried out on all parameters except Hct, which had a Gaussian distribution and was therefore analysed using the paired *t*-test. **P<0.005, ***P<0.0001; ※ = Paired *t*-test analysis

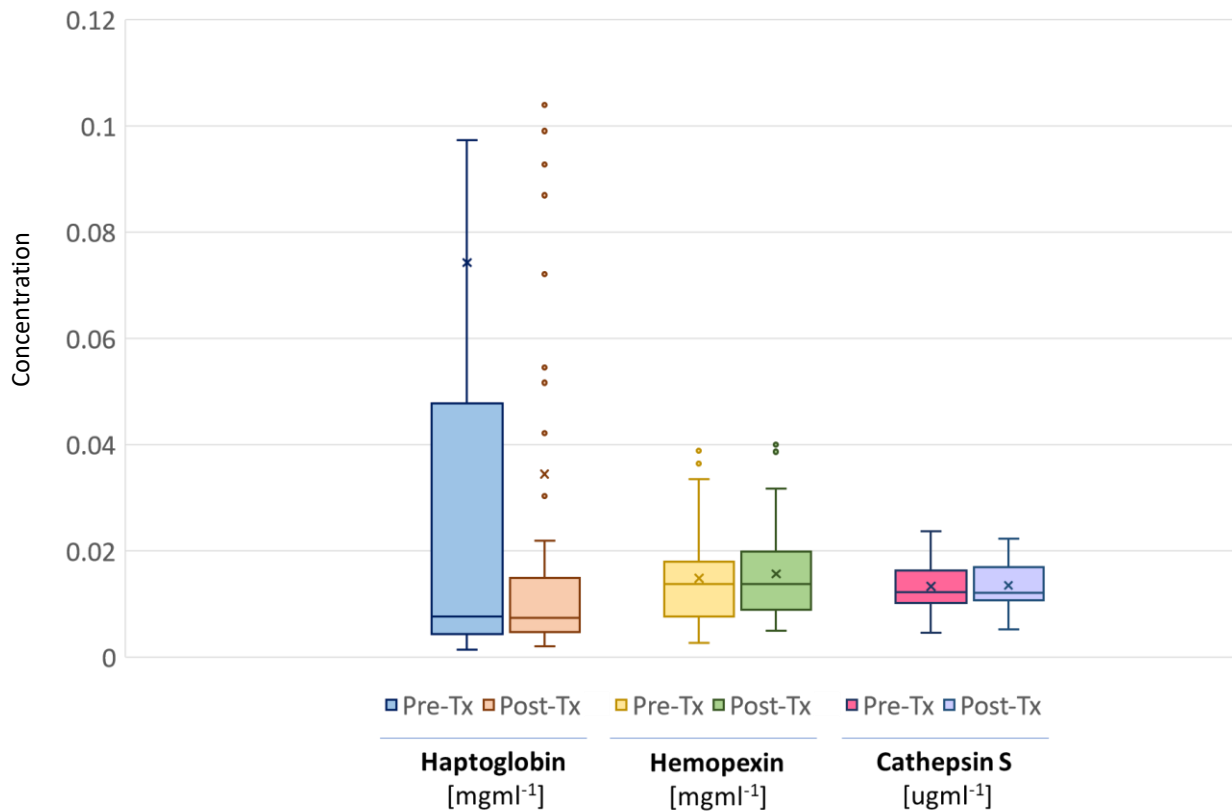


Figure 5.4. Box plots showing different levels of plasma haptoglobin (mgml⁻¹), hemopexin (mgml⁻¹), and CTSS (ugml⁻¹) pre- and post-transfusion.

The differences between pre-Tx and post-Tx levels analysed by Wilcoxon Signed-Rank test (two-tailed) were not statistically significant (haptoglobin $P=0.035$; hemopexin $P=0.159$; CTSS $P=0.25$), where $P<0.05$ denoted significant difference. The box spans an interquartile range. The median and mean for a particular sample group is represented by horizontal lines and plus signs, respectively.

However, for haptoglobin, the differences in pre- and post-transfusion levels in two patients approached statistical significance, where pre-transfusion haptoglobin levels were in the low normal range: patients A3 and A7 (32.40 ± 4.94 mgdl⁻¹ and 10.64 ± 3.88 mgdl⁻¹ for pre- and post-transfusion, respectively).

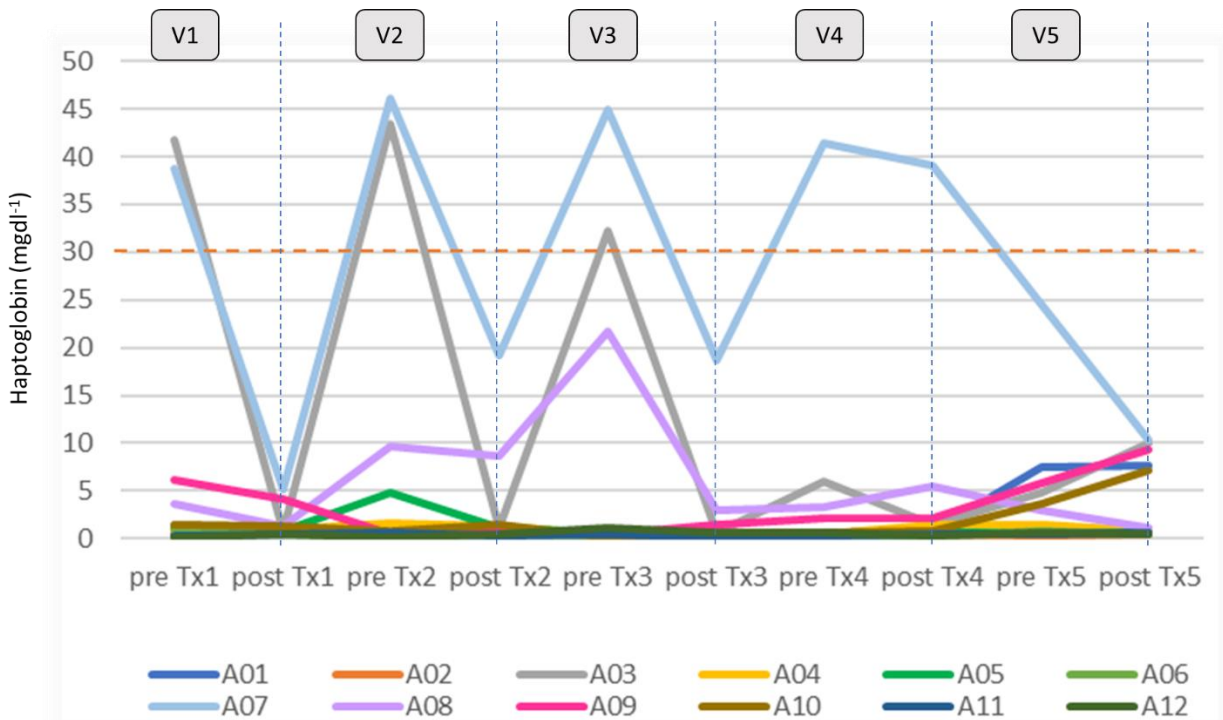


Figure 5.5. Haptoglobin pre- and one-hour post-transfusion and concentration (mgdl⁻¹) shown for five visits for each individual patient.

Pre-Tx and Post-Tx in X-axis; concentration (mgdl⁻¹) in Y-axis. Each line represents one TDT patient. Orange dash line is the lower limit of normal haptoglobin level (30 mgdl⁻¹). The blue vertical dash lines represent each post-Tx test. V designates visit, e.g., V1= visit1, V2= visit2. Note that patients A3 and A7 displayed particularly sharp declining levels of post-transfusion haptoglobin.

5.3 Discussion

Currently, there is no definitive marker of haemolysis that would indicate the actual clinical severity of TDT and NTDT patients. It has been shown that Hb might not be a good marker in the chronic haemolytic patients, although it is an acceptable marker in the acute anaemic setting (258, 268). In this chapter, we have evaluated the clinical application of haptoglobin, hemopexin and CTSS observed to exhibit significantly altered abundance in the β -thalassaemic patients' plasma EVs (Chapter 4). The hypothesis tested in this chapter was that these proteins may act as biomarkers that may correlate better to the pathophysiology of the disease. We have also endeavoured to begin to understand how these markers could be utilised for predicting the clinical need for transfusion.

5.3.1 Clinical severity of thalassaemia

Haptoglobin, hemopexin and CTSS were identified due to their altered abundance in the *in vivo* circulating thalassaemic EVs compared to controls (see Chapter 4). Also, as elaborated in the section 4.3.3.5 of Chapter 4, haptoglobin and hemopexin are directly related to haemolysis condition and the pathophysiology of thalassaemia. In this chapter, we have confirmed that these three proteins significantly changed their concentration in plasma in concordance with the disease severity. TDT patients were observed to have the lowest level of both haptoglobin ($5.439 \pm 1.021 \text{ mgml}^{-1}$) and hemopexin ($0.015 \pm 0.001 \text{ mgml}^{-1}$) and had the highest level of CTSS ($13435.29 \pm 392.03 \text{ pgml}^{-1}$) among all the groups. These levels were significantly different from the thalassaemia intermedia or the NTDT group ($P < 0.0001$) and reflecting the more severe haemolysis observed in the TDT patients when compared to the other two groups.

Previous studies of blood parameters for use as an indication of the severity of thalassaemic disease are very limited. Vinchi *et al.* (2016) reported the severe drop of serum haptoglobin, hemopexin, and transferrin in both β -thalassaemia major receiving regular transfusion ($n = 60$) and β -thalassaemia intermedia groups ($n = 7$). Our study was in agreement with their findings (serum hemopexin in the thalassaemic group was $< 0.1 \text{ mgml}^{-1}$ vs. $\sim 0.6 \text{ mgml}^{-1}$ in controls; $P < 0.0001$; data interpreted from a bar chart) (443). Serum haptoglobin and

hemopexin showed differences in their concentrations in blood of SCD patients, measured by the ELISA method in a recent study of the potential of haptoglobin to distinguish severities between sickle cell anaemia, Hb SC disease, and healthy control groups (435). This study was a forerunner in ascertaining the clinical use of serum haptoglobin and hemopexin as biomarkers of disease severity in haemoglobinopathies. Hence, the results of our clinical follow-up study indicated that the three proteins may all be good biomarkers that reflect the clinical severity of the TDT patients.

5.3.2 NTDT patients

For NTDT patients, one of the key unsolved patient management issues is determining when to trigger the provision of transfusion to the patients. On the one hand, despite the NTDT group generally not requiring regular transfusion, this patient group is still prone to develop many complications related to chronic anaemia (224). On the other hand, a substantial number of patients may receive inappropriate transfusions when they can actually tolerate a lower baseline of Hb (241). The literature describes the criteria for decision making (228), but according to these criteria, only Hb $<5 \text{ gdl}^{-1}$ is a measurable laboratory parameter. Nonetheless, Hb as a marker for administering transfusion has limitations in representing the clinical status of NTDT patients (255), because patients with chronic haemolysis tend to tolerate a low Hb level. Direct evidence of how much volume or percentage of haemolysis needs to occur in order to change Hb level is not available. A single study revealed a drop of 3% Hct ($\sim \text{Hb } 1 \text{ gdl}^{-1}$) per 1 gdl^{-1} of free Hb (462). A recent survey of transfusion practice in NTDT patients from 11 medical centres has confirmed that the majority of physicians use clinical symptoms rather than Hb level to transfuse patients (268).

Results presented in this chapter suggested that the correlations between Hb and the other markers were poor, with only IDB being significantly correlated with Hb level. Whereas, both haptoglobin and hemopexin levels correlated with plasma Hb, %haemolysis, LDH, IDB, and reticulocyte counts. This finding highlighted the limitation of Hb as a marker for the severity of the disease in the NTDT subtype. Additionally, plasma haptoglobin and hemopexin were superior in detecting the IVH portion of haemolysis that would occur in the patients. This is because both markers, especially haptoglobin, had moderate to strong statistical correlations with the IVH markers, i.e., plasma Hb, %haemolysis, and LDH (Table 5.3).

Plasma CTSS also demonstrated moderate to strong correlations with several haemolysis markers (Table 5.3) in NTDT patients. The levels of CTSS in the NTDT correlated with numbers of WBC. CTSS is located inside lysosomal compartments of professional antigen-presenting cells (457). Tato *et al.* (2017) recently reported the release of CTSS from activated macrophages and its potential as a marker for inflammation in autoimmune diseases (421). Regarding β -thalassaemia, previous reports observed an increase in proinflammatory markers (463, 464) and the roles of macrophages in modulating thalassaemic erythroid proliferation and differentiation (465). Thus, with further exploration, CTSS has the potential to be a good marker of myeloid compartment activities and inflammation, particularly macrophages, in haemolytic settings.

Future studies with a larger cohort of patients and a more extensive follow-up period, particularly capturing haemolytic crises, are essential to prove the advantages of these proteins as haemolysis biomarkers in the NTDT patients.

5.3.3 TDT patients

In the TDT group, a striking decrease of plasma haptoglobin after transfusion was observed in two patients (A3 and A7 in Figure 5.5). In those patients, pre-transfusion haptoglobin levels returned to low normal ($>30 \text{ mgdl}^{-1}$); whereas, this was not observed in ten other TDT patients who consistently had extremely low haptoglobin levels. Thus, our data emphasised the non-homogenous disease severity observed among TDT patients. Moreover, we postulated, for the first time, that blood transfusion could potentially worsen the protective mechanisms in TDT patients who have less severe clinical features and already have haemolysis induced by transfusion.

Plasma hemopexin demonstrated a good correlation with Hb and Hct (Figure 5.2), which in turn, could potentially complement Hb as a marker for optimising blood transfusion dosage and timing for individual patients. Both haptoglobin and hemopexin showed significant correlations with other haemolytic markers (LDH, IDB) and the marrow responsive marker, reticulocyte count (see Table 5.5). No direct relationship was found between the haemolytic markers in thalassaemic patients who receive blood transfusions. However, in the non-thalassaemic setting, L'Acqua and colleagues (2015) assessed the effects of red blood cell

transfusion compared with saline/albumin infusion in critically ill children. A significant increase in plasma Hb, IDB, and non-transferrin bound iron was recorded in recently transfused patients (466), whereas other studies only showed the increase of the EVH markers in long-term stored RBC units (467, 468).

Therefore, our project has revealed the significant alteration of haemolytic markers, particularly the IVH markers (plasma Hb; $P < 0.0001$ and %haemolysis; $P = 0.003$) in the TDT patients. These findings are in agreement with what was observed in post-transfusion status of the non-thalassaemic patients (466). It is possibly explained by the minimal level of haemolysis that occurs after transfusion, even with compatible blood or the presence of EVs in the transfused bag due to RBC storage lesions (469-471). Although it would be interesting to follow the haptoglobin and hemopexin cycle, we did not continue monitoring these markers after the one-hour post-transfusion sampling time. This limitation was necessary for ethical reasons - the pre-anaemic background of the recruited patients and the inconvenience of their follow-up as out-patients had to be considered.

Smith and McCulloh (2015) reported 24 to 48 hours of restoration time for hemopexin, and 14 days for haptoglobin to return to normal plasma levels after the haemolytic event (449). In our study, only two out of 12 TDT patients demonstrated the restoration of haptoglobin to low normal level. Note that the intervals between transfusions for these two patients were six-week and four-week for A3 and A7 patients, respectively. Therefore, ideally, baseline levels of the two proteins could be assessed if we were able to measure plasma hemopexin at 48 hours and haptoglobin at the two-week interval after transfusion. A longer monitoring period with a larger patient sample is required to confirm these observations.

Importantly, this is the first study to identify the lowest recorded level of haptoglobin ($5.44 \pm 1.02 \text{ mgdl}^{-1}$ for TDT group; see Appendix I for individual data). Dilutional tests were performed to improve the ELISA manufacturer's protocol in order to be able to measure the extremely low levels of haptoglobin and hemopexin in TDT patients. The low measurable levels recorded by ELISA were also validated through the observed correlation with the other markers of haemolysis (Table 5.5). Therefore, we proposed here the benefit of the high sensitivity ELISA method for detecting low-level plasma haptoglobin. Measurements of both haptoglobin and hemopexin would benefit the future clinical management of patients as they can lead to the set-up of new cut-off values for a follow-up study in the setting of consistently low plasma

levels of these two proteins, e.g., in haemoglobinopathy diseases. Furthermore, if therapeutic haptoglobin and/or hemopexin are available on prescription in the future, ELISA-based tool would be useful to monitor their abundances following drug administration. Future studies on the inter- and intra-assays with greater number of samples are required to validate our findings. In a clinical context of the developing countries, including Thailand, these biomarkers harnessed together would be beneficial for monitoring the status of thalassaemic patients, because they are plasma proteins and are relatively easy to measure in a cost-effective way when compared to multiple clinical parameters of erythropoiesis and haemolysis such as serum erythropoietin with soluble transferrin receptor.

5.4 Chapter summary

This work has described the successful preliminary clinical evaluation of haptoglobin, hemopexin and CTSS and has demonstrated their potential useful as biomarkers for indicating the clinical severity of the thalassaemia diseases.

The use of haptoglobin, hemopexin, and CTSS was postulated as markers for monitoring the transfusion requirements of NTDT patients, in conjunction with the standard Hb level measurement. Notably, hemopexin showed better correlation with plasma Hb and haemolysis percentage, known indicators of IVH, than Hb levels in the NTDT patient group. Moreover, the altered levels of the three proteins were observed to be of relevance across thalassaemic patient groups. We also demonstrated, for the first time, the significant alteration of CTSS levels in TDT and to a lesser extent in NTDT, which highlights its potential to contribute as an inflammatory marker for monitoring of haemoglobinopathy diseases.

Although this study has followed a small cohort of TDT and NTDT patients, it has demonstrated that the three biomarkers may have potential utility in the clinical management of TDT and NTDT patients. For the future, this work will need to be expanded to conduct a larger trial of patients for a longer clinical follow-up to generate more longitudinal data.

CHAPTER 6

CONCLUSIONS AND FUTURE PERSPECTIVES

Thalassaemic patients can present with a broad spectrum of clinical manifestations even with the same diagnosis and the same genetic background (267). The underlying causes of such diversity is not fully understood. The work conducted in this thesis has explored EVs as one potential factor which could explain the clinical variations observed. We have studied the behaviour of patient cells during *in vitro* erythroid culture, compared EVs from *in vivo* and *in vitro* sources and through this work, identified potential biomarkers for clinical management of thalassaemia patients. Finally, this project also explored genetic variation through the analysis of the relevant genes (see Appendix III).

6.1 *In vitro* erythropoiesis of HbE/ β -thalassaemic patients

This work has successfully adapted the originally erythroid culture method described by Griffiths *et al.* (128) by the addition of dexamethasone (DXM), for the *in vitro* culture of CD34⁺ cells isolated from peripheral blood of HbE/ β^0 -thalassaemia. This was used to monitor cell proliferation, maturation, viability, and enucleation rates compared to healthy controls. Ineffective erythropoiesis is the hallmark of thalassaemia, characterised by the combination of increased cell proliferation and decreased erythroid production due to intramedullary apoptosis (212, 213). Previous studies reported an increase in apoptosis of thalassaemic RBC precursors during the polychromatophilic stage (159). However, although patients' erythroid cells were successfully cultured to reticulocytes, we did not observe enhanced cell death at the polychromatophilic normoblast state (159). This could be explained by the different genetics of thalassaemic patient groups studied or could be due to the specific *ex vivo* culture conditions used. The lack of ineffective erythropoiesis in erythroid cultures was also reported by others (216, 218, 409). We did, however, observe slower cell maturation and lower enucleation rates as measured on day 21 of the culture in thalassaemia samples compared to controls.

The discrepancy of the results between previous studies of cultured β -thalassaemia and our work exists. A study by Mathias *et al.* (2000) that cultured CD34⁺ progenitor cells isolated from bone marrow of β -thalassaemia major patients and observed *ex vivo* ineffective erythropoiesis of thalassaemic cells at the polychromatophilic stage (151). Another study that

observed an increase of apoptosis in *ex vivo* erythropoiesis of CD34⁺ cells isolated from peripheral blood of HbE/ β -thalassaemia when compared to controls ($10.01 \pm 1.45\%$ vs. $5.92 \pm 1.16\%$) (472). Other studies explored apoptosis of cells obtained directly from bone marrow of β -thalassaemia major (211, 214). However, more recent work by Forster *et al.* (2016) also cultured CD34⁺ cells obtained from peripheral blood of five TDT β -thalassaemic patients and did not observe an increase in apoptosis of cells during the 14-day culture period when compared to the healthy controls (216).

One major difference between Mathias paper and our own study was that they used a one-stage cell culture system with hydrocortisone and, similarly, no corticosteroid was added in Lithanatum study. In our work, the DXM additive was added up to day 11 in an optimised three-stage culture system (128) which may have ameliorated the oxidative stress experienced. Another difference is the presence in the culture media of SCF. One study of thalassaemic cell cultures has highlighted the dependence on SCF with or without DXM for thalassaemic cells to survive and mature to reticulocytes (410). The cells were observed to have the greatest proliferation in the culture protocol containing both SCF and DXM which is similar to the conditions observed in our cultures. This evidence is corroborated with our proteomic work on corticosteroid additive cells that showed an upregulation of SCF/KL expression over controls (see section 3.2.3 and Table 3.1 in Chapter 3). Thus, our optimisation of the three-stage culture protocol (128) with DXM may mimic stress erythropoiesis and could ameliorate ineffective erythropoiesis of thalassaemic cell culture. The alternative potential explanation is that the culture system only permits the more functional cells to survive, which was suggested by Satchwell *et al.* (2013) in the study of cultured MNCs of congenital dyserythropoietic anaemia (type II) patients, a disease characterised by *SEC23B* mutation resulting in dyserythropoiesis of erythroid cells (154).

6.1.1 Proteomic study of *in vitro*-derived thalassaemic EVs

The work in Chapter 3 provided the first information of proteomic profiles of the adult *in vitro* thalassaemic reticulocyte membranes as well as the *in vitro* EVs-derived from these reticulocytes. We reported approximately 2500 and 600 proteins from the former and the latter sources, with 162 proteins shared across both sources (Table 3.6 and Figure 3.15). The bulk of proteins identified in both the reticulocyte membrane and the EV samples were

involved with metabolic processes. Importantly, a recent study reported the proteome of EVs isolated from reticulocytes produced using *in vitro* culture of human cord blood CD34⁺ cells. This study identified 367 individual proteins; many of these proteins were also detected in our study (413).

When the reticulocyte membrane list was compared to the list derived from the reticulocyte EVs, the proteins that increased in abundance in both reticulocyte membranes and EVs of the patients were proteins that are known to be involved in cell maturation and facilitation the enucleation process (393, 395-397). No evidence of increased oxidative injury was found from this proteomics study. Again, this suggests that under the conditions of culture in the laboratory, the cells are experiencing less oxidative stress or the HbE/ β -thalassaemia patient samples *ex vivo* cultured here are not as disturbed as previously studied thalassaemia patients.

6.1.2 Future work around *in vitro* culture of thalassaemia

6.1.2.1 Development of a synthetic cellular model of human β -thalassaemia

With the difficulties of assessing the best cell culture system for studying the very small number of CD34⁺ HSCs available from minimal blood samples obtained from patients with thalassaemia, it was clear that a better system is required to facilitate the study of this disease. Lee *et al.* (2013) engineered a potential culture model using lentivirus-mediated human β -thalassaemia knockdown of *HBB* in cultured CD34⁺ cells obtained from adult donors (186). Using this model, it was observed that around the polychromatophilic stage, the majority of cells underwent apoptosis (186). Thus, the study of this β -thalassaemia model may shed light on the pathophysiology of *ex vivo* ineffective erythropoiesis. Additionally, the recent availability of adult erythroid cell lines, in particular, Bristol Erythroid Line Adult, (BEL-A) (184), offer a potential opportunity to develop thalassaemic cell lines for reproducible studies on a known genetic background. This could be conducted by generating patient-specific lines or using gene-editing technology of the current BEL-A line or any other appropriate erythroid immortalised line. These lines have recently been shown to be amenable to gene editing (185, 473).

6.1.2.2 Monitoring decreased differentiation of erythroid precursor cells

One of the interesting findings observed during the culture of thalassaemic cells was delayed in differentiation when compared to healthy control cultures. This work needs to be expanded further in future studies, but similar observations were reported in previous studies of thalassaemic cultures (159, 218). The proposed mechanisms that hinder cell differentiation in thalassaemia could have potentially resulted from alterations in two transcription factors: DNA-binding protein inhibitor (ID1) and Forkhead box O3 (Foxo3).

The activation of ID1 by JAK/STAT pathway was found inhibiting cell differentiation in β -thalassaemia, which has sustained JAK2 activation. This could possibly explain the delay of cell maturation (474). A mouse model deficient in Foxo3 (murine homolog of human Foxo3a) decreased differentiation of erythroid progenitor (475). Interestingly, it was proposed that the ineffective erythropoiesis was caused by the loss of Foxo3, a transcription factor that regulates maturation of terminal erythropoiesis (475). Another study administered resveratrol (a natural antioxidant from plants) that activates Foxo3, and this resulted in amelioration of ineffective erythropoiesis, confirming the role of Foxo3 in this phenomenon (476). Therefore, in future work, it would be interesting to evaluate whether ID1 and Foxo3 indeed contribute to ineffective erythropoiesis in β -thalassaemia in humans and determining whether treatment with resveratrol could improve their symptoms. Ultimately, such studies may lead to a breakthrough in therapeutic options in the future, especially if coupled with the use of model systems derived from immortalised cell line models (see above) which would enhance reproducibility of the results.

6.2 Identification and clinical applications of haptoglobin, hemopexin, and cathepsin S as biomarkers

Although thalassaemia is one of the most common monogenic gene disorders globally and the main pathophysiology of the disease is haemolytic anaemia, surprisingly, there is lack of studies of the parameters used to monitor clinical severity in the patients. Moreover, the very limited evidence is available about the effects and appropriateness of blood transfusion in

these patients. We have explored *in vivo* sources of patient EVs by carrying out a proteomics study of plasma-derived EVs which successfully showed that antioxidants, chaperones, iron-sequestering proteins and cathepsin S exhibited increase abundance in HbE/ β -thalassaemic EVs; whilst, haptoglobin and hemopexin are reduced in thalassaemic patients' EVs (419). We then went on to show that there were significantly altered levels of plasma haptoglobin, hemopexin, and cathepsin S (CTSS) in different groups of thalassaemia patients (TDT, NTDT, carriers and controls) by conducting a small longitudinal study.

These three proteins identified from the proteomics of thalassaemic EVs (Chapter 4) were closely correlated with the pathophysiology of the disease and other blood parameters of haemolysis, as shown by statistical analyses in Chapter 5 of this thesis. Such parameters include lactate dehydrogenase, indirect bilirubin, and reticulocyte counts (Table 5.4 and Table 5.6). We specifically postulated the use of haptoglobin and hemopexin to monitor transfusion requirements of NTDT patients, instead of relying on Hb only as the current practices suggest (255). Because these two proteins correlated well with markers of intravascular haemolysis (i.e., plasma Hb and haemolysis percentage) for this group of patients, when Hb did not. In addition, we propose that CTSS should also be monitored as this provides an indication of the degree of systemic inflammation in the patient (421), and so has potential as a biomarker for the degree of inflammation in haemoglobinopathy diseases. This initial study has illustrated the potential utility of these markers and merits further study of a larger cohort of patients with a longer clinical follow-up in future work.

Lastly, the work in this thesis reports the lowest measurable haptoglobin levels across the cohort of thalassaemia patients, and this would allow us to monitor blood level of this protein both for the follow-up purpose and, in the future, after therapeutic administration (477).

6.3 Genetic studies of the thalassaemic patients

With the limitations of Hb analysis for diagnosis (478) and the discrepancies observed between clinical manifestations and available, diagnosis in some of the patients recruited to this project, a parallel genetic assessment of the patients was also performed. Although not presented in a specific results chapter, this body of work represents is a substantial

undertaking and provides important additional information on the patients studied in this thesis, and so is presented in Appendix III. This work confirmed the diagnosis of 27 patient cases, provided a new diagnosis to one patient, amended diagnoses of seven patients, and has identified new α -alleles (i.e., eight Hb Constant Spring, two Hb Paksé, and one Hb Westmead alleles) in 11 patient cases. The Hb Westmead [*HBA2*:c.369C>G] is a rare allele of *HBA2* mutation reported to date in only two unrelated families in the Thai population (479). The *HBA1*, *HBA2*, *HBB* and *KLF1* genes were also Sanger sequenced in 46 thalassaemic patients enrolled in the study, but no new mutations were observed.

6.4 Final summary

Taken together, this thesis has achieved its aims to explore the proteomes of *in vitro* and *in vivo* thalassaemic patients EV samples and identified potential biomarkers for predicting clinical severity and transfusion requirement of thalassaemic patients. The initial longitudinal study that has been conducted on a wider group of thalassaemic patients has shown that the biomarkers identified have the potential for clinical management of such patients. Further studies on a larger patient cohort are needed to validate our findings and, ultimately, we hope the work initiated in this thesis will provide benefits to patients who have suffered from this haemoglobinopathic disease.

REFERENCES

1. Palis J. Primitive and definitive erythropoiesis in mammals. *Frontiers in physiology*. 2014;5:3. PubMed PMID: 24478716. Pubmed Central PMCID: PMC3904103. Epub 2014/01/31. eng.
2. Higgins JM. Red blood cell population dynamics. *Clinics in laboratory medicine*. 2015 Mar;35(1):43-57. PubMed PMID: 25676371. Pubmed Central PMCID: PMC4717490. Epub 2015/02/14. eng.
3. Zivot A, Lipton JM, Narla A, Blanc L. Erythropoiesis: insights into pathophysiology and treatments in 2017. *Molecular medicine (Cambridge, Mass)*. 2018 Mar 23;24(1):11. PubMed PMID: 30134792. Pubmed Central PMCID: PMC6016880. Epub 2018/08/24. eng.
4. Sender R, Fuchs S, Milo R. Revised Estimates for the Number of Human and Bacteria Cells in the Body. *PLoS biology*. 2016 Aug;14(8):e1002533. PubMed PMID: 27541692. Pubmed Central PMCID: PMC4991899. Epub 2016/08/20. eng.
5. Dzierzak E, Philipsen S. Erythropoiesis: development and differentiation. *Cold Spring Harbor perspectives in medicine*. 2013 Apr 1;3(4):a011601. PubMed PMID: 23545573. Pubmed Central PMCID: PMC3684002. Epub 2013/04/03. eng.
6. Adams GB, Scadden DT. The hematopoietic stem cell in its place. *Nature immunology*. 2006 Apr;7(4):333-7. PubMed PMID: 16550195. Epub 2006/03/22. eng.
7. Seita J, Weissman IL. Hematopoietic stem cell: self-renewal versus differentiation. *Wiley interdisciplinary reviews Systems biology and medicine*. 2010 Nov-Dec;2(6):640-53. PubMed PMID: 20890962. Pubmed Central PMCID: PMC2950323. Epub 2010/10/05. eng.
8. Iscove NN. The role of erythropoietin in regulation of population size and cell cycling of early and late erythroid precursors in mouse bone marrow. *Cell and tissue kinetics*. 1977 Jul;10(4):323-34. PubMed PMID: 884703. Epub 1977/07/01. eng.
9. Hu J, Liu J, Xue F, Halverson G, Reid M, Guo A, et al. Isolation and functional characterization of human erythroblasts at distinct stages: implications for understanding of normal and disordered erythropoiesis in vivo. *Blood*. 2013 Apr 18;121(16):3246-53. PubMed PMID: 23422750. Pubmed Central PMCID: PMC3630836. Epub 2013/02/21. eng.
10. Wu H, Liu X, Jaenisch R, Lodish HF. Generation of committed erythroid BFU-E and CFU-E progenitors does not require erythropoietin or the erythropoietin receptor. *Cell*. 1995 Oct 6;83(1):59-67. PubMed PMID: 7553874. Epub 1995/10/06. eng.
11. Hattangadi SM, Wong P, Zhang L, Flygare J, Lodish HF. From stem cell to red cell: regulation of erythropoiesis at multiple levels by multiple proteins, RNAs, and chromatin modifications. *Blood*. 2011 Dec 8;118(24):6258-68. PubMed PMID: 21998215. Pubmed Central PMCID: PMC3236116. Epub 2011/10/15. eng.
12. Chasis JA, Mohandas N. Erythroblastic islands: niches for erythropoiesis. *Blood*. 2008 Aug 1;112(3):470-8. PubMed PMID: 18650462. Pubmed Central PMCID: PMC2481536. Epub 2008/07/25. eng.
13. Giarratana MC, Kobari L, Lapillonne H, Chalmers D, Kiger L, Cynober T, et al. Ex vivo generation of fully mature human red blood cells from hematopoietic stem cells. *Nature biotechnology*. 2005 Jan;23(1):69-74. PubMed PMID: 15619619. Epub 2004/12/28. eng.
14. Satchwell TJ, Hawley BR, Bell AJ, Ribeiro ML, Toye AM. The cytoskeletal binding domain of band 3 is required for multiprotein complex formation and retention during erythropoiesis. *Haematologica*. 2015 Jan;100(1):133-42. PubMed PMID: 25344524. Pubmed Central PMCID: PMC4281326. Epub 2014/10/26. eng.

15. Satchwell TJ, Bell AJ, Pellegrin S, Kupzig S, Ridgwell K, Daniels G, et al. Critical band 3 multiprotein complex interactions establish early during human erythropoiesis. *Blood*. 2011 Jul 7;118(1):182-91. PubMed PMID: 21527529. Pubmed Central PMCID: PMC4340578. Epub 2011/04/30. eng.
16. Mankelow TJ, Griffiths RE, Trompeter S, Flatt JF, Cogan NM, Massey EJ, et al. Autophagic vesicles on mature human reticulocytes explain phosphatidylserine-positive red cells in sickle cell disease. *Blood*. 2015 Oct 8;126(15):1831-4. PubMed PMID: 26276668. Pubmed Central PMCID: PMC4608391. Epub 2015/08/16. eng.
17. Liu J, Han X, An X. Novel methods for studying normal and disordered erythropoiesis. *Science China Life sciences*. 2015 Dec;58(12):1270-5. PubMed PMID: 26588913. Epub 2015/11/22. eng.
18. Tsiftoglou AS, Vizirianakis IS, Strouboulis J. Erythropoiesis: model systems, molecular regulators, and developmental programs. *IUBMB life*. 2009 Aug;61(8):800-30. PubMed PMID: 19621348. Epub 2009/07/22. eng.
19. Moura PL, Hawley BR, Mankelow TJ, Griffiths RE, Dobbe JGG, Streekstra GJ, et al. Non-muscle Myosin II drives vesicle loss during human reticulocyte maturation. *Haematologica*. 2018 Aug 3. PubMed PMID: 30076174. Epub 2018/08/05. eng.
20. Xie Y, Shi X, Sheng K, Han G, Li W, Zhao Q, et al. PI3K/Akt signaling transduction pathway, erythropoiesis and glycolysis in hypoxia (Review). *Molecular medicine reports*. 2019 Feb;19(2):783-91. PubMed PMID: 30535469. Pubmed Central PMCID: PMC6323245. Epub 2018/12/12. eng.
21. Lentjes MH, Niessen HE, Akiyama Y, de Bruine AP, Melotte V, van Engeland M. The emerging role of GATA transcription factors in development and disease. *Expert reviews in molecular medicine*. 2016 Mar 8;18:e3. PubMed PMID: 26953528. Pubmed Central PMCID: PMC4836206. Epub 2016/03/10. eng.
22. Evans T, Reitman M, Felsenfeld G. An erythrocyte-specific DNA-binding factor recognizes a regulatory sequence common to all chicken globin genes. *Proceedings of the National Academy of Sciences of the United States of America*. 1988 Aug;85(16):5976-80. PubMed PMID: 3413070. Pubmed Central PMCID: PMC281888. Epub 1988/08/01. eng.
23. Orkin SH. GATA-binding transcription factors in hematopoietic cells. *Blood*. 1992 Aug 1;80(3):575-81. PubMed PMID: 1638017. Epub 1992/08/01. eng.
24. Takai J, Moriguchi T, Suzuki M, Yu L, Ohneda K, Yamamoto M. The Gata1 5' region harbors distinct cis-regulatory modules that direct gene activation in erythroid cells and gene inactivation in HSCs. *Blood*. 2013 Nov 14;122(20):3450-60. PubMed PMID: 24021675. Epub 2013/09/12. eng.
25. Pevny L, Lin CS, D'Agati V, Simon MC, Orkin SH, Costantini F. Development of hematopoietic cells lacking transcription factor GATA-1. *Development (Cambridge, England)*. 1995 Jan;121(1):163-72. PubMed PMID: 7867497. Epub 1995/01/01. eng.
26. Moriguchi T, Yamamoto M. A regulatory network governing Gata1 and Gata2 gene transcription orchestrates erythroid lineage differentiation. *International journal of hematology*. 2014 Nov;100(5):417-24. PubMed PMID: 24638828. Epub 2014/03/19. eng.
27. Zon LI, Youssoufian H, Mather C, Lodish HF, Orkin SH. Activation of the erythropoietin receptor promoter by transcription factor GATA-1. *Proceedings of the National Academy of Sciences of the United States of America*. 1991 Dec 1;88(23):10638-41. PubMed PMID: 1660143. Pubmed Central PMCID: PMC52985. Epub 1991/12/01. eng.

28. Wall L, deBoer E, Grosveld F. The human beta-globin gene 3' enhancer contains multiple binding sites for an erythroid-specific protein. *Genes & development*. 1988 Sep;2(9):1089-100. PubMed PMID: 2461328. Epub 1988/09/01. eng.
29. Ferreira R, Ohneda K, Yamamoto M, Philipsen S. GATA1 function, a paradigm for transcription factors in hematopoiesis. *Molecular and cellular biology*. 2005 Feb;25(4):1215-27. PubMed PMID: 15684376. Pubmed Central PMCID: PMC548021. Epub 2005/02/03. eng.
30. Cantor AB, Orkin SH. Transcriptional regulation of erythropoiesis: an affair involving multiple partners. *Oncogene*. 2002 May 13;21(21):3368-76. PubMed PMID: 12032775. Epub 2002/05/29. eng.
31. Letting DL, Chen YY, Rakowski C, Reedy S, Blobel GA. Context-dependent regulation of GATA-1 by friend of GATA-1. *Proceedings of the National Academy of Sciences of the United States of America*. 2004 Jan 13;101(2):476-81. PubMed PMID: 14695898. Pubmed Central PMCID: PMC327172. Epub 2003/12/30. eng.
32. Pal S, Cantor AB, Johnson KD, Moran TB, Boyer ME, Orkin SH, et al. Coregulator-dependent facilitation of chromatin occupancy by GATA-1. *Proceedings of the National Academy of Sciences of the United States of America*. 2004 Jan 27;101(4):980-5. PubMed PMID: 14715908. Pubmed Central PMCID: PMC327128. Epub 2004/01/13. eng.
33. Nichols KE, Crispino JD, Poncz M, White JG, Orkin SH, Maris JM, et al. Familial dyserythropoietic anaemia and thrombocytopenia due to an inherited mutation in GATA1. *Nature genetics*. 2000 Mar;24(3):266-70. PubMed PMID: 10700180. Epub 2000/03/04. eng.
34. Crispino JD, Lodish MB, MacKay JP, Orkin SH. Use of altered specificity mutants to probe a specific protein-protein interaction in differentiation: the GATA-1:FOG complex. *Molecular cell*. 1999 Feb;3(2):219-28. PubMed PMID: 10078204. Epub 1999/03/17. eng.
35. Miccio A, Blobel GA. Role of the GATA-1/FOG-1/NuRD pathway in the expression of human beta-like globin genes. *Molecular and cellular biology*. 2010 Jul;30(14):3460-70. PubMed PMID: 20439494. Pubmed Central PMCID: PMC2897567. Epub 2010/05/05. eng.
36. Perkins A, Xu X, Higgs DR, Patrinos GP, Arnaud L, Bieker JJ, et al. Kruppeling erythropoiesis: an unexpected broad spectrum of human red blood cell disorders due to KLF1 variants. *Blood*. 2016 Apr 14;127(15):1856-62. PubMed PMID: 26903544. Pubmed Central PMCID: PMC4832505. Epub 2016/02/24. eng.
37. Perkins AC, Sharpe AH, Orkin SH. Lethal beta-thalassaemia in mice lacking the erythroid CACCC-transcription factor EKLF. *Nature*. 1995 May 25;375(6529):318-22. PubMed PMID: 7753195. Epub 1995/05/25. eng.
38. Nuez B, Michalovich D, Bygrave A, Ploemacher R, Grosveld F. Defective haematopoiesis in fetal liver resulting from inactivation of the EKLF gene. *Nature*. 1995 May 25;375(6529):316-8. PubMed PMID: 7753194. Epub 1995/05/25. eng.
39. Siatecka M, Bieker JJ. The multifunctional role of EKLF/KLF1 during erythropoiesis. *Blood*. 2011 Aug 25;118(8):2044-54. PubMed PMID: 21613252. Pubmed Central PMCID: PMC3292426. Epub 2011/05/27. eng.
40. Hodge D, Coghill E, Keys J, Maguire T, Hartmann B, McDowall A, et al. A global role for EKLF in definitive and primitive erythropoiesis. *Blood*. 2006 Apr 15;107(8):3359-70. PubMed PMID: 16380451. Pubmed Central PMCID: PMC1895762. Epub 2005/12/29. eng.
41. Miller IJ, Bieker JJ. A novel, erythroid cell-specific murine transcription factor that binds to the CACCC element and is related to the Kruppel family of nuclear proteins. *Molecular and cellular biology*. 1993 May;13(5):2776-86. PubMed PMID: 7682653. Pubmed Central PMCID: PMC359658. Epub 1993/05/01. eng.

42. Schoenfelder S, Sexton T, Chakalova L, Cope NF, Horton A, Andrews S, et al. Preferential associations between co-regulated genes reveal a transcriptional interactome in erythroid cells. *Nature genetics*. 2010 Jan;42(1):53-61. PubMed PMID: 20010836. Pubmed Central PMCID: PMC3237402. Epub 2009/12/17. eng.
43. Zhang W, Kadam S, Emerson BM, Bieker JJ. Site-specific acetylation by p300 or CREB binding protein regulates erythroid Kruppel-like factor transcriptional activity via its interaction with the SWI-SNF complex. *Molecular and cellular biology*. 2001 Apr;21(7):2413-22. PubMed PMID: 11259590. Pubmed Central PMCID: PMC86874. Epub 2001/03/22. eng.
44. Sengupta T, Chen K, Milot E, Bieker JJ. Acetylation of EKLF is essential for epigenetic modification and transcriptional activation of the beta-globin locus. *Molecular and cellular biology*. 2008 Oct;28(20):6160-70. PubMed PMID: 18710946. Pubmed Central PMCID: PMC2577412. Epub 2008/08/20. eng.
45. Ouyang L, Chen X, Bieker JJ. Regulation of erythroid Kruppel-like factor (EKLF) transcriptional activity by phosphorylation of a protein kinase casein kinase II site within its interaction domain. *The Journal of biological chemistry*. 1998 Sep 4;273(36):23019-25. PubMed PMID: 9722526. Epub 1998/08/29. eng.
46. Drissen R, Palstra RJ, Gillemans N, Splinter E, Grosveld F, Philipsen S, et al. The active spatial organization of the beta-globin locus requires the transcription factor EKLF. *Genes & development*. 2004 Oct 15;18(20):2485-90. PubMed PMID: 15489291. Pubmed Central PMCID: PMC529536. Epub 2004/10/19. eng.
47. Noordermeer D, de Laat W. Joining the loops: beta-globin gene regulation. *IUBMB life*. 2008 Dec;60(12):824-33. PubMed PMID: 18767169. Epub 2008/09/04. eng.
48. Im H, Grass JA, Johnson KD, Kim SI, Boyer ME, Imbalzano AN, et al. Chromatin domain activation via GATA-1 utilization of a small subset of dispersed GATA motifs within a broad chromosomal region. *Proceedings of the National Academy of Sciences of the United States of America*. 2005 Nov 22;102(47):17065-70. PubMed PMID: 16286657. Pubmed Central PMCID: PMC1287986. Epub 2005/11/16. eng.
49. Zhou D, Liu K, Sun CW, Pawlik KM, Townes TM. KLF1 regulates BCL11A expression and gamma- to beta-globin gene switching. *Nature genetics*. 2010 Sep;42(9):742-4. PubMed PMID: 20676097. Epub 2010/08/03. eng.
50. Borg J, Papadopoulos P, Georgitsi M, Gutierrez L, Grech G, Fanis P, et al. Haploinsufficiency for the erythroid transcription factor KLF1 causes hereditary persistence of fetal hemoglobin. *Nature genetics*. 2010 Sep;42(9):801-5. PubMed PMID: 20676099. Pubmed Central PMCID: PMC2930131. Epub 2010/08/03. eng.
51. Merika M, Orkin SH. Functional synergy and physical interactions of the erythroid transcription factor GATA-1 with the Kruppel family proteins Sp1 and EKLF. *Molecular and cellular biology*. 1995 May;15(5):2437-47. PubMed PMID: 7739528. Pubmed Central PMCID: PMC230473. Epub 1995/05/01. eng.
52. Sengupta T, Cohet N, Morle F, Bieker JJ. Distinct modes of gene regulation by a cell-specific transcriptional activator. *Proceedings of the National Academy of Sciences of the United States of America*. 2009 Mar 17;106(11):4213-8. PubMed PMID: 19251649. Pubmed Central PMCID: PMC2657397. Epub 2009/03/03. eng.
53. Mas C, Lussier-Price M, Soni S, Morse T, Arseneault G, Di Lello P, et al. Structural and functional characterization of an atypical activation domain in erythroid Kruppel-like factor (EKLF). *Proceedings of the National Academy of Sciences of the United States of America*. 2011 Jun 28;108(26):10484-9. PubMed PMID: 21670263. Pubmed Central PMCID: PMC3127900. Epub 2011/06/15. eng.

54. Zhang W, Bieker JJ. Acetylation and modulation of erythroid Kruppel-like factor (EKLF) activity by interaction with histone acetyltransferases. *Proceedings of the National Academy of Sciences of the United States of America*. 1998 Aug 18;95(17):9855-60. PubMed PMID: 9707565. Pubmed Central PMCID: PMC21426. Epub 1998/08/26. eng.
55. Menzel S, Garner C, Gut I, Matsuda F, Yamaguchi M, Heath S, et al. A QTL influencing F cell production maps to a gene encoding a zinc-finger protein on chromosome 2p15. *Nature genetics*. 2007 Oct;39(10):1197-9. PubMed PMID: 17767159. Epub 2007/09/04. eng.
56. Uda M, Galanello R, Sanna S, Lettre G, Sankaran VG, Chen W, et al. Genome-wide association study shows BCL11A associated with persistent fetal hemoglobin and amelioration of the phenotype of beta-thalassemia. *Proceedings of the National Academy of Sciences of the United States of America*. 2008 Feb 05;105(5):1620-5. PubMed PMID: 18245381. Pubmed Central PMCID: PMC2234194. Epub 2008/02/05. eng.
57. Sankaran VG, Menne TF, Xu J, Akie TE, Lettre G, Van Handel B, et al. Human fetal hemoglobin expression is regulated by the developmental stage-specific repressor BCL11A. *Science (New York, NY)*. 2008 Dec 19;322(5909):1839-42. PubMed PMID: 19056937. Epub 2008/12/06. eng.
58. Xu J, Sankaran VG, Ni M, Menne TF, Puram RV, Kim W, et al. Transcriptional silencing of {gamma}-globin by BCL11A involves long-range interactions and cooperation with SOX6. *Genes & development*. 2010 Apr 15;24(8):783-98. PubMed PMID: 20395365. Pubmed Central PMCID: PMC2854393. Epub 2010/04/17. eng.
59. Liu N, Hargreaves VV, Zhu Q, Kurland JV, Hong J, Kim W, et al. Direct Promoter Repression by BCL11A Controls the Fetal to Adult Hemoglobin Switch. *Cell*. 2018 Apr 5;173(2):430-42 e17. PubMed PMID: 29606353. Pubmed Central PMCID: PMC5889339. Epub 2018/04/03. eng.
60. Kim SI, Bresnick EH. Transcriptional control of erythropoiesis: emerging mechanisms and principles. *Oncogene*. 2007 Oct 15;26(47):6777-94. PubMed PMID: 17934485. Epub 2007/10/16. eng.
61. D'Souza SL, Elefanty AG, Keller G. SCL/Tal-1 is essential for hematopoietic commitment of the hemangioblast but not for its development. *Blood*. 2005 May 15;105(10):3862-70. PubMed PMID: 15677567. Pubmed Central PMCID: PMC1895073. Epub 2005/01/29. eng.
62. Wadman IA, Osada H, Grutz GG, Agulnick AD, Westphal H, Forster A, et al. The LIM-only protein Lmo2 is a bridging molecule assembling an erythroid, DNA-binding complex which includes the TAL1, E47, GATA-1 and Ldb1/NLI proteins. *The EMBO journal*. 1997 Jun 2;16(11):3145-57. PubMed PMID: 9214632. Pubmed Central PMCID: PMC1169933. Epub 1997/06/02. eng.
63. Hewitt KJ, Johnson KD, Gao X, Keles S, Bresnick EH. The Hematopoietic Stem and Progenitor Cell Cistrome: GATA Factor-Dependent cis-Regulatory Mechanisms. *Current topics in developmental biology*. 2016;118:45-76. PubMed PMID: 27137654. Epub 2016/05/04. eng.
64. Steiner M, Schneider L, Yillah J, Gerlach K, Kuvardina ON, Meyer A, et al. FUSE binding protein 1 (FUBP1) expression is upregulated by T-cell acute lymphocytic leukemia protein 1 (TAL1) and required for efficient erythroid differentiation. *PLoS one*. 2019;14(1):e0210515. PubMed PMID: 30653565. Pubmed Central PMCID: PMC6336336. Epub 2019/01/18. eng.
65. Fried W. Erythropoietin and erythropoiesis. *Experimental hematology*. 2009 Sep;37(9):1007-15. PubMed PMID: 19500646. Epub 2009/06/09. eng.
66. Rawlings JS, Rosler KM, Harrison DA. The JAK/STAT signaling pathway. *Journal of Cell Science*. 2004;117(8):1281-3.

67. Grebien F, Kerenyi MA, Kovacic B, Kolbe T, Becker V, Dolznig H, et al. Stat5 activation enables erythropoiesis in the absence of EpoR and Jak2. *Blood*. 2008;111(9):4511-22.
68. Haase VH. Regulation of erythropoiesis by hypoxia-inducible factors. *Blood reviews*. 2013 Jan;27(1):41-53. PubMed PMID: 23291219. Pubmed Central PMCID: PMC3731139. Epub 2013/01/08. eng.
69. Yamashita T, Ohneda O, Sakiyama A, Iwata F, Ohneda K, Fujii-Kuriyama Y. The microenvironment for erythropoiesis is regulated by HIF-2alpha through VCAM-1 in endothelial cells. *Blood*. 2008 Aug 15;112(4):1482-92. PubMed PMID: 18451309. Epub 2008/05/03. eng.
70. Peyssonnaud C, Nizet V, Johnson RS. Role of the hypoxia inducible factors HIF in iron metabolism. *Cell cycle (Georgetown, Tex)*. 2008 Jan 1;7(1):28-32. PubMed PMID: 18212530. Epub 2008/01/24. eng.
71. R. K. Stem cell factor. 2003. In: *Cancer Medicine* [Internet]. Hamilton (ON): BC Decker. 6th Available from: <https://www.ncbi.nlm.nih.gov/books/NBK12671/>.
72. Munugalavadla V, Kapur R. Role of c-Kit and erythropoietin receptor in erythropoiesis. *Critical reviews in oncology/hematology*. 2005 Apr;54(1):63-75. PubMed PMID: 15780908. Epub 2005/03/23. eng.
73. Sui X, Krantz SB, You M, Zhao Z. Synergistic activation of MAP kinase (ERK1/2) by erythropoietin and stem cell factor is essential for expanded erythropoiesis. *Blood*. 1998 Aug 15;92(4):1142-9. PubMed PMID: 9694701. Epub 1998/08/08. eng.
74. Ratajczak J, Zhang Q, Pertusini E, Wojczyk BS, Wasik MA, Ratajczak MZ. The role of insulin (INS) and insulin-like growth factor-I (IGF-I) in regulating human erythropoiesis. *Studies in vitro under serum-free conditions--comparison to other cytokines and growth factors. Leukemia*. 1998 Mar;12(3):371-81. PubMed PMID: 9529132. Epub 1998/04/07. eng.
75. Yang YC, Clark SC. Interleukin-3: molecular biology and biologic activities. *Hematology/oncology clinics of North America*. 1989 Sep;3(3):441-52. PubMed PMID: 2698876. Epub 1989/09/01. eng.
76. Ihle JN. Interleukin-3 and hematopoiesis. *Chemical immunology*. 1992;51:65-106. PubMed PMID: 1567546. Epub 1992/01/01. eng.
77. Bryder D, Jacobsen SE. Interleukin-3 supports expansion of long-term multilineage repopulating activity after multiple stem cell divisions in vitro. *Blood*. 2000 Sep 1;96(5):1748-55. PubMed PMID: 10961873. Epub 2000/08/29. eng.
78. Parganas E, Wang D, Stravopodis D, Topham DJ, Marine JC, Teglund S, et al. Jak2 is essential for signaling through a variety of cytokine receptors. *Cell*. 1998 May 1;93(3):385-95. PubMed PMID: 9590173. Epub 1998/05/20. eng.
79. Migliaccio G, Migliaccio AR, Visser JW. Synergism between erythropoietin and interleukin-3 in the induction of hematopoietic stem cell proliferation and erythroid burst colony formation. *Blood*. 1988 Sep;72(3):944-51. PubMed PMID: 3262001. Epub 1988/09/01. eng.
80. Reddy EP, Korapati A, Chaturvedi P, Rane S. IL-3 signaling and the role of Src kinases, JAKs and STATs: a covert liaison unveiled. *Oncogene*. 2000 May 15;19(21):2532-47. PubMed PMID: 10851052. Epub 2000/06/13. eng.
81. Aglietta M, Sanavio F, Stacchini A, Morelli S, Fubini L, Severino A, et al. Interleukin-3 in vivo: kinetic of response of target cells. *Blood*. 1993 Oct 1;82(7):2054-61. PubMed PMID: 8400256. Epub 1993/10/01. eng.
82. Aron DC. Insulin-like growth factor I and erythropoiesis. *BioFactors (Oxford, England)*. 1992 Apr;3(4):211-6. PubMed PMID: 1376602. Epub 1992/04/01. eng.

83. Shimon I, Shpilberg O. The insulin-like growth factor system in regulation of normal and malignant hematopoiesis. *Leukemia research*. 1995 Apr;19(4):233-40. PubMed PMID: 7538616. Epub 1995/04/01. eng.
84. Miyagawa S, Kobayashi M, Konishi N, Sato T, Ueda K. Insulin and insulin-like growth factor I support the proliferation of erythroid progenitor cells in bone marrow through the sharing of receptors. *British journal of haematology*. 2000 Jun;109(3):555-62. PubMed PMID: 10886204. Epub 2000/07/11. eng.
85. Sawada K, Krantz SB, Dessypris EN, Koury ST, Sawyer ST. Human colony-forming units-erythroid do not require accessory cells, but do require direct interaction with insulin-like growth factor I and/or insulin for erythroid development. *The Journal of clinical investigation*. 1989 May;83(5):1701-9. PubMed PMID: 2651478. Pubmed Central PMCID: PMC303879. Epub 1989/05/01. eng.
86. Paulson RF, Shi L, Wu DC. Stress erythropoiesis: new signals and new stress progenitor cells. *Current opinion in hematology*. 2011 May;18(3):139-45. PubMed PMID: 21372709. Pubmed Central PMCID: PMC3099455. Epub 2011/03/05. eng.
87. Lenox LE, Shi L, Hegde S, Paulson RF. Extramedullary erythropoiesis in the adult liver requires BMP-4/Smad5-dependent signaling. *Experimental hematology*. 2009 May;37(5):549-58. PubMed PMID: 19375646. Pubmed Central PMCID: PMC2671639. Epub 2009/04/21. eng.
88. Bunn HF. Erythropoietin. *Cold Spring Harbor perspectives in medicine*. 2013 Mar 1;3(3):a011619. PubMed PMID: 23457296. Pubmed Central PMCID: PMC3579209. Epub 2013/03/05. eng.
89. Porpiglia E, Hidalgo D, Koulis M, Tzafirri AR, Socolovsky M. Stat5 signaling specifies basal versus stress erythropoietic responses through distinct binary and graded dynamic modalities. *PLoS biology*. 2012 Aug;10(8):e1001383. PubMed PMID: 22969412. Pubmed Central PMCID: PMC3433736. Epub 2012/09/13. eng.
90. Varricchio L, Tirelli V, Masselli E, Ghinassi B, Saha N, Besmer P, et al. The expression of the glucocorticoid receptor in human erythroblasts is uniquely regulated by KIT ligand: implications for stress erythropoiesis. *Stem cells and development*. 2012 Oct 10;21(15):2852-65. PubMed PMID: 22533504. Pubmed Central PMCID: PMC3623384. Epub 2012/04/27. eng.
91. Lenox LE, Perry JM, Paulson RF. BMP4 and Madh5 regulate the erythroid response to acute anemia. *Blood*. 2005 Apr 1;105(7):2741-8. PubMed PMID: 15591122. Epub 2004/12/14. eng.
92. Harandi OF, Hedge S, Wu DC, McKeone D, Paulson RF. Murine erythroid short-term radioprotection requires a BMP4-dependent, self-renewing population of stress erythroid progenitors. *The Journal of clinical investigation*. 2010 Dec;120(12):4507-19. PubMed PMID: 21060151. Pubmed Central PMCID: PMC2993581. Epub 2010/11/10. eng.
93. Xiang J, Wu DC, Chen Y, Paulson RF. In vitro culture of stress erythroid progenitors identifies distinct progenitor populations and analogous human progenitors. *Blood*. 2015 Mar 12;125(11):1803-12. PubMed PMID: 25608563. Pubmed Central PMCID: PMC4357585. Epub 2015/01/23. eng.
94. Bennett LF, Liao C, Paulson RF. Stress Erythropoiesis Model Systems. *Methods in molecular biology (Clifton, NJ)*. 2018;1698:91-102. PubMed PMID: 29076085. Epub 2017/10/28. eng.
95. Hao S, Xiang J, Wu DC, Fraser JW, Ruan B, Cai J, et al. Gdf15 regulates murine stress erythroid progenitor proliferation and the development of the stress erythropoiesis niche.

- Blood advances. 2019 Jul 23;3(14):2205-17. PubMed PMID: 31324641. Pubmed Central PMCID: PMC6650738. Epub 2019/07/22. eng.
96. Tanno T, Noel P, Miller JL. Growth differentiation factor 15 in erythroid health and disease. *Current opinion in hematology*. 2010 May;17(3):184-90. PubMed PMID: 20182355. Pubmed Central PMCID: PMC2884377. Epub 2010/02/26. eng.
97. Kim A, Nemeth E. New insights into iron regulation and erythropoiesis. *Current opinion in hematology*. 2015 May;22(3):199-205. PubMed PMID: 25710710. Pubmed Central PMCID: PMC4509743. Epub 2015/02/25. eng.
98. Perry JM, Harandi OF, Porayette P, Hegde S, Kannan AK, Paulson RF. Maintenance of the BMP4-dependent stress erythropoiesis pathway in the murine spleen requires hedgehog signaling. *Blood*. 2009 Jan 22;113(4):911-8. PubMed PMID: 18927434. Pubmed Central PMCID: PMC2630276. Epub 2008/10/18. eng.
99. Dulmovits BM, Blanc L. Stress erythropoiesis: selenium to the rescue! *Blood*. 2018 Jun 7;131(23):2512-3. PubMed PMID: 29880648. Epub 2018/06/09. eng.
100. Kim TS, Hanak M, Trampont PC, Braciale TJ. Stress-associated erythropoiesis initiation is regulated by type 1 conventional dendritic cells. *The Journal of clinical investigation*. 2015 Oct 1;125(10):3965-80. PubMed PMID: 26389678. Pubmed Central PMCID: PMC4607133. Epub 2015/09/22. eng.
101. Dolznig H, Grebien F, Deiner EM, Stangl K, Kolbus A, Habermann B, et al. Erythroid progenitor renewal versus differentiation: genetic evidence for cell autonomous, essential functions of EpoR, Stat5 and the GR. *Oncogene*. 2006 May 11;25(20):2890-900. PubMed PMID: 16407844. Pubmed Central PMCID: PMC3035873. Epub 2006/01/13. eng.
102. Bauer A, Tronche F, Wessely O, Kellendonk C, Reichardt HM, Steinlein P, et al. The glucocorticoid receptor is required for stress erythropoiesis. *Genes & development*. 1999 Nov 15;13(22):2996-3002. PubMed PMID: 10580006. Pubmed Central PMCID: PMC317156. Epub 1999/12/02. eng.
103. Varricchio L, Masselli E, Alfani E, Battistini A, Migliaccio G, Vannucchi AM, et al. The dominant negative beta isoform of the glucocorticoid receptor is uniquely expressed in erythroid cells expanded from polycythemia vera patients. *Blood*. 2011 Jul 14;118(2):425-36. PubMed PMID: 21355091. Pubmed Central PMCID: PMC3138692. Epub 2011/03/01. eng.
104. von Lindern M, Zauner W, Mellitzer G, Steinlein P, Fritsch G, Huber K, et al. The glucocorticoid receptor cooperates with the erythropoietin receptor and c-Kit to enhance and sustain proliferation of erythroid progenitors in vitro. *Blood*. 1999 Jul 15;94(2):550-9. PubMed PMID: 10397722. Epub 1999/07/09. eng.
105. Lodish H, Flygare J, Chou S. From stem cell to erythroblast: regulation of red cell production at multiple levels by multiple hormones. *IUBMB life*. 2010 Jul;62(7):492-6. PubMed PMID: 20306512. Pubmed Central PMCID: PMC2893266. Epub 2010/03/23. eng.
106. Wessely O, Deiner EM, Beug H, von Lindern M. The glucocorticoid receptor is a key regulator of the decision between self-renewal and differentiation in erythroid progenitors. *The EMBO journal*. 1997 Jan 15;16(2):267-80. PubMed PMID: 9029148. Pubmed Central PMCID: PMC1169634. Epub 1997/01/15. eng.
107. Zhang L, Prak L, Rayon-Estrada V, Thiru P, Flygare J, Lim B, et al. ZFP36L2 is required for self-renewal of early burst-forming unit erythroid progenitors. *Nature*. 2013 Jul 4;499(7456):92-6. PubMed PMID: 23748442. Pubmed Central PMCID: PMC3702661. Epub 2013/06/12. eng.
108. Falchi M, Varricchio L, Martelli F, Masiello F, Federici G, Zingariello M, et al. Dexamethasone targeted directly to macrophages induces macrophage niches that promote

- erythroid expansion. *Haematologica*. 2015 Feb;100(2):178-87. PubMed PMID: 25533803. Pubmed Central PMCID: PMC4803138. Epub 2014/12/24. eng.
109. Heideveld E, Masiello F, Marra M, Esteghamat F, Yagci N, von Lindern M, et al. CD14+ cells from peripheral blood positively regulate hematopoietic stem and progenitor cell survival resulting in increased erythroid yield. *Haematologica*. 2015 Nov;100(11):1396-406. PubMed PMID: 26294724. Pubmed Central PMCID: PMC4825294. Epub 2015/08/22. eng.
110. Heideveld E, Hampton-O'Neil LA, Cross SJ, van Alphen FPJ, van den Biggelaar M, Teye AM, et al. Glucocorticoids induce differentiation of monocytes towards macrophages that share functional and phenotypical aspects with erythroblastic island macrophages. *Haematologica*. 2018 Mar;103(3):395-405. PubMed PMID: 29284682. Pubmed Central PMCID: PMC5830394. Epub 2017/12/30. eng.
111. Labunskyy VM, Hatfield DL, Gladyshev VN. Selenoproteins: molecular pathways and physiological roles. *Physiological reviews*. 2014 Jul;94(3):739-77. PubMed PMID: 24987004. Pubmed Central PMCID: PMC4101630. Epub 2014/07/06. eng.
112. Paulson RF, Nettleford SK, Liao C, Chen Y, Hao S, Blatzinger M, et al. The role of Selenoprotein N in the differentiation of erythroid progenitors during stress erythropoiesis. *bioRxiv*. 2018:506345.
113. Kaushal N, Hegde S, Lumadue J, Paulson RF, Prabhu KS. The regulation of erythropoiesis by selenium in mice. *Antioxidants & redox signaling*. 2011 Apr 15;14(8):1403-12. PubMed PMID: 20969477. Pubmed Central PMCID: PMC3061201. Epub 2010/10/26. eng.
114. Liao C, Hardison RC, Kennett MJ, Carlson BA, Paulson RF, Prabhu KS. Selenoproteins regulate stress erythroid progenitors and spleen microenvironment during stress erythropoiesis. *Blood*. 2018 Jun 7;131(23):2568-80. PubMed PMID: 29615406. Pubmed Central PMCID: PMC5992864. Epub 2018/04/05. eng.
115. Liao C, Carlson BA, Paulson RF, Prabhu KS. The intricate role of selenium and selenoproteins in erythropoiesis. *Free radical biology & medicine*. 2018 Nov 1;127:165-71. PubMed PMID: 29719207. Pubmed Central PMCID: PMC6168382. Epub 2018/05/03. eng.
116. Liao C, Prabhu KS, Paulson RF. Monocyte-derived macrophages expand the murine stress erythropoietic niche during the recovery from anemia. *Blood*. 2018 Dec 13;132(24):2580-93. PubMed PMID: 30322871. Pubmed Central PMCID: PMC6293871. Epub 2018/10/17. eng.
117. Behringer RR, Ryan TM, Palmiter RD, Brinster RL, Townes TM. Human gamma- to beta-globin gene switching in transgenic mice. *Genes & development*. 1990 Mar;4(3):380-9. PubMed PMID: 1692558. Epub 1990/03/01. eng.
118. Tallack MR, Perkins AC. Three fingers on the switch: Kruppel-like factor 1 regulation of gamma-globin to beta-globin gene switching. *Current opinion in hematology*. 2013 May;20(3):193-200. PubMed PMID: 23474875. Epub 2013/03/12. eng.
119. Wallace HA, Marques-Kranc F, Richardson M, Luna-Crespo F, Sharpe JA, Hughes J, et al. Manipulating the mouse genome to engineer precise functional syntenic replacements with human sequence. *Cell*. 2007 Jan 12;128(1):197-209. PubMed PMID: 17218265. Epub 2007/01/16. eng.
120. Vernimmen D, Marques-Kranc F, Sharpe JA, Sloane-Stanley JA, Wood WG, Wallace HA, et al. Chromosome looping at the human alpha-globin locus is mediated via the major upstream regulatory element (HS -40). *Blood*. 2009 Nov 5;114(19):4253-60. PubMed PMID: 19696202. Epub 2009/08/22. eng.
121. Yang B, Kirby S, Lewis J, Detloff PJ, Maeda N, Smithies O. A mouse model for beta 0-thalassemia. *Proceedings of the National Academy of Sciences of the United States of*

- America. 1995 Dec 5;92(25):11608-12. PubMed PMID: 8524813. Pubmed Central PMCID: PMC40451. Epub 1995/12/05. eng.
122. Ciavatta DJ, Ryan TM, Farmer SC, Townes TM. Mouse model of human beta zero thalassemia: targeted deletion of the mouse beta maj- and beta min-globin genes in embryonic stem cells. *Proceedings of the National Academy of Sciences of the United States of America*. 1995 Sep 26;92(20):9259-63. PubMed PMID: 7568113. Pubmed Central PMCID: PMC40964. Epub 1995/09/26. eng.
123. McColl B, Vadolas J. Animal models of beta-hemoglobinopathies: utility and limitations. *Journal of blood medicine*. 2016;7:263-74. PubMed PMID: 27853395. Pubmed Central PMCID: PMC5104300. Epub 2016/11/18. eng.
124. May C, Rivella S, Chadburn A, Sadelain M. Successful treatment of murine beta-thalassemia intermedia by transfer of the human beta-globin gene. *Blood*. 2002 Mar 15;99(6):1902-8. PubMed PMID: 11877258. Epub 2002/03/06. eng.
125. Miccio A, Cesari R, Lotti F, Rossi C, Sanvito F, Ponzoni M, et al. In vivo selection of genetically modified erythroblastic progenitors leads to long-term correction of beta-thalassemia. *Proceedings of the National Academy of Sciences of the United States of America*. 2008 Jul 29;105(30):10547-52. PubMed PMID: 18650378. Pubmed Central PMCID: PMC2492493. Epub 2008/07/25. eng.
126. An X, Schulz VP, Li J, Wu K, Liu J, Xue F, et al. Global transcriptome analyses of human and murine terminal erythroid differentiation. *Blood*. 2014 May 29;123(22):3466-77. PubMed PMID: 24637361. Pubmed Central PMCID: PMC4041167. Epub 2014/03/19. eng.
127. Migliaccio G, Sanchez M, Masiello F, Tirelli V, Varricchio L, Whitsett C, et al. Humanized culture medium for clinical expansion of human erythroblasts. *Cell transplantation*. 2010;19(4):453-69. PubMed PMID: 20149301. Pubmed Central PMCID: PMC4397648. Epub 2010/02/13. eng.
128. Griffiths RE, Kupzig S, Cogan N, Mankelow TJ, Betin VM, Trakarnsanga K, et al. Maturing reticulocytes internalize plasma membrane in glycophorin A-containing vesicles that fuse with autophagosomes before exocytosis. *Blood*. 2012 Jun 28;119(26):6296-306. PubMed PMID: 22490681. Pubmed Central PMCID: PMC3383192. Epub 2012/04/12. eng.
129. Zeuner A, Martelli F, Vaglio S, Federici G, Whitsett C, Migliaccio AR. Concise review: stem cell-derived erythrocytes as upcoming players in blood transfusion. *Stem cells (Dayton, Ohio)*. 2012 Aug;30(8):1587-96. PubMed PMID: 22644674. Pubmed Central PMCID: PMC3697769. Epub 2012/05/31. eng.
130. Severn CE, Macedo H, Eagle MJ, Rooney P, Mantalaris A, Toye AM. Polyurethane scaffolds seeded with CD34(+) cells maintain early stem cells whilst also facilitating prolonged egress of haematopoietic progenitors. *Scientific reports*. 2016 Aug 30;6:32149. PubMed PMID: 27573994. Pubmed Central PMCID: PMC5004174. Epub 2016/08/31. eng.
131. Migliaccio G, Di Pietro R, di Giacomo V, Di Baldassarre A, Migliaccio AR, Maccioni L, et al. In vitro mass production of human erythroid cells from the blood of normal donors and of thalassemic patients. *Blood cells, molecules & diseases*. 2002 Mar-Apr;28(2):169-80. PubMed PMID: 12064913. Epub 2002/06/18. eng.
132. Giarratana MC, Rouard H, Dumont A, Kiger L, Safeukui I, Le Pennec PY, et al. Proof of principle for transfusion of in vitro-generated red blood cells. *Blood*. 2011 Nov 10;118(19):5071-9. PubMed PMID: 21885599. Pubmed Central PMCID: PMC3217398. Epub 2011/09/03. eng.
133. van den Akker E, Satchwell TJ, Pellegrin S, Daniels G, Toye AM. The majority of the in vitro erythroid expansion potential resides in CD34(-) cells, outweighing the contribution of

- CD34(+) cells and significantly increasing the erythroblast yield from peripheral blood samples. *Haematologica*. 2010 Sep;95(9):1594-8. PubMed PMID: 20378567. Pubmed Central PMCID: PMC2930963. Epub 2010/04/10. eng.
134. Leberbauer C, Boulme F, Unfried G, Huber J, Beug H, Mullner EW. Different steroids co-regulate long-term expansion versus terminal differentiation in primary human erythroid progenitors. *Blood*. 2005 Jan 1;105(1):85-94. PubMed PMID: 15358620. Epub 2004/09/11. eng.
135. Fujimi A, Matsunaga T, Kobune M, Kawano Y, Nagaya T, Tanaka I, et al. Ex vivo large-scale generation of human red blood cells from cord blood CD34+ cells by co-culturing with macrophages. *International journal of hematology*. 2008 May;87(4):339-50. PubMed PMID: 18369691. Epub 2008/03/29. eng.
136. Olivier EN, Qiu C, Velho M, Hirsch RE, Bouhassira EE. Large-scale production of embryonic red blood cells from human embryonic stem cells. *Experimental hematology*. 2006 Dec;34(12):1635-42. PubMed PMID: 17157159. Epub 2006/12/13. eng.
137. Trakarnsanga K, Wilson MC, Lau W, Singleton BK, Parsons SF, Sakuntanaga P, et al. Induction of adult levels of beta-globin in human erythroid cells that intrinsically express embryonic or fetal globin by transduction with KLF1 and BCL11A-XL. *Haematologica*. 2014 Nov;99(11):1677-85. PubMed PMID: 25107887. Pubmed Central PMCID: PMC4222483. Epub 2014/08/12. eng.
138. Dias J, Gumenyuk M, Kang H, Vodyanik M, Yu J, Thomson JA, et al. Generation of red blood cells from human induced pluripotent stem cells. *Stem cells and development*. 2011 Sep;20(9):1639-47. PubMed PMID: 21434814. Pubmed Central PMCID: PMC3161101. Epub 2011/03/26. eng.
139. Kupzig S, Parsons SF, Curnow E, Anstee DJ, Blair A. Superior survival of ex vivo cultured human reticulocytes following transfusion into mice. *Haematologica*. 2017 Mar;102(3):476-83. PubMed PMID: 27909219. Pubmed Central PMCID: PMC5394952. Epub 2016/12/03. eng.
140. Watanapokasin Y, Chuncharunee S, Sanmund D, Kongnium W, Winichagoon P, Rodgers GP, et al. In vivo and in vitro studies of fetal hemoglobin induction by hydroxyurea in beta-thalassemia/hemoglobin E patients. *Experimental hematology*. 2005 Dec;33(12):1486-92. PubMed PMID: 16338491. Epub 2005/12/13. eng.
141. Pecoraro A, Rigano P, Troia A, Calzolari R, Scazzone C, Maggio A, et al. Quantification of HBG mRNA in primary erythroid cultures: prediction of the response to hydroxyurea in sickle cell and beta-thalassemia. *European journal of haematology*. 2014 Jan;92(1):66-72. PubMed PMID: 24112139. Epub 2013/10/12. eng.
142. Watanapokasin R, Sanmund D, Winichagoon P, Muta K, Fucharoen S. Hydroxyurea responses and fetal hemoglobin induction in beta-thalassemia/HbE patients' peripheral blood erythroid cell culture. *Annals of hematology*. 2006 Mar;85(3):164-9. PubMed PMID: 16389564. Epub 2006/01/04. eng.
143. Lithanatudom P, Wannatung T, Leecharoenkiat A, Svasti S, Fucharoen S, Smith DR. Enhanced activation of autophagy in beta-thalassemia/Hb E erythroblasts during erythropoiesis. *Annals of hematology*. 2011 Jul;90(7):747-58. PubMed PMID: 21221583. Epub 2011/01/12. eng.
144. Anstee DJ, Gampel A, Toye AM. Ex-vivo generation of human red cells for transfusion. *Current opinion in hematology*. 2012 May;19(3):163-9. PubMed PMID: 22406823. Epub 2012/03/13. eng.
145. Wilson MC, Trakarnsanga K, Heesom KJ, Cogan N, Green C, Toye AM, et al. Comparison of the Proteome of Adult and Cord Erythroid Cells, and Changes in the Proteome Following

- Reticulocyte Maturation. *Molecular & cellular proteomics* : MCP. 2016 Jun;15(6):1938-46. PubMed PMID: 27006477. Pubmed Central PMCID: PMC5083095. Epub 2016/03/24. eng.
146. Lo B, Parham L. Ethical issues in stem cell research. *Endocrine reviews*. 2009 May;30(3):204-13. PubMed PMID: 19366754. Pubmed Central PMCID: PMC2726839. Epub 2009/04/16. eng.
147. Jacobs K, Shoemaker C, Rudersdorf R, Neill SD, Kaufman RJ, Mufson A, et al. Isolation and characterization of genomic and cDNA clones of human erythropoietin. *Nature*. 1985 Feb 28-Mar 6;313(6005):806-10. PubMed PMID: 3838366. Epub 1985/02/06. eng.
148. Yang YC, Ciarletta AB, Temple PA, Chung MP, Kovacic S, Witek-Giannotti JS, et al. Human IL-3 (multi-CSF): identification by expression cloning of a novel hematopoietic growth factor related to murine IL-3. *Cell*. 1986 Oct 10;47(1):3-10. PubMed PMID: 3489530. Epub 1986/10/10. eng.
149. Zsebo KM, Williams DA, Geissler EN, Broudy VC, Martin FH, Atkins HL, et al. Stem cell factor is encoded at the Sl locus of the mouse and is the ligand for the c-kit tyrosine kinase receptor. *Cell*. 1990 Oct 5;63(1):213-24. PubMed PMID: 1698556. Epub 1990/10/05. eng.
150. Fibach E, Manor D, Oppenheim A, Rachmilewitz EA. Proliferation and maturation of human erythroid progenitors in liquid culture. *Blood*. 1989 Jan;73(1):100-3. PubMed PMID: 2910352. Epub 1989/01/01. eng.
151. Malik P, Fisher TC, Barsky LL, Zeng L, Izadi P, Hiti AL, et al. An in vitro model of human red blood cell production from hematopoietic progenitor cells. *Blood*. 1998 Apr 15;91(8):2664-71. PubMed PMID: 9531574. Epub 1998/05/16. eng.
152. Neildez-Nguyen TM, Wajcman H, Marden MC, Bensidhoum M, Moncollin V, Giarratana MC, et al. Human erythroid cells produced ex vivo at large scale differentiate into red blood cells in vivo. *Nature biotechnology*. 2002 May;20(5):467-72. PubMed PMID: 11981559. Epub 2002/05/01. eng.
153. Migliaccio AR, Whitsett C, Migliaccio G. Erythroid cells in vitro: from developmental biology to blood transfusion products. *Current opinion in hematology*. 2009 Jul;16(4):259-68. PubMed PMID: 19444099. Epub 2009/05/16. eng.
154. Satchwell TJ, Pellegrin S, Bianchi P, Hawley BR, Gampel A, Mordue KE, et al. Characteristic phenotypes associated with congenital dyserythropoietic anemia (type II) manifest at different stages of erythropoiesis. *Haematologica*. 2013 Nov;98(11):1788-96. PubMed PMID: 23935019. Pubmed Central PMCID: PMC3815181. Epub 2013/08/13. eng.
155. Huisjes R, Satchwell TJ, Verhagen LP, Schiffelers RM, van Solinge WW, Toye AM, et al. Quantitative measurement of red cell surface protein expression reveals new biomarkers for hereditary spherocytosis. *International journal of laboratory hematology*. 2018 Aug;40(4):e74-e7. PubMed PMID: 29746727. Epub 2018/05/11. eng.
156. Pellegrin S, Haydn-Smith KL, Hampton-O'Neil LA, Hawley BR, Heesom KJ, Fermo E, et al. Transduction with BBF2H7/CREB3L2 upregulates SEC23A protein in erythroblasts and partially corrects the hypo-glycosylation phenotype associated with CD41. *British journal of haematology*. 2019 Mar;184(5):876-81. PubMed PMID: 29536501. Pubmed Central PMCID: PMC6491999. Epub 2018/03/15. eng.
157. Boulad F, Wang X, Qu J, Taylor C, Ferro L, Karponi G, et al. Safe mobilization of CD34+ cells in adults with beta-thalassemia and validation of effective globin gene transfer for clinical investigation. *Blood*. 2014 Mar 6;123(10):1483-6. PubMed PMID: 24429337. Pubmed Central PMCID: PMC3945860. Epub 2014/01/17. eng.
158. Karponi G, Psatha N, Lederer CW, Adair JE, Zervou F, Zogas N, et al. Plerixafor+G-CSF-mobilized CD34+ cells represent an optimal graft source for thalassemia gene therapy. *Blood*.

- 2015 Jul 30;126(5):616-9. PubMed PMID: 26089395. Pubmed Central PMCID: PMC4520876. Epub 2015/06/20. eng.
159. Mathias LA, Fisher TC, Zeng L, Meiselman HJ, Weinberg KI, Hiti AL, et al. Ineffective erythropoiesis in beta-thalassemia major is due to apoptosis at the polychromatophilic normoblast stage. *Experimental hematology*. 2000 Dec;28(12):1343-53. PubMed PMID: 11146156. Epub 2001/01/09. eng.
160. Arlet JB, Ribeil JA, Guillem F, Negre O, Hazoume A, Marcion G, et al. HSP70 sequestration by free alpha-globin promotes ineffective erythropoiesis in beta-thalassaemia. *Nature*. 2014 Oct 9;514(7521):242-6. PubMed PMID: 25156257. Epub 2014/08/27. eng.
161. Ribeil JA, Zermati Y, Vandekerckhove J, Cathelin S, Kersual J, Dussiot M, et al. Hsp70 regulates erythropoiesis by preventing caspase-3-mediated cleavage of GATA-1. *Nature*. 2007 Jan 4;445(7123):102-5. PubMed PMID: 17167422. Epub 2006/12/15. eng.
162. Psatha N, Reik A, Phelps S, Zhou Y, Dalas D, Yannaki E, et al. Disruption of the BCL11A Erythroid Enhancer Reactivates Fetal Hemoglobin in Erythroid Cells of Patients with beta-Thalassemia Major. *Molecular therapy Methods & clinical development*. 2018 Sep 21;10:313-26. PubMed PMID: 30182035. Pubmed Central PMCID: PMC6120587. Epub 2018/09/06. eng.
163. Wilber A, Hargrove PW, Kim YS, Riberdy JM, Sankaran VG, Papanikolaou E, et al. Therapeutic levels of fetal hemoglobin in erythroid progeny of beta-thalassemic CD34+ cells after lentiviral vector-mediated gene transfer. *Blood*. 2011 Mar 10;117(10):2817-26. PubMed PMID: 21156846. Pubmed Central PMCID: PMC3062294. Epub 2010/12/16. eng.
164. Finotti A, Breda L, Lederer CW, Bianchi N, Zuccato C, Kleanthous M, et al. Recent trends in the gene therapy of beta-thalassemia. *Journal of blood medicine*. 2015;6:69-85. PubMed PMID: 25737641. Pubmed Central PMCID: PMC4342371. Epub 2015/03/05. eng.
165. Takahashi K, Yamanaka S. Induction of pluripotent stem cells from mouse embryonic and adult fibroblast cultures by defined factors. *Cell*. 2006 Aug 25;126(4):663-76. PubMed PMID: 16904174. Epub 2006/08/15. eng.
166. Ochi K, Takayama N, Hirose S, Nakahata T, Nakauchi H, Eto K. Multicolor staining of globin subtypes reveals impaired globin switching during erythropoiesis in human pluripotent stem cells. *Stem cells translational medicine*. 2014 Jul;3(7):792-800. PubMed PMID: 24873860. Pubmed Central PMCID: PMC4073826. Epub 2014/05/31. eng.
167. Kobari L, Yates F, Oudrhiri N, Francina A, Kiger L, Mazurier C, et al. Human induced pluripotent stem cells can reach complete terminal maturation: in vivo and in vitro evidence in the erythropoietic differentiation model. *Haematologica*. 2012 Dec;97(12):1795-803. PubMed PMID: 22733021. Pubmed Central PMCID: PMC3590085. Epub 2012/06/27. eng.
168. Tubsuwan A, Abed S, Deichmann A, Kardel MD, Bartholoma C, Cheung A, et al. Parallel assessment of globin lentiviral transfer in induced pluripotent stem cells and adult hematopoietic stem cells derived from the same transplanted beta-thalassemia patient. *Stem cells (Dayton, Ohio)*. 2013 Sep;31(9):1785-94. PubMed PMID: 23712774. Epub 2013/05/29. eng.
169. Okita K, Ichisaka T, Yamanaka S. Generation of germline-competent induced pluripotent stem cells. *Nature*. 2007 Jul 19;448(7151):313-7. PubMed PMID: 17554338. Epub 2007/06/08. eng.
170. Dong A, Rivella S, Breda L. Gene therapy for hemoglobinopathies: progress and challenges. *Translational research : the journal of laboratory and clinical medicine*. 2013 Apr;161(4):293-306. PubMed PMID: 23337292. Pubmed Central PMCID: PMC3716457. Epub 2013/01/23. eng.

171. Ma N, Liao B, Zhang H, Wang L, Shan Y, Xue Y, et al. Transcription activator-like effector nuclease (TALEN)-mediated gene correction in integration-free beta-thalassemia induced pluripotent stem cells. *The Journal of biological chemistry*. 2013 Nov 29;288(48):34671-9. PubMed PMID: 24155235. Pubmed Central PMCID: PMC3843079. Epub 2013/10/25. eng.
172. Ou Z, Niu X, He W, Chen Y, Song B, Xian Y, et al. The Combination of CRISPR/Cas9 and iPSC Technologies in the Gene Therapy of Human beta-thalassemia in Mice. *Scientific reports*. 2016 Sep 1;6:32463. PubMed PMID: 27581487. Pubmed Central PMCID: PMC5007518. Epub 2016/09/02. eng.
173. Wattanapanitch M, Damkham N, Potirat P, Trakarnsanga K, Janan M, Y UP, et al. One-step genetic correction of hemoglobin E/beta-thalassemia patient-derived iPSCs by the CRISPR/Cas9 system. *Stem cell research & therapy*. 2018 Feb 26;9(1):46. PubMed PMID: 29482624. Pubmed Central PMCID: PMC5828150. Epub 2018/02/28. eng.
174. Cardano M, Marsoner F, Marcatili M, Karnavas T, Zasso J, Lanterna LA, et al. Establishment of induced pluripotent stem cell (iPSC) line from 55-year old male patient with hemorrhagic Moyamoya disease. *Stem cell research*. 2016 Nov;17(3):623-6. PubMed PMID: 27934594. Epub 2016/12/10. eng.
175. Zhang S, Lv Z, Liu Y, Li Q, Gong W, Liu L, et al. Development of human induced pluripotent stem cell (iPSC) line from a 60year old female patient with multiple schwannoma. *Stem cell research*. 2017 Mar;19:31-3. PubMed PMID: 28413001. Epub 2017/04/18. eng.
176. Marsoner F, Marcatili M, Karnavas T, Bottai D, D'Agostino A, Scarone S, et al. Generation and characterization of an induced pluripotent stem cell (iPSC) line from a patient with clozapine-resistant Schizophrenia. *Stem cell research*. 2016 Nov;17(3):661-4. PubMed PMID: 27934603. Epub 2016/12/10. eng.
177. Ross SB, Fraser ST, Bagnall RD, Semsarian C. Peripheral blood derived induced pluripotent stem cells (iPSCs) from a female with familial hypertrophic cardiomyopathy. *Stem cell research*. 2017 Apr;20:76-9. PubMed PMID: 28395744. Epub 2017/04/12. eng.
178. Lebedeva OS, Lagarkova MA. Pluripotent Stem Cells for Modelling and Cell Therapy of Parkinson's Disease. *Biochemistry Biokhimiia*. 2018 Sep;83(9):1046-56. PubMed PMID: 30472943. Epub 2018/11/27. eng.
179. Wongkumool W, Maneepitasut W, Tong-Ngam P, Tangprasittipap A, Munkongdee T, Boonchuay C, et al. Establishment of MUI009 - A human induced pluripotent stem cells from a 32year old male with homozygous beta degrees -thalassemia coinherited with heterozygous alpha-thalassemia 2. *Stem cell research*. 2017 Apr;20:80-3. PubMed PMID: 28395745. Epub 2017/04/12. eng.
180. Tangprasittipap A, Satirapod C, Jittorntrum B, Lertritanan S, Anurathaphan U, Phanthong P, et al. Generation of iPSC line MU011.A-hiPS from homozygous alpha-thalassemia fetal skin fibroblasts. *Stem cell research*. 2015 Nov;15(3):506-9. PubMed PMID: 26432158. Epub 2015/10/04. eng.
181. Wongkumool W, Maneepitasut W, Munkongdee T, Tong-Ngam P, Tangprasittipap A, Svasti S, et al. Derivation of the human induced pluripotent stem cell line MUI017-A from a patient with homozygous Hemoglobin Constant Spring. *Stem cell research*. 2017 Apr;20:84-7. PubMed PMID: 28395746. Epub 2017/04/12. eng.
182. Phanthong P, Borwornpinyo S, Kitiyanant N, Jearawiriyapaisarn N, Nuntakarn L, Saetan J, et al. Enhancement of beta-Globin Gene Expression in Thalassemic IVS2-654 Induced Pluripotent Stem Cell-Derived Erythroid Cells by Modified U7 snRNA. *Stem cells translational medicine*. 2017 Apr;6(4):1059-69. PubMed PMID: 28213976. Pubmed Central PMCID: PMC5442829. Epub 2017/02/19. eng.

183. Kurita R, Suda N, Sudo K, Miharada K, Hiroyama T, Miyoshi H, et al. Establishment of immortalized human erythroid progenitor cell lines able to produce enucleated red blood cells. *PloS one*. 2013;8(3):e59890. PubMed PMID: 23533656. Pubmed Central PMCID: PMC3606290. Epub 2013/03/28. eng.
184. Trakarnsanga K, Griffiths RE, Wilson MC, Blair A, Satchwell TJ, Meinders M, et al. An immortalized adult human erythroid line facilitates sustainable and scalable generation of functional red cells. *Nature communications*. 2017 Mar 14;8:14750. PubMed PMID: 28290447. Pubmed Central PMCID: PMC5355882. Epub 2017/03/16. eng.
185. Hawsworth J, Satchwell TJ, Meinders M, Daniels DE, Regan F, Thornton NM, et al. Enhancement of red blood cell transfusion compatibility using CRISPR-mediated erythroblast gene editing. *EMBO molecular medicine*. 2018 Jun;10(6). PubMed PMID: 29700043. Pubmed Central PMCID: PMC5991592. Epub 2018/04/28. eng.
186. Lee YT, Kim KS, Byrnes C, de Vasconcellos JF, Noh SJ, Rabel A, et al. A synthetic model of human beta-thalassemia erythropoiesis using CD34+ cells from healthy adult donors. *PloS one*. 2013;8(7):e68307. PubMed PMID: 23861885. Pubmed Central PMCID: PMC3704632. Epub 2013/07/19. eng.
187. D'Alessandro A, Dzieciatkowska M, Nemkov T, Hansen KC. Red blood cell proteomics update: is there more to discover? *Blood transfusion = Trasfusione del sangue*. 2017 Mar;15(2):182-7. PubMed PMID: 28263177. Pubmed Central PMCID: PMC5336341. Epub 2017/03/07. eng.
188. Palis J SB. Hematology of the fetus and newborn. In: Lichtman MA KT, Prchal JT, and Levi MM. , editor. *Williams Hematology*. 8th edition. New York: New York: McGraw-Hill.; 2011. p. 87-104.
189. Cao A, Galanello R. Beta-thalassemia. *Genetics in medicine : official journal of the American College of Medical Genetics*. 2010 Feb;12(2):61-76. PubMed PMID: 20098328. Epub 2010/01/26. eng.
190. Clarke GM, Higgins TN. Laboratory investigation of hemoglobinopathies and thalassemias: review and update. *Clinical chemistry*. 2000 Aug;46(8 Pt 2):1284-90. PubMed PMID: 10926923. Epub 2000/08/06. eng.
191. Weatherall DJ. Phenotype-genotype relationships in monogenic disease: lessons from the thalassaemias. *Nature reviews Genetics*. 2001 Apr;2(4):245-55. PubMed PMID: 11283697. Epub 2001/04/03. eng.
192. Sankaran VG, Xu J, Orkin SH. Advances in the understanding of haemoglobin switching. *British journal of haematology*. 2010 Apr;149(2):181-94. PubMed PMID: 20201948. Pubmed Central PMCID: PMC4153468. Epub 2010/03/06. eng.
193. Wijgerde M, Grosveld F, Fraser P. Transcription complex stability and chromatin dynamics in vivo. *Nature*. 1995 Sep 21;377(6546):209-13. PubMed PMID: 7675106. Epub 1995/09/21. eng.
194. Wijgerde M, Gribnau J, Trimborn T, Nuez B, Philipsen S, Grosveld F, et al. The role of EKLF in human beta-globin gene competition. *Genes & development*. 1996 Nov 15;10(22):2894-902. PubMed PMID: 8918890. Epub 1996/11/15. eng.
195. Liu D, Zhang X, Yu L, Cai R, Ma X, Zheng C, et al. KLF1 mutations are relatively more common in a thalassemia endemic region and ameliorate the severity of beta-thalassemia. *Blood*. 2014 Jul 31;124(5):803-11. PubMed PMID: 24829204. Pubmed Central PMCID: PMC4118488. Epub 2014/05/16. eng.

196. Bauer DE, Kamran SC, Orkin SH. Reawakening fetal hemoglobin: prospects for new therapies for the beta-globin disorders. *Blood*. 2012 Oct 11;120(15):2945-53. PubMed PMID: 22904296. Pubmed Central PMCID: PMC4467860. Epub 2012/08/21. eng.
197. Thein SL. Molecular basis of beta thalassemia and potential therapeutic targets. *Blood cells, molecules & diseases*. 2017 Jun 20. PubMed PMID: 28651846. Epub 2017/06/28. eng.
198. Sankaran VG, Nathan DG. Reversing the hemoglobin switch. *The New England journal of medicine*. 2010 Dec 2;363(23):2258-60. PubMed PMID: 21121839. Epub 2010/12/03. eng.
199. Sankaran VG, Xu J, Ragozy T, Ippolito GC, Walkley CR, Maika SD, et al. Developmental and species-divergent globin switching are driven by BCL11A. *Nature*. 2009 Aug 27;460(7259):1093-7. PubMed PMID: 19657335. Pubmed Central PMCID: PMC3749913. Epub 2009/08/07. eng.
200. Weatherall DJ. Thalassaemia: the long road from bedside to genome. *Nature reviews Genetics*. 2004 Aug;5(8):625-31. PubMed PMID: 15266345. Epub 2004/07/22. eng.
201. Weatherall DJC, J.B. . *The Thalassaemia Syndromes, Fourth Edition*. 4th Edn. ed. Oxford: Blackwell Sciences Ltd; 2001.
202. Thein SL. Pathophysiology of beta thalassemia--a guide to molecular therapies. *Hematology American Society of Hematology Education Program*. 2005:31-7. PubMed PMID: 16304356. Epub 2005/11/24. eng.
203. Modell B, Darlison M. Global epidemiology of haemoglobin disorders and derived service indicators. *Bulletin of the World Health Organization*. 2008 Jun;86(6):480-7. PubMed PMID: 18568278. Pubmed Central PMCID: PMC2647473. Epub 2008/06/24. eng.
204. Williams TN, Weatherall DJ. World distribution, population genetics, and health burden of the hemoglobinopathies. *Cold Spring Harbor perspectives in medicine*. 2012 Sep 1;2(9):a011692. PubMed PMID: 22951448. Pubmed Central PMCID: PMC3426822. Epub 2012/09/07. eng.
205. JBS H. Disease and evolution. *La Ricerca Scientifica*. 1949;19:68-76.
206. Clegg JB, Weatherall DJ. Thalassaemia and malaria: new insights into an old problem. *Proceedings of the Association of American Physicians*. 1999 Jul-Aug;111(4):278-82. PubMed PMID: 10417734. Epub 1999/07/27. eng.
207. Willcox M, Bjorkman A, Brohult J. Falciparum malaria and beta-thalassaemia trait in northern Liberia. *Annals of tropical medicine and parasitology*. 1983 Aug;77(4):335-47. PubMed PMID: 6357119. Epub 1983/08/01. eng.
208. Yuan J, Kannan R, Shinar E, Rachmilewitz EA, Low PS. Isolation, characterization, and immunoprecipitation studies of immune complexes from membranes of beta-thalassaemic erythrocytes. *Blood*. 1992 Jun 1;79(11):3007-13. PubMed PMID: 1586745. Epub 1992/06/01. eng.
209. Schrier SL. Pathophysiology of thalassemia. *Current opinion in hematology*. 2002 Mar;9(2):123-6. PubMed PMID: 11844995. Epub 2002/02/15. eng.
210. Huff RL, Hennessy TG, Austin RE, Garcia JF, Roberts BM, Lawrence JH. Plasma and red cell iron turnover in normal subjects and in patients having various hematopoietic disorders. *The Journal of clinical investigation*. 1950 Aug;29(8):1041-52. PubMed PMID: 15436873. Pubmed Central PMCID: PMC436143. Epub 1950/08/01. eng.
211. Centis F, Tabellini L, Lucarelli G, Buffi O, Tonucci P, Persini B, et al. The importance of erythroid expansion in determining the extent of apoptosis in erythroid precursors in patients with beta-thalassemia major. *Blood*. 2000 Nov 15;96(10):3624-9. PubMed PMID: 11071663. Epub 2000/11/09. eng.

212. Rivella S. Ineffective erythropoiesis and thalassemias. *Current opinion in hematology*. 2009 May;16(3):187-94. PubMed PMID: 19318943. Pubmed Central PMCID: PMC3703923. Epub 2009/03/26. eng.
213. Oikonomidou PR, Rivella S. What can we learn from ineffective erythropoiesis in thalassemia? *Blood reviews*. 2018 Mar;32(2):130-43. PubMed PMID: 29054350. Pubmed Central PMCID: PMC5882559. Epub 2017/10/22. eng.
214. Yuan J, Angelucci E, Lucarelli G, Aljurf M, Snyder LM, Kiefer CR, et al. Accelerated programmed cell death (apoptosis) in erythroid precursors of patients with severe beta-thalassemia (Cooley's anemia). *Blood*. 1993 Jul 15;82(2):374-7. PubMed PMID: 8329696. Epub 1993/07/15. eng.
215. Libani IV, Guy EC, Melchiori L, Schiro R, Ramos P, Breda L, et al. Decreased differentiation of erythroid cells exacerbates ineffective erythropoiesis in beta-thalassemia. *Blood*. 2008 Aug 1;112(3):875-85. PubMed PMID: 18480424. Pubmed Central PMCID: PMC2481539. Epub 2008/05/16. eng.
216. Forster L, Cornwall S, Finlayson J, Ghassemifar R. Cell cycle, proliferation and apoptosis in erythroblasts cultured from patients with beta-thalassaemia major. *British journal of haematology*. 2016 Nov;175(3):539-42. PubMed PMID: 26763683. Epub 2016/10/28. eng.
217. Voskou S, Aslan M, Fanis P, Phylactides M, Kleanthous M. Oxidative stress in beta-thalassaemia and sickle cell disease. *Redox biology*. 2015 Dec;6:226-39. PubMed PMID: 26285072. Pubmed Central PMCID: PMC4543215. Epub 2015/08/19. eng.
218. Leecharoenkiat A, Wannatung T, Lithanatudom P, Svasti S, Fucharoen S, Chokchaichamnankit D, et al. Increased oxidative metabolism is associated with erythroid precursor expansion in beta0-thalassaemia/Hb E disease. *Blood cells, molecules & diseases*. 2011 Oct 15;47(3):143-57. PubMed PMID: 21783389. Epub 2011/07/26. eng.
219. Amer J, Goldfarb A, Fibach E. Flow cytometric measurement of reactive oxygen species production by normal and thalassaemic red blood cells. *European journal of haematology*. 2003 Feb;70(2):84-90. PubMed PMID: 12581189. Epub 2003/02/13. eng.
220. Gardenghi S, Marongiu MF, Ramos P, Guy E, Breda L, Chadburn A, et al. Ineffective erythropoiesis in beta-thalassemia is characterized by increased iron absorption mediated by down-regulation of hepcidin and up-regulation of ferroportin. *Blood*. 2007 Jun 1;109(11):5027-35. PubMed PMID: 17299088. Pubmed Central PMCID: PMC1885515. Epub 2007/02/15. eng.
221. Pasricha SR, Frazer DM, Bowden DK, Anderson GJ. Transfusion suppresses erythropoiesis and increases hepcidin in adult patients with beta-thalassemia major: a longitudinal study. *Blood*. 2013 Jul 4;122(1):124-33. PubMed PMID: 23656728. Epub 2013/05/10. eng.
222. Eldor A, Rachmilewitz EA. The hypercoagulable state in thalassemia. *Blood*. 2002 Jan 1;99(1):36-43. PubMed PMID: 11756150. Epub 2002/01/05. eng.
223. Weatherall DJ. The definition and epidemiology of non-transfusion-dependent thalassemia. *Blood reviews*. 2012 Apr;26 Suppl 1:S3-6. PubMed PMID: 22631040. Epub 2012/05/29. eng.
224. Taher A, Vichinsky E, Musallam K, Cappellini MD, Viprakasit V. In: Weatherall D, editor. *Guidelines for the Management of Non Transfusion Dependent Thalassaemia (NTDT)*. Nicosia, Cyprus: 2013 Thalassaemia International Federation.; 2013.
225. In: rd, Cappellini MD, Cohen A, Porter J, Taher A, Viprakasit V, editors. *Guidelines for the Management of Transfusion Dependent Thalassaemia (TDT)*. Nicosia CY: 2014 Thalassaemia International Federation.; 2014.

226. Borgna-Pignatti C, Rugolotto S, De Stefano P, Zhao H, Cappellini MD, Del Vecchio GC, et al. Survival and complications in patients with thalassemia major treated with transfusion and deferoxamine. *Haematologica*. 2004 Oct;89(10):1187-93. PubMed PMID: 15477202. Epub 2004/10/13. eng.
227. Cazzola M, De Stefano P, Ponchio L, Locatelli F, Beguin Y, Dessi C, et al. Relationship between transfusion regimen and suppression of erythropoiesis in beta-thalassaemia major. *British journal of haematology*. 1995 Mar;89(3):473-8. PubMed PMID: 7734344. Epub 1995/03/01. eng.
228. Taher AT, Musallam KM, Cappellini MD, Weatherall DJ. Optimal management of beta thalassaemia intermedia. *British journal of haematology*. 2011 Mar;152(5):512-23. PubMed PMID: 21250971. Epub 2011/01/22. eng.
229. Fucharoen S, Weatherall DJ. The hemoglobin E thalassemyias. *Cold Spring Harbor perspectives in medicine*. 2012 Aug 01;2(8). PubMed PMID: 22908199. Pubmed Central PMCID: PMC3405827. Epub 2012/08/22. eng.
230. Orkin SH, Kazazian HH, Jr., Antonarakis SE, Ostrer H, Goff SC, Sexton JP. Abnormal RNA processing due to the exon mutation of beta E-globin gene. *Nature*. 1982 Dec 23;300(5894):768-9. PubMed PMID: 7177196. Epub 1982/12/23. eng.
231. Olivieri NF, Pakbaz Z, Vichinsky E. HbE/beta-thalassemia: basis of marked clinical diversity. *Hematology/oncology clinics of North America*. 2010 Dec;24(6):1055-70. PubMed PMID: 21075280. Epub 2010/11/16. eng.
232. Winichagoon P, Fucharoen S, Wilairat P, Chihara K, Fukumaki Y. Role of alternatively spliced beta E-globin mRNA on clinical severity of beta-thalassemia/hemoglobin E disease. *The Southeast Asian journal of tropical medicine and public health*. 1995;26 Suppl 1:241-5. PubMed PMID: 8629114. Epub 1995/01/01. eng.
233. Roche CJ, Malashkevich V, Balazs TC, Dantsker D, Chen Q, Moreira J, et al. Structural and functional studies indicating altered redox properties of hemoglobin E: implications for production of bioactive nitric oxide. *The Journal of biological chemistry*. 2011 Jul 1;286(26):23452-66. PubMed PMID: 21531715. Pubmed Central PMCID: PMC3123109. Epub 2011/05/03. eng.
234. Chiu DT, van den Berg J, Kuypers FA, Hung IJ, Wei JS, Liu TZ. Correlation of membrane lipid peroxidation with oxidation of hemoglobin variants: possibly related to the rates of heme release. *Free radical biology & medicine*. 1996;21(1):89-95. PubMed PMID: 8791096. Epub 1996/01/01. eng.
235. Datta P, Basu S, Chakravarty SB, Chakravarty A, Banerjee D, Chandra S, et al. Enhanced oxidative cross-linking of hemoglobin E with spectrin and loss of erythrocyte membrane asymmetry in hemoglobin E beta-thalassemia. *Blood cells, molecules & diseases*. 2006 Sep-Oct;37(2):77-81. PubMed PMID: 16877015. Epub 2006/08/01. eng.
236. Pootrakul P, Sirankapracha P, Hemsorach S, Mounsub W, Kumbunlue R, Piangitjagum A, et al. A correlation of erythrokinetics, ineffective erythropoiesis, and erythroid precursor apoptosis in Thai patients with thalassemia. *Blood*. 2000 Oct 1;96(7):2606-12. PubMed PMID: 11001918. Epub 2000/09/26. eng.
237. Rees DC, Styles L, Vichinsky EP, Clegg JB, Weatherall DJ. The hemoglobin E syndromes. *Annals of the New York Academy of Sciences*. 1998 Jun 30;850:334-43. PubMed PMID: 9668555. Epub 1998/07/21. eng.
238. Jetsrisuparb A, Sanchaisuriya K, Fucharoen G, Fucharoen S, Wiangnon S, Jetsrisuparb C, et al. Development of severe anemia during fever episodes in patients with hemoglobin E

- trait and hemoglobin H disease combinations. *Journal of pediatric hematology/oncology*. 2006 Apr;28(4):249-53. PubMed PMID: 16679924. Epub 2006/05/09. eng.
239. Gibbons R HD, Olivieri NF, Wood WG. The β and $\delta\beta$ thalassaemias in association with structural haemoglobin variants. In: Weatherall DJ CJ, eds., editor. *The Thalassaemia Syndromes*. 4th ed. Oxford, United Kingdom: Blackwell Science; 2001. p. 393-449.
240. Panigrahi I, Agarwal S, Gupta T, Singhal P, Pradhan M. Hemoglobin E-beta thalassemia: factors affecting phenotype. *Indian pediatrics*. 2005 Apr;42(4):357-62. PubMed PMID: 15876597. Epub 2005/05/07. eng.
241. Premawardhena A, Fisher CA, Olivieri NF, de Silva S, Arambepola M, Perera W, et al. Haemoglobin E beta thalassaemia in Sri Lanka. *Lancet (London, England)*. 2005 Oct 22-28;366(9495):1467-70. PubMed PMID: 16243092. Epub 2005/10/26. eng.
242. Rees DC. Hemoglobin F and hemoglobin E/beta-thalassemia. *Journal of pediatric hematology/oncology*. 2000 Nov-Dec;22(6):567-72. PubMed PMID: 11132232. Epub 2000/12/29. eng.
243. Olivieri NF, Pakbaz Z, Vichinsky E. Hb E/beta-thalassaemia: a common & clinically diverse disorder. *The Indian journal of medical research*. 2011 Oct;134:522-31. PubMed PMID: 22089616. Pubmed Central PMCID: PMC3237252. Epub 2011/11/18. eng.
244. Vichinsky E. Hemoglobin e syndromes. *Hematology American Society of Hematology Education Program*. 2007:79-83. PubMed PMID: 18024613. Epub 2007/11/21. eng.
245. Schrier SL, Bunyaratvej A, Khuhapinant A, Fucharoen S, Aljurf M, Snyder LM, et al. The unusual pathobiology of hemoglobin constant spring red blood cells. *Blood*. 1997 Mar 1;89(5):1762-9. PubMed PMID: 9057661. Epub 1997/03/01. eng.
246. Liebhaber SA, Cash FE, Ballas SK. Human alpha-globin gene expression. The dominant role of the alpha 2-locus in mRNA and protein synthesis. *The Journal of biological chemistry*. 1986 Nov 15;261(32):15327-33. PubMed PMID: 3771577. Epub 1986/11/15. eng.
247. Molchanova TP, Pobedimskaya DD, Huisman TH. The differences in quantities of alpha 2- and alpha 1-globin gene variants in heterozygotes. *British journal of haematology*. 1994 Oct;88(2):300-6. PubMed PMID: 7803274. Epub 1994/10/01. eng.
248. Shakin SH, Liebhaber SA. Translational profiles of alpha 1-, alpha 2-, and beta-globin messenger ribonucleic acids in human reticulocytes. *The Journal of clinical investigation*. 1986 Oct;78(4):1125-9. PubMed PMID: 3760187. Pubmed Central PMCID: PMC423777. Epub 1986/10/01. eng.
249. Wilber A, Nienhuis AW, Persons DA. Transcriptional regulation of fetal to adult hemoglobin switching: new therapeutic opportunities. *Blood*. 2011 Apr 14;117(15):3945-53. PubMed PMID: 21321359. Pubmed Central PMCID: PMC3087525. Epub 2011/02/16. eng.
250. Chen FE, Ooi C, Ha SY, Cheung BM, Todd D, Liang R, et al. Genetic and clinical features of hemoglobin H disease in Chinese patients. *The New England journal of medicine*. 2000 Aug 24;343(8):544-50. PubMed PMID: 10954762. Epub 2000/08/24. eng.
251. Fucharoen S, Viprakasit V. Hb H disease: clinical course and disease modifiers. *Hematology American Society of Hematology Education Program*. 2009:26-34. PubMed PMID: 20008179. Epub 2009/12/17. eng.
252. Kormoczi GF, Saemann MD, Buchta C, Peck-Radosavljevic M, Mayr WR, Schwartz DW, et al. Influence of clinical factors on the haemolysis marker haptoglobin. *European journal of clinical investigation*. 2006 Mar;36(3):202-9. PubMed PMID: 16506966. Epub 2006/03/02. eng.
253. FAO/WHO. Preventing micronutrient deficiencies. ICN: Fact Sheet Number One. The International Conference on Nutrition; December, 1992; Rome, Italy 1992.

254. Barcellini W, Fattizzo B, Zaninoni A, Radice T, Nichele I, Di Bona E, et al. Clinical heterogeneity and predictors of outcome in primary autoimmune hemolytic anemia: a GIMEMA study of 308 patients. *Blood*. 2014 Nov 6;124(19):2930-6. PubMed PMID: 25232059. Epub 2014/09/19. eng.
255. Taher AT, Radwan A, Viprakasit V. When to consider transfusion therapy for patients with non-transfusion-dependent thalassaemia. *Vox sanguinis*. 2015 Jan;108(1):1-10. PubMed PMID: 25286743. Pubmed Central PMCID: PMC4302976. Epub 2014/10/08. eng.
256. Fairbanks VF, Ziesmer SC, O'Brien PC. Methods for measuring plasma hemoglobin in micromolar concentration compared. *Clinical chemistry*. 1992 Jan;38(1):132-40. PubMed PMID: 1733585. Epub 1992/01/01. eng.
257. Harboe M. A method for determination of hemoglobin in plasma by near-ultraviolet spectrophotometry. *Scandinavian journal of clinical and laboratory investigation*. 1959;11:66-70. PubMed PMID: 13646603. Epub 1959/01/01. eng.
258. Barcellini W, Fattizzo B. Clinical Applications of Hemolytic Markers in the Differential Diagnosis and Management of Hemolytic Anemia. *Disease markers*. 2015;2015:635670. PubMed PMID: 26819490. Pubmed Central PMCID: PMC4706896. Epub 2016/01/29. eng.
259. Fretzayas A, Moustaki M, Liapi O, Karpathios T. Gilbert syndrome. *European journal of pediatrics*. 2012 Jan;171(1):11-5. PubMed PMID: 22160004. Epub 2011/12/14. eng.
260. Kato GJ, McGowan V, Machado RF, Little JA, Taylor Jt, Morris CR, et al. Lactate dehydrogenase as a biomarker of hemolysis-associated nitric oxide resistance, priapism, leg ulceration, pulmonary hypertension, and death in patients with sickle cell disease. *Blood*. 2006 Mar 15;107(6):2279-85. PubMed PMID: 16291595. Pubmed Central PMCID: PMC1895723. Epub 2005/11/18. eng.
261. Porter JB, Garbowski M. The pathophysiology of transfusional iron overload. *Hematology/oncology clinics of North America*. 2014 Aug;28(4):683-701, vi. PubMed PMID: 25064708. Epub 2014/07/30. eng.
262. Porter JB, de Witte T, Cappellini MD, Gattermann N. New insights into transfusion-related iron toxicity: Implications for the oncologist. *Critical reviews in oncology/hematology*. 2016 Mar;99:261-71. PubMed PMID: 26806144. Epub 2016/01/26. eng.
263. Musallam KM, Cappellini MD, Taher AT. Iron overload in beta-thalassemia intermedia: an emerging concern. *Current opinion in hematology*. 2013 May;20(3):187-92. PubMed PMID: 23426199. Epub 2013/02/22. eng.
264. De Domenico I, Ward DM, Kaplan J. Hcpidin and ferroportin: the new players in iron metabolism. *Seminars in liver disease*. 2011 Aug;31(3):272-9. PubMed PMID: 21901657. Pubmed Central PMCID: PMC3706197. Epub 2011/09/09. eng.
265. Kim CH. Homeostatic and pathogenic extramedullary hematopoiesis. *Journal of blood medicine*. 2010;1:13-9. PubMed PMID: 22282679. Pubmed Central PMCID: PMC3262334. Epub 2010/01/01. eng.
266. Cappellini MD, Porter JB, Viprakasit V, Taher AT. A paradigm shift on beta-thalassaemia treatment: How will we manage this old disease with new therapies? *Blood reviews*. 2018 Jul;32(4):300-11. PubMed PMID: 29455932. Epub 2018/02/20. eng.
267. Taher AT, Weatherall DJ, Cappellini MD. Thalassaemia. *Lancet (London, England)*. 2018 Jan 13;391(10116):155-67. PubMed PMID: 28774421. Epub 2017/08/05. eng.
268. Lal A, Wong TE, Andrews J, Balasa VV, Chung JH, Forester CM, et al. Transfusion practices and complications in thalassemia. *Transfusion*. 2018 Sep 27. PubMed PMID: 30260477. Epub 2018/09/28. eng.

269. Garner C, Dew TK, Sherwood R, Rees D, Thein SL. Heterocellular hereditary persistence of fetal haemoglobin affects the haematological parameters of beta-thalassaemia trait. *British journal of haematology*. 2003 Oct;123(2):353-8. PubMed PMID: 14531920. Epub 2003/10/09. eng.
270. Huang S, Wong C, Antonarakis SE, Ro-lien T, Lo WH, Kazazian HH, Jr. The same "TATA" box beta-thalassaemia mutation in Chinese and US blacks: another example of independent origins of mutation. *Human genetics*. 1986 Oct;74(2):162-4. PubMed PMID: 3021607. Epub 1986/10/01. eng.
271. Ward AJ, Cooper TA. The pathobiology of splicing. *The Journal of pathology*. 2010 Jan;220(2):152-63. PubMed PMID: 19918805. Pubmed Central PMCID: PMC2855871. Epub 2009/11/18. eng.
272. Hall GW, Thein S. Nonsense codon mutations in the terminal exon of the beta-globin gene are not associated with a reduction in beta-mRNA accumulation: a mechanism for the phenotype of dominant beta-thalassaemia. *Blood*. 1994 Apr 15;83(8):2031-7. PubMed PMID: 8161774. Epub 1994/04/15. eng.
273. Craig JE, Kelly SJ, Barnetson R, Thein SL. Molecular characterization of a novel 10.3 kb deletion causing beta-thalassaemia with unusually high Hb A2. *British journal of haematology*. 1992 Dec;82(4):735-44. PubMed PMID: 1482661. Epub 1992/12/01. eng.
274. Yu C, Niakan KK, Matsushita M, Stamatoyannopoulos G, Orkin SH, Raskind WH. X-linked thrombocytopenia with thalassaemia from a mutation in the amino finger of GATA-1 affecting DNA binding rather than FOG-1 interaction. *Blood*. 2002 Sep 15;100(6):2040-5. PubMed PMID: 12200364. Pubmed Central PMCID: PMC2808424. Epub 2002/08/30. eng.
275. Weatherall DJ, Clegg JB, Knox-Macaulay HH, Bunch C, Hopkins CR, Temperley IJ. A genetically determined disorder with features both of thalassaemia and congenital dyserythropoietic anaemia. *British journal of haematology*. 1973 Jun;24(6):681-702. PubMed PMID: 4351905. Epub 1973/06/01. eng.
276. Stamatoyannopoulos G, Woodson R, Papayannopoulou T, Heywood D, Kurachi S. Inclusion-body beta-thalassaemia trait. A form of beta thalassaemia producing clinical manifestations in simple heterozygotes. *The New England journal of medicine*. 1974 Apr 25;290(17):939-43. PubMed PMID: 4361439. Epub 1974/04/25. eng.
277. Thein S. Structural variants with a beta-thalassaemia phenotype. In: Steinberg MH FB, Higgs DR, Nagel RL, editor. *Disorders of hemoglobin: Genetics, pathophysiology, and clinical management*. 1st ed. Cambridge, UK: Cambridge University Press; 2001. p. 342-55.
278. Thein SL. Is it dominantly inherited beta thalassaemia or just a beta-chain variant that is highly unstable? *British journal of haematology*. 1999 Oct;107(1):12-21. PubMed PMID: 10520021. Epub 1999/10/16. eng.
279. Thein SL WW. The molecular basis of β thalassaemia, $\delta\beta$ thalassaemia, and hereditary persistence of fetal hemoglobin. In: Steinberg MH FB, Higgs DR, Weatherall DJ, editor. *Disorders of hemoglobin: Genetics, pathophysiology, and clinical management*. 2nd ed. Cambridge, UK: Cambridge University Press; 2009. p. 323-56.
280. Olivieri NF, Muraca GM, O'Donnell A, Premawardhena A, Fisher C, Weatherall DJ. Studies in haemoglobin E beta-thalassaemia. *British journal of haematology*. 2008 May;141(3):388-97. PubMed PMID: 18410572. Epub 2008/04/16. eng.
281. Olivieri NF, Thayalsuthan V, O'Donnell A, Premawardhena A, Rigobon C, Muraca G, et al. Emerging insights in the management of hemoglobin E beta thalassaemia. *Annals of the New York Academy of Sciences*. 2010 Aug;1202:155-7. PubMed PMID: 20712787. Epub 2010/08/18. eng.

282. O'Donnell A, Premawardhena A, Arambepola M, Allen SJ, Peto TE, Fisher CA, et al. Age-related changes in adaptation to severe anemia in childhood in developing countries. *Proceedings of the National Academy of Sciences of the United States of America*. 2007 May 29;104(22):9440-4. PubMed PMID: 17517643. Pubmed Central PMCID: PMC1890513. Epub 2007/05/23. eng.
283. Allen A, Fisher C, Premawardhena A, Peto T, Allen S, Arambepola M, et al. Adaptation to anemia in hemoglobin E-ss thalassemia. *Blood*. 2010 Dec 9;116(24):5368-70. PubMed PMID: 20833979. Epub 2010/09/14. eng.
284. Craig JE, Rochette J, Sampietro M, Wilkie AO, Barnetson R, Hatton CS, et al. Genetic heterogeneity in heterocellular hereditary persistence of fetal hemoglobin. *Blood*. 1997 Jul 1;90(1):428-34. PubMed PMID: 9207480. Epub 1997/07/01. eng.
285. Forget BG. Molecular basis of hereditary persistence of fetal hemoglobin. *Annals of the New York Academy of Sciences*. 1998 Jun 30;850:38-44. PubMed PMID: 9668525. Epub 1998/07/21. eng.
286. Ye L, Wang J, Tan Y, Beyer AI, Xie F, Muench MO, et al. Genome editing using CRISPR-Cas9 to create the HPFH genotype in HSPCs: An approach for treating sickle cell disease and beta-thalassemia. *Proceedings of the National Academy of Sciences of the United States of America*. 2016 Sep 20;113(38):10661-5. PubMed PMID: 27601644. Pubmed Central PMCID: PMC5035856. Epub 2016/09/08. eng.
287. Wienert B, Martyn GE, Funnell APW, Quinlan KGR, Crossley M. Wake-up Sleepy Gene: Reactivating Fetal Globin for beta-Hemoglobinopathies. *Trends in genetics : TIG*. 2018 Dec;34(12):927-40. PubMed PMID: 30287096. Epub 2018/10/06. eng.
288. Martyn GE, Wienert B, Yang L, Shah M, Norton LJ, Burdach J, et al. Natural regulatory mutations elevate the fetal globin gene via disruption of BCL11A or ZBTB7A binding. *Nature genetics*. 2018 Apr;50(4):498-503. PubMed PMID: 29610478. Epub 2018/04/04. eng.
289. Huang P, Keller CA, Giardine B, Grevet JD, Davies JOJ, Hughes JR, et al. Comparative analysis of three-dimensional chromosomal architecture identifies a novel fetal hemoglobin regulatory element. *Genes & development*. 2017 Aug 15;31(16):1704-13. PubMed PMID: 28916711. Pubmed Central PMCID: PMC5647940. Epub 2017/09/17. eng.
290. Masuda T, Wang X, Maeda M, Canver MC, Sher F, Funnell AP, et al. Transcription factors LRF and BCL11A independently repress expression of fetal hemoglobin. *Science (New York, NY)*. 2016 Jan 15;351(6270):285-9. PubMed PMID: 26816381. Pubmed Central PMCID: PMC4778394. Epub 2016/01/28. eng.
291. Skene PJ, Henikoff S. An efficient targeted nuclease strategy for high-resolution mapping of DNA binding sites. *eLife*. 2017 Jan 16;6. PubMed PMID: 28079019. Pubmed Central PMCID: PMC5310842. Epub 2017/01/13. eng.
292. Thein SL, Weatherall DJ. A non-deletion hereditary persistence of fetal hemoglobin (HPFH) determinant not linked to the beta-globin gene complex. *Progress in clinical and biological research*. 1989;316B:97-111. PubMed PMID: 2482508. Epub 1989/01/01. eng.
293. Cappellini MD, Fiorelli G, Bernini LF. Interaction between homozygous beta (0) thalassaemia and the Swiss type of hereditary persistence of fetal haemoglobin. *British journal of haematology*. 1981 Aug;48(4):561-72. PubMed PMID: 6168279. Epub 1981/08/01. eng.
294. Rochette J, Craig JE, Thein SL. Fetal hemoglobin levels in adults. *Blood reviews*. 1994 Dec;8(4):213-24. PubMed PMID: 7534152. Epub 1994/12/01. eng.

295. Rees DC, Porter JB, Clegg JB, Weatherall DJ. Why are hemoglobin F levels increased in HbE/beta thalassemia? *Blood*. 1999 Nov 1;94(9):3199-204. PubMed PMID: 10556208. Epub 1999/11/11. eng.
296. Garner C, Tatu T, Reittie JE, Littlewood T, Darley J, Cervino S, et al. Genetic influences on F cells and other hematologic variables: a twin heritability study. *Blood*. 2000 Jan 1;95(1):342-6. PubMed PMID: 10607722. Epub 1999/12/23. eng.
297. Craig JE, Rochette J, Fisher CA, Weatherall DJ, Marc S, Lathrop GM, et al. Dissecting the loci controlling fetal haemoglobin production on chromosomes 11p and 6q by the regressive approach. *Nature genetics*. 1996 Jan;12(1):58-64. PubMed PMID: 8528252. Epub 1996/01/01. eng.
298. Thein SL, Menzel S. Discovering the genetics underlying foetal haemoglobin production in adults. *British journal of haematology*. 2009 May;145(4):455-67. PubMed PMID: 19344402. Epub 2009/04/07. eng.
299. Thein SL, Menzel S, Lathrop M, Garner C. Control of fetal hemoglobin: new insights emerging from genomics and clinical implications. *Human molecular genetics*. 2009 Oct 15;18(R2):R216-23. PubMed PMID: 19808799. Pubmed Central PMCID: PMC2758709. Epub 2009/10/08. eng.
300. Singleton BK, Lau W, Fairweather VS, Burton NM, Wilson MC, Parsons SF, et al. Mutations in the second zinc finger of human EKLF reduce promoter affinity but give rise to benign and disease phenotypes. *Blood*. 2011 Sep 15;118(11):3137-45. PubMed PMID: 21778342. Epub 2011/07/23. eng.
301. Yien YY, Bieker JJ. EKLF/KLF1, a tissue-restricted integrator of transcriptional control, chromatin remodeling, and lineage determination. *Molecular and cellular biology*. 2013 Jan;33(1):4-13. PubMed PMID: 23090966. Pubmed Central PMCID: PMC3536305. Epub 2012/10/24. eng.
302. Gnanapragasam MN, McGrath KE, Catherman S, Xue L, Palis J, Bieker JJ. EKLF/KLF1-regulated cell cycle exit is essential for erythroblast enucleation. *Blood*. 2016 Sep 22;128(12):1631-41. PubMed PMID: 27480112. Pubmed Central PMCID: PMC5034741. Epub 2016/08/03. eng.
303. Lee JS, Ngo H, Kim D, Chung JH. Erythroid Kruppel-like factor is recruited to the CACCC box in the beta-globin promoter but not to the CACCC box in the gamma-globin promoter: the role of the neighboring promoter elements. *Proceedings of the National Academy of Sciences of the United States of America*. 2000 Mar 14;97(6):2468-73. PubMed PMID: 10706605. Pubmed Central PMCID: PMC15952. Epub 2000/03/08. eng.
304. Vinjamur DS, Alhashem YN, Mohamad SF, Amin P, Williams DC, Jr., Lloyd JA. Kruppel-Like Transcription Factor KLF1 Is Required for Optimal gamma- and beta-Globin Expression in Human Fetal Erythroblasts. *PloS one*. 2016;11(2):e0146802. PubMed PMID: 26840243. Pubmed Central PMCID: PMC4739742. Epub 2016/02/04. eng.
305. Bieker JJ. Putting a finger on the switch. *Nature genetics*. 2010 Sep;42(9):733-4. PubMed PMID: 20802474. Pubmed Central PMCID: PMC3234686. Epub 2010/08/31. eng.
306. Borg J, Patrinos GP, Felice AE, Philipsen S. Erythroid phenotypes associated with KLF1 mutations. *Haematologica*. 2011 May;96(5):635-8. PubMed PMID: 21531944. Pubmed Central PMCID: PMC3084906. Epub 2011/05/03. eng.
307. Khamphikham P, Sripichai O, Munkongdee T, Fucharoen S, Tongsimma S, Smith DR. Genetic variation of Kruppel-like factor 1 (KLF1) and fetal hemoglobin (HbF) levels in beta(0)-thalassemia/HbE disease. *International journal of hematology*. 2018 Mar;107(3):297-310. PubMed PMID: 29067594. Epub 2017/10/27. eng.

308. Sankaran VG, Xu J, Byron R, Greisman HA, Fisher C, Weatherall DJ, et al. A functional element necessary for fetal hemoglobin silencing. *The New England journal of medicine*. 2011 Sep 1;365(9):807-14. PubMed PMID: 21879898. Pubmed Central PMCID: PMC3174767. Epub 2011/09/02. eng.
309. Xu J, Bauer DE, Kerenyi MA, Vo TD, Hou S, Hsu YJ, et al. Corepressor-dependent silencing of fetal hemoglobin expression by BCL11A. *Proceedings of the National Academy of Sciences of the United States of America*. 2013 Apr 16;110(16):6518-23. PubMed PMID: 23576758. Pubmed Central PMCID: PMC3631619. Epub 2013/04/12. eng.
310. Bauer DE, Kamran SC, Lessard S, Xu J, Fujiwara Y, Lin C, et al. An erythroid enhancer of BCL11A subject to genetic variation determines fetal hemoglobin level. *Science (New York, NY)*. 2013 Oct 11;342(6155):253-7. PubMed PMID: 24115442. Pubmed Central PMCID: PMC4018826. Epub 2013/10/12. eng.
311. Canver MC, Smith EC, Sher F, Pinello L, Sanjana NE, Shalem O, et al. BCL11A enhancer dissection by Cas9-mediated in situ saturating mutagenesis. *Nature*. 2015 Nov 12;527(7577):192-7. PubMed PMID: 26375006. Pubmed Central PMCID: PMC4644101. Epub 2015/09/17. eng.
312. Labie D, Pagnier J, Lapoumeroulie C, Rouabhi F, Dunda-Belkhodja O, Chardin P, et al. Common haplotype dependency of high G gamma-globin gene expression and high Hb F levels in beta-thalassemia and sickle cell anemia patients. *Proceedings of the National Academy of Sciences of the United States of America*. 1985 Apr;82(7):2111-4. PubMed PMID: 2580306. Pubmed Central PMCID: PMC397502. Epub 1985/04/01. eng.
313. Efremov GD, Gjorgovski I, Stojanovski N, Diaz-Chico JC, Harano T, Kutlar F, et al. One haplotype is associated with the Swiss type of hereditary persistence of fetal hemoglobin in the Yugoslavian population. *Human genetics*. 1987 Oct;77(2):132-6. PubMed PMID: 2443439. Epub 1987/10/01. eng.
314. Thein SL, Menzel S, Peng X, Best S, Jiang J, Close J, et al. Intergenic variants of HBS1L-MYB are responsible for a major quantitative trait locus on chromosome 6q23 influencing fetal hemoglobin levels in adults. *Proceedings of the National Academy of Sciences of the United States of America*. 2007 Jul 3;104(27):11346-51. PubMed PMID: 17592125. Pubmed Central PMCID: PMC2040901. Epub 2007/06/27. eng.
315. Stadhouders R, Aktuna S, Thongjuea S, Aghajani-refah A, Pourfarzad F, van Ijcken W, et al. HBS1L-MYB intergenic variants modulate fetal hemoglobin via long-range MYB enhancers. *The Journal of clinical investigation*. 2014 Apr;124(4):1699-710. PubMed PMID: 24614105. Pubmed Central PMCID: PMC3973089. Epub 2014/03/13. eng.
316. Compe E, Egly JM. Nucleotide Excision Repair and Transcriptional Regulation: TFIIH and Beyond. *Annual review of biochemistry*. 2016 Jun 2;85:265-90. PubMed PMID: 27294439. Epub 2016/06/15. eng.
317. Viprakasit V, Gibbons RJ, Broughton BC, Tolmie JL, Brown D, Lunt P, et al. Mutations in the general transcription factor TFIIH result in beta-thalassaemia in individuals with trichothiodystrophy. *Human molecular genetics*. 2001 Nov 15;10(24):2797-802. PubMed PMID: 11734544. Epub 2001/12/06. eng.
318. Tkach M, Thery C. Communication by Extracellular Vesicles: Where We Are and Where We Need to Go. *Cell*. 2016 Mar 10;164(6):1226-32. PubMed PMID: 26967288. Epub 2016/03/12. eng.
319. Robbins PD, Morelli AE. Regulation of immune responses by extracellular vesicles. *Nature reviews Immunology*. 2014 Mar;14(3):195-208. PubMed PMID: 24566916. Pubmed Central PMCID: PMC4350779. Epub 2014/02/26. eng.

320. Tripisciano C, Weiss R, Eichhorn T, Spittler A, Heuser T, Fischer MB, et al. Different Potential of Extracellular Vesicles to Support Thrombin Generation: Contributions of Phosphatidylserine, Tissue Factor, and Cellular Origin. *Scientific reports*. 2017 Jul 26;7(1):6522. PubMed PMID: 28747771. Pubmed Central PMCID: PMC5529579. Epub 2017/07/28. eng.
321. They C, Witwer KW, Aikawa E, Alcaraz MJ, Anderson JD, Andriantsitohaina R, et al. Minimal information for studies of extracellular vesicles 2018 (MISEV2018): a position statement of the International Society for Extracellular Vesicles and update of the MISEV2014 guidelines. *Journal of extracellular vesicles*. 2018;7(1):1535750. PubMed PMID: 30637094. Pubmed Central PMCID: PMC6322352. Epub 2019/01/15. eng.
322. Lotvall J, Hill AF, Hochberg F, Buzas EI, Di Vizio D, Gardiner C, et al. Minimal experimental requirements for definition of extracellular vesicles and their functions: a position statement from the International Society for Extracellular Vesicles. *Journal of extracellular vesicles*. 2014;3:26913. PubMed PMID: 25536934. Pubmed Central PMCID: PMC4275645. Epub 2014/12/30. eng.
323. Gyorgy B, Szabo TG, Pasztoi M, Pal Z, Misjak P, Aradi B, et al. Membrane vesicles, current state-of-the-art: emerging role of extracellular vesicles. *Cellular and molecular life sciences : CMLS*. 2011 Aug;68(16):2667-88. PubMed PMID: 21560073. Pubmed Central PMCID: PMC3142546. Epub 2011/05/12. eng.
324. van der Pol E, Boing AN, Gool EL, Nieuwland R. Recent developments in the nomenclature, presence, isolation, detection and clinical impact of extracellular vesicles. *Journal of thrombosis and haemostasis : JTH*. 2016 Jan;14(1):48-56. PubMed PMID: 26564379. Epub 2015/11/14. eng.
325. Shah R, Patel T, Freedman JE. Circulating Extracellular Vesicles in Human Disease. *The New England journal of medicine*. 2018 Sep 6;379(10):958-66. PubMed PMID: 30184457. Epub 2018/09/06. eng.
326. Said AS, Rogers SC, Doctor A. Physiologic Impact of Circulating RBC Microparticles upon Blood-Vascular Interactions. *Frontiers in physiology*. 2017;8:1120. PubMed PMID: 29379445. Pubmed Central PMCID: PMC5770796. Epub 2018/01/31. eng.
327. Bevers EM, Comfurius P, Dekkers DW, Zwaal RF. Lipid translocation across the plasma membrane of mammalian cells. *Biochimica et biophysica acta*. 1999 Aug 18;1439(3):317-30. PubMed PMID: 10446420. Epub 1999/08/14. eng.
328. Nagata S, Suzuki J, Segawa K, Fujii T. Exposure of phosphatidylserine on the cell surface. *Cell death and differentiation*. 2016 Jun;23(6):952-61. PubMed PMID: 26891692. Pubmed Central PMCID: PMC4987739. Epub 2016/02/20. eng.
329. Bosman GJ, Lasonder E, Groenen-Dopp YA, Willekens FL, Werre JM. The proteome of erythrocyte-derived microparticles from plasma: new clues for erythrocyte aging and vesiculation. *Journal of proteomics*. 2012 Dec 5;76 Spec No.:203-10. PubMed PMID: 22669077. Epub 2012/06/07. eng.
330. Ravichandran KS. Beginnings of a good apoptotic meal: the find-me and eat-me signaling pathways. *Immunity*. 2011 Oct 28;35(4):445-55. PubMed PMID: 22035837. Pubmed Central PMCID: PMC3241945. Epub 2011/11/01. eng.
331. They C, Zitvogel L, Amigorena S. Exosomes: composition, biogenesis and function. *Nature reviews Immunology*. 2002 Aug;2(8):569-79. PubMed PMID: 12154376. Epub 2002/08/03. eng.

332. Kuo WP, Tigges JC, Toxavidis V, Ghiran I. Red Blood Cells: A Source of Extracellular Vesicles. *Methods in molecular biology* (Clifton, NJ). 2017;1660:15-22. PubMed PMID: 28828644. Epub 2017/08/23. eng.
333. Westerman M, Porter JB. Red blood cell-derived microparticles: An overview. *Blood cells, molecules & diseases*. 2016 Jul;59:134-9. PubMed PMID: 27282583. Epub 2016/06/11. eng.
334. Camus SM, Gausseres B, Bonnin P, Loufrani L, Grimaud L, Charue D, et al. Erythrocyte microparticles can induce kidney vaso-occlusions in a murine model of sickle cell disease. *Blood*. 2012 Dec 13;120(25):5050-8. PubMed PMID: 22976952. Epub 2012/09/15. eng.
335. Nebor D, Bowers A, Connes P, Hardy-Dessources MD, Knight-Madden J, Cumming V, et al. Plasma concentration of platelet-derived microparticles is related to painful vaso-occlusive phenotype severity in sickle cell anemia. *PloS one*. 2014;9(1):e87243. PubMed PMID: 24475257. Pubmed Central PMCID: PMC3901744. Epub 2014/01/30. eng.
336. Camus SM, De Moraes JA, Bonnin P, Abbyad P, Le Jeune S, Lionnet F, et al. Circulating cell membrane microparticles transfer heme to endothelial cells and trigger vasoocclusions in sickle cell disease. *Blood*. 2015 Jun 11;125(24):3805-14. PubMed PMID: 25827830. Pubmed Central PMCID: PMC4490297. Epub 2015/04/02. eng.
337. Liu C, Zhao W, Christ GJ, Gladwin MT, Kim-Shapiro DB. Nitric oxide scavenging by red cell microparticles. *Free radical biology & medicine*. 2013 Dec;65:1164-73. PubMed PMID: 24051181. Pubmed Central PMCID: PMC3859830. Epub 2013/09/21. eng.
338. Kasar M, Boga C, Yeral M, Asma S, Kozanoglu I, Ozdogu H. Clinical significance of circulating blood and endothelial cell microparticles in sickle-cell disease. *Journal of thrombosis and thrombolysis*. 2014;38(2):167-75. PubMed PMID: 24254379. Epub 2013/11/21. eng.
339. Mankelov TJ, Griffiths RE, Trompeter S, Flatt JF, Cogan NM, Massey EJ, et al. The ins and outs of reticulocyte maturation revisited: The role of autophagy in sickle cell disease. *Autophagy*. 2016;12(3):590-1. PubMed PMID: 27046252. Pubmed Central PMCID: PMC4836018. Epub 2016/04/06. eng.
340. De Franceschi L, Bertoldi M, Matte A, Santos Franco S, Pantaleo A, Ferru E, et al. Oxidative stress and beta-thalassemic erythroid cells behind the molecular defect. *Oxidative medicine and cellular longevity*. 2013;2013:985210. PubMed PMID: 24205432. Pubmed Central PMCID: PMC3800594. Epub 2013/11/10. eng.
341. Hugel B, Martinez MC, Kunzelmann C, Freyssinet JM. Membrane microparticles: two sides of the coin. *Physiology (Bethesda, Md)*. 2005 Feb;20:22-7. PubMed PMID: 15653836. Epub 2005/01/18. eng.
342. Shinar E, Rachmilewitz EA. Oxidative denaturation of red blood cells in thalassemia. *Seminars in hematology*. 1990 Jan;27(1):70-82. PubMed PMID: 2405497. Epub 1990/01/01. eng.
343. Hirsch RE, Sibmooh N, Fucharoen S, Friedman JM. HbE/beta-Thalassemia and Oxidative Stress: The Key to Pathophysiological Mechanisms and Novel Therapeutics. *Antioxidants & redox signaling*. 2017 May 10;26(14):794-813. PubMed PMID: 27650096. Pubmed Central PMCID: PMC5421591. Epub 2016/09/22. eng.
344. Kalpravidh RW, Tangjaidee T, Hatairaktham S, Charoensakdi R, Panichkul N, Siritanaratkul N, et al. Glutathione redox system in beta -thalassemia/Hb E patients. *TheScientificWorldJournal*. 2013;2013:543973. PubMed PMID: 24223032. Pubmed Central PMCID: PMC3816076. Epub 2013/11/14. eng.

345. Rifkind JM, Nagababu E. Hemoglobin redox reactions and red blood cell aging. *Antioxidants & redox signaling*. 2013 Jun 10;18(17):2274-83. PubMed PMID: 23025272. Pubmed Central PMCID: PMC3638511. Epub 2012/10/03. eng.
346. Nagababu E, Mohanty JG, Friedman JS, Rifkind JM. Role of peroxiredoxin-2 in protecting RBCs from hydrogen peroxide-induced oxidative stress. *Free radical research*. 2013 Mar;47(3):164-71. PubMed PMID: 23215741. Pubmed Central PMCID: PMC5911927. Epub 2012/12/12. eng.
347. Westerman M, Pizzey A, Hirschman J, Cerino M, Weil-Weiner Y, Ramotar P, et al. Microvesicles in haemoglobinopathies offer insights into mechanisms of hypercoagulability, haemolysis and the effects of therapy. *British journal of haematology*. 2008 Jul;142(1):126-35. PubMed PMID: 18422994. Epub 2008/04/22. eng.
348. Ferru E, Pantaleo A, Carta F, Mannu F, Khadjavi A, Gallo V, et al. Thalassaemic erythrocytes release microparticles loaded with hemichromes by redox activation of p72Syk kinase. *Haematologica*. 2014 Mar;99(3):570-8. PubMed PMID: 24038029. Pubmed Central PMCID: PMC3943323. Epub 2013/09/17. eng.
349. Pantaleo A, De Franceschi L, Ferru E, Vono R, Turrini F. Current knowledge about the functional roles of phosphorylative changes of membrane proteins in normal and diseased red cells. *Journal of proteomics*. 2010 Jan 3;73(3):445-55. PubMed PMID: 19758581. Epub 2009/09/18. eng.
350. Raposo G, Nijman HW, Stoorvogel W, Liejendekker R, Harding CV, Melief CJ, et al. B lymphocytes secrete antigen-presenting vesicles. *The Journal of experimental medicine*. 1996 Mar 1;183(3):1161-72. PubMed PMID: 8642258. Pubmed Central PMCID: PMC2192324. Epub 1996/03/01. eng.
351. Cizmar P, Yuana Y. Detection and Characterization of Extracellular Vesicles by Transmission and Cryo-Transmission Electron Microscopy. *Methods in molecular biology (Clifton, NJ)*. 2017;1660:221-32. PubMed PMID: 28828660. Epub 2017/08/23. eng.
352. Sokolova V, Ludwig AK, Hornung S, Rotan O, Horn PA, Epple M, et al. Characterisation of exosomes derived from human cells by nanoparticle tracking analysis and scanning electron microscopy. *Colloids and surfaces B, Biointerfaces*. 2011 Oct 1;87(1):146-50. PubMed PMID: 21640565. Epub 2011/06/07. eng.
353. Chuo ST, Chien JC, Lai CP. Imaging extracellular vesicles: current and emerging methods. *Journal of biomedical science*. 2018 Dec 24;25(1):91. PubMed PMID: 30580764. Pubmed Central PMCID: PMC6304785. Epub 2018/12/26. eng.
354. Cloutier N, Tan S, Boudreau LH, Cramb C, Subbaiah R, Lahey L, et al. The exposure of autoantigens by microparticles underlies the formation of potent inflammatory components: the microparticle-associated immune complexes. *EMBO molecular medicine*. 2013 Feb;5(2):235-49. PubMed PMID: 23165896. Pubmed Central PMCID: PMC3569640. Epub 2012/11/21. eng.
355. van der Vlist EJ, Nolte-'t Hoen EN, Stoorvogel W, Arkesteijn GJ, Wauben MH. Fluorescent labeling of nano-sized vesicles released by cells and subsequent quantitative and qualitative analysis by high-resolution flow cytometry. *Nature protocols*. 2012 Jun 14;7(7):1311-26. PubMed PMID: 22722367. Epub 2012/06/23. eng.
356. Welsh JA, Holloway JA, Wilkinson JS, Englyst NA. Extracellular Vesicle Flow Cytometry Analysis and Standardization. *Frontiers in cell and developmental biology*. 2017;5:78. PubMed PMID: 28913335. Pubmed Central PMCID: PMC5582084. Epub 2017/09/16. eng.

357. Lacroix R, Robert S, Poncelet P, Dignat-George F. Overcoming limitations of microparticle measurement by flow cytometry. *Seminars in thrombosis and hemostasis*. 2010 Nov;36(8):807-18. PubMed PMID: 21049381. Epub 2010/11/05. eng.
358. Pattanapanyasat K, Nulsri E, Fucharoen S, Lerdwana S, Lamchiagdhase P, Siritanaratkul N, et al. Flow cytometric quantitation of red blood cell vesicles in thalassemia. *Cytometry Part B, Clinical cytometry*. 2004 Jan;57(1):23-31. PubMed PMID: 14696060. Epub 2003/12/30. eng.
359. Dragovic RA, Gardiner C, Brooks AS, Tannetta DS, Ferguson DJ, Hole P, et al. Sizing and phenotyping of cellular vesicles using Nanoparticle Tracking Analysis. *Nanomedicine : nanotechnology, biology, and medicine*. 2011 Dec;7(6):780-8. PubMed PMID: 21601655. Pubmed Central PMCID: PMC3280380. Epub 2011/05/24. eng.
360. Gardiner C, Ferreira YJ, Dragovic RA, Redman CW, Sargent IL. Extracellular vesicle sizing and enumeration by nanoparticle tracking analysis. *Journal of extracellular vesicles*. 2013;2. PubMed PMID: 24009893. Pubmed Central PMCID: PMC3760643. Epub 2013/09/07. eng.
361. Witwer KW, Buzas EI, Bemis LT, Bora A, Lasser C, Lotvall J, et al. Standardization of sample collection, isolation and analysis methods in extracellular vesicle research. *Journal of extracellular vesicles*. 2013;2. PubMed PMID: 24009894. Pubmed Central PMCID: PMC3760646. Epub 2013/09/07. eng.
362. Vogel R, Coumans FA, Maltesen RG, Boing AN, Bonnington KE, Broekman ML, et al. A standardized method to determine the concentration of extracellular vesicles using tunable resistive pulse sensing. *Journal of extracellular vesicles*. 2016;5:31242. PubMed PMID: 27680301. Pubmed Central PMCID: PMC5040823. Epub 2016/09/30. eng.
363. Maas SL, Broekman ML, de Vrij J. Tunable Resistive Pulse Sensing for the Characterization of Extracellular Vesicles. *Methods in molecular biology (Clifton, NJ)*. 2017;1545:21-33. PubMed PMID: 27943204. Epub 2016/12/13. eng.
364. Erdbrugger U, Lannigan J. Analytical challenges of extracellular vesicle detection: A comparison of different techniques. *Cytometry Part A : the journal of the International Society for Analytical Cytology*. 2016 Feb;89(2):123-34. PubMed PMID: 26651033. Epub 2015/12/10. eng.
365. Taylor SC, Posch A. The design of a quantitative western blot experiment. *BioMed research international*. 2014;2014:361590. PubMed PMID: 24738055. Pubmed Central PMCID: PMC3971489. Epub 2014/04/17. eng.
366. Mishra M, Tiwari S, Gomes AV. Protein purification and analysis: next generation Western blotting techniques. *Expert review of proteomics*. 2017 Nov;14(11):1037-53. PubMed PMID: 28974114. Epub 2017/10/05. eng.
367. Adan A, Alizada G, Kiraz Y, Baran Y, Nalbant A. Flow cytometry: basic principles and applications. *Critical reviews in biotechnology*. 2017 Mar;37(2):163-76. PubMed PMID: 26767547. Epub 2016/01/16. eng.
368. Gauthier DJ, Sobota JA, Ferraro F, Mains RE, Lazure C. Flow cytometry-assisted purification and proteomic analysis of the corticotropes dense-core secretory granules. *Proteomics*. 2008 Sep;8(18):3848-61. PubMed PMID: 18704904. Pubmed Central PMCID: PMC2989539. Epub 2008/08/16. eng.
369. Glish GL, Vachet RW. The basics of mass spectrometry in the twenty-first century. *Nature reviews Drug discovery*. 2003 Feb;2(2):140-50. PubMed PMID: 12563305. Epub 2003/02/04. eng.

370. Jensen ON. Interpreting the protein language using proteomics. *Nature reviews Molecular cell biology*. 2006 Jun;7(6):391-403. PubMed PMID: 16723975. Epub 2006/05/26. eng.
371. Bantscheff M, Lemeer S, Savitski MM, Kuster B. Quantitative mass spectrometry in proteomics: critical review update from 2007 to the present. *Analytical and bioanalytical chemistry*. 2012 Sep;404(4):939-65. PubMed PMID: 22772140. Epub 2012/07/10. eng.
372. Mann M. Functional and quantitative proteomics using SILAC. *Nature reviews Molecular cell biology*. 2006 Dec;7(12):952-8. PubMed PMID: 17139335. Epub 2006/12/02. eng.
373. Bendall SC, Hughes C, Stewart MH, Doble B, Bhatia M, Lajoie GA. Prevention of amino acid conversion in SILAC experiments with embryonic stem cells. *Molecular & cellular proteomics : MCP*. 2008 Sep;7(9):1587-97. PubMed PMID: 18487603. Pubmed Central PMCID: PMC2556023. Epub 2008/05/20. eng.
374. Bhattacharya D, Saha S, Basu S, Chakravarty S, Chakravarty A, Banerjee D, et al. Differential regulation of redox proteins and chaperones in HbEbeta-thalassemia erythrocyte proteome. *Proteomics Clinical applications*. 2010 May;4(5):480-8. PubMed PMID: 21137065. Epub 2010/12/08. eng.
375. Weeraphan C, Srisomsap C, Chokchaichamnankit D, Subhasitanont P, Hatairaktham S, Charoensakdi R, et al. Role of curcuminoids in ameliorating oxidative modification in beta-thalassemia/Hb E plasma proteome. *The Journal of nutritional biochemistry*. 2013 Mar;24(3):578-85. PubMed PMID: 22818714. Epub 2012/07/24. eng.
376. Panachan J, Chokchaichamnankit D, Weeraphan C, Srisomsap C, Masaratana P, Hatairaktham S, et al. Differentially expressed plasma proteins of beta-thalassemia/hemoglobin E patients in response to curcuminoids/vitamin E antioxidant cocktails. *Hematology (Amsterdam, Netherlands)*. 2019 Dec;24(1):300-7. PubMed PMID: 30661467. Epub 2019/01/22. eng.
377. Rosa-Fernandes L, Rocha VB, Carregari VC, Urbani A, Palmisano G. A Perspective on Extracellular Vesicles Proteomics. *Frontiers in chemistry*. 2017;5:102. PubMed PMID: 29209607. Pubmed Central PMCID: PMC5702361. Epub 2017/12/07. eng.
378. Mears R, Craven RA, Hanrahan S, Totty N, Upton C, Young SL, et al. Proteomic analysis of melanoma-derived exosomes by two-dimensional polyacrylamide gel electrophoresis and mass spectrometry. *Proteomics*. 2004 Dec;4(12):4019-31. PubMed PMID: 15478216. Epub 2004/10/13. eng.
379. Xiao D, Ohlendorf J, Chen Y, Taylor DD, Rai SN, Waigel S, et al. Identifying mRNA, microRNA and protein profiles of melanoma exosomes. *PloS one*. 2012;7(10):e46874. PubMed PMID: 23056502. Pubmed Central PMCID: PMC3467276. Epub 2012/10/12. eng.
380. Chaichompoo P, Kumya P, Khowawisetsut L, Chiangjong W, Chaiyarit S, Pongsakul N, et al. Characterizations and proteome analysis of platelet-free plasma-derived microparticles in beta-thalassemia/hemoglobin E patients. *Journal of proteomics*. 2012 Dec 5;76 Spec No.:239-50. PubMed PMID: 22705320. Epub 2012/06/19. eng.
381. Gyorgy B, Paloczi K, Kovacs A, Barabas E, Beko G, Varnai K, et al. Improved circulating microparticle analysis in acid-citrate dextrose (ACD) anticoagulant tube. *Thrombosis research*. 2014 Feb;133(2):285-92. PubMed PMID: 24360116. Epub 2013/12/24. eng.
382. Mullier F, Bailly N, Chatelain C, Chatelain B, Dogne JM. Pre-analytical issues in the measurement of circulating microparticles: current recommendations and pending questions. *Journal of thrombosis and haemostasis : JTH*. 2013 Apr;11(4):693-6. PubMed PMID: 23410207. Epub 2013/02/16. eng.

383. Blott SJ, Pye K. GRADISTAT: a grain size distribution and statistics package for the analysis of unconsolidated sediments. *Earth Surface Processes and Landforms*. 2001;26(11):1237-48.
384. Technology I. Particle Size Distribution. Available from: <https://www.innopharmalabs.com/tech/applications-and-processes/particle-size-distribution>.
385. UniProt Consortium T. UniProt: the universal protein knowledgebase. *Nucleic acids research*. 2018 Mar 16;46(5):2699. PubMed PMID: 29425356. Pubmed Central PMCID: PMC5861450. Epub 2018/02/10. eng.
386. Miharada K, Hiroyama T, Sudo K, Nagasawa T, Nakamura Y. Efficient enucleation of erythroblasts differentiated in vitro from hematopoietic stem and progenitor cells. *Nature biotechnology*. 2006 Oct;24(10):1255-6. PubMed PMID: 16980975. Epub 2006/09/19. eng.
387. van den Akker E, Satchwell TJ, Pellegrin S, Flatt JF, Maigre M, Daniels G, et al. Investigating the key membrane protein changes during in vitro erythropoiesis of protein 4.2 (-) cells (mutations Chartres 1 and 2). *Haematologica*. 2010 Aug;95(8):1278-86. PubMed PMID: 20179084. Pubmed Central PMCID: PMC2913075. Epub 2010/02/25. eng.
388. Satchwell TJ, Bell AJ, Hawley BR, Pellegrin S, Mordue KE, van Deursen CT, et al. Severe Ankyrin-R deficiency results in impaired surface retention and lysosomal degradation of RhAG in human erythroblasts. *Haematologica*. 2016 Sep;101(9):1018-27. PubMed PMID: 27247322. Pubmed Central PMCID: PMC5060018. Epub 2016/06/02. eng.
389. Wu CJ, Krishnamurti L, Kutok JL, Biernacki M, Rogers S, Zhang W, et al. Evidence for ineffective erythropoiesis in severe sickle cell disease. *Blood*. 2005 Nov 15;106(10):3639-45. PubMed PMID: 16091448. Pubmed Central PMCID: PMC1895054. Epub 2005/08/11. eng.
390. Douay L, Giarratana MC. Ex vivo generation of human red blood cells: a new advance in stem cell engineering. *Methods in molecular biology (Clifton, NJ)*. 2009;482:127-40. PubMed PMID: 19089353. Epub 2008/12/18. eng.
391. Chakrabarti A, Bhattacharya D, Basu A, Basu S, Saha S, Halder S. Differential expression of red cell proteins in hemoglobinopathy. *Proteomics Clinical applications*. 2011 Feb;5(1-2):98-108. PubMed PMID: 21246741. Epub 2011/01/20. eng.
392. Sriiam S, Leecharoenkiat A, Lithanatudom P, Wannatung T, Svasti S, Fucharoen S, et al. Proteomic analysis of hemoglobin H-constant spring (Hb H-CS) erythroblasts. *Blood cells, molecules & diseases*. 2012 Feb 15;48(2):77-85. PubMed PMID: 22154201. Epub 2011/12/14. eng.
393. Shin JW, Spinler KR, Swift J, Chasis JA, Mohandas N, Discher DE. Lamins regulate cell trafficking and lineage maturation of adult human hematopoietic cells. *Proceedings of the National Academy of Sciences of the United States of America*. 2013 Nov 19;110(47):18892-7. PubMed PMID: 24191023. Pubmed Central PMCID: PMC3839750. Epub 2013/11/06. eng.
394. Ozdemir A, Machida K, Imataka H, Catling AD. Identification of the T-complex protein as a binding partner for newly synthesized cytoplasmic dynein intermediate chain 2. *Biochemical and biophysical research communications*. 2016 Jan 1;469(1):126-31. PubMed PMID: 26616053. Epub 2015/12/01. eng.
395. Thom CS, Traxler EA, Khandros E, Nickas JM, Zhou OY, Lazarus JE, et al. Trim58 degrades Dynein and regulates terminal erythropoiesis. *Developmental cell*. 2014 Sep 29;30(6):688-700. PubMed PMID: 25241935. Pubmed Central PMCID: PMC4203341. Epub 2014/09/23. eng.

396. Kalfa TA, Zheng Y. Rho GTPases in erythroid maturation. *Current opinion in hematology*. 2014 May;21(3):165-71. PubMed PMID: 24492678. Pubmed Central PMCID: PMC4104204. Epub 2014/02/05. eng.
397. Zimdahl B, Ito T, Blevins A, Bajaj J, Konuma T, Weeks J, et al. Lis1 regulates asymmetric division in hematopoietic stem cells and in leukemia. *Nature genetics*. 2014 Mar;46(3):245-52. PubMed PMID: 24487275. Pubmed Central PMCID: PMC4267534. Epub 2014/02/04. eng.
398. Ghaffari S. Oxidative stress in the regulation of normal and neoplastic hematopoiesis. *Antioxidants & redox signaling*. 2008 Nov;10(11):1923-40. PubMed PMID: 18707226. Pubmed Central PMCID: PMC2932538. Epub 2008/08/19. eng.
399. Ponka P, Schulman HM. Regulation of heme biosynthesis: distinct regulatory features in erythroid cells. *Stem cells (Dayton, Ohio)*. 1993 May;11 Suppl 1:24-35. PubMed PMID: 8318916. Epub 1993/05/01. eng.
400. Bryk AH, Wisniewski JR. Quantitative Analysis of Human Red Blood Cell Proteome. *Journal of proteome research*. 2017 Aug 4;16(8):2752-61. PubMed PMID: 28689405. Epub 2017/07/12. eng.
401. Moroff G, Seetharaman S, Kurtz JW, Greco NJ, Mullen MD, Lane TA, et al. Retention of cellular properties of PBPCs following liquid storage and cryopreservation. *Transfusion*. 2004 Feb;44(2):245-52. PubMed PMID: 14962316. Epub 2004/02/14. eng.
402. Martinson JA, Loudovaris M, Smith SL, Bender JG, Vachula M, van Epps DE, et al. Ex vivo expansion of frozen/thawed CD34+ cells isolated from frozen human apheresis products. *Journal of hematotherapy*. 1997 Feb;6(1):69-75. PubMed PMID: 9112220. Epub 1997/02/01. eng.
403. Laroche V, McKenna DH, Moroff G, Schierman T, Kadidlo D, McCullough J. Cell loss and recovery in umbilical cord blood processing: a comparison of postthaw and postwash samples. *Transfusion*. 2005 Dec;45(12):1909-16. PubMed PMID: 16371043. Epub 2005/12/24. eng.
404. Meyer TP, Hofmann B, Zaisserer J, Jacobs VR, Fuchs B, Rapp S, et al. Analysis and cryopreservation of hematopoietic stem and progenitor cells from umbilical cord blood. *Cytotherapy*. 2006;8(3):265-76. PubMed PMID: 16793735. Epub 2006/06/24. eng.
405. Pope B, Hokin B, Grant R. Effect of umbilical cord blood prefreeze variables on postthaw viability. *Transfusion*. 2015 Mar;55(3):629-35. PubMed PMID: 25332061. Epub 2014/10/22. eng.
406. Stellacci E, Di Noia A, Di Baldassarre A, Migliaccio G, Battistini A, Migliaccio AR. Interaction between the glucocorticoid and erythropoietin receptors in human erythroid cells. *Experimental hematology*. 2009 May;37(5):559-72. PubMed PMID: 19375647. Pubmed Central PMCID: PMC2689622. Epub 2009/04/21. eng.
407. von Lindern M, Deiner EM, Dolznig H, Parren-Van Amelsvoort M, Hayman MJ, Mullner EW, et al. Leukemic transformation of normal murine erythroid progenitors: v- and c-ErbB act through signaling pathways activated by the EpoR and c-Kit in stress erythropoiesis. *Oncogene*. 2001 Jun 21;20(28):3651-64. PubMed PMID: 11439328. Epub 2001/07/06. eng.
408. Shieh BH, Travis J. The reactive site of human alpha 2-antiplasmin. *The Journal of biological chemistry*. 1987 May 5;262(13):6055-9. PubMed PMID: 2437112. Epub 1987/05/05. eng.
409. Wannatung T, Lithanatudom P, Leecharoenkiat A, Svasti S, Fucharoen S, Smith DR. Increased erythropoiesis of beta-thalassaemia/Hb E proerythroblasts is mediated by high basal levels of ERK1/2 activation. *British journal of haematology*. 2009 Sep;146(5):557-68. PubMed PMID: 19594742. Epub 2009/07/15. eng.

410. Gabbianelli M, Morsilli O, Massa A, Pasquini L, Cianciulli P, Testa U, et al. Effective erythropoiesis and HbF reactivation induced by kit ligand in beta-thalassemia. *Blood*. 2008 Jan 1;111(1):421-9. PubMed PMID: 17951528. Epub 2007/10/24. eng.
411. Chu TTT, Sinha A, Malleret B, Suwanarusk R, Park JE, Naidu R, et al. Quantitative mass spectrometry of human reticulocytes reveal proteome-wide modifications during maturation. *British journal of haematology*. 2018 Jan;180(1):118-33. PubMed PMID: 29094334. Epub 2017/11/03. eng.
412. Gautier EF, Ducamp S, Leduc M, Salnot V, Guillonneau F, Dussiot M, et al. Comprehensive Proteomic Analysis of Human Erythropoiesis. *Cell reports*. 2016 Aug 2;16(5):1470-84. PubMed PMID: 27452463. Pubmed Central PMCID: PMC5274717. Epub 2016/07/28. eng.
413. Diaz-Varela M, de Menezes-Neto A, Perez-Zsolt D, Gamez-Valero A, Segui-Barber J, Izquierdo-Useros N, et al. Proteomics study of human cord blood reticulocyte-derived exosomes. *Scientific reports*. 2018 Sep 19;8(1):14046. PubMed PMID: 30232403. Pubmed Central PMCID: PMC6145868. Epub 2018/09/21. eng.
414. Elsayh KI, Zahran AM, El-Abaseri TB, Mohamed AO, El-Metwally TH. Hypoxia biomarkers, oxidative stress, and circulating microparticles in pediatric patients with thalassemia in Upper Egypt. *Clinical and applied thrombosis/hemostasis : official journal of the International Academy of Clinical and Applied Thrombosis/Hemostasis*. 2014 Jul;20(5):536-45. PubMed PMID: 23314673. Epub 2013/01/15. eng.
415. Alaarg A, Schiffelers RM, van Solinge WW, van Wijk R. Red blood cell vesiculation in hereditary hemolytic anemia. *Frontiers in physiology*. 2013 Dec 13;4:365. PubMed PMID: 24379786. Pubmed Central PMCID: PMC3862113. Epub 2014/01/01. eng.
416. Hebbel RP, Key NS. Microparticles in sickle cell anaemia: promise and pitfalls. *British journal of haematology*. 2016 Jul;174(1):16-29. PubMed PMID: 27136195. Epub 2016/05/03. eng.
417. Agouti I, Cointe S, Robert S, Judicone C, Loundou A, Driss F, et al. Platelet and not erythrocyte microparticles are procoagulant in transfused thalassaemia major patients. *British journal of haematology*. 2015 Nov;171(4):615-24. PubMed PMID: 26205481. Epub 2015/07/25. eng.
418. Pattanapanyasat K, Gonwong S, Chaichompoo P, Noulsri E, Lerdwana S, Sukapirom K, et al. Activated platelet-derived microparticles in thalassaemia. *British journal of haematology*. 2007 Feb;136(3):462-71. PubMed PMID: 17278261. Epub 2007/02/06. eng.
419. Kittivorapart J, Crew VK, Wilson MC, Heesom KJ, Siritanaratkul N, Teye AM. Quantitative proteomics of plasma vesicles identify novel biomarkers for hemoglobin E/beta-thalassemic patients. *Blood advances*. 2018 Jan 23;2(2):95-104. PubMed PMID: 29365317. Pubmed Central PMCID: PMC5787864. Epub 2018/01/25. eng.
420. Gell D, Kong Y, Eaton SA, Weiss MJ, Mackay JP. Biophysical characterization of the alpha-globin binding protein alpha-hemoglobin stabilizing protein. *The Journal of biological chemistry*. 2002 Oct 25;277(43):40602-9. PubMed PMID: 12192002. Epub 2002/08/23. eng.
421. Tato M, Kumar SV, Liu Y, Mulay SR, Moll S, Popper B, et al. Cathepsin S inhibition combines control of systemic and peripheral pathomechanisms of autoimmune tissue injury. *Scientific reports*. 2017 Jun 5;7(1):2775. PubMed PMID: 28584258. Pubmed Central PMCID: PMC5459853. Epub 2017/06/07. eng.
422. Gamez-Valero A, Monguio-Tortajada M, Carreras-Planella L, Franquesa M, Beyer K, Borrás FE. Size-Exclusion Chromatography-based isolation minimally alters Extracellular Vesicles' characteristics compared to precipitating agents. *Scientific reports*. 2016 Sep

- 19;6:33641. PubMed PMID: 27640641. Pubmed Central PMCID: PMC5027519. Epub 2016/09/20. eng.
423. van der Pol E, Coumans FA, Grootemaat AE, Gardiner C, Sargent IL, Harrison P, et al. Particle size distribution of exosomes and microvesicles determined by transmission electron microscopy, flow cytometry, nanoparticle tracking analysis, and resistive pulse sensing. *Journal of thrombosis and haemostasis : JTH.* 2014 Jul;12(7):1182-92. PubMed PMID: 24818656. Epub 2014/05/14. eng.
424. Varga Z, Yuana Y, Grootemaat AE, van der Pol E, Gollwitzer C, Krumrey M, et al. Towards traceable size determination of extracellular vesicles. *Journal of extracellular vesicles.* 2014;3. PubMed PMID: 24511372. Pubmed Central PMCID: PMC3916677. Epub 2014/02/11. eng.
425. Shao H, Im H, Castro CM, Breakefield X, Weissleder R, Lee H. New Technologies for Analysis of Extracellular Vesicles. *Chemical reviews.* 2018 Feb 28;118(4):1917-50. PubMed PMID: 29384376. Pubmed Central PMCID: PMC6029891. Epub 2018/02/01. eng.
426. Levin C, Koren A, Rebibo-Sabbah A, Koifman N, Brenner B, Aharon A. Extracellular Vesicle Characteristics in beta-thalassemia as Potential Biomarkers for Spleen Functional Status and Ineffective Erythropoiesis. *Frontiers in physiology.* 2018;9:1214. PubMed PMID: 30214417. Pubmed Central PMCID: PMC6125348. Epub 2018/09/15. eng.
427. Weatherall DJ, Clegg JB. Inherited haemoglobin disorders: an increasing global health problem. *Bulletin of the World Health Organization.* 2001;79(8):704-12. PubMed PMID: 11545326. Pubmed Central PMCID: PMC2566499. Epub 2001/09/08. eng.
428. Weiss MJ, dos Santos CO. Chaperoning erythropoiesis. *Blood.* 2009 Mar 5;113(10):2136-44. PubMed PMID: 19109556. Pubmed Central PMCID: PMC2652363. Epub 2008/12/26. eng.
429. Viprakasit V, Tanphaichitr VS, Chinchang W, Sangkla P, Weiss MJ, Higgs DR. Evaluation of alpha hemoglobin stabilizing protein (AHSP) as a genetic modifier in patients with beta thalassemia. *Blood.* 2004 May 1;103(9):3296-9. PubMed PMID: 14715623. Epub 2004/01/13. eng.
430. Sripichai O, Whitacre J, Munkongdee T, Kumkhaek C, Makarasara W, Winichagoon P, et al. Genetic analysis of candidate modifier polymorphisms in Hb E-beta 0-thalassemia patients. *Annals of the New York Academy of Sciences.* 2005;1054:433-8. PubMed PMID: 16339693. Epub 2005/12/13. eng.
431. Cappellini MD, Refaldi C, Bignamini D, Zanaboni L, Fiorelli G. Molecular Analysis of Alpha Hemoglobin Stabilizing Protein (AHSP) in Caucasian Patients with different Beta-Thalassemia Phenotypes. *Blood.* 2004 2004-11-16 00:00:00;104:3770-.
432. Musallam KM, Rivella S, Vichinsky E, Rachmilewitz EA. Non-transfusion-dependent thalassemias. *Haematologica.* 2013 Jun;98(6):833-44. PubMed PMID: 23729725. Pubmed Central PMCID: PMC3669437. Epub 2013/06/05. eng.
433. Schaer DJ, Buehler PW, Alayash AI, Belcher JD, Vercellotti GM. Hemolysis and free hemoglobin revisited: exploring hemoglobin and heme scavengers as a novel class of therapeutic proteins. *Blood.* 2013 Feb 21;121(8):1276-84. PubMed PMID: 23264591. Pubmed Central PMCID: PMC3578950. Epub 2012/12/25. eng.
434. Belcher JD, Nath KA, Vercellotti GM. Vasculotoxic and Proinflammatory Effects of Plasma Heme: Cell Signaling and Cytoprotective Responses. *ISRN oxidative medicine.* 2013;2013. PubMed PMID: 25506596. Pubmed Central PMCID: PMC4261193. Epub 2013/01/01. eng.

435. Santiago RP, Guarda CC, Figueiredo CVB, Fiuza LM, Aleluia MM, Adanho CSA, et al. Serum haptoglobin and hemopexin levels are depleted in pediatric sickle cell disease patients. *Blood cells, molecules & diseases*. 2018 Sep;72:34-6. PubMed PMID: 30033157. Epub 2018/07/24. eng.
436. kato GJ GM. Mechanisms and clinical complications of hemolysis in sickle cell disease and thalassemia In: Steinberg MH FB, Higgs DR, Weatherall DJ, editor. *Disorders of hemoglobin: Genetics, pathophysiology, and clinical management*. 2nd ed. Cambridge, UK: Cambridge University Press; 2009. p. 201-24.
437. Moller HJ, Nielsen MJ, Bartram J, Dick MC, Height SE, Moestrup SK, et al. Soluble CD163 levels in children with sickle cell disease. *British journal of haematology*. 2011 Apr;153(1):105-10. PubMed PMID: 21332709. Epub 2011/02/22. eng.
438. Thomsen JH, Etzerodt A, Svendsen P, Moestrup SK. The haptoglobin-CD163-heme oxygenase-1 pathway for hemoglobin scavenging. *Oxidative medicine and cellular longevity*. 2013;2013:523652. PubMed PMID: 23781295. Pubmed Central PMCID: PMC3678498. Epub 2013/06/20. eng.
439. O'Driscoll S, Height SE, Dick MC, Rees DC. Serum lactate dehydrogenase activity as a biomarker in children with sickle cell disease. *British journal of haematology*. 2008 Jan;140(2):206-9. PubMed PMID: 18028483. Epub 2007/11/22. eng.
440. Muller-Eberhard U, Javid J, Liem HH, Hanstein A, Hanna M. Plasma concentrations of hemopexin, haptoglobin and heme in patients with various hemolytic diseases. *Blood*. 1968 Nov;32(5):811-5. PubMed PMID: 5687939. Epub 1968/11/01. eng.
441. Yamak B OS. Haptoglobin in thalassemia. *Acta Haemat*. 1969;42:176-82.
442. Ragab SM, Safan MA, Badr EA. Study of serum haptoglobin level and its relation to erythropoietic activity in Beta thalassemia children. *Mediterranean journal of hematology and infectious diseases*. 2015;7(1):e2015019. PubMed PMID: 25745546. Pubmed Central PMCID: PMC4344174. Epub 2015/03/10. eng.
443. Vinchi F, Vercellotti GM, Belcher JD, Fibach E, Zreid H, Rasras R, Ghoti H, Muckenthaler MU, Rachmilewitz EA. Systemic heme and iron overload results in depletion of serum hemopexin, haptoglobin, and transferrin and correlates with markers of endothelial activation and lipid oxidation in beta thalassemia major and intermedia. *Blood*. 2016;128:2469.
444. Huebers HA, Beguin Y, Pootrakul P, Einspahr D, Finch CA. Intact transferrin receptors in human plasma and their relation to erythropoiesis. *Blood*. 1990 Jan 1;75(1):102-7. PubMed PMID: 2294984. Epub 1990/01/01. eng.
445. Beguin Y, Clemons GK, Pootrakul P, Fillet G. Quantitative assessment of erythropoiesis and functional classification of anemia based on measurements of serum transferrin receptor and erythropoietin. *Blood*. 1993 Feb 15;81(4):1067-76. PubMed PMID: 8427988. Epub 1993/02/15. eng.
446. Fillet G, Beguin Y. Monitoring of erythropoiesis by the serum transferrin receptor and erythropoietin. *Acta clinica Belgica*. 2001 May-Jun;56(3):146-54. PubMed PMID: 11484511. Epub 2001/08/04. eng.
447. Rees DC, Williams TN, Maitland K, Clegg JB, Weatherall DJ. Alpha thalassaemia is associated with increased soluble transferrin receptor levels. *British journal of haematology*. 1998 Nov;103(2):365-9. PubMed PMID: 9827906. Epub 1998/11/25. eng.
448. Carter K, Worwood M. Haptoglobin: a review of the major allele frequencies worldwide and their association with diseases. *International journal of laboratory hematology*. 2007 Apr;29(2):92-110. PubMed PMID: 17474882. Epub 2007/05/04. eng.

449. Smith A, McCulloh RJ. Hemopexin and haptoglobin: allies against heme toxicity from hemoglobin not contenders. *Frontiers in physiology*. 2015;6:187. PubMed PMID: 26175690. Pubmed Central PMCID: PMC4485156. Epub 2015/07/16. eng.
450. Gupta S, Ahern K, Nakhil F, Forte F. Clinical usefulness of haptoglobin levels to evaluate hemolysis in recently transfused patients. *Advances in hematology*. 2011;2011:389854. PubMed PMID: 21860624. Pubmed Central PMCID: PMC3153881. Epub 2011/08/24. eng.
451. Shih AW, McFarlane A, Verhovsek M. Haptoglobin testing in hemolysis: measurement and interpretation. *American journal of hematology*. 2014 Apr;89(4):443-7. PubMed PMID: 24809098. Epub 2014/05/09. eng.
452. Marchand A, Galen RS, Van Lente F. The predictive value of serum haptoglobin in hemolytic disease. *Jama*. 1980 May 16;243(19):1909-11. PubMed PMID: 7365971. Epub 1980/05/16. eng.
453. Delanghe JR, Langlois MR. Hemopexin: a review of biological aspects and the role in laboratory medicine. *Clinica chimica acta; international journal of clinical chemistry*. 2001 Oct;312(1-2):13-23. PubMed PMID: 11580905. Epub 2001/10/03. eng.
454. Vladutiu AO, Kim JS. Absence of beta-globulin band in the serum protein electropherogram of a patient with liver disease. *Clinical chemistry*. 1981 Feb;27(2):334-6. PubMed PMID: 6161719. Epub 1981/02/01. eng.
455. Moran MJ, Fontanellas A, Santos JL, Enriquez de Salamanca R. Correlation between levels of free and protein-bound plasma porphyrin and urinary porphyrins in porphyria cutanea tarda. *The international journal of biochemistry & cell biology*. 1995 Jun;27(6):585-8. PubMed PMID: 7671136. Epub 1995/06/01. eng.
456. Kirschke H. Cathepsin S. In: Salvesen NDRGS, editor. *Handbook of Proteolytic Enzymes*. one. London, UK: Elsevier Ltd.; 2013. p. 1824-30.
457. Lutzner N, Kalbacher H. Quantifying cathepsin S activity in antigen presenting cells using a novel specific substrate. *The Journal of biological chemistry*. 2008 Dec 26;283(52):36185-94. PubMed PMID: 18957408. Pubmed Central PMCID: PMC2662293. Epub 2008/10/30. eng.
458. Turk V, Stoka V, Vasiljeva O, Renko M, Sun T, Turk B, et al. Cysteine cathepsins: from structure, function and regulation to new frontiers. *Biochimica et biophysica acta*. 2012 Jan;1824(1):68-88. PubMed PMID: 22024571. Epub 2011/10/26. eng.
459. Pozgan U, Caglic D, Rozman B, Nagase H, Turk V, Turk B. Expression and activity profiling of selected cysteine cathepsins and matrix metalloproteinases in synovial fluids from patients with rheumatoid arthritis and osteoarthritis. *Biological chemistry*. 2010 May;391(5):571-9. PubMed PMID: 20180636. Epub 2010/02/26. eng.
460. Laboratories A. Haptoglobin: National Reference Laboratories; 2006-2012. Available from: www.aruplab.com.
461. Faber J, Fonseca LM. How sample size influences research outcomes. *Dental press journal of orthodontics*. 2014 Jul-Aug;19(4):27-9. PubMed PMID: 25279518. Pubmed Central PMCID: PMC4296634. Epub 2014/10/04. eng.
462. Paluszkiwicz A, Kellner J, Elshehabi M, Schneditz D. Effect of hemolysis and free hemoglobin on optical hematocrit measurements in the extracorporeal circulation. *ASAIO journal (American Society for Artificial Internal Organs : 1992)*. 2008 Mar-Apr;54(2):181-4. PubMed PMID: 18356652. Epub 2008/03/22. eng.
463. Wanachiwanawin W, Wiener E, Siripanyaphinyo U, Chinprasertsuk S, Mawas F, Fucharoen S, et al. Serum levels of tumor necrosis factor-alpha, interleukin-1, and interferon-gamma in beta(o)-thalassemia/HbE and their clinical significance. *Journal of interferon &*

cytokine research : the official journal of the International Society for Interferon and Cytokine Research. 1999 Feb;19(2):105-11. PubMed PMID: 10090395. Epub 1999/03/25. eng.

464. Voskaridou E, Christoulas D, Papatheodorou A, Plata E, Xirakia C, Tsaftaris P, et al. Angiogenic Molecules and Inflammatory Cytokines in Patients with Thalassemia Major and Double Heterozygous HbS/Beta-Thalassemia; the impact of Deferasirox. *Blood*. 2009;114(22):2018-.

465. Ramos P, Casu C, Gardenghi S, Breda L, Crielaard BJ, Guy E, et al. Macrophages support pathological erythropoiesis in polycythemia vera and beta-thalassemia. *Nature medicine*. 2013 Apr;19(4):437-45. PubMed PMID: 23502961. Pubmed Central PMCID: PMC3618568. Epub 2013/03/19. eng.

466. L'Acqua C, Bandyopadhyay S, Francis RO, McMahon DJ, Nellis M, Sheth S, et al. Red blood cell transfusion is associated with increased hemolysis and an acute phase response in a subset of critically ill children. *American journal of hematology*. 2015 Oct;90(10):915-20. PubMed PMID: 26183122. Pubmed Central PMCID: PMC4831067. Epub 2015/07/18. eng.

467. Rapido F, Brittenham GM, Bandyopadhyay S, La Carpio F, L'Acqua C, McMahon DJ, et al. Prolonged red cell storage before transfusion increases extravascular hemolysis. *The Journal of clinical investigation*. 2017 Jan 3;127(1):375-82. PubMed PMID: 27941245. Pubmed Central PMCID: PMC5199711. Epub 2016/12/13. eng.

468. Hod EA, Brittenham GM, Billote GB, Francis RO, Ginzburg YZ, Hendrickson JE, et al. Transfusion of human volunteers with older, stored red blood cells produces extravascular hemolysis and circulating non-transferrin-bound iron. *Blood*. 2011 Dec 15;118(25):6675-82. PubMed PMID: 22021369. Pubmed Central PMCID: PMC3242722. Epub 2011/10/25. eng.

469. Kim-Shapiro DB, Lee J, Gladwin MT. Storage lesion: role of red blood cell breakdown. *Transfusion*. 2011 Apr;51(4):844-51. PubMed PMID: 21496045. Pubmed Central PMCID: PMC3080238. Epub 2011/04/19. eng.

470. Burnouf T, Chou ML, Goubran H, Cognasse F, Garraud O, Seghatchian J. An overview of the role of microparticles/microvesicles in blood components: Are they clinically beneficial or harmful? *Transfusion and apheresis science : official journal of the World Apheresis Association : official journal of the European Society for Haemapheresis*. 2015 Oct;53(2):137-45. PubMed PMID: 26596959. Epub 2015/11/26. eng.

471. Garcia-Roa M, Del Carmen Vicente-Ayuso M, Bobes AM, Pedraza AC, Gonzalez-Fernandez A, Martin MP, et al. Red blood cell storage time and transfusion: current practice, concerns and future perspectives. *Blood transfusion = Trasfusione del sangue*. 2017 May;15(3):222-31. PubMed PMID: 28518049. Pubmed Central PMCID: PMC5448828. Epub 2017/05/19. eng.

472. Lithanatudom P, Leechaoenkiat A, Wannatung T, Svasti S, Fucharoen S, Smith DR. A mechanism of ineffective erythropoiesis in beta-thalassemia/Hb E disease. *Haematologica*. 2010 May;95(5):716-23. PubMed PMID: 20015891. Pubmed Central PMCID: PMC2864376. Epub 2009/12/18. eng.

473. Cyranoski D. CRISPR gene-editing tested in a person for the first time. *Nature*. 2016 Nov 24;539(7630):479. PubMed PMID: 27882996. Epub 2016/11/25. eng.

474. Melchiori L, Gardenghi S, Rivella S. beta-Thalassemia: Hijacking Ineffective Erythropoiesis and Iron Overload. *Advances in hematology*. 2010;2010:938640. PubMed PMID: 20508726. Pubmed Central PMCID: PMC2873658. Epub 2010/05/29. eng.

475. Marinkovic D, Zhang X, Yalcin S, Luciano JP, Brugnara C, Huber T, et al. Foxo3 is required for the regulation of oxidative stress in erythropoiesis. *The Journal of clinical*

- investigation. 2007 Aug;117(8):2133-44. PubMed PMID: 17671650. Pubmed Central PMCID: PMC1934587. Epub 2007/08/03. eng.
476. Zhang X, Camprecios G, Rimmele P, Liang R, Yalcin S, Mungamuri SK, et al. FOXO3-mTOR metabolic cooperation in the regulation of erythroid cell maturation and homeostasis. *American journal of hematology*. 2014 Oct;89(10):954-63. PubMed PMID: 24966026. Pubmed Central PMCID: PMC4201594. Epub 2014/06/27. eng.
477. Quimby KR, Hambleton IR, Landis RC. Intravenous infusion of haptoglobin for the prevention of adverse clinical outcome in Sickle Cell Disease. *Medical hypotheses*. 2015 Oct;85(4):424-32. PubMed PMID: 26141635. Epub 2015/07/05. eng.
478. Pornprasert S, Panyasai S, Treesuwan K. Unmasking Hb Pakse (codon 142, TAA>TAT, alpha2) and its combinations in patients also carrying Hb Constant Spring (codon 142, TAA>CAA, alpha2) in northern Thailand. *Hemoglobin*. 2012;36(5):491-6. PubMed PMID: 22881835. Epub 2012/08/14. eng.
479. Viprakasit V, Ekwattanakit S, Chalaow N, Riolueang S, Wijit S, Tanyut P, et al. Clinical presentation and molecular identification of four uncommon alpha globin variants in Thailand. Initiation codon mutation of alpha2-globin Gene (HBA2:c.1delA), donor splice site mutation of alpha1-globin gene (IVSI-1, HBA1:c.95 + 1G>A), hemoglobin Queens Park/Chao Pra Ya (HBA1:c.98T>A) and hemoglobin Westmead (HBA2:c.369C>G). *Acta haematologica*. 2014;131(2):88-94. PubMed PMID: 24081251. Epub 2013/10/02. eng.

APPENDIX

Appendix I

Demographic data, initial diagnoses, laboratory parameters, medications, and ELISA results of all the patients recruited in the clinical follow-up trial

Note: Coding

A = Transfusion dependant thalassaemia (TDT) group

B = Non-transfusion-dependent thalassaemia (NTDT) group

C = thalassaemic traits

D = healthy controls

Green and yellow columns represent all the relevant tested performed in Thailand

Orange colour denotes the ELISA test results performed at NHSBT, Filton, UK

Sample	Age	Sex	Date	Diagnosis	Hb (g/dL)	Hct (%)	WBC (/mm3)	Platelet (/mm3)	Corrected Retic count (%)	Ferritin (ng/ml)	IDB	LDH	Haptoglobin (mg/ml, 0.3-2.0)	Plasma Hb (mg/dl)	Hemolysis (%)	Haptoglobin bin (mg/ml)	Hemopexin (mg/ml)	CTSS (pg/ml)
C01	39	F	10/11/2017	β-thal trait	12.7	41.4	5200	257,000	1.04	63.4	0.4	354	0.8	0.02	0.09	144.61	0.67	5118.18
C02	56	F	10/11/2017	Hb E trait	13.1	41.8	6900	338,000	1.63	238.8	0.14	434	2	0.01	0.04	470.72	0.69	3611.82
C03	37	f	25/04/2018	β-thal trait	10.2	33.1	5000	372000	1.02	78	0.22	303	0.82	0.00	0.00	201.00	1.78	3355.45
C04	26	m	20/06/2018	β-thal trait	14.7	46.2	7900	302000	1.20	776	0.43	381	0.48	0.11	0.40	3.46	1.18	2023.73
C05	33	m	20/06/2018	α-thal1	12.8	42	7200	312000	0.89	354	0.3	322	1.52	0.06	0.28	339.61	2.79	3475.45
C06	28	m	20/06/2018	α-thal1	15.9	50.2	9900	265000	1.95	225	0.23	340	1.52	0.03	0.09	443.20	2.81	7472.73
C07	31	m	20/06/2018	Hb E trait	14.4	44.5	9700	269000	2.48	567	0.3	360	1.79	0.12	0.41	452.28	2.80	5125.45
C08	25	F	10/11/2017	Hb E trait	10.7	33.1	8900	311000	1.15	21.9	0.3	239	0.7	0.04	0.25	259.10	1.95	1355.45

Sample	Age	Sex	Date	Hb (g/dL)	Hct (%)	WBC (/mm3)	Platelet (/mm3)	Corrected Retic count (%)	Ferritin (ng/ml)	IDB	LDH	Haptoglobin (mg/ml, 0.3-2.0)	Plasma Hb (mg/dl)	Hemolysis (%)	Haptoglobin bin (mg/ml)	Hemopexin (mg/ml)	CTSS (pg/ml)
D01	39	M	10/11/2017	12.8	39.7	6,600	299,000	1.31	7.9	0.27	264	1.3	0.02	0.09	248.91	2.97	4734.55
D02	29	F	22/11/2017	13.1	40.8	6,900	184,000	1.42	157.3	0.19	284	1.4	0.02	0.09	364.83	2.98	2053.81
D03	44	m	20/06/2018	15	45.2	9200	218000	1.81	272	0.22	326	1.06	0.05	0.19	93.53	1.19	3016.10
D04	38	f	20/06/2018	13.5	41	7200	276000	1.14	70	0.2	279	0.79	0.02	0.08	211.76	1.06	3285.59
D05	29	f	20/06/2018	12.7	39.4	7300	399000	1.39	90.8	0.17	277	0.83	0.04	0.19	151.83	2.79	2102.54
D06	38	m	20/06/2018	16.5	49.4	6700	303000	1.72	377	0.33	365	0.66	0.13	0.40	3.41	2.76	7660.91
D07	37	m	20/06/2018	14.1	45	10200	295000	1.44	228.5	0.19	432	1.59	0.02	0.08	369.29	2.90	5312.73

Appendix II

Primers used for PCR amplifications and Sanger sequencing

Amplified region	Primer*	Primer sequence	Primer position†	Product size (bp)	PCR amplification enzyme and annealing temp. (°C)
<i>HBB</i> exon 1+2	HBB_1+2_F	5'-TCCTAAGCCAGTGCCAGAA-3'	5' UTR (-211 to -193)	741	BioTaq, 65
	HBB_1+2_R	5'-CCCTGTTACTTATCCCCTTCC-3'	intron 2 (+65 to +85)		
<i>HBB</i> exon 3	HBB_3_F	5'-ATGGTTGGGATAAGGCTGGAT-3'	intron 2 (-85 to -65)	533	BioTaq, 65
	HBB_3_R	5'-ATATGCATCAGGGGCTGTTG-3'	3' UTR (+300 to +319)		
<i>HBB</i> IVS-II	HBB_intr2_F	5'-TATCATGCCTCTTTGCCACCA	intron 2 (-253 to -234)	190	BioTaq, 65
	HBB_intr2_R	5'-AATCCAGCCTTATCCCAACC-3'	intron 2 (-83 to -64)		
<i>KLF1</i> exon 1	KLF1_1_F	5'-TTGACTTGGCTTTGGACACAG-3'	5' UTR (-237 to -217)	507	BioTaq, 65
<i>KLF1</i> exon 2a	KLF1_1_R	5'-CCCTAGACCACCTCCTCAC-3'	intron 1 (+164 to +183)	594	Phusion, 65
	KLF1_2a_F	5'-TGGGGAAGTGGGACAGACAGA-3'	intron 1 (-136 to -116)		
<i>KLF1</i> exon 2b	KLF1_2a_R	5'-AAGTAGCCACCCGAGGAGCC-3'	exon 2 (+439 to +458)	637	Phusion, 68
	KLF1_2b_F	5'-GGATCACTCGGGTTGGGTG-3'	exon 2 (+303 to +321)		
<i>KLF1</i> exon 3	KLF1_2b_R	5'-CACTCACTCTCAGAGGCCAGC-3'	intron 2 (+93 to +113)	516	BioTaq, 65
	KLF1_3_F	5'-TTACAGGGGAAGAAGGGTTGC-3'	intron 2 (-206 to -186)		
<i>KLF1</i> exon 3	KLF1_3_R	5'-GCGAGTCCAGGAGAGGGTC-3'	3' UTR (+116 to +134)		
<i>HBA1</i> exon 1	HBA1_1_F	5'-GGAGTGGCGGGTGGAGGGT-3'	5' UTR (-250 to -232)	604	Phusion, 68
	HBA1_1_R	5'-GTTGGGCATGTCGTCCAC-3'	exon 2 (+125 to +142)		
<i>HBA1</i> exon 2	HBA1_2_F	5'-CACCCCTCACTCTGCTTCTC-3'	intron 1 (-27 to -8)	506	Phusion, 68
	HBA1_2_R	5'-CGGTATTTGGAGGTCAGCAC-3'	exon 3 (+106 to +125)		
<i>HBA1</i> exon 3	HBA1_3_F	5'-CCTACTGACCCTCTTCTCTGC-3'	intron 2 (-24 to -5)	476	Phusion, 68
	HBA1_3_R	5'-AGCAAATGCATCCTCAAAGC-3'	3' UTR (+303 to +323)		
<i>HBA2</i> exon 1	HBA2_1_F	5'-GGGCTCCGCGCCAGCCAATGAG-3'	5' UTR (-122 to -101)	330	Phusion, 70
	HBA2_1_R	5'-GGGGAGAAGCAGAGTGAGG-3'	intron 1 (-23 to -5)		
<i>HBA2</i> exon 2	HBA2_2_F	5'-CACCCCTCACTCTGCTTCTC-3'	intron 1 (-27 to -8)	470	AmpliTaq, 68
	HBA2_2_R	5'-AGAAGCCAGGAACTTGTC-3'	exon 3 (+77 to +96)		
<i>HBA2</i> exon 3	HBA2_3_F	5'-CTCTCAGGGCAGAGGATCAC-3'	intron 2 (+52 to +71)	416	AmpliTaq, 65
	HBA2_3_R	5'-CTGCAGAGAGGCTTGGTC-3'	3' UTR (+177 to +196)		

*F and R denote forward (sense) and reverse (antisense) direction, respectively.

†Primer positions are relative to the respective exon/intron boundary.

Appendix III

Table summarised genetic backgrounds of all the thalassaemia patients recruited in the project

Patients	Mutations	Diagnosis	Patients	Mutations	Diagnosis	Patients	Mutations	Diagnosis
1	HBB:c.79G>A	β^0/β^E	17	HBB:c.79G>A	β^0/β^E	34	HBA2:c.427T>C	HbH-CS
	HBB:c.126_129delCTTT			HBB:c.-28A>G				
2	HBB:c.79G>A	β^0/β^E with Hb Westmead	18	HBB:c.92+1G>T	β^0/β^0	35	HBB:c.79G>A	β^E/β^E with heterozygous CS
	HBB:c.126_129delCTTT			HBB:c.92+1G>T			HBA2:c.427T>C	
	HBA2:c.369C>G			HBB:c.79G>A			HBB:c.79G>A	
3	HBB:c.79G>A	β^0/β^E	19	HBB:c.92+5G>C	β^0/β^E with heterozygous CS	36	HBA2:c.427T>C	HbH-CS
	HBB:c.92+1G>A			HBA2:c.427T>C				
4	HBB:c.79G>A	β^0/β^E	20	HBB:c.79G>A	β^E/β^E with homozygous CS	39	HBB:c.79G>A	β^E/β^E
	HBB:c.108C>A			HBB:c.79G>A			HBB:c.79G>A	
5	HBB:c.79G>A	β^0/β^E	21	HBB:c.79G>A	β^0/β^E	40	HBA2:c.427T>C	HbH-CS
	HBB:c.92+5G>C			HBB:c.52A>T			HBA2:c.429A>T	
6	HBB:c.79G>A	β^0/β^E	22	HBB:c.79G>A	β^0/β^E	41	HBA2:c.427T>C	HbH-CS
	HBB:c.316-197C>T			HBB:c.92+5G>C			HBA2:c.427T>C	
7	HBB:c.79G>A	β^0/β^E	23	HBA2:c.427T>C	HbH-CS	42	HBA2:c.427T>C	HbH disease
	HBB:c.316-197C>T			HBB:c.79G>A			HBB:c.79G>A	
8	HBB:c.79G>A	β^0/β^E	24	HBB:c.79G>A	β^0/β^E	43	HBB:c.79G>A	β^E/β^E
	HBB:c.126_129delCTTT			HBB:c.126_129delCTTT			HBB:c.79G>A	
9	HBB:c.79G>A	β^0/β^E	25	HBB:c.79G>A	β^0/β^E	44	HBB:c.79G>A	β^0/β^E
	HBB:c.316-197C>T			HBB:c.126_129delCTTT			HBB:c.126_129delCTTT	
10	HBB:c.79G>A	β^0/β^E	26	HBB:c.79G>A	β^0/β^E	45	HBB:c.79G>A	β^0/β^E
	HBB:c.92+1G>T			HBB:c.126_129delCTTT			HBB:c.126_129delCTTT	
11	HBB:c.79G>A	β^0/β^E	27	HBB:c.79G>A	β^0/β^E	46	HBB:c.79G>A	β^0/β^E
	HBB:c.52A>T			HBB:c.52A>T			HBB:c.126_129delCTTT	
12	HBB:c.79G>A	β^0/β^E	28	HBB:c.79G>A	β^0/β^E	46	HBB:c.79G>A	β^0/β^E
	HBB:c.126_129delCTTT			HBB:c.316-197C>T			HBB:c.126_129delCTTT	
13	HBB:c.79G>A	CSEABart's disease (Hb Paksé)	29	HBB:c.79G>A	β^0/β^E	46	HBB:c.79G>A	β^0/β^E
	HBA2:c.429A>T			HBB:c.126_129delCTTT			HBB:c.126_129delCTTT	
14	HBB:c.79G>A	β^0/β^E	30	HBB:c.79G>A	β^0/β^E	46	HBB:c.79G>A	β^0/β^E
	HBB:c.52A>T			HBB:c.92+5G>C			HBB:c.79G>A	
15	HBB:c.79G>A	β^0/β^E	31	HBB:c.316-197C>T	β^0/β^E	46	HBB:c.79G>A	β^0/β^E
	HBB:c.126_129delCTTT			HBA2:c.427T>C			HbH-CS	
16	HBB:c.79G>A	β^E/β^E	33	HBB:c.79G>A	β^E/β^E	46	HBB:c.79G>A	β^E/β^E
	HBB:c.79G>A			HBB:c.79G>A				